GEOLOGIJA

2010 | št.: **53/1**

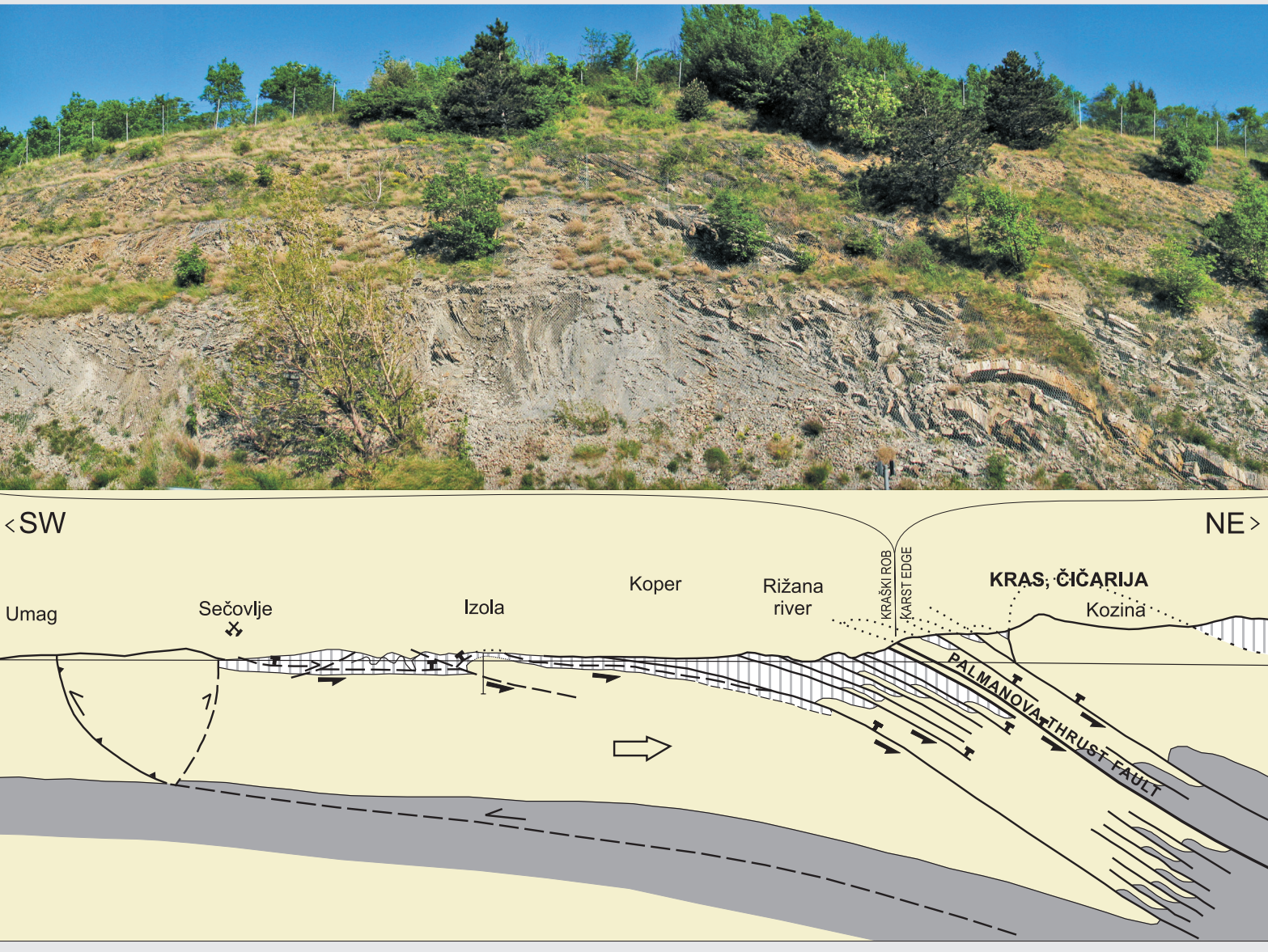

Geološki zavod Slovenije
Geological Survey of Slovenia

ISSN 0016-7789
ISSN 1854-620X

GEOLOGIJA

53/1 – 2010

GEOLOGIJA	2010	53/1	1–108	Ljubljana

GEOLOGIJA
ISSN 0016-7789
© Geološki zavod Slovenije

Izdajatelj: Geološki zavod Slovenije, zanj direktor Marko Komac
Publisher: Geological Survey of Slovenia, represented by Director Marko Komac
Financirata Javna agencija za knjigo Republike Slovenije in Geološki zavod Slovenije
Financed by the Slovenian Book Agency and the Geological Survey of Slovenia

Vsebina številke 53/1 je bila sprejeta na seji Uredniškega odbora, dne 2. 6. 2010.
Manuscripts of the Volume 53/1 accepted by Editorial and Scientific Advisory Board on June 2, 2010.

Glavna in odgovorna urednica / Editor-in-Chief: Mateja Gosar

Uredniški in recenzijski odbor / Scientific Advisory Board:

Dunja Aljinović, Rudarsko-geološki naftni fakultet, Zagreb
Mihael Brenčič, Naravoslovnotehniška fakulteta, Univerza v Ljubljani
Giovanni Battista Carulli, Dip. di Sci. Geol., Ambientali e Marine, Università di Trieste
Katica Drobne, Znanstveno Raziskovalni Center SAZU, Ljubljana
Matija Drovenik, Slovenska akademija znanosti in umetnosti, Ljubljana
Jadran Faganeli, Nacionalni inštitut za biologijo, Morska biološka postaja Piran
Janos Haas, Etvös Lorand University, Budapest
Bogdan Jurkovšek, Geološki zavod Slovenije, Ljubljana
Roman Koch, Institut für Paläontologie, Universität Erlangen-Nürnberg
Marko Komac, Geološki zavod Slovenije, Ljubljana
Harald Lobitzer, Geologische Bundesanstalt, Wien
Rinaldo Nicolich, D.I.N.M.A., Sezione Georisorse e Ambiente, Università di Trieste
Bojan Ogorelec, Geološki zavod Slovenije, Ljubljana
Simon Pirc, Naravoslovnotehniška fakulteta, Univerza v Ljubljani
Mario Pleničar, Slovenska akademija znanosti in umetnosti, Ljubljana
Danilo Ravnik, Naravoslovnotehniška fakulteta, Univerza v Ljubljani
Mihael Ribičič, Naravoslovnotehniška fakulteta, Univerza v Ljubljani
Marko Šparica, Institut za geološka istraživanja, Zagreb
Sašo Šturm, Institut »Jožef Stefan«, Ljubljana
Dragica Turnšek, Slovenska akademija znanosti in umetnosti, Ljubljana
Miran Veselič, Fakulteta za gradbeništvo in geodezijo, Univerza v Ljubljani

Tehnična urednica / Technical Editor: Bernarda Bole
Naslov uredništva / Editorial Office: GEOLOGIJA Geološki zavod Slovenije / Geological Survey of Slovenia
Dimičeva ulica 14, SI-1000 Ljubljana, Slovenija
Tel.: +386 (01) 2809-700, Fax: +386 (01) 2809-753, e-mail: urednik@geologija-revija.si
Spletni naslov / URL: http://www.geologija-revija.si/

GEOLOGIJA izhaja dvakrat letno. GEOLOGIJA is published two times a year.
GEOLOGIJA je na voljo tudi preko medknjižnične izmenjave publikacij. / GEOLOGIJA is available also on exchange basis.

Baze, v katerih je Geologija indeksirana / Indexation bases of Geologija: GeoRef, Chemical Abstracts, PASCAL, Zoological Record

Cena / Price

Posamezni izvod / Single Issue	Letna naročnina / Annual Subscription
Posameznik / Individual: 15 €	Posameznik / Individual: 25 €
Institucija / Institutional: 25 €	Institucija / Institutional: 40 €

Tisk / Printed by: Tiskarna Formatisk d.o.o.

Slika na naslovni strani: Prerez Umag – Kozina preko Istrsko-Furlanske podrivne cone s Palmanovskim narivnim prelomom (krajevno Črnokalski narivni prelom) v sredini. Na fotografiji Palmanovski narivni prelom v useku avtoceste pod hribom Čelo nasproti Doline (Dorligo delle Valle). (Placer et al., članek v tej številki, foto: B. Celarc).
Cover page: Cross-section Umag – Kozina across Istria-Friuli Underthrust Zone with the Palmanova Thrust Fault (local Črni kal Thrust Fault) in central position. On photography Palmanova Thrust Fault in the highway cut under Čelo hill opposite to Dolina (S. Dorligo delle Valle) village. (Placer et al., paper in this issue, photo: B. Celarc).

GEOLOGIJA *53/1*, 1–108, Ljubljana 2010

VSEBINA – CONTENTS

GEOLOGIJA *53/1*, 5-20, Ljubljana 2010

Pohorje eclogites revisited: Evidence for ultrahigh-pressure metamorphic conditions

Ultravisokotlačni metamorfizem pohorskega eklogita

Mirijam VRABEC

University of Ljubljana, Faculty of Natural Sciences and Engineering, Department of Geology, Aškerčeva 12, SI-1000 Ljubljana, Slovenia; e-mail: mirijam.vrabec@ntf.uni-lj.si

Prejeto / Received 4. 3. 2010; Sprejeto / Accepted 20. 5. 2010

Key words: ultrahigh-pressure metamorphism, eclogite, geothermobarometry, collisional orogen, Pohorje, Eastern Alps, Slovenia

Ključne besede: ultravisokotlačna metamorfoza, eklogit, geotermobarometrija, kolizijski orogeni, Pohorje, Vzhodne Alpe, Slovenija

Abstract

Kyanite eclogites from the Pohorje Mountains, Slovenia, are providing the first evidence of ultrahigh-pressure Eo-Alpine metamorphism in the Eastern Alps. Polycrystalline quartz inclusions in garnet, omphacite and kyanite are surrounded by radial fractures and exhibit microtextures diagnostic for the recovery after coesite breakdown. The non-stoichiometric supersilicic omphacites found in Pohorje eclogites contain up to 5 mol % of Ca-Eskola molecule. Such clinopyroxenes are known to be stable exclusively at high-pressure conditions exceeding 3 GPa. Their breakdown during decompression resulted in exolution of quartz rods and needles that are oriented parallel to omphacite c-axis. The absence of coesite is a consequence of near-isothermal decompression during the first stages of exhumation.

Pressure and temperature conditions for the formation of the peak metamorphic mineral assemblages have been assessed through a consideration of a) Fe^{2+}-Mg partitioning between garnet and omphacite pairs, based on different calibrations; b) the equilibrium between garnet + clinopyroxene + phengite ± kyanite ± quartz/coesite assemblage. Estimated peak pressure and temperature conditions of 3.0-3.1 GPa and 750-783 °C are well within the coesite, i.e. the ultrahigh-pressure stability field.

Izvleček

Pohorski kianitovi eklogiti predstavljajo prvi dokaz za obstoj eo-alpinske ultravisokotlačne metamorfoze v Vzhodnih Alpah. Radialne razpoke okoli polikristalnih kremenovih vključkov v granatu, omfacitu in kianitu ter njihove specifične mikrostrukture pričajo o obstoju coesita, ki je med ekshumacijo zaradi dekompresije prešel v kremen. Popolna odsotnost coesita je posledica izotermne dekompresije v začetni stopnji ekshumacije pohorskih eklogitov. Nestehiometrični omfaciti z visoko vsebnostjo SiO_2, ki vsebujejo do 5 mol % Ca-Eskola molekule in so obstojni izključno pri tlakih večjih od 3 GPa, potrjujejo izpostavljenost pohorskih eklogitov ultravisokotlačnim metamorfnim pogojem. Zaradi dekompresije so se v njih izločile kremenove iglice in paličice, ki so orientirane vzporedno z omfacitovo c-osjo.

Tlačni in temperaturni pogoji nastanka pohorskih eklogitov so bili določeni s pomočjo različnih geotermometrov, ki temeljijo na izmenjavi Fe^{2+} in Mg ionov med granatom in omfacitom, kot tudi na osnovi ravnotežja med mineralnimi fazami: granat + monoklinski piroksen + fengit ± kianit ± kremen/coesit. Izračunane tlačne in temperaturne vrednosti se gibljejo v razponu od 3.0-3.1 GPa in 750-783 °C ter odgovarjajo ultravisokotlačnemu (coesitovemu) stabilnostnemu območju.

Introduction

Ultrahigh-pressure (UHP) metamorphism is an important type of orogenic metamorphism that has been recognized in many Phanerozoic collision belts (e.g. Liou et al., 1998; Chopin, 2003, and references therein). Well investigated intracratonic collisional orogens that exhibit scattered effects of subsolidus UHP recrystallization include the Quinling-Dabie-Sulu belt of east-central China, the Kokchetav Complex of northern Kazahstan, the Dora Maira massif of the Western Alps, and the Western Gneiss Region (WGR) of Norway (Liou et al., 1994; Coleman & Wang, 1995; Ernst et al., 1995). This four classic and several other UHP terranes (Figure 1) share common structural and lithological characteristics (Liou, 2000). Supracrustal rocks of these UHP regions experienced subduction-zone metamorphism at mantle depths, followed by a retrograde amphibolite-granulite facies overprint during exhumation, and finally thermal recrystallization and defor-

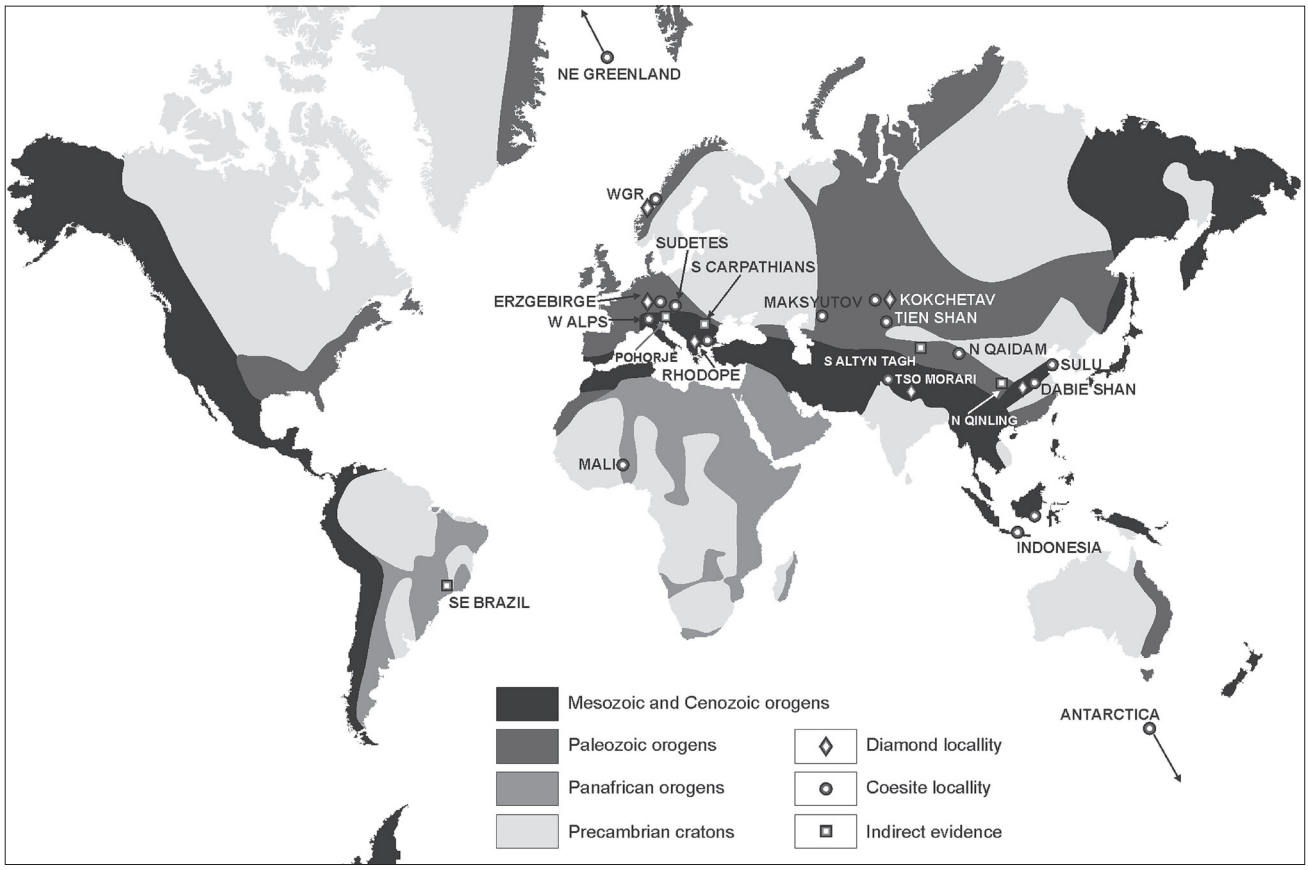

Figure 1. Distribution of recognized UHP metamorphic terranes in the world through time and space. So far, evidence of UHP metamorphism was not found only in Australia and North America (modified from Liou et al., 1998; Chopin, 2003).

mation during postcollisional granitic intrusions and orogeny.

With the discovery of UHP metamorphism geologists realized that, contrary to general belief, continental crust in convergent settings may be subducted to enormous depths, and that the most formidable geodynamic problems concerning UHP metamorphic rocks are not the mechanisms of their deep burial, but the mechanisms which facilitated their subsequent exhumation to the Earth's surface without a complete breakdown of the UHP mineral assemblages. From the recurrent occurrences both in time and space, since late Proterozoic, it is clear that UHP metamorphism is a common process, inherent to continental collision.

Ultrahigh-pressure metamorphism is synonymous with eclogite-facies metamorphism that has occured within the stability field of coesite (Figure 2). Unequivocal identification of UHP conditions depends on the presence of relict coesite or diamond, high-pressure polymorphs of silica and carbon, as direct indicators of metamorphic pressures of at least 3 GPa (coesite) or 4 GPa (diamond). But since the metastable preservation of relict UHP phases during exhumation and decompression is now known to be very rare, a simple microscopic identification of UHP metamorphic rocks is normally not possible, and the evidence for UHP conditions must be deduced from indirect petrographic and microtextural observations. In absence of an actual coesite relict, polycrystalline quartz aggregates are strongly indicative tex-

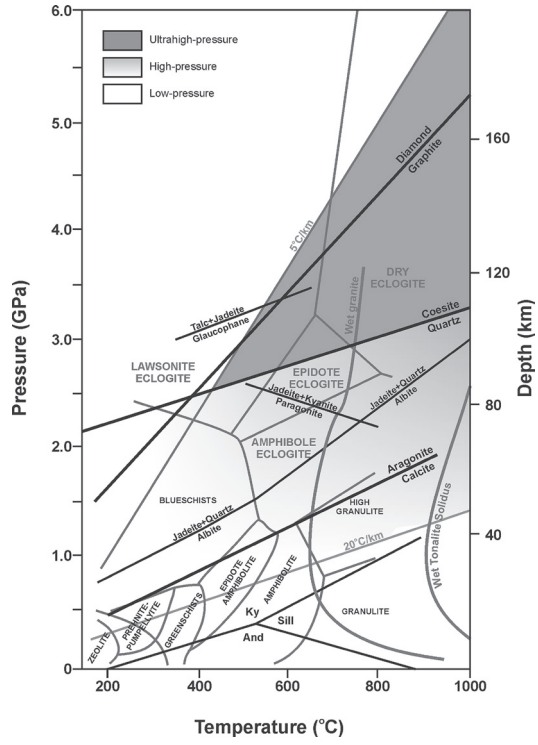

Figure 2. Simplified P-T facies diagram. UHP eclogites are defined as metabasic rocks with a dominant plagioclase-free, eclogite-facies mineral paragenesis of garnet and omphacitic clinopyroxene, but with additional petrographic or mineral-chemistry features that indicate equilibration at pressures within the coesite P-T stability field. Subdivision of the eclogite facies field is based on Okamoto & Maruyama (1999). Also shown are the stability fields for diamond and coesite according to Holland & Powell (1998).

tural feature of former coesite existence (Smith, 1984; Gillet et al., 1984) but tend to disappear due to recrystallization during prolonged thermal annealing. A further distinctive petrographic feature of partly or completely replaced coesite inclusions is the developement of radial expansion cracks, extending from the inclusion boundary into the enclosing mineral. This reflects the roughly 10 % volume increase on transition from coesite to α-quartz. Several other uncommon petrological features and assemblages that have been reported from various UHP metamorphic rocks provide additional evidence for UHP metamorphism. Quartz rods have been observed in omphacite from eclogites of several UHP terranes. In all cases, SiO_2 needles and rods in omphacite have been interpreted as exsolution products from a preexisting supersilicic clinopyroxene that contained excess silica at peak metamorphic conditions (e.g. Smith, 1984; Liou et al., 1998; Katayama et al., 2000; Schmädicke and Müller, 2000; Zhang & Liou, 2000; Dobrzhinetskaya et al., 2002). Potassium-bearing clinopyroxene with extremely high potassium content (up to 1.5 wt% K_2O) is stable at pressures of 4–10 GPa. During decompression, potassic clinopyroxene develops characteristic textures with oriented precipitates of K-feldspar (Sobolev & Shatsky, 1990). Orthopyroxene exsolutions in garnet require formation pressures in excess of 6 GPa and hence over 200 km of depth. Exsolutions suggest the existence of a super-silicic precursor garnet with several mol % of majorite component (van Roermund et al., 2001). α-PbO_2-type TiO_2 inclusions in garnet indicate achieved pressures in the range from 4.5 to 6.5 GPa at a temperature of 1000 °C (Huang et al., 2000). Although the indirect indicators of UHP metamorphism are very useful since the preservation of metastable coesite and diamond is very rare, they cannot be used alone as a proof that UHP metamorphism was achieved. When direct mineral indicators are absent, converging indirect pieces of evidence, together with reliable geothermobarometrical calculations, are needed to verify the existence of UHP metamorphism.

Pohorje in north-eastern Slovenia (Figure 3) is the south-easternmost prolongation of the Eastern Alps. It is a part of the extensive Alpine orogen where UHP metamorphism was documented in the Western Alps (e.g. Chopin, 1984) and was shown to be related to the Tertiary orogeny (e.g. Tilton et al., 1991). Metamorphic processes related to the older, Cretaceous Alpine orogeny are mainly recognized in the Austroalpine units of the Eastern Alps (e.g. Thöni & Jagoutz, 1992). So far, up to high-pressure (HP) eclogite facies metamorphic conditions were recognized in the Koralpe and Saualpe areas situated just north of Pohorje (Miller, 1990). The Pohorje Mountains consist of a stack of Cretaceous Austroalpine nappes, predominately composed of micashists, gneisses and amphibolites, but also include several lenses of eclogitic rocks that are of special interest since they have high preservation potential for ultrahigh-pressure metamorphic indicators. Eclogites from Pohorje were previously investigated by Hinterlechner-Ravnik (1982), Hinterlechner-Ravnik et al. (1991) and Koch (1999). Geothermobarometric estimations from the first two works are rather broad, with estimated pressure ranging from 1.2–1.8 GPa at temperature from 460–900 °C. Pressure and temperature estimates by Koch (1999) fall into the same (high-pressure) range, but are more narrowly constrained to 1.5 GPa at 760 °C.

First two samples of eclogites from Pohorje indicating possible UHP conditions were investigated by Janák et al. (2004). This work presents new samples from several new localities bringing undisputed mineralogical, petrological, microtextural and microchemical evidence for ultra-

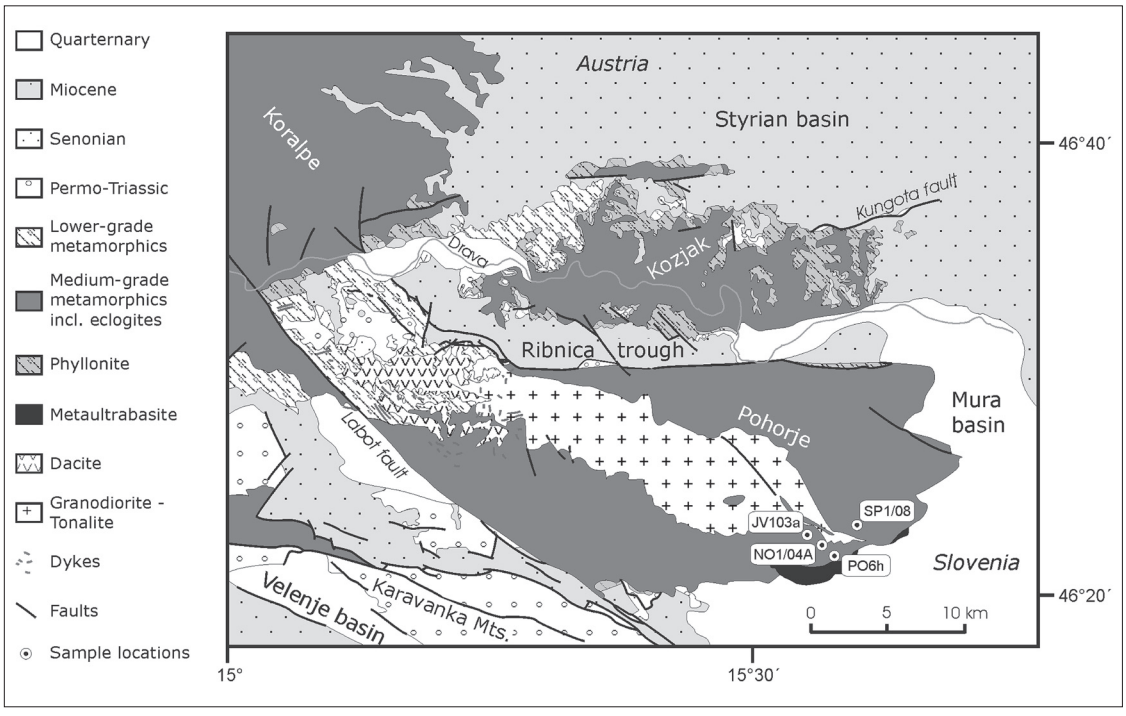

Figure 3. Simplified geologic map of Pohorje and adjacent areas (modified from Mioč & Žnidarčič, 1977) showing locations of the investigated eclogite samples.

high-pressure metamorphism of eclogites in the Austroalpine units of the Eastern Alps, exposed in the Pohorje Mountains of Slovenia. The evidence for ultrahigh-pressure conditions is strongly supported by extensive and precise geothermobarometric calculations based on different widely accepted calibrations.

Methods

Electron Probe Micro-Analysis

Representative microchemical analyses of the main constituent minerals were determined by EPMA technique using a CAMECA SX-100 electron microprobe at Dionýz Štúr Institute of Geology in Bratislava. Bombarding of micro-volumes of sample with a focused electron beam (5–30 keV) induced emission of X-ray photons. The wavelengths of collected X-rays were identified by recording their WDS spectra (Wavelength Dispersive Spectroscopy). Analytical conditions were 15 keV accelerating voltage and 20 nA beam current, with a peak counting time of 20 s and a beam diameter of 2–10 μm. Raw counts were corrected using a PAP routine.

Garnet-clinopyroxene Fe^{2+}-Mg exchange geothermometery

Temperature conditions of metamorphism were obtained using the partitioning of Fe^{2+} and Mg between co-existing garnet and clinopyroxene (omphacite). Due to the common appearance of clinopyroxene and garnet in a mineral assemblage of high-grade metamorphic rocks of basic and ultrabasic composition this is one of the most widely used methods in geothermometry of such rocks. When these two minerals are contiguous phases, they effectively exchange the two elements and the exchange balance is a function of temperature.

The exchange of iron and magnesium between clinopyroxene and garnet is represented by exchange reaction:

pyrope + 3 *hedenbergite* → *almandine* + 3 *diopside*

The equilibrium constant for the considered equilibrium is expressed by the following function:

$$K_{eq} = \frac{a_{Fe}^{grt}}{a_{Mg}^{grt}} \cdot \left[\frac{a_{Mg}^{cpx}}{a_{Fe}^{cpx}} \right]^3$$

where a_i^j is the activity of component i in phase j. If the minerals are ideal solid solutions, activities are equivalent to concentrations and

$$K_{eq} = \frac{X_{Fe}^{grt}}{X_{Mg}^{grt}} \cdot \frac{X_{Mg}^{cpx}}{X_{Fe}^{cpx}} = \frac{\left(Fe^{2+}/Mg\right)^{grt}}{\left(Fe^{2+}/Mg\right)^{cpx}} = K_D$$

where K_D is the distribution coefficient, X_{Fe}^{grt} is the mole fraction of Fe^{2+} in the three equivalent divalent sites in garnet structure, X_{Fe}^{cpx} is the mole fraction of Fe^{2+} in the clinopyroxene, etc. If the minerals are not ideal (i.e. their compositions differ from those of pure ideal end-members used in experiments) compositional differences are corrected by the introduction of activities, which express the thermodynamically effective concentrations of components. Then

$$a = X \cdot \gamma$$

where γ is defined as the activity coefficient and thus

$$K_{eq} = \frac{X_{Fe}^{grt}}{X_{Mg}^{grt}} \cdot \frac{X_{Mg}^{cpx}}{X_{Fe}^{cpx}} \cdot \frac{\gamma_{Fe}^{grt}}{\gamma_{Mg}^{grt}} \cdot \frac{\gamma_{Mg}^{cpx}}{\gamma_{Fe}^{cpx}} = K_D \cdot K_\gamma$$

Temperatures have been estimated using six different quantitative calibrations of the garnet-clinopyroxene system revealing garnet-clinopyroxene Fe^{2+}-Mg exchange geothermometers of Ellis & Green (1979), Powel (1985), Krogh (1988), Pattison & Newton (1989), Ai (1994) and Krogh Ravna (2000).

Ellis & Green (1979) determined the distribution coefficient as a function of P, T and Ca-content in garnet (X_{Ca}^{grt}) and derived the empirical relation:

$$T_{EG-79}(^\circ C) = \frac{3104 \cdot X_{Ca}^{grt} + 3030 + 10.86 \cdot P(kb)}{\ln K_D + 1.9034} - 273$$

where X_{Ca}^{grt} is defined as

$$X_{Ca}^{grt} = \frac{Ca}{Ca + Mg + Fe^{2+}}$$

They have shown that K_D is apparently independent of the Mg/(Mg + Fe^{2+}) content in clinopyroxene and garnet, but that there is a marked dependence of K_D upon the Ca-content of garnet. This Ca-effect is believed to be caused by a combination of non-ideal Ca-Mg substitutions in garnet and clinopyroxene. Consequently, a rectilinear correction for X_{Ca}^{grt} in garnet was proposed.

Powell (1985) made an upgrade to Ellis & Green (1979) geothermometer defining:

$$T_{P-85}(^\circ C) = \frac{2790 + 10 \cdot P(kb) + 3140 \cdot X_{Ca}^{grt}}{\ln K_D + 1.735} - 273$$

which gives slightly lower temperatures than calibration of Ellis & Green (1979).

Krogh (1988) suggested a curvilinear relationship between $\ln K_D$ and X_{Ca}^{grt} in garnet:

$$T_{K-88}(^\circ C) =$$

$$= \frac{1879 + 6731 \cdot X_{Ca}^{grt} - 6173 \cdot (X_{Ca}^{grt})^2 + 100 \cdot P(GPa)}{\ln K_D + 1.393} - 273$$

at least for the compositional range X_{Ca}^{grt} = 0.10–0.50. The Ca-content in garnet was calculated as:

$$X_{Ca}^{grt} = \frac{Ca}{Ca + Mn + Fe^{2+} + Mg}$$

Calculated temperatures do not vary with the Mg/(Mg + Fe^{2+}) content in garnet and Na-content in the clinopyroxene. Temperatures below 900°C are a bit lower than those obtained by the method

of Powell (1985), and the difference is larger for lower temperatures and lower values of X_{Ca}^{grt}.

Pattison & Newton (1989) performed multiple regression of a large set of data on the Fe^{2+}-Mg equilibrium between garnet and clinopyroxene resulting in the following relationship:

$$T_{PN-89}(^{\circ}C) =$$

$$= \frac{561 + 3395 \cdot X_{Ca}^{grt} - 2388 \cdot (X_{Ca}^{grt})^2 + 9781 \cdot X_{Mg}^{grt} - 31026 \cdot (X_{Mg}^{grt})^2}{\ln K_D + 0.512} +$$

$$+ \frac{26217 \cdot (X_{Mg}^{grt})^3 + 103.7 \cdot P(GPa)}{\ln K_D + 0.512} - 273$$

which includes the curvilinear corrections for X_{Ca}^{grt} and also for Mg-number ($Mg_{\#}$) in garnet:

$$Mg_{\#} = 100 \cdot X_{Mg}^{grt} = 100 \cdot \frac{Mg}{Mg + Fe^{2+}}$$

This thermometer works well with experimental data of Pattison & Newton (1989) but commonly yields unrealistically low temperatures for natural rocks. An important feature discovered by Pattison & Newton (1989) and later supported by other researchers (e.g. Ai, 1994; Berman et al., 1995) is that K_D decreases with decreasing X_{Mg}^{grt} at all temperatures.

Ai (1994) investigated about 300 garnet-clinopyroxene pairs and by multiple regression arrived to the expression:

$$T_{A-94}(^{\circ}C) =$$

$$= \frac{1987 + 3648.55 \cdot X_{Ca}^{grt} - 1629 \cdot (X_{Ca}^{grt})^2 - 659 \cdot X_{Mg}^{grt}}{\ln K_D + 1.076} +$$

$$+ \frac{176.6 \cdot P(GPa)}{\ln K_D + 1.076} - 273$$

with curvilinear correction for X_{Ca}^{grt} and rectilinear correction for X_{Mg}^{grt} in garnet. Ai's thermometer is suitable especially for the systems with low-Ca and high-Mg garnets.

In addition to significant dependence between the distribution coefficient K_D and X_{Ca}^{grt} and X_{Mg}^{grt}, Krogh Ravna (2000) incorporated the effect of Mn-content in garnet X_{Mn}^{grt}:

$$X_{Mn}^{grt} = \frac{Mn}{Ca + Mn + Fe^{2+} + Mg}$$

and proposed the following P-T-compositional relationship:

$$T_{KR-00}(^{\circ}C) =$$

$$= \frac{1939 + 3270 \cdot X_{Ca}^{grt} - 1396 \cdot (X_{Ca}^{grt})^2 + 3319 \cdot X_{Mn}^{grt} - 3535 \cdot (X_{Mn}^{grt})^2}{\ln K_D + 1.223} +$$

$$+ \frac{1105 \cdot X_{Mg}^{grt} - 3561 \cdot (X_{Mg}^{grt})^2 + 2324 \cdot (X_{Mg}^{grt})^3 + 169.4 \cdot P(GPa)}{\ln K_D + 1.223} - 273$$

which confirmed his conclusion from 1988 that the Fe^{2+}-Mg equilibrium between co-existing garnet and clinopyroxene is independent of the variations in the Na-content of the clinopyroxene, at least in the X_{Na}^{cpx} range from 0 to 0.51. This means that the jadeite content in clinopyroxene has a certain influence on calculated temperatures only at higher X_{Na}^{cpx} values. Since the natural jadeite content of eclogites is commonly lower than the recommended value, Na is not a problematic additional component in the garnet-clinopyroxene exchange thermometer for eclogites. Application of this thermometer gives reasonable results for most compositional ranges covered by garnet-clinopyroxene pairs from natural rocks.

The uncertainty of the garnet-clinopyroxene geothermometer is usually estimated to ±30 to 50 °C and in most cases almost all of the above-mentioned geothermometers, give temperatures within this interval. However, there is one important drawback that should always be considered when using Fe^{2+}-Mg exchange geothermometers. The problem is that generally the data is only available for total iron content (Fe^{tot}), therefore it is not known how much garnet and clinopyroxene iron is present in the exchanging ferrous (Fe^{2+}) and non-exchanging ferric (Fe^{3+}) states. There are several methods to calculate the Fe^{3+}/Fe^{2+} ratio in garnet and clinopyroxene (charge balance criteria, equalizing the amount of Fe^{3+} with the Na excess over (Al^{tot}+Cr), standard titration method, etc.) but they are unfortunately very sensitive to analytical errors and not always reliable.

Garnets are less of a problem than clinopyroxenes because of their customary higher Fe^{tot} contents and much lower Fe^{3+}/Fe^{2+} ratios (Carswell et al., 1997). In Fe-rich garnets all iron can be treated as ferrous without affecting the calculated temperatures significantly. But in Fe-poor garnets the underestimation of Fe^{3+} will result in higher K_D value, and consequently, in underestimated temperatures (Krogh Ravna, 2000). In common eclogites the Fe^{3+}/Fe^{tot} ratio is reported to be low, in the range of 0.0–0.06 (Carswell et al., 2000; Schmid et al., 2003) and can be therefore calculated by using stoichiometric charge balance.

Clinopyroxenes are more problematic, especially because they tend to be non-stoichiometric under HP/UHP conditions due to the presence of the Ca-Eskola molecule. The most problematic are Fe-poor clinopyroxenes which show a large spread in calculated Fe^{3+}/Fe^{tot} ratios. The charge balance calculations are unsuitable in this case. The published Fe^{3+}/Fe^{tot} ratios from omphacites vary between 0.0 and 0.5 (Carswell et al., 1997) and were proven by Mössbauer studies (Carswell et al., 2000) and micro-XANES (Schmid et al., 2003).

For eclogitic rocks from Pohorje, the Fe^{3+}/Fe^{tot} ratio directly determined by Mössbauer spectroscopy is reported to vary between 0.15 to 0.41 in omphacite, with a mean of 0.30, and tends to be low and constant in garnets, with the value of 0.02–0.03 (Koch, 1999).

Geobarometry based on garnet-clinopyroxene-phengite-kyanite-quartz/coesite assemblage

Reliable geobarometers applicable to HP and UHP metamorphic rocks are rather scarce. In eclogites containing an assemblage of garnet +

clinopyroxene + phengite ± kyanite ± quartz/coesite, an equilibrium between these phases may be used for thermobarometric estimations. Such geobarometer is based on net-transfer reactions representing a balanced reactions among phases (or components of phases) in which progress of the reactions result in a change in the modal amounts of the phases. This means that net-transfer reactions cause the production and consumption of phases and therefore result in large volume changes making the equilibrium constants pressure sensitive.

Possible net-transfer reactions defining this equilibrium are given as follows (Krogh Ravna & Terry, 2001; Krogh Ravna & Paquin, 2003):

[phe]: 3 *diopside* + 2 *kyanite* → 1 *grossular* + 1 *pyrope* + 2 *coesite/quartz*

[di, grs]: 1 *pyrope* + 3 *muscovite* + 4 *coesite/quartz* → 3 *Al-celadonite* + 4 *kyanite*

[prp]: 3 *muscovite* + 3 *diopside* + 2 *coesite/quartz* → 3 *Al-celadonite* + 1 *grossular* + 2 *kyanite*

[SiO_2, ky]: 6 *diopside* + 3 *muscovite* → 2 *grossular* + 1 *pyrope* + 3 *celadonite*

These reactions define an invariant point in both the coesite and quartz stability field, depending on which SiO_2 polymorph is stable. Phases in square brackets are absent in the reactions.

For pressure calculations the calibrations of Waters & Martin (1996), Krogh Ravna & Terry (2001) and Krogh Ravna & Terry (2004) have been applied.

Waters & Martin (1996) calibrated geobarometer aplicable to HP and UHP eclogites with the garnet + clinopyroxene + phengite assemblage, using the reaction [SiO_2, ky] and thermodynamic data set of Holland & Powell (1990):

$$P_{WM-96}(kbar) = 28.5 + 0.02044 \cdot T - 0.003539 \cdot T \cdot \ln K$$

where lnK term is calculated as follows:

$$\ln K = 6 \ln a_{di} - \ln a_{prp} - 2 \ln a_{grs} + 3 \ln a_{invphe}$$

The phengite activity may be calculated from:

$$a_{invphe} = \frac{a_{ideal\,ms}}{a_{ideal\,cel}} = \frac{X_{Al\,M_1} \cdot X_{Al\,T_1}}{X_{Mg\,M_1} \cdot X_{Si\,T_1}}$$

with $X_{Al\,T_1} = 4 - Si$, $X_{Si\,T_1} = Si - 2$ and M_1 the octahedral cation sites. Activity model for diopside was taken from Holland (1990) and for garnet from Newton & Haselton (1981).

Krogh Ravna & Terry (2001, 2004) used all four above reactions and constructed geobarometric expressions for UHP (with coesite) and HP (with quartz) assemblages. The corresponding equilibrium constants are:

$$K^{[phe,coe/qtz]} = \frac{a_{prp}^{grt} \cdot a_{grs}^{grt} \cdot \left(a_{SiO_2}^{coe/qtz}\right)^2}{\left(a_{di}^{cpx}\right)^3 \cdot \left(a_{Al_2SiO_5}^{ky}\right)^2} \quad K^{[di,grs,coe/qtz]} = \frac{\left(a_{cel}^{phe}\right)^3 \cdot \left(a_{Al_2SiO_5}^{ky}\right)^4}{a_{prp}^{grt} \cdot \left(a_{ms}^{phe}\right)^3 \cdot \left(a_{SiO_2}^{coe/qtz}\right)^4}$$

$$K^{[prp,coe/qtz]} = \frac{a_{grs}^{grt} \cdot \left(a_{cel}^{phe}\right)^3 \cdot \left(a_{Al_2SiO_5}^{ky}\right)^2}{\left(a_{di}^{cpx}\right)^3 \cdot \left(a_{ms}^{phe}\right)^3 \cdot \left(a_{SiO_2}^{coe/qtz}\right)^2} \quad K^{[SiO_2,ky]} = \frac{a_{prp}^{grt} \cdot \left(a_{grs}^{grt}\right)^2 \cdot \left(a_{cel}^{phe}\right)^3}{\left(a_{di}^{cpx}\right)^6 \cdot \left(a_{ms}^{phe}\right)^3}$$

For the above reactions they formulated linearized barometric expressions, which are:

$$P_{KRT-04}^{[phe,qtz]}(GPa) = 7.235 - 0.000659 \cdot T + 0.001162 \cdot T \cdot \ln K^{[phe,qtz]}$$

$$P_{KRT-04}^{[phe,coe]}(GPa) = 11.422 - 0.001676 \cdot T + 0.002157 \cdot T \cdot \ln K^{[phe,coe]}$$

$$P_{KRT-04}^{[di,grs,qtz]}(GPa) = -2.624 + 0.005741 \cdot T + 0.0004549 \cdot T \cdot \ln K^{[di,grs,qtz]}$$

$$P_{KRT-04}^{[di,grs,coe]}(GPa) = -0.899 + 0.003929 \cdot T + 0.0002962 \cdot T \cdot \ln K^{[di,grs,coe]}$$

$$P_{KRT-04}^{[prp,qtz]}(GPa) = 0.355 + 0.003695 \cdot T + 0.0003059 \cdot T \cdot \ln K^{[prp,qtz]}$$

$$P_{KRT-04}^{[prp,coe]}(GPa) = 0.568 + 0.003345 \cdot T + 0.0002705 \cdot T \cdot \ln K^{[prp,coe]}$$

$$P_{KRT-04}^{[SiO_2,ky]}(GPa) = 1.801 + 0.002781 \cdot T + 0.0002425 \cdot T \cdot \ln K^{[SiO_2,ky]}$$

The intersection of "quartz absent" lines defines a single point within the coesite (UHP) stability field, and analogously, the intersection of "coesite absent" lines defines another single point within the quartz (HP) stability field (Figure 4). Therefore the intersection of any two of these sets of lines uniquely defines P and T for a single sample.

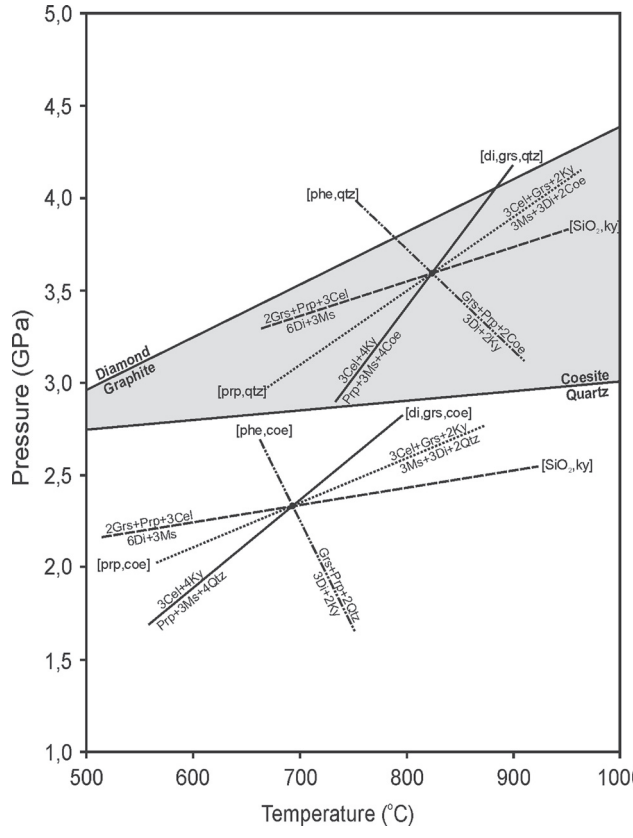

Figure 4. The intersection of reaction lines in the quartz and coesite stability fields (after Krogh Ravna & Terry, 2004). Phases in square brackets are absent in the reactions.

The content of ferric iron was calculated as:

$$Fe^{3+} = 2 - (Al + Cr + Ti)$$

The uncertainty limits for this thermobarometer are ±65°C and ±0.32 GPa. These geothermobarometric methods are supposedly less affected by subsequent thermal re-equilibration than common cation exchange thermometers, and the methods

also diminish the problems related to estimation of Fe^{3+} in omphacite (Krogh Ravna & Paquin, 2003). Activity models for phengite, clinopyroxene and garnet were taken from Holland & Powell (1998), Holland (1990) and Ganguly et al. (1996), respectively.

For calculating peak metamorphic conditions for a specific eclogite sample, garnet with maximum $a_{py}^{grt} \cdot \left(a_{grs}^{grt}\right)^2$, omphacite with minimum a_{di}^{cpx} (and thus maximum jadeite content) and phengite with maximum a_{cel}^{phe} (maximum Si content) are required. Analyses of phases used for geothermobarometryare given in Table 1.

matrix often accompanied with elongated grains of blue kyanite.

The eclogites consist of garnet, omphacite, kyanite, and zoisite as major primary mineral phases. In some samples crystals of phengitic mica, quartz (after coesite?), rutile and rarely zircon are also present. Among the secondary mineral phases are mainly amphibole, diopside, plagioclase, biotite, sapphirine, corundum and spinel. They occur in the coronas, symplectites and fractures of the primary minerals. Secondary minerals developed after peak metamorphic conditions and are related to the exhumation of these rocks.

Table 1. Representative microprobe analyses of mineral compositions used for thermobarometry.

Sample	JV103a	NO1/04A	PO6h	SP1/08	JV103a	NO1/04A	PO6h	SP1/08	JV103a	NO1/04A	PO6h	SP1/08
Mineral	Grt	Grt	Grt	Grt	Cpx	Cpx	Cpx	Cpx	Phe	Phe	Phe	Phe
SiO_2	40.99	40.80	40.83	40.35	55.02	5.5	55.28	54.92	53.36	51.53	51.00	52.66
TiO_2	0.01	0.02	0.02	0.00	0.11	0.12	0.14	0.10	0.02	0.00	0.74	0.02
Al_2O_3	23.16	22.99	23.06	22.58	8.34	8.03	8.04	7.95	26.87	26.84	27.59	27.05
Cr_2O_3	0.00	0.14	0.04	0.27	0.02	0.19	0.18	0.06	0.30	0.37	0.08	0.05
FeO	15.77	13.92	13.91	14.88	2.55	2.45	2.48	2.28	1.48	1.71	1.03	1.20
MnO	0.38	0.26	0.28	0.34	0.02	0.02	0.00	0.06	0.00	0.01	0.00	0.00
MgO	13.37	15.02	14.22	12.91	12.30	12.43	12.71	12.08	3.62	4.00	4.22	3.90
CaO	7.81	7.42	7.76	7.60	18.19	18.83	18.80	18.22	0.11	0.08	0.00	0.16
Na_2O	0.01	0.02	0.00	0.03	3.73	3.69	3.75	3.75	0.06	0.08	0.32	0.06
K_2O	nd	nd	nd	nd	bd	bd	bd	bd	9.11	10.06	10.46	9.50
Total	101.50	100.59	100.12	98.97	100.28	100.81	101.38	99.42	94.93	94.68	95.44	94.60
Si	2.978	2.960	2.984	3.005	1.958	1.954	1.949	1.970	3.510	3.431	3.377	3.482
Ti	0.001	0.001	0.001	0.000	0.003	0.003	0.004	0.003	0.001	0.000	0.037	0.001
Al	1.983	1.966	1.987	1.983	0.350	0.336	0.334	0.336	2.083	2.107	2.154	2.108
Cr	0.000	0.008	0.002	0.016	0.001	0.005	0.005	0.002	0.016	0.019	0.004	0.003
Fe^{3+}	0.061	0.106	0.039	0.000	0.000	0.000	0.011	0.000	0.000	0.035	0.000	0.000
Fe^{2+}	0.897	0.739	0.811	0.931	0.076	0.073	0.062	0.068	0.081	0.060	0.057	0.066
Mn	0.023	0.016	0.017	0.021	0.001	0.001	0.000	0.002	0.000	0.001	0.000	0.000
Mg	1.447	1.624	1.549	1.433	0.652	0.657	0.668	0.646	0.355	0.397	0.416	0.385
Ca	0.608	0.577	0.608	0.607	0.694	0.716	0.710	0.700	0.008	0.006	0.000	0.011
Na	0.001	0.003	0.000	0.005	0.258	0.254	0.257	0.261	0.008	0.010	0.041	0.008
K	0.000	0.000	0.000	0.000	0.000	0.000	0.000	0.000	0.765	0.855	0.884	0.801
Total	7.999	8.000	7.998	8.001	3.993	3.999	4.000	3.988	6.827	6.921	6.970	6.866

Analyses (in wt%) of garnet (Grt), clinopyroxene (Cpx) and phengite (Phe). Garnet is normalized to 12, clinopyroxene to 6 and phengite to 11 oxygens. Abbreviations are as follows: bd - below detection; nd - not determined.

Results

Petrography and mineral chemistry

Eclogites from four localities in the Pohorje Mountains have been investigated (Figure 3). The dominant rock type is weakly retrograded eclogite, which occurrs in bands, lenses and boudins within the surrounding continental crustal rocks (orthogneisses, paragneisses and micaschists). In macroscopic scale, eclogites contain big distinctive grains of garnet surrounded by omphacite

Garnets form euhedral to subhedral crystals with size ranging from large porphyroblasts up to several mm in diameter, to very tiny inclusions of few microns, which are found within kyanite and omphacite crystals. Garnets are texturally uniform, unzoned (Figure 5a), and nearly homogeneous in composition, as major element zoning is absent in all observed grains. Garnets with 27–55 mol% of pyrope, 25–48 mol% of almandine and spessartine, and 18–27 mol% of grossular and andradite content belong to the almandine-pyrope-grossular series with high pyrope content, as

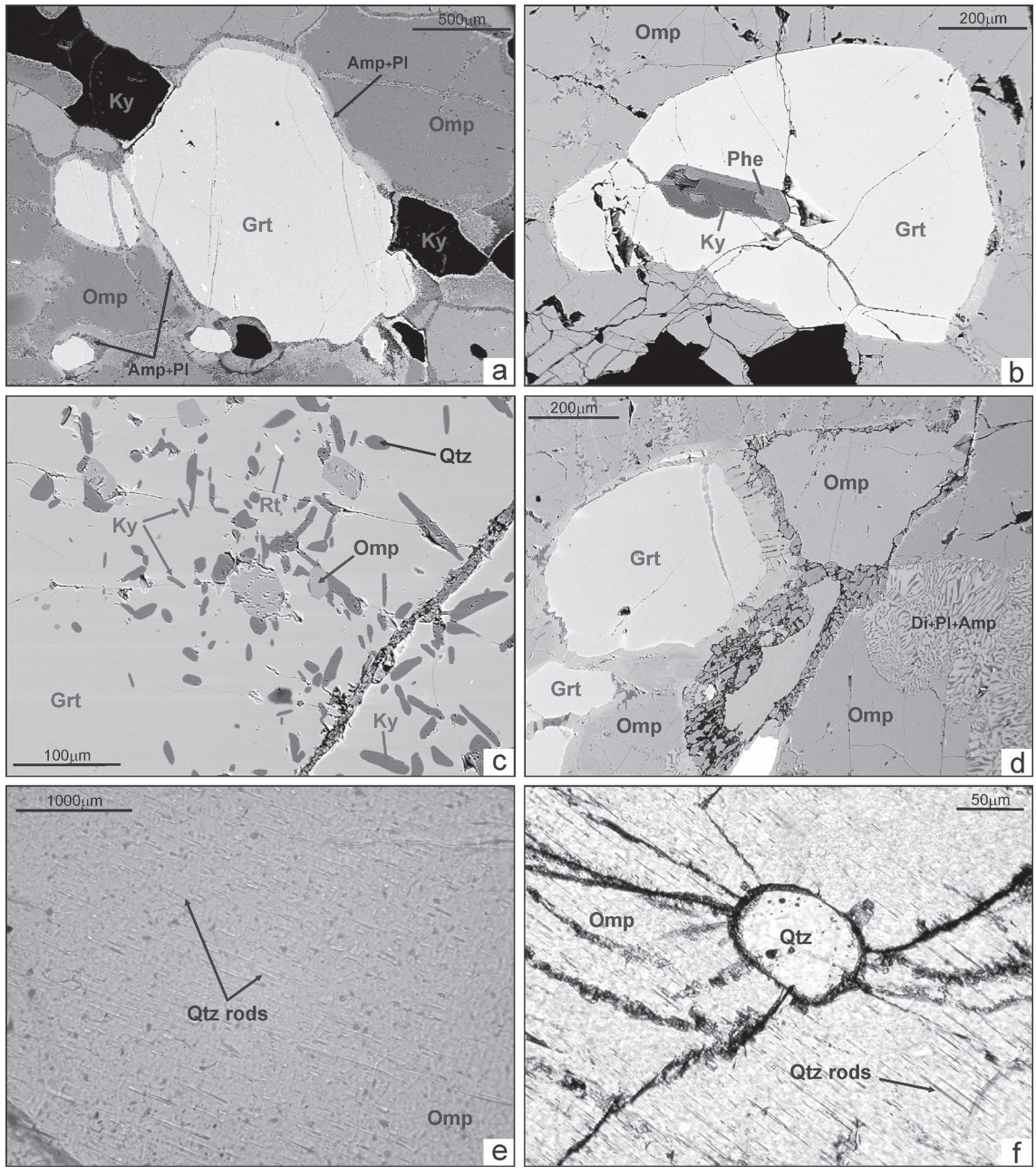

Figure 5. Primary and secondary mineral phases in eclogites.
(a) Photomicrograph – backscattered electron image (BSE) of unzoned homogenous garnet grains lacking any inclusions. Symplectitic rims of amphibole + plagioclase are replacing garnet rims in contact with omphacite.
(b, c) Typical inclusions in garnet belong to phengite, kyanite, omphacite, quartz and rutile (BSE).
(d) Homogenous omphacites are replaced by symplectites of diopside + plagioclase + amphibole.
(e) Quartz rods and needles in matrix omphacite shown in plane-polarized light. Quartz rods are distinctly oriented and parallel to omphacite c-axis.
(f) Omphacite with tiny quartz exolutions is hosting quartz inclusion surrounded by radial fractures (BSE). Abbreviations after KRETZ (1983).

it is common for UHP metamorphic rocks (CHOPIN, 1984). Inclusions in garnet are relatively rare; these are typically omphacite, rutile, kyanite, quartz and phengite (Figure 5b, c). Garnet rims are commonly resorbed by amphibole + plagioclase symplectite (Figure 5a).

Omphacite occurs in large anhedral grains in the matrix (Figure 5d) or as inclusions in garnet (Figure 5c) and kyanite. Similarly to garnets, omphacites also show uniform grains and almost homogenous composition for all major oxides. The jadeite component of omphacites, calculated from KATAYAMA et al. (2000):

$$Jd = Na - Fe^{3+} - 2 \cdot Ti$$

varies between 18–37 mol%. The total cation deficiency (omphacite cation totals are less than 4.00 per six oxygen atoms) and excess Al on the octahedral site suggest the existence of non-stoichiometric pyroxenes or pyroxenes with octahedral vacancies. Ca and Al combine and form the Ca-Eskola molecule (CaEs – $Ca_{0.5}\square_{0.5}AlSi_2O_6$; empty rectangle $\square$ represents a vacancy on the M2 site). The cation sum of natural clinopyroxenes, calculated on the basis of six oxygens, decreases progressively from the theoretical value of 4.00 as the

^{VI}Al content increases (Cawthorne & Collerson, 1974). The Ca-Eskola clinopyroxene, which is stable at peak metamorphic conditions, is highly unstable at lower pressure (Smyth, 1980). It rapidly breaks down to Ca-Tschermak component (CaTs – $CaAl_2SiO_6$) and quartz, following the retrograde reaction:

$$2 \cdot Ca_{0.5}\square_{0.5}AlSi_2O_6 \rightarrow CaAl_2SiO_6 + 3 \cdot SiO_2$$

which can be simplified to:

$$2 \cdot CaEs \rightarrow CaTs + 3 \cdot Qtz$$

The Ca-Tschermak component is assigned to be equivalent to the ^{IV}Al content (Katayama et al., 2000), and may be calculated from:

$$CaTs = 2 - Si = {}^{IV}Al$$

The decompressional breakdown of Ca-Eskola molecule results in the exsolution of tiny needles and rods of quartz that are the most striking feature of matrix omphacites from Pohorje eclogites (Figure 5e, f). They display an orientation parallel to the c-axis of omphacite. Microprobe analysis of quartz needles show essentially pure SiO_2. The amount of the Ca-Eskola component in omphacites from Pohorje samples, calculated from Katayama et al. (2000):

$$CaEs = {}^{TOT}Al - 2 \cdot {}^{IV}Al - K - (Na - Fe^{3+} - 2 \cdot Ti)$$

is reaching 5 mol%. Integral analysis of omphacite, together with SiO_2 precipitates, under defocused electron beam (25–30 μm) yields even higher values, up to 9 mol%. Omphacite is very sensitive to retrogression. During decompression, omphacitic clinopyroxene must reduce its jadeite content, which results in the production of plagioclase. The typical product of omphacite retrogression is the formation of symplectites of fine-grained diopside + plagioclase + amphibole (Figure 5d).

Phengite occurs sporadically in the matrix (Figure 6a) and as minor inclusions in garnet (Figure 5b) and omphacite. Measured phengite grains were nearly homogenous in composition since the content of major cations is close to constant. Phengite belongs to white micas which result from solid solution between muscovite and celadonite and is formed by an inverse Tschermak substitution starting from muscovite. The amount of celadonite component present is evident from the Si content of phengite, which rapidly increases with

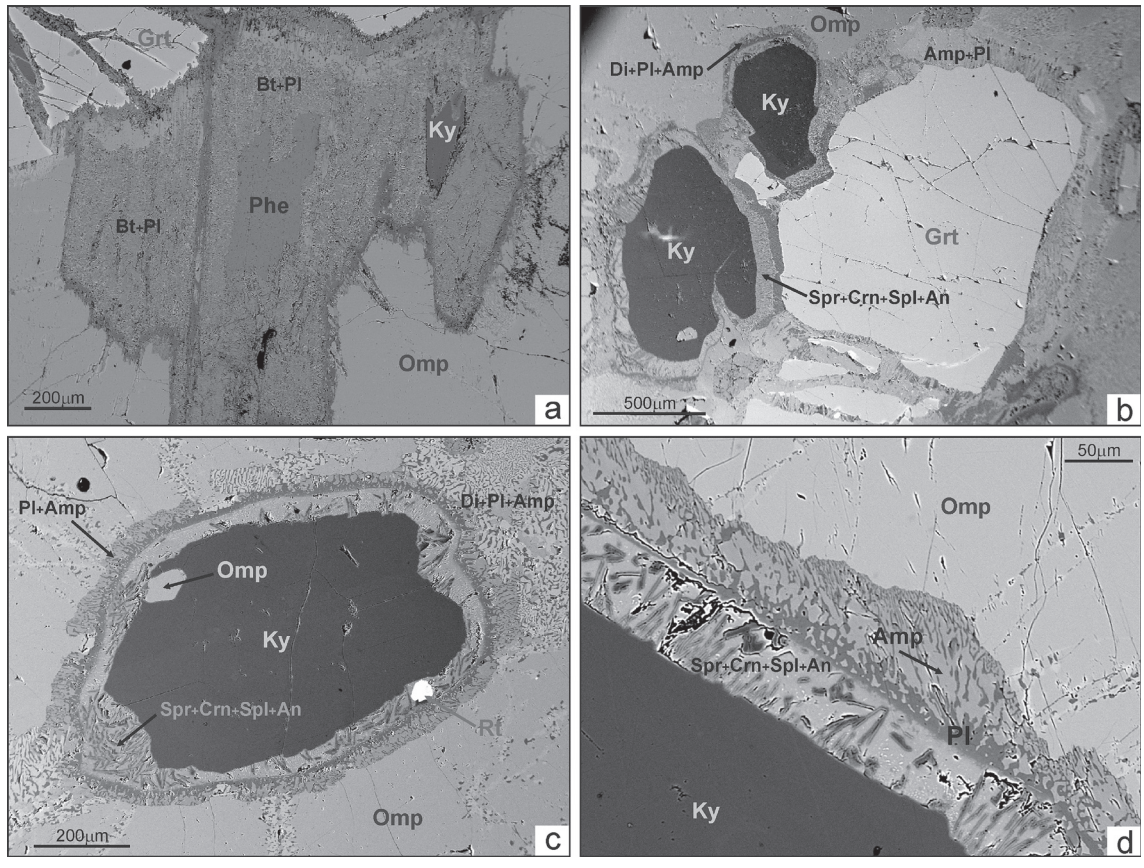

Figure 6. Primary and secondary mineral phases in eclogites (photomicrographs – backscattered electron images).
(a) Preserved remnant of phengite with clearly visible cleavage is surrounded by symplectitic intergrowth of biotite and plagioclase.
(b) Dark-gray kyanite grains in comparison with garnet and omphacite. All minerals shown are surrounded by symplectites of secondary mineral phases. The most typical are amphibole + plagioclase after garnet, diopside + plagioclase + amphibole after omphacite and sapphirine + corundum + spinel + anorthite after kyanite.
(c) Kyanite with omphacite inclusion is surrounded by coronas of secondary minerals. Two distinct symplectitic belts are present. Inner corona, next to kyanite, consists of sapphirine + corundum + spinel + anorthite. Outer corona, next to omphacite, is made of plagioclase + amphibole ± diopside.
(d) Detail of kyanite corona in which separate symplectitic constituents are clearly visible. Abbreviations after Kretz (1983).

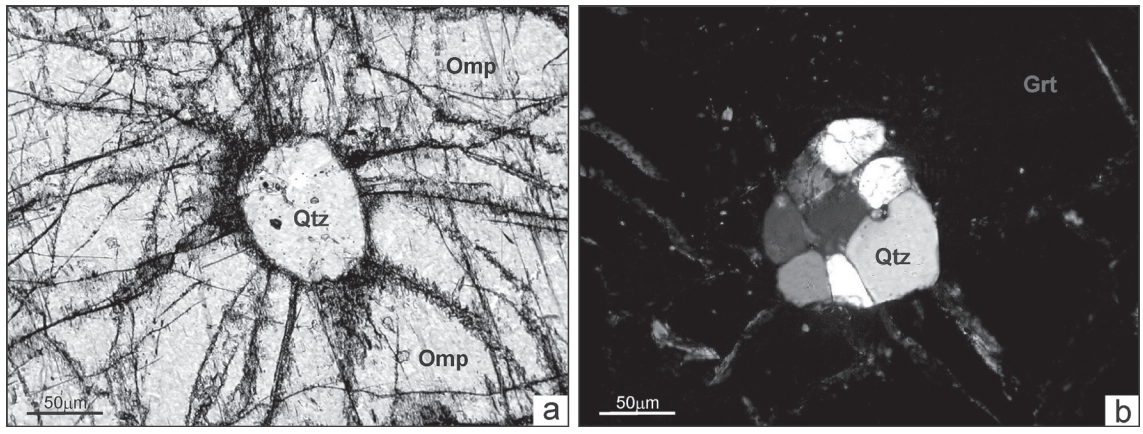

Figure 7. Quartz (former coesite?) inclusions in eclogites.
(a) Radial fractures surrounding quartz inclusion in omphacite under plane-polarized light.
(b) Polycrystalline polygonal quartz inclusion (PPQ) surrounded by tiny radial fractures within garnet host under crossed polars.
Abbreviations after KRETZ (1983).

increasing pressure (HERMANN, 2002). The strong variation of phengite composition as a function of pressure makes phengite a crucial mineral component for determination of UHP metamorphism (MASSONE & SZPURZKA, 1997). Investigated phengite grains from Pohorje eclogites contain up to 3.5 Si per formula unit (pfu). The biotite + plagioclase intergrowths are typical replacements of phengite (Figure 6a).

Kyanite forms frequently twinned subhedral grains (Figure 6b) and small rod-like inclusions within garnet (Figure 5c) and omphacite minerals. Rare inclusions found in kyanite belong to garnet, omphacite (Figure 6c) and quartz. Microprobe analysis of all measured kyanite grains revealed almost pure Al_2SiO_5. Retrogression of kyanite is expressed by development of complex coronas consisting of sapphirine + corundum + spinel + anorthite (Figure 6b, c, d). The width of the corona is progressively increasing with the increasing degree of retrogression. Spinel belongs to Fe-Mg spinels. Sapphirines contain up to 1.4 Si pfu and are clearly peraluminous. Growth of corundum and tiny lamellar grains of sapphirine is restricted only to domains formerly occupied by kyanite.

Zoisite mainly forms individual elongated grains but may also be found as minor inclusions in garnet and omphacite. It contains rare inclusions of rutile.

Quartz inclusions are present in garnet (Figure 5c), omphacite (Figure 5f, 7a) and kyanite. They are frequently surrounded by radial fractures (Figure 7a) which may imply the possibility for the existence of former coesite. Some of the quartz inclusions surrounded by radial fractures, are aggregates of several polycrystalline quartz grains (Figure 7b). They strongly resemble the PPQ (polycrystalline polygonal quartz) and MPQ (multicrystalline polygonal quartz) textures described by WAIN et al. (2000). Those quartz inclusions are interpreted as possible pseudomorphs after coesite.

Table 2. Calculated temperatures and pressures.

	Temperature (°C)								
Sample	EG-79	P-85	K-88	PN-89	A-94	KR-00	Minimum	Maximum	Average
JV103a	843	822	802	573	741	748	741	843	791
NO1/04A	921	903	888	777	817	820	817	921	870
PO6h	824	803	781	588	710	717	710	824	767
SP1/08	801	779	755	516	694	702	694	801	746
	Temperatures calculated at 3 GPa.								

Geothermometers: EG-79: ELLIS & GREEN (1979), P-85: POWEL (1985), K-88: KROGH (1988), PN-89: PATTISON & NEWTON (1989), A-94: AI (1994), KR-00: KROGH RAVNA (2000). PN-89 calibration is excluded from minimum and average temperature calculations.

	Pressure (GPa)							
Sample	KRT-04$^{[phe, qtz]}$	KRT-04$^{[di, grs, qtz]}$	KRT-04$^{[prp, qtz]}$	KRT-04$^{[SiO2, ky]}$	WM-96	Minimum	Maximum	Average
JV103a	2.9	3.2	3.1	3.1	3.0	2.9	3.2	3.1
NO1/04A	2.9	3.2	3.1	3.1	2.9	2.9	3.2	3.1
PO6h	2.9	3.2	3.1	3.1	2.8	2.8	3.2	3.0
SP1/08	2.9	3.2	3.1	3.1	3.0	2.9	3.2	3.1
	Pressures calculated at 800 °C.							

Geobarometers: WM-96: WATERS & MARTIN (1996), KRT-04: KROGH RAVNA & TERRY (2001, 2004).

Geothermobarometry

Calculated temperatures from different calibrations of the garnet-clinopyroxene system (Ellis & Green, 1979; Powell, 1985; Krogh, 1988; Pattison & Newton, 1989; Ai, 1994; Krogh Ravna, 2000) differ substantially (Table 2, Figure 8). The unrealistically low temperatures were obtained by Pattison & Newton's (1989) geothermometer, while the highest temperatures were calculated from the calibration of Ellis & Green (1979). Powel (1985) and Krogh (1988) calibrations give reasonable

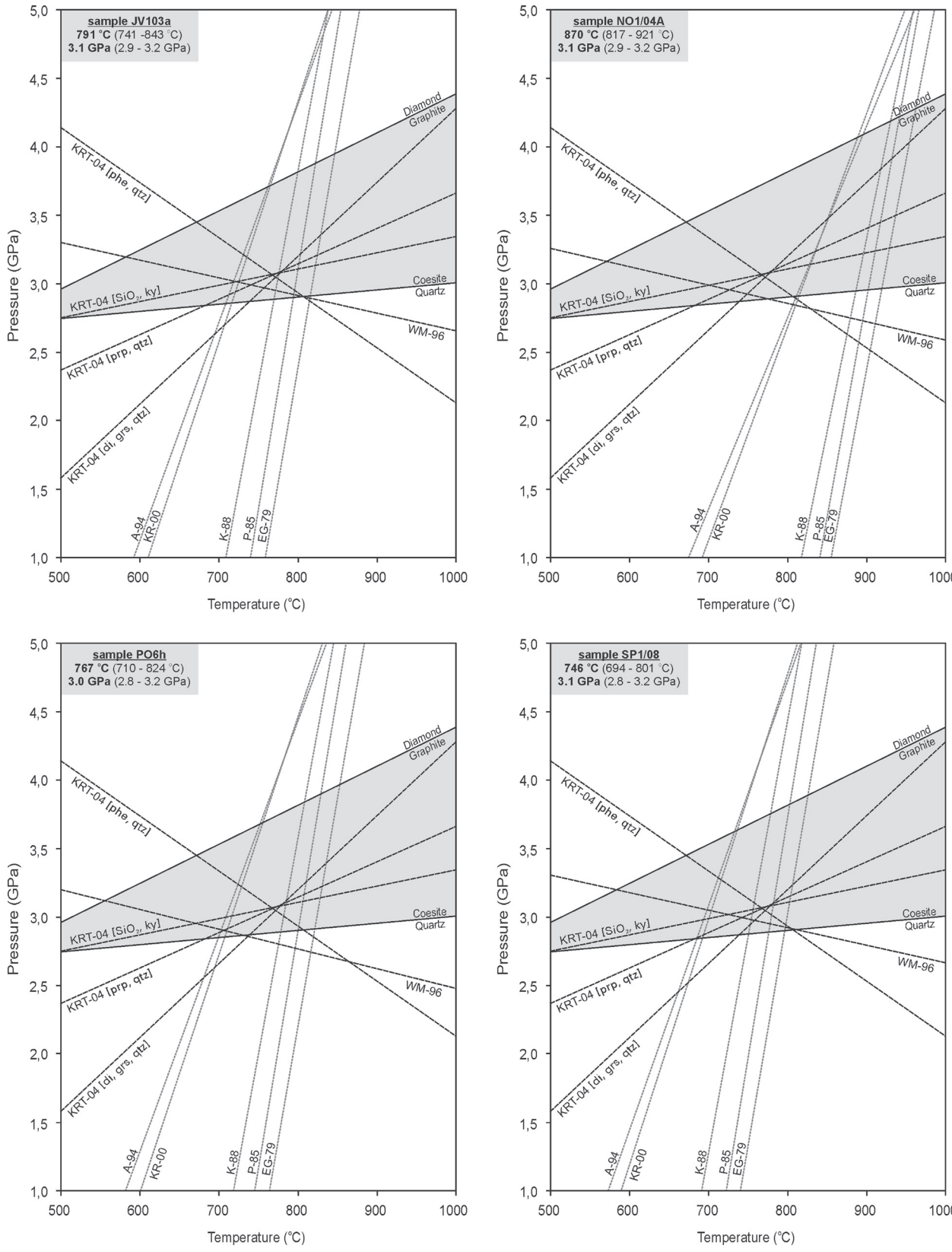

Figure 8. Comparison of geothermobarometric results calculated with different geothermometers and geobarometers. Geothermometers: EG-79: Ellis & Green (1979), P-85: Powel (1985), K-88: Krogh (1988), A-94: Ai (1994), KR-00: Krogh Ravna (2000). Geobarometers: WM-96: Waters & Martin (1996), KRT-04: Krogh Ravna & Terry (2001, 2004). Abbreviations after Kretz (1983).

results but obtained temperatures are still very high. The most reliable are temperatures obtained by geothermometers of Ai (1994) and Krogh Ravna (2000). With the exception of Pattison & Newton's (1989) calibration which obviously underestimates peak temperature conditions in mafic and ultramafic lithologies, the temperature intervals calculated at 3.0 GPa pressure range from 741 to 843 °C for JV103a sample, from 817 to 921 °C for NO1/04A sample, from 710 to 824 °C for PO6h sample, and from 694 to 801 °C for SP1/08 sample. Average peak temperatures obtained are 791 °C (JV103a sample), 870 °C (NO1/04A sample), 767 °C (PO6h sample), and 746 °C (SP1/08 sample).

Peak pressure estimations of Waters & Martin (1996) and Krogh Ravna & Terry (2001, 2004) calibrations yielded consistent results (Table 2, Figure 8). The intersections between these two geobarometers and the geothermometers of Ai (1994) and Krogh Ravna (2000) define average peak pressures of 3.0 GPa for PO6h sample and 3.1 GPa for JV103a, NO1/04A and SP1/08 samples, calculated at 800 °C. Excellent fitting is obtained mostly between Waters & Martin (1996) geothermobarometer, the pyrope absent reaction with coesite and the SiO_2-kyanite absent reaction from Krogh Ravna & Terry (2001, 2004) calibration system.

The combination of garnet-clinopyroxene Fe^{2+}-Mg exchange geothermometer (Krogh Ravna, 2000) with the geobarometric calibrations based on the net-transfer reactions in the garnet-clinopyroxene-phengite-kyanite-quartz/coesite system (Krogh Ravna & Terry, 2004), resulted in similar but more precise estimations of peak metamorphic conditions. The intersections between the used geothermometer and geobarometers define optimized maximum pressure of 3.0 GPa for samples JV103a, PO6h and SP1/08 at temperature range from 750 to 782 °C; and pressure of 3.1 GPa at temperature 783 °C for NO1/04A sample (Figure 9).

All estimated peak pressure and temperature values consistently plot above the quartz-coesite transformation curve and thus correspond well to the ultrahigh-pressure stability field of coesite (Figure 8, 9). The quartz-coesite and graphite-diamond transformation boundaries were calculated from thermodynamic data of Holland & Powell (1998).

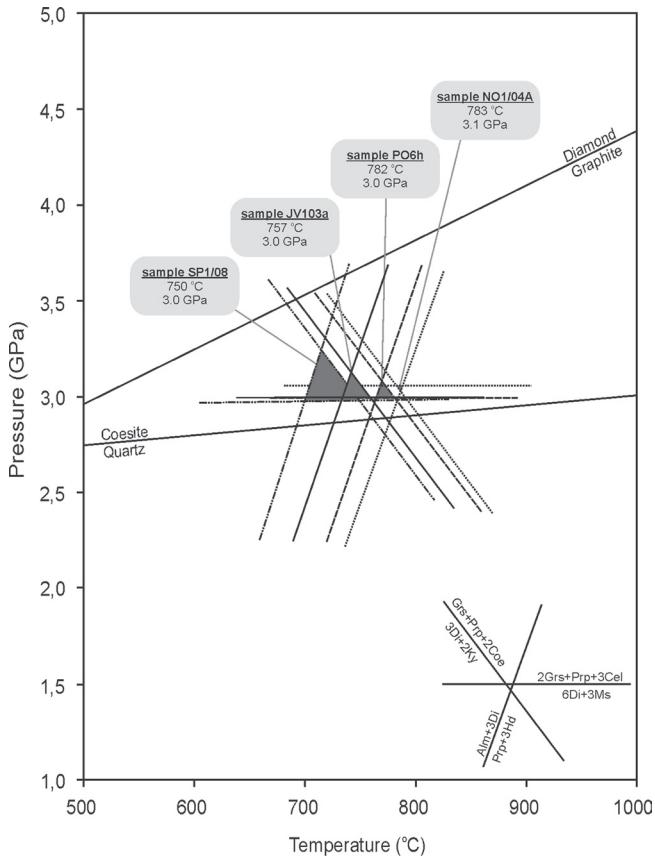

Figure 9. Results from geothermobarometry. Combination of garnet + omphacite + phengite + kyanite + quartz/coesite assemblage (Krogh Ravna & Terry, 2004) with garnet-clinopyroxene Fe^{2+}-Mg exchange thermometer (Krogh Ravna, 2000). The quartz-coesite and graphite-diamond curves are calculated from thermodynamic data of Holland & Powell (1998). Abbreviations after Kretz (1983).

Discussion

UHP metamorphism in eclogites from Pohorje is evident both from microtextural observations and from the results of geothermobarometric calculations of peak metamorphic conditions, which revealed very high pressures and temperatures of 3.0–3.1 GPa and 750–783 °C. These values correspond well to the coesite, i.e. ultrahigh-pressure, stability field. Pressures calculated in this work are much higher than the former estimates of 1.8 GPa by Hinterlechner-Ravnik et al. (1991) or 1.5 GPa by Koch (1999).

Remnants of coesite, a direct mineral indicator of UHP conditions, were not found but its existence is clearly revealed from: (1) radial fractures around quartz inclusions within robust host minerals (garnet, kyanite and omphacite) that were caused by expansion ensuing the transformation of high-pressure coesite to its low-pressure polymorph; and (2) polycrystalline appearance of these inclusions interpreted as a pseudomorphs after former coesite due to their distinctive PPQ and MPQ microtextures (Wain et al., 2000).

Radial fractures around quartz inclusions may imply the possibility for the existence of former coesite and are therefore an indicator of possible UHP conditions. The roughly 10% of volume increase in coesite-quartz transformation process produces considerable overpressure (more than three times the lithostatic pressure), which buffers the inclusion at the coesite-quartz transformation boundary (Gillet et al., 1984).

The multistage transformation of coesite to strain-free quartz was described from experimental studies (Mosenfelder & Bohlen, 1997) and also observed in UHP rocks from many well-established UHP localities (e.g. Wain et al., 2000). Transformation begins with the growth of quartz on the coesite-host contact, which is followed by the development of shear cracks with no open volume (Hirth & Tullis, 1994), providing new sites for quartz growth. With progressing transformation, quartz rim around coesite inclusion succes-

sively changes from textureless to fibrous radial texture and to more irregular, feather-like texture. In the final stage of transformation, quartz inclusions exhibit typical radial palisade texture; if any relic coesite is present, palisades of quartz radiate from it. When absolutely no coesite is preserved, its former existence may be deduced from the three different sequential textural types of quartz inclusions: PRQ, PPQ and MPQ (Wain et al., 2000). Polycrystalline radial-texture quartz (PRQ) inclusions develop prior to radial fracturing in the host mineral and result from stress release. They consist of individual strain-free palisades, which often radiate from a core zone. The core zone is made of quartz which has irregular mosaic texture, sutured boundaries and undulatory extinction. Polycrystalline quartz inclusions with mosaic texture and sutured contacts containing 30–100 grains also belong to the PRQ group. With proceeding recovery, the number of grains per inclusion is continuously reduced. Polycrystalline polygonal quartz (PPQ) inclusions consist of 10–50 polygonal strain-free quartz grains. Their formation post-dates radial fracturing. The next step of recovery is represented by multicrystalline polygonal quartz (MPQ) inclusions with 2-10 monocrystalline quartz grains per inclusion. Eventually, the recovery is completed when the whole inclusion recrystallizes to a single unstrained monocrystalline quartz surrounded by radial fractures.

Additional evidence for UHP metamorphism is coming from the presence of highly pressure-sensitive non-stoichiometric supersilicic clinopyroxenes that directly indicate high pressure and temperature conditions (Gasparik & Lindsley, 1980; Fockenberg & Schreyer, 1997). They were reported as a typical constituent of eclogites from various UHP terranes (summarized by Bruno et al., 2002). Such clinopyroxenes containing Ca-Escola molecule in solid solution favourably form at high pressures exceeding 3 GPa (Schmädicke & Müller, 2000). Due to the pressure decrease quartz needles and rods form as an exsolution product from supersilicic clinopyroxene. They are oriented along the c-axis of omphacite and are resulting from the omphacitic clinopyroxene that contained excess silica at peak metamorphic conditions (Zhang & Liou, 2000). The occurrence of oriented quartz needles and rods in matrix omphacites is typical feature of many UHP eclogites (e.g. Liou et al., 1998). The eclogites from Pohorje show both, direct and indirect, evidence for pyroxene containing the Ca-Eskola component: the presence of clinopyroxene with Ca-Eskola molecule in solid solution, and quartz rods and needles as an exolution product.

The survival of coesite relics depends on many factors, like the presence of sufficiently rigid host mineral, the extent of metamorphic re-equilibration of a mineral assemblage during exhumation, the trend of exhumation P-T path, the rate of exhumation, the presence of fluid phase on the reactant side of retrograde reactions (e.g. Mosenfelder & Bohlen, 1997; Hermann, 2002). Continental crustal rocks entering the UHP realm are not completely dry, as one would expect. The majority of UHP assemblages contains hydrous minerals, like phengitic mica and epidote, that are stable under UHP conditions and may evolve small amounts of fluids by dehydration reactions (Chopin, 2003). Therefore, UHP parageneses may only be preserved if the entire exhumation path is situated within the stability field of phengite. This can happen either when continuous cooling is accompanying exhumation or when the entire exhumation process occurred at T<700°C (Hermann, 2002). In contrast, in terranes that show isothermal decompression, breakdown of phengite and concomitant partial melting may cause a complete recrystallization of the subducted crustal rocks during exhumation, and thus destruction of all UHP mineral assemblages.

Granulite facies metamorphism is usually required for sapphirine formation (Ackermand et al., 1975). Composition of sapphirines from Pohorje eclogites is clearly peraluminous and is significantly different from the composition of sapphirines that are stable within granulite facies conditions (Higgins et al., 1979). Furthermore, the formation of sapphirine is very dependent on H_2O activity, and for this reason is by itself not an indication that typical granulite facies conditions were reached (Simon & Chopin, 2001). Therefore it is proposed that sapphirine in Pohorje eclogites formed during decompression at lower-temperature conditions than those common for granulite-facies. Presence of sapphirine in coronas around kyanite in eclogites from Pohorje clearly indicates that during the early stages of decompression high temperature conditions persisted. Due to this near-isothermal decompression, fracturing and introduction of fluids was possible already at high temperatures. Because the Pohorje eclogites crossed the transformation border between coesite and quartz at such high temperatures, there was no possibility for the survival of coesite.

The only known UHP metamorphism of Alpine eclogites so far was documented in the Western Alps, e.g. Dora Maira Massif (Chopin, 1984), Zermatt-Saas Zone (Reinecke, 1991), and is of Tertiary age (Tilton et al., 1991; Rubatto et al., 1998). The determined P-T conditions of Eo-Alpine metamorphism in Pohorje are the highest reported within the Austroalpine units of the Eastern Alps. Thus, the Pohorje eclogites are the first evidence of UHP metamorphism in Eastern Alps, and also the first evidence that UHP metamorphic conditions were also reached during the Cretaceous orogeny.

Conclusions

Kyanite eclogites from Pohorje experienced UHP metamorphic conditions of 3.0–3.1 GPa at temperature range from 750 to 783 °C.

Radial fractures around polycrystalline quartz inclusions with microtextures diagnostic for recovery after coesite, together with oriented quartz exolutions in clinopyroxene, and omphacites with Ca-Eskola molecule are the microtextural evidence for UHP metamorphism.

During the first stages of exhumation, eclogites were exposed to near-isothermal decompression that lead to complete breakdown of coesite.

Pohorje eclogites record the highest pressure conditions of Eo-Alpine metamorphism in the Alps and thus provide the first evidence that UHP metamorphism in the Alps occurred already during the Cretaceous orogeny.

UHP eclogites from Pohorje represent the first occurrence of UHP metamorphic rocks within the Eastern Alps.

References

Ackermand, D., Seifert, F. & Schreyer, W. 1975: Instability of sapphirine at high pressures. Contrib. Mineral. Petrol. (Berlin) 50: 79–92.

Ai, Y. 1994: A revision of the garnet-clinopyroxene Fe^{2+}-Mg exchange geothermometer. Contrib. Mineral. Petrol. (Berlin) 115: 467–473.

Berman, R.G., Aranovich, L.Y. & Pattison, D.R.M. 1995: Reassessment of the garnet-clinopyroxene Fe-Mg exchange thermometer: II. Thermodynamic analysis. Contrib. Mineral. Petrol. (Berlin) 119: 30–42.

Bruno, M., Compagnoni, R., Hirajima, T. & Rubbo, M. 2002: Jadeite with Ca-Eskola molecule from an ultra-high pressure metagranodiorite, Dora-Maira Massif, Western Alps. Contrib. Mineral. Petrol. (Berlin) 142: 515–519.

Carswell, D.A., O'Brien, P.J., Wilson, R.N. & Zhai, M. 1997: Thermobarometry of phengite-bearing eclogites in the Dabie Mountains of central China. J. Metamorphic Geol. (Oxford) 15: 239–252.

Carswell, D.A., Wilson, R.N. & Zhai, M. 2000: Metamorphic evolution, mineral chemistry and thermobarometry of shists and ortogneisses hosting ultra-high pressure eclogites in the Dabie Shan of central China. Lithos (Amsterdam) 52: 121–155.

Cawthorne, W.G. & Collerson, K.D. 1974: The recalculation of pyroxene end-member parameters and the estimation of ferrous and ferric iron content from electron microprobe analyses. Am. Mineral. (Washington) 59: 1203–1208.

Chopin, C. 1984: Coesite and pure pyrope in high-grade blueschists of the Western Alps: a first record and some consequences. Contrib. Mineral. Petrol. (Berlin) 86: 107–118.

Chopin, C. 2003: Ultrahigh-pressure metamorphism: tracing continental crust into the mantle. Earth Planet. Sci. Lett. (Amsterdam) 212: 1–14.

Coleman, R.G. & Wang, X. 1995: Overview of the geology and tectonics of UHPM. In: Coleman, R.G. & Wang, X. (eds.): Ultrahigh-pressure metamorphism. Cambridge University Press (Cambridge): 1–32.

Dobrzhinetskaya, L.F., Schweinehage, R., Massone, H.J. & Green, H.W. 2002: Silica precipitates in omphacite from eclogite at Alpe Arami, Switzerland: evidence of deep subduction. J. Metamorphic Geol. (Oxford) 20: 481–492.

Ellis, D. & Green, D.H. 1979: An experimental study of the effect of Ca upon garnet-clinopyroxene Fe-Mg exchange equilibria. Contrib. Mineral. Petrol. (Berlin) 71: 13–22.

Ernst, W.G., Liou, J.G. & Coleman, R.G. 1995: Comparative petrotectonic study of five Eurasian ultrahigh-pressure metamorphic complexes. Int. Geol. Rev. (London) 37: 191–211.

Fockenberg, T. & Schreyer, W. 1997: Synthesis and chemistry of unusual excess-Si aluminous enstatite in the system MgO-Al_2O_3-SiO_2 (MAS). Eur. J. Mineral. (Stuttgart) 8: 1293–1299.

Ganguly, J., Cheng, W. & Tirone, M. 1996: Thermodynamics of aluminosilicate garnet solid solution: new experimental data, an optimized model, and thermometric applications. Contrib. Mineral. Petrol. (Berlin) 126: 137–151.

Gasparik, T. & Lindsley, D.H. 1980: Phase equilibria at high pressure of pyroxenes containing monovalent and trivalent ions. In: Prewitt, C.T. (ed.): Reviews in Mineralogy, 7. Mineral. Soc. Am. (Washington): 309–339.

Gillet, P., Ingrin, J. & Chopin, C. 1984: Coesite in subducted continental crust: P-T history deduced from an elastic model. Earth Planet. Sci. Lett. (Amsterdam) 70: 426–436.

Hermann, J. 2002: Experimental constraints on phase relations in subducted continental crust. Contrib. Mineral. Petrol. (Berlin) 143: 219–235.

Higgins, J.B., Ribbe, P.H. & Herd, R.H. 1979: Sapphirine I. Crustal chemical contributions. Contrib. Mineral. Petrol. (Berlin) 68: 349–356.

Hinterlechner-Ravnik, A. 1982: Pohorski eklogit. Geologija (Ljubljana) 25/2: 251–288.

Hinterlechner-Ravnik, A., Sassi, F.P. & Visona, D. 1991: The Austridic eclogites, metabasites and metaultrabasites from the Pohorje area (Eastern Alps, Yugoslavia): 1. The eclogites and related rocks. Rendiconti Fisiche Accademia Lincei (Milano) 2: 157–173.

Hirth, G. & Tullis, J. 1994: The brittle-plastic transition in experimentally deformed quartz aggregates. J. Geophys. Res. (Washington): 11731–11747.

Holland, T.J.B. & Powell, R. 1990: An enlargened and updated internally consistent thermodynamic dataset with uncertainties and correlations: The system K_2O-Na_2O-CaO-MgO-MnO-FeO-Fe_2O_3-Al_2O_3-TiO_2-SiO_2-C-H_2-O_2. J. Metamorphic Geol. (Oxford) 8: 89–124.

Holland, T.J.B. 1990: Activities of components in omphacitic solid solutions. An application of Landau theory of mixtures. Contrib. Mineral. Petrol. (Berlin) 105: 446–453.

Holland, T.J.B. & Powell, R. 1998: An internally consistent thermodynamic data set for phases of petrological interest. J. Metamorphic Geol. (Oxford) 16: 309–344.

Huang, S.L., Shen, P., Chu, H.T. & Yui, T.F. 2000: Nanometer-size α-PbO_2-type TiO_2 in garnet: A thermobarometer for ultrahigh-pressure metamorphism. Science, (Washington) 288: 321–324.

Janák, M., Froitzheim, N., Lupták, B., Vrabec, M. & Krogh Ravna, E.J. 2004: First evidence for ultrahigh-pressure metamorphism of eclogites in Pohorje, Slovenia: Tracing deep continental sub-

duction in the Eastern Alps. Tectonics (Washington) 23: TC5014, doi:10.1029/2004TC001641.

Katayama, I., Parkinson, C.D., Okamoto, K., Nakajima, Y. & Maruyama, S. 2000: Supersilicic clinopyroxene and silica exsolution in UHPM eclogite and pelitic gneiss from the Kokchetav massif, Kazakhstan. Am. Mineral. (Washington) 85: 1368–1374.

Koch, M. 1999: Metamorphe Entwicklung von Eklogiten des Pohorje-Gebirges, Slowenien: Diplomarbeit. Mineralogisches Institut Ruprecht-Karls-Universität Heidelberg (Heidelberg): 1–105.

Kretz, R. 1983: Symbols for rock-forming minerals. Am. Mineral. (Washington) 68: 277–279.

Krogh, E.J. 1988: The garnet-clinopyroxene Fe-Mg geothermometer – a reinterpretation of existing experimental data. Contrib. Mineral. Petrol. (Berlin) 99: 44–48.

Krogh Ravna, E.J. 2000: The garnet-clinopyroxene Fe^{2+}-Mg geothermometer: an updated calibration. J. Metamorphic Geol. (Oxford) 8: 211–219.

Krogh Ravna, E.J. & Terry, M.P. 2001: Geothermobarometry of phengite-kyanite-quartz/coesite eclogites. In: Eleventh Annual V. M. Goldschmidt Conference, Abstract 3145: cd-rom.

Krogh Ravna, E.J. & Paquin, J. 2003: Thermobarometric metodologies applicable to eclogites and garnet ultrabasites. In: Carswell, D.A. & Compagnoni, R. (eds.): Ultra-high pressure metamorphism. EMU Notes in Mineralogy, 5. Eötvös University Press (Budapest): 1–508 cd-rom.

Krogh Ravna, E.J. & Terry, M.P. 2004: Geothermobarometry of UHP and HP eclogites and schists – an evaluation of equilibria among garnet-clinopyroxene-kyanite-phengite-quartz/coesite. J. Metamorphic Geol. (Oxford) 22: 579–592.

Liou, J.G. 2000: Petrotectonic summary of less intensively studied UHP regions. In: Ernst, W. G. & Liou, J. G. (eds.): Ultrahigh-pressure metamorphism and geodynamics in collision-type orogenic belts. International Book Series 4. Geol. Soc. Am. (New York): 20–35.

Liou, J.G., Zhang, R. & Ernst, W.G. 1994: An introduction to ultrahigh-P metamorphism. The Island Arc (Carlton South) 3: 1–24.

Liou, J.G., Hang, W.G.E., Rumble, D. & Maruyama, S. 1998: High-pressure minerals from deeply subducted metamorphic rocks. In: Hemley, R.J. (ed.): Ultrahigh pressure mineralogy: Physics and chemistry of the Earth's deep interior. Reviews in Mineralogy, 37. Mineral. Soc. Am. (Washington): 33–96.

Massone, H.J. & Szpurzka, Z. 1997: Thermodynamic properties of white micas on the basis of high-pressure experiments in the system K_2O-MgO-Al_2O_3-SiO_2-H_2O and K_2O-FeO-Al_2O_3-SiO_2-H_2O. Lithos (Amsterdam) 41: 229–250.

Miller, C. 1990: Petrology of the type locality eclogites from the Koralpe and Saualpe (Eastern Alps), Austria. Schweiz. Mineral. Petrogr. Mitt. (Zürich) 70: 287–300.

Mioč, P. & Žnidarčič, M. 1977: Osnovna geološka karta SFRJ, list Slovenj Gradec, 1:100.000. Zvezni geološki zavod (Beograd).

Mosenfelder, J.L. & Bohlen, S.R. 1997: Kinetics of coesite to quartz transformation. Earth Planet. Sci. Lett. (Amsterdam) 153: 133–147.

Newton, R.C. & Haselton, H.T. 1981: Termodynamics of the garnet-plagioclase-$AlSiO_5$-quartz geobarometer. In: Newton, R.C., Navrotsky, A. & Wood, B.J. (eds.): Termodynamics of minerals and melts. Adv. Phys. Geochem., 1. Springer Verlag (Berlin), 131–147.

Okamoto, K. & Maruyama, S. 1999: The high pressure stability limits of lawsonite in the MORB + H_2O system. Am. Mineral. (Washington) 84: 362–273.

Pattison, D.R.M. & Newton, R.C. 1989: Reversed experimental calibration of the garnet-clinopyroxene Fe-Mg exchange thermometer. Contrib. Mineral. Petrol. (Berlin) 101: 87–103.

Powell, R. 1985: Regression diagnostics and robust regression in geothermometer/geobarometer calibration: the garnet-clinopyroxene geothermometer revisited. J. Metamorphic Geol. (Oxford) 3: 231–243.

Reinecke, T. 1991: Very-high-pressure metamorphism and uplift of coesite bearing metasediments from the Zermatt-Saas zone, Western Alps. Eur. J. Mineral. (Stuttgart) 3: 7–17.

Rubatto, D., Gebauer, D. & Fanning, M. 1998: Jurassic formation and Eocene subduction of the Zermatt-Saas Fee ophiolites: implications for the geodynamic evolution of the central and Western Alps. Contrib. Mineral. Petrol. (Berlin) 132: 269–287.

Schmädicke, E. & Müller, W.F. 2000: Unusual exolution phenomena in omphacite and partial replacement of phengite by phlogopite + kyanite in an eclogite from Erzgebirge. Contrib. Mineral. Petrol. (Berlin) 139: 629–642.

Schmid, R., Wilke, M., Oberhänsli, R., Janssens, K., Falkenberg, G., Franz, F. & Gaab, A. 2003: MicroXAES determination of ferric iron and its application in geothermobarometry. Lithos (Amsterdam) 70: 381–392.

Simon, G. & Chopin, C. 2001: Enstatite-sapphirine crack-related assemblages in ultrahigh-pressure pyrope megablasts, Dora-Maira massif, western Alps. Contrib. Mineral. Petrol. (Berlin) 140: 422–440.

Smith, D. 1984: Coesite in clinopyroxene in the Caledonides and its implications for geodynamics. Nature (London) 310: 641–644.

Sobolev, N.V. & Shatsky, V.S. 1990: Diamond inclusions in ganet from metamorphic rocks: a new environment for diamond formation. Nature (London) 343: 742–746.

Thöni, M. & Jagoutz, E. 1992: Some new aspects of dating eclogites in orogenic belts: Sm-Nd, Rb-Sr, and Pb-Pb isotopic results from the Austroalpine Saualpe and Koralpe type locality (Carinthia/Styria, southeastern Austria). Geochim. Cosmochim. Acta (New York) 56: 347–368.

Tilton, G.R., Schreyer, W. & Schertl, H.P. 1991: Pb-Sr-Nd isotopic behaviour of deeply subducted crustal rocks from the Dora Maira Massif, Western Alps, Italy-II: what is the age of

ultrahigh-pressure metamorphism? Contrib. Mineral. Petrol. (Berlin) 108: 22–33.

VAN ROERMUND, H.L.M., DRURY, M.R., BARNHOORN, A. & DE RONDE, A. 2001: Relict majoritic garnet microstructures from ultra-deep orogenic peridotites in Western Norway. J. Petrol. (Oxford) 42: 117–130.

WAIN, A., WATERS, D., JEPHCOAT, A. & OLIJYNK, H. 2000: The high-pressure to ultra-high pressure eclogite transition in the Western Gneiss Region, Norway. Eur. J. Mineral. (Stuttgart) 12: 667–687.

WATERS, D. J. & MARTIN, H. N. 1996: Geobarometry of phengite-bearing eclogites. Terra Abstr. (Oxford) 5(1), 410–411.

ZHANG, R. Y. & LIOU, J. G. 2000: Exsolution lamellae in minerals from ultrahigh-pressure rocks. In: ERNST, W.G. & LIOU, J.G. (eds.): Ultrahigh pressure metamorphism and geodynamics in collision-type orogenic belts. International Book Series 4. Geol. Soc. Am. (New York): 216–228.

GEOLOGIJA *53/1*, 21-36, Ljubljana 2010

Garnet peridotites from Pohorje: Petrography, geothermobarometry and metamorphic evolution

Petrografija, geotermobarometrija in metamorfni razvoj granatovega peridotita na Pohorju

Mirijam VRABEC

University of Ljubljana, Faculty of Natural Sciences and Engineering, Department of Geology, Aškerčeva 12, SI-1000 Ljubljana, Slovenia; e-mail: mirijam.vrabec@ntf.uni-lj.si

Prejeto / Received 15. 3. 2010; Sprejeto / Accepted 20. 5. 2010

Key words: ultrahigh-pressure metamorphism, garnet peridotite, geothermobarometry, collisional orogen, Pohorje, Eastern Alps, Slovenia

Ključne besede: ultravisokotlačna metamorfoza, granatov peridotit, geotermobarometrija, kolizijski orogeni, Pohorje, Vzhodne Alpe, Slovenija

Abstract

Ultrahigh-pressure (UHP) metamorphism has been recorded in Eo-Alpine garnet peridotites from the Pohorje Mts., Slovenia, belonging to the Eastern Alps. The garnet peridotite bodies are found within serpentinized metaultrabasites in the SE edge of Pohorje and are closely associated with UHP kyanite eclogites. These rocks belong to the Lower Central Austroalpine basement unit of the Eastern Alps, exposed in the proximity of the Periadriatic fault system.

Garnet peridotites show signs of a complex four-stage metamorphic history. The protolith stage is represented by a low-P high-T assemblage of olivine + Al-rich orthopyroxene + Al-rich clinopyroxene + Cr-spinel. Due to metamorphism, primary clinopyroxene shows exsolutions of garnet, orthopyroxene, amphibole, Cr-spinel and ilmenite. The UHP metamorphic stage is defined by the assemblage garnet + olivine + Al-poor orthopyroxene + clinopyroxene + Cr-spinel. Subsequent decompression and final retrogression stage resulted in formation of kelyphitic rims around garnet and crystallization of tremolite, chlorite, serpentine and talc.

Pressure and temperature estimates indicate that garnet peridotites reached the peak of metamorphism at 4 GPa and 900 °C, that is well within the UHP stability field. Garnet peridotites in the Pohorje Mountains experienced UHP metamorphism during the Cretaceous orogeny and thus record the highest-pressure conditions of all Eo-Alpine metamorphism in the Alps.

Izvleček

Granatovi peridotiti na JV robu Pohorja kažejo znake metamorfoze pri ultravisokotlačnih pogojih. Nastopajo v obliki majhnih teles znotraj serpentiniziranih metaultrabazičnih kamnin in so v tesni povezavi z ultravisokotlačnimi kianitovimi eklogiti. Tako peridotiti kot eklogiti pripadajo kamninam Spodnjega srednjega avstroalpina Vzhodnih Alp.

Metamorfni razvoj granatovih peridotitov je potekal v štirih fazah. Protolitna faza obsega nizkotlačno in visokotemperaturno mineralno združbo olivin + visoko-Al ortopiroksen + visoko-Al klinopiroksen + Cr-spinel. Med metamorfozo so se v primarnih klinopiroksenih formirale eksolucijske lamele granata, ortopiroksena, amfibola, Cr-spinela in ilmenita. Fazo ultravisokotlačne metamorfoze označujejo minerali granat + olivin + nizko-Al ortopiroksen + klinopiroksen + Cr-spinel. Sledili sta dekompresijska in kot zadnja retrogradna faza, ki je nastopila pri najnižjih P-T pogojih. To zaznamujejo nizkotemperaturni minerali, kot so tremolit, klorit, serpentin in lojevec.

Geotermobarometrični izračuni kažejo, da so bili granatovi peridotiti na Pohorju med viškom metamorfoze v času kredne orogeneze izpostavljeni tlaku 4 GPa in temperaturi preko 900 °C, kar ustreza polju ultravisokotlačne metamorfoze. Tako predstavljajo najvišje tlačne pogoje, dosežene med eo-alpinsko orogenezo na območju celotnega Alpskega orogen.

Introduction

Garnet peridotites are commonly associated with eclogites in UHP metamorphic terranes (Liou et al., 1998; Carswell & Compagnoni, 2003; Chopin, 2003). Peridotite massifs are important features of orogenic belts worldwide. Spinel peridotite is predominant in such bodies, but garnet peridotite is common in continental collision belts, particularly in Eurasian UHP metamorphic terranes (garnet peridotites and pyroxenites have been reported from 11 of the 15 or so HP/UHP terranes). These so-called 'orogenic' or 'Alpine-type' peridotites include several garnet-bearing rock types, such as

lherzolites, harzburgites, wehrlites, dunites and pyroxenites, generally referred to as garnet peridotites. These rocks mostly occur not only within metamorphosed continental crust, but also within units of oceanic affinity (e.g. Brueckner & Medaris, 2000 and references therein). Although volumetrically minor, these UHP metamorphic rocks provide an opportunity to evaluate the tectonothermal conditions related to the interaction of mantle and crust during UHP metamorphism as well as important information on orogenic processes in deep orogenic root zones and the upper mantle (e.g. Zhang et al., 1994; Dobrzhinetskaya et al., 1996; van Roermund & Drury, 1998).

Most garnet peridotites are depleted upper mantle material, variously modified by metasomatism, but some originated by low-pressure crystallization from ultramafic-mafic igneous complexes. All presently known garnet peridotites in Eurasian HP/UHP terranes can be divided into two groups, one having a high P/T ratio and the other a low P/T ratio (Medaris, 2000; Figure 1). Nearly all of the peridotite occurences in the high P/T group can be related to subduction processes and are isofacial and approximately contemporaneous with associated UHP crustal rocks that contain coesite and diamond. The single exception is the Western Gneiss Region, Norway, where the garnet peridotites are relicts of old, cold lithosphere that formed earlier and under different conditions than those prevailing during the overprinting Caledonian metamorphism. Peridotites in the low P/T group are associated with HP crustal rocks that are characterized by HP granulites and strongly retrogressed eclogites, in which little evidence for the presence of coesite or diamond was found so far. The extremely high temperatures of the low P/T group would seem to require the influence of upwelling asthenosphere.

Garnet peridotites are thought to have evolved in at least four different tectonothermal settings (Medaris, 2000): (1) emplacement of peridotites (serpentinites or igneous complexes, e.g. ophiolite components or ultramafic differentiates of mafic intrusions) into the oceanic or continental crust prior to UHP metamorphism, followed by transport of peridotites and associated crust to UHP conditions (high P/T) by a subducting plate; (2) transfer of peridotites from a mantle wedge to the crust of an underlying, subducting plate (high P/T); such peridotites are initially either spinel- or garnet-bearing, depending on the depth of derivation; (3) originating from upwelling asthenosphere that passed through a high-temperature spinel peridotite stage, followed by cooling into the garnet peridotite field (low P/T); and (4) extraction of garnet peridotites from ancient subcontinental lithosphere, perhaps by deep-seated faulting within a continental plate (high P/T).

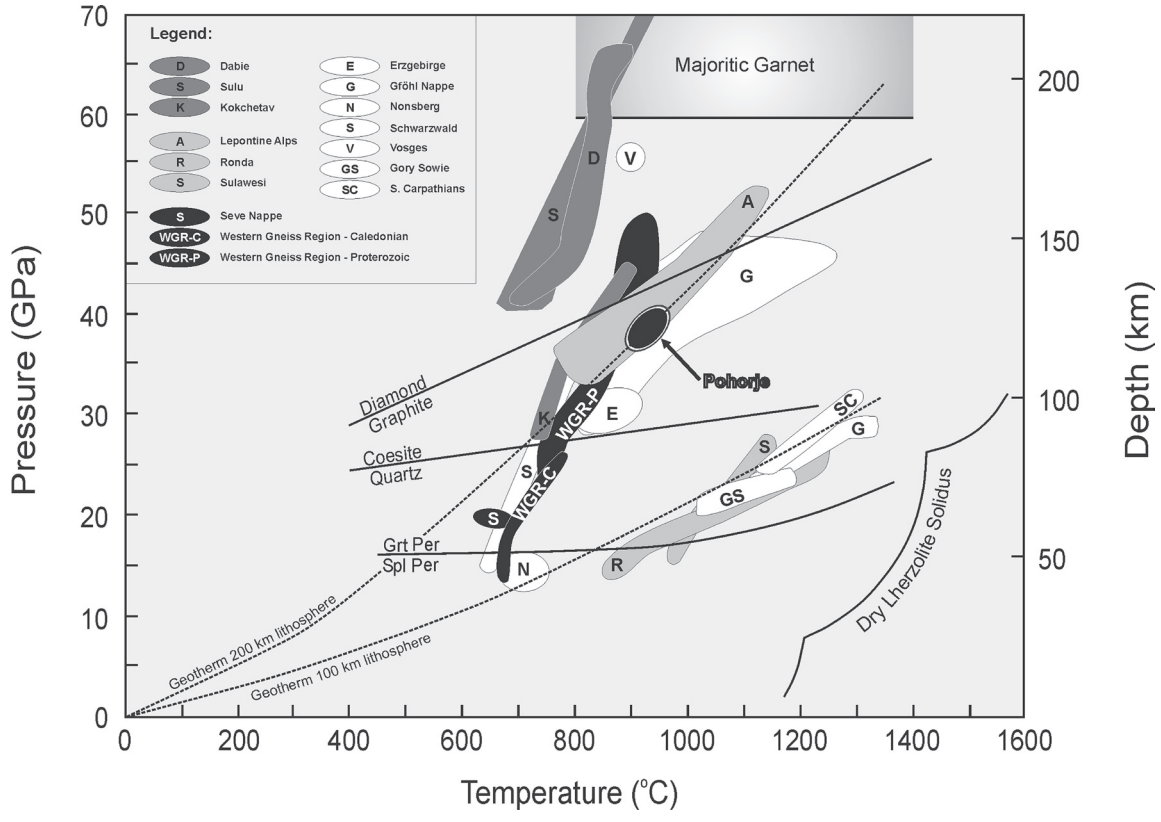

Figure 1. P-T estimates for Pohorje garnet peridotites in comparison with well established UHP terranes:
(1) Asian UHP terranes (dark grey color);
(2) Scandinavian Caledonides (black color);
(3) European Variscan terranes (white color); and
(4) Alpine terranes (pale grey color; after Medaris, 2000).
Shown for reference are equilibria for diamond-graphite (Bundy, 1980), coesite-quartz (Bohlen & Boettcher, 1982), and spinel-garnet peridotite (O'Hara et al., 1971). Also shown are steady-state conductive geotherms for 200 km and 100 km thick lithosphere, a dry lherzolite solidus (Takahashi, 1986), and a stability field for majoritic garnet containing 3 to 5 vol% pyroxene.

Garnet peridotite bodies in the Alps are known from two main regions. Alpe Arami, Monte Duria and Cima di Gagnone garnet peridotites belong to the Adula-Cima Lunga unit (Ernst, 1978; Nimis & Trommsdorff, 2001; Paquin & Altherr, 2001), and are of Tertiary age (Becker, 1993; Gebauer, 1996), whereas garnet peridotites from Nonsberg area in the Ulten zone (Obata & Morten, 1987; Nimis & Morten, 2000) are of Variscan age (Tumiati et al., 2003). Metamorphic processes related to the Cretaceous (so-called Eo-Alpine) events in the Alps have been recognized mainly in the Austroalpine units (e.g. Thöni & Jagoutz, 1992; Hoinkes et al., 1999; Schmid et al., 2004; Schuster et al., 2004). In the Eastern Alps, the metamorphic grade of Cretaceous metamorphism reached UHP facies in the south-easternmost parts, in the Pohorje Mountains of Slovenia, belonging to the Lower Central Austroalpine unit (Janák et al., 2004; Vrabec, 2010).

In kyanite eclogites from Pohorje Mountains UHP metamorphism have been recently documented (Janák et al., 2004; Vrabec, 2010). The eclogites are closely associated with serpentinized metaultrabasites in which investigated garnet peridotite remnants are preserved (Janák et al., 2006). Early estimates of the P-T conditions experienced by the Pohorje garnet peridotites were in the range of 750–1050 °C and 2.4–3.6 GPa (Hinterlechner-Ravnik et al., 1991; Visona et al., 1991).

This paper presents the evidence for UHP metamorphism of garnet-bearing ultramafic rocks in the Austroalpine units of the Eastern Alps, exposed in the Pohorje Mountains of Slovenia. Described here are the mineralogical, petrological and geothermobarometrical features of garnet peridotites constraining their multi-stage metamorphic evolution. The obtained results offer additional evidence for UHP metamorphism in the Eastern Alps.

Geological Background

The Pohorje massif is built up of three Eo-Alpine Cretaceous nappes (Mioč & Žnidarčič, 1977; Fodor et al., 2003) that belong to pre-Neogene metamorphic sequences of the Austroalpine units of the Eastern Alps (Figure 2). The lowest nappe that is termed the Pohorje nappe (Janák et al., 2006) represents the Lower Central Austroalpine (Janák et al., 2004) and consists of medium- to high-grade metamorphic rocks, predominantly micaschists, gneisses and amphibolites with marble and quarzite lenses. It also contains several eclogite lenses and a body of metaultrabasic rocks. The Pohorje nappe is overlain by a nappe composed of weakly metamorphosed Paleozoic rocks, mainly low-grade metamorphic slates and phyllites. The uppermost nappe is built up of Permo-Triasic clastic sedimentary rocks, mainly sandstones and conglomerates. The two latter nappes represent the Upper Central Austroalpine. The entire nappe stack is overlain by Early Miocene sediments which belong to the syn-rift basin fill of the Pannonian Basin (Fodor et al., 2003).

The magmatic intrusion in the central part of Pohorje is of Miocene age (18–19 Ma; Trajanova et al., 2008; Fodor et al., 2007). It is of granodioritic to tonalitic composition (Zupančič, 1994), with a very small gabbroic enclave in its SE part. The main intrusion was followed by the formation of aplite and pegmatite veins, and lamprophyric dykes. In the western part of Pohorje, shallow dacite bodies and dykes intrude both the granodiorite body and the country rocks, suggesting that the dacite intrusion is somewhat younger than the granodiorite one. The Pohorje nappe is folded into an ESE-WNW-striking antiform, the core of which is occupied by the intrusion. Therefore, neither the original basal contact of the Pohorje nappe nor

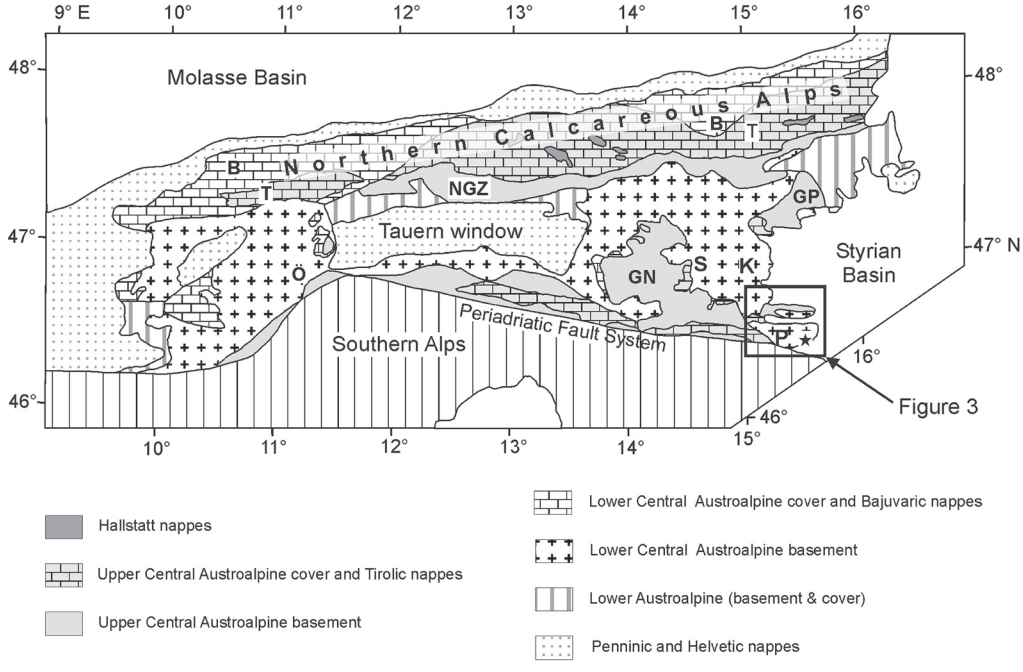

Figure 2. Tectonic map of the Eastern Alps. B-Bajuvaric, GN-Gurktal nappe, GP-Graz Paleozoic, K-Koralpe, NGZ-Northern Grauwacke zone, Ö-Southern Ötztal nappe, P-Pohorje, S-Saualpe, T-Tirolic. Modified after Neubauer & Höck (2000) and Schmid et al. (2004).

any deeper tectonic units are exposed in the Pohorje area.

North and south of the granodiorite intrusion, eclogite bodies, lenses and bands of different sizes are found within country rocks. Numerous lenses, boudins and bands of eclogites also occur within the metaultrabasite body, located in the southeasternmost part of Pohorje Mountains near Slovenska Bistrica. Metaultrabasites form a body of ca. 5 x 1 km size, which is termed the Slovenska Bistrica ultramafic complex (SBUC; Janák et al., 2006; Figure 3). Some outcrops of garnet peridotites also occur away from this body, further to the west. The main protoliths of the Slovenska Bistrica ultramafic complex are harzburgites and dunites (cf. Hinterlechner-Ravnik, 1987; Hinterlechner-Ravnik et al., 1991). Because of extensive serpentinization, only a few less-altered bodies of garnet peridotites, garnet pyroxenites and coronitic metatroctolites are preserved (Hinterlechner-Ravnik, 1987; Hinterlechner-Ravnik et al., 1991). The country rocks of the eclogites and the Slovenska Bistrica ultramafic complex are amphibolites, orthogneisses, paragneisses and micaschists. These rocks form a strongly foliated matrix around elongated lenses and boudins of eclogites and ultrabasites, including the Slovenska Bistrica ultramafic complex.

The timing of HP/UHP metamorphism in the Pohorje nappe is Cretaceous, as documented by dating of eclogites with garnet Sm-Nd and zircon U-Pb ages of 91 Ma (Miller et al., 2005). Almost identical ages have been obtained from dating of garnet (93–87 Ma; Thöni, 2002) and zircon (92 Ma; Janák et al., 2009) of gneisses and micaschists. This age is similar to that of Koralpe and Saualpe eclogite facies metamorphism (Thöni & Jagoutz, 1992; Thöni & Miller, 1996; Miller & Thöni, 1997; Thöni, 2002). Tertiary K-Ar mica ages (19–13 Ma) as well as apatite and zircon fission track ages (19–10 Ma) were obtained from the country rocks of eclogites and metaultrabasites in the Pohorje nappe (Fodor et al., 2002). This suggests that the peak of metamorphism was attained during the Cretaceous, and final cooling occurred in the Early to Midd Miocene. Upper Cretaceous (75–70 Ma) cooling ages were determined in the Koralpe area, the north-westward extension of the Pohorje nappe (Schuster et al., 2004), indicating that the Koralpe rocks were exhumed during the Upper Cretaceous. Also the major exhumation of the Pohorje nappe, from UHP depth to crustal depth, most probably occurred already during the Upper Cretaceous. The final stage of exhumation to the surface was achieved in the Miocene by east- to north-east-directed low-angle extensional shearing, associated with the main opening phase of the Pannonian basin and leading to the core complex structure of the Pohorje Mountains (Fodor et al., 2003). The Miocene shearing event reactivated and overprinted the nappe boundaries in the Pohorje area (Janák et al., 2006). Therefore, direct structural evidence for the kinematics of Cretaceous exhumation has not yet been found.

Methods

Electron Probe Micro-Analysis

Microchemical analyses of the main constituent minerals were determined by Electron Probe Micro-Analysis (EPMA) technique using a CAMECA SX-100 electron microprobe at Dionýz Štúr Institute of Geology in Bratislava. Bombarding of micro-volumes of sample with a focused electron beam (5–30 keV) induced emission of X-ray photons. The wavelengths of collected X-rays

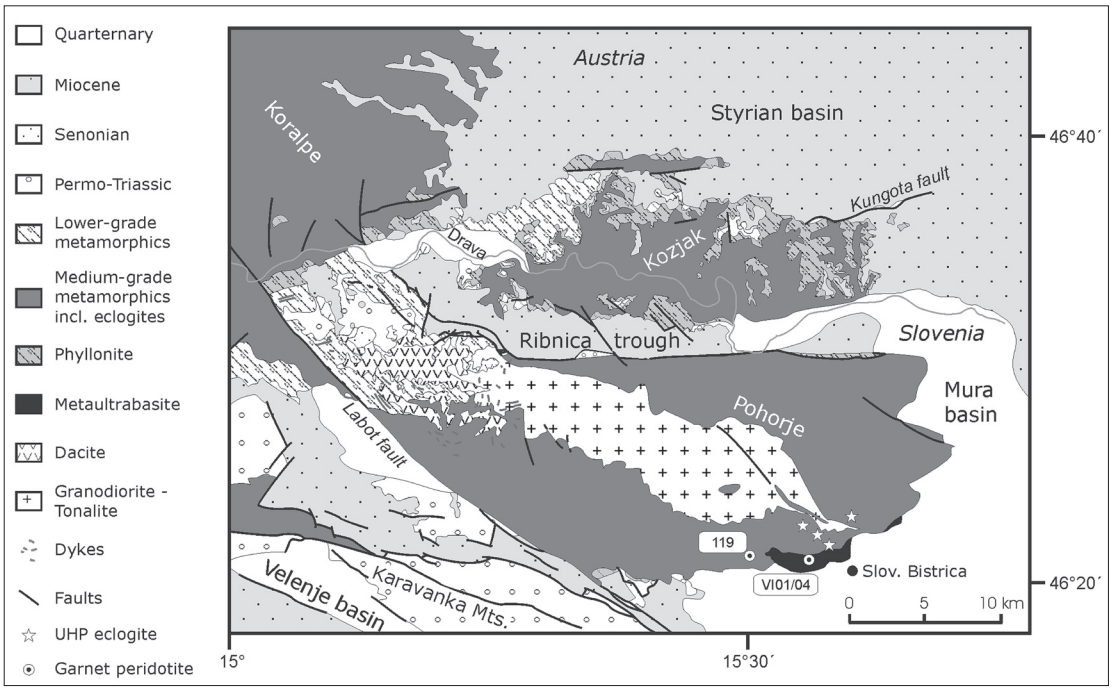

Figure 3. Simplified geological map of Pohorje and adjacent areas (modified from Mioč & Žnidarčič, 1977) showing locations of the investigated garnet peridotites. Locality VI01/04 is outcroping within the SBUC near Visole while the other one, locality 119, is exposed farther west, near Prihovca.

were identified by recording their WDS spectra (Wavelength Dispersive Spectroscopy). Analytical conditions were 15 keV accelerating voltage and 20 nA beam current, with a peak counting time of 20 s and a beam diameter of 2–10 μm. Raw counts were corrected using a PAP routine.

Representative analyses of mineral phases are given in Table 1.

Table 1. Representative microprobe analyses of mineral compositions. I – protolith stage, II – metamorphic stage, III – decompression stage, IV – retrogression stage.

Sample	119	119	119	119	119	119	119	119	119	119	119
Mineral	Ol II	Grt II	Grt II^{exs}	Cpx I, II	Opx II^{exs}	Opx II	Opx III	Spl I, II	Spl III	Amp III	Amp IV
SiO_2	40.70	41.40	41.95	54.02	58.26	57.73	56.50	0.01	0.04	45.23	56.16
TiO_2	0.00	0.01	0.04	0.03	0.01	0.05	0.01	0.14	0.00	0.35	0.11
Al_2O_3	0.03	23.20	22.70	0.93	0.85	0.74	1.97	27.78	69.64	12.49	2.26
Cr_2O_3	0.01	0.12	1.05	0.16	0.17	0.11	0.03	35.43	0.00	0.77	0.30
FeO	10.69	10.02	12.13	1.78	6.93	6.55	6.32	25.50	7.79	5.18	3.73
MnO	0.10	0.24	0.46	0.02	0.10	0.10	0.08	0.29	0.00	0.02	0.08
MgO	49.90	18.80	16.56	17.52	34.81	35.64	34.70	10.30	23.20	18.41	21.89
CaO	0.02	5.46	5.81	24.90	0.56	0.20	0.21	0.00	0.06	12.14	12.93
Na_2O	0.00	0.00	0.00	0.42	0.00	0.00	0.01	0.00	0.00	2.70	0.30
K_2O	0.00	0.00	0.00	0.02	0.00	0.00	0.01	0.00	0.00	0.07	0.02
Total	101.44	99.25	100.70	99.80	101.69	101.12	99.84	99.45	100.73	97.36	97.79
Si	0.986	2.983	3.018	1.968	1.979	1.963	1.950	0.000	0.001	6.390	7.743
Ti	0.000	0.001	0.002	0.001	0.000	0.001	0.000	0.003	0.000	0.037	0.012
Al	0.001	1.971	1.925	0.040	0.034	0.030	0.080	1.004	1.994	2.080	0.367
Cr	0.000	0.007	0.060	0.005	0.005	0.003	0.001	0.858	0.000	0.086	0.032
Fe^{2+}	0.217	0.602	0.730	0.054	0.197	0.186	0.183	0.640	0.157	0.574	0.430
Mn	0.002	0.015	0.028	0.001	0.003	0.003	0.002	0.008	0.000	0.002	0.010
Mg	1.802	2.019	1.776	0.951	1.762	1.806	1.785	0.471	0.840	3.876	4.499
Ca	0.000	0.422	0.448	0.972	0.020	0.007	0.008	0.000	0.002	1.838	1.910
Na	0.000	0.000	0.000	0.030	0.000	0.000	0.000	0.000	0.000	0.740	0.082
K	0.000	0.000	0.000	0.001	0.000	0.000	0.000	0.000	0.000	0.013	0.004
Total	3.008	8.020	7.987	4.022	4.000	3.999	4.009	2.984	2.994	15.636	15.088
X_{Mg}	0.89	0.78	0.71	0.95	0.90	0.92	0.91	0.42	0.84	0.94	0.91
Cr*								0.46	0.00		
Sample	VI01/04	VI01/04	VI01/04	VI01/04	VI01/04	VI01/04	VI01/04	VI01/04	VI01/04	VI01/04	VI01/04
Mineral	Ol II	Grt II	Cpx I	Cpx II, III	Opx I	Opx II	Opx III	Spl I, II	Spl III	Amp III	Amp IV
SiO_2	40.62	41.73	52.95	55.28	56.73	57.33	55.65	0.04	0.09	44.70	56.89
TiO_2	0.00	0.00	0.00	0.00	0.00	0.00	0.00	0.10	0.00	0.13	0.03
Al_2O_3	0.00	22.99	4.87	1.05	2.19	0.81	1.82	26.68	65.96	13.85	1.20
Cr_2O_3	0.000	0.48	0.16	0.21	0.00	0.00	0.03	37.29	0.85	1.23	0.21
FeO	12.239	10.94	3.36	1.66	8.05	7.55	9.71	22.97	11.71	3.77	2.25
MnO	0.210	0.45	0.09	0.02	0.08	0.18	0.14	0.34	0.15	0.04	0.05
MgO	47.510	17.64	17.65	17.42	33.69	34.13	32.80	10.28	20.73	18.58	23.33
CaO	0.029	6.16	21.320	24.680	0.130	0.110	0.189	0.00	0.04	12.57	13.27
Na_2O	0.000	0.00	0.290	0.500	0.000	0.000	0.093	0.00	0.00	2.36	0.13
K_2O	0.000	0.00	0.010	0.010	0.000	0.000	0.027	0.00	0.00	0.07	0.02
Total	100.61	100.39	100.699	100.834	100.865	100.105	100.468	97.70	99.53	97.30	97.38
Si	1.000	2.993	1.901	1.984	1.949	1.982	1.941	0.001	0.002	6.287	7.823
Ti	0.000	0.000	0.000	0.000	0.000	0.000	0.000	0.002	0.000	0.014	0.003
Al	0.000	1.943	0.206	0.044	0.089	0.033	0.075	0.983	1.952	2.296	0.195
Cr	0.000	0.027	0.005	0.006	0.000	0.000	0.001	0.921	0.017	0.137	0.023
Fe^{2+}	0.252	0.653	0.099	0.048	0.231	0.218	0.283	0.591	0.243	0.406	0.258
Mn	0.004	0.027	0.003	0.001	0.002	0.005	0.004	0.009	0.003	0.005	0.005
Mg	1.74	1.886	0.944	0.932	1.725	1.758	1.706	0.479	0.775	3.894	4.783
Ca	0.00	0.474	0.820	0.949	0.005	0.004	0.007	0.000	0.001	1.894	1.956
Na	0.00	0.000	0.020	0.035	0.000	0.000	0.006	0.000	0.000	0.644	0.036
K	0.00	0.000	0.000	0.000	0.000	0.000	0.001	0.000	0.000	0.013	0.004
Total	3.000	8.003	3.998	3.999	4.001	4.000	4.025	2.986	2.993	15.590	15.085
X_{Mg}	0.87	0.75	0.90	0.95	0.89	0.89	0.86	0.45	0.76	0.98	0.95
Cr*								0.48	0.86		

Analyses (in wt%) of olivine (Ol), garnet (Grt), clinopyroxene (Cpx), orthopyroxene (Opx), spinel (Spl) and amphibole (Amp). Olivine is normalized to 4, garnet to 12, clinopyroxene to 6, orthopyroxene to 6, spinel to 4 and amphibole to 23 oxygens. Exs - exsolution in clinopyroxene.

Garnet-olivine Fe^{2+}-Mg exchange geothermometery

Garnet-olivine Fe^{2+}-Mg exchange thermometer is based on the partitioning of iron and magnesium between the coexisting garnet and olivine and may be represented by the exchange reaction:

2 *pyrope* + 3 *fayalite* → 2 *almandine* + 3 *forsterite*

The distribution coefficient K_D is defined as:

$$K_D = \frac{X_{Mg}^{ol} \cdot X_{Fe}^{grt}}{X_{Fe}^{ol} \cdot X_{Mg}^{grt}}$$

where X_{Mg}^{ol} is the mole fraction of Mg in olivine, X_{Fe}^{grt} is the mole fraction of Fe^{2+} in the garnet, etc.

Garnet-olivine Fe^{2+}-Mg exchange thermometer has been successfully calibrated by O'Neill & Wood (1979) and later corrected by O'Neill (1980) yielding the following equation:

$$T_{OW-80}(^{\circ}C) = \\ = \frac{902 + DV + (X_{Mg}^{ol} - X_{Fe}^{ol}) \cdot (498 + 1.51(P - 30))}{\ln K_D + 0.357} + \\ + \frac{-98 \cdot (X_{Mg}^{grt} - X_{Fe}^{grt}) + 1347 \cdot X_{Ca}^{grt}}{\ln K_D + 0.357} - 273$$

DV term is incorporating thermal expansion and compressibilities for all four phases and is given by:

$$DV = 462.5 \cdot (1.0191 + (T - 1073)) \cdot (2.87 \cdot 10^{-5}) \cdot (P - 2.63 \cdot 10^{-4} \cdot P^2 - 29.76) + \\ + 262.4 \cdot (1.0292 + (T - 1073)) \cdot (4.5 \cdot 10^{-5}) \cdot (P - 3.9 \cdot 10^{-4} \cdot P^2 - 29.65) - \\ - 454 \cdot (1.020 + (T - 1073)) \cdot (2.84 \cdot 10^{-5}) \cdot (P - 2.36 \cdot 10^{-4} \cdot P^2 - 29.79) - \\ - 278.3 \cdot (1.0234 + (T - 1073)) \cdot (2.3 \cdot 10^{-5}) \cdot (P - 4.5 \cdot 10^{-4} \cdot P^2 - 29.6)$$

where P is in kbars. The four parts of the DV term are volume expressions for almandine, forsterite, pyrope and fayalite, respectively. Since the DV term involves temperature, upper equation for T_{OW-80} is best solved iteratively by estimating initial value of T (°C) at pressure P (kbar). Since the DV term is small, this method converges rapidly. At P equal to the experimental pressure of 30 kbar, the DV term is zero.

This geothermometer is most sensitive in the temperature and composition regions where K_D is substantially greater than 1. It serves as a reliable geothermometer for magnesium-rich garnet-olivine assemblages equilibrated close to, or within, the temperature range 900–1400 °C and pressures up to about 60 kbar. For a fixed K_D, the influence of pressure is to increase the calculated temperature by between 3 and 6 °C per kbar (O'Neill & Wood, 1979).

In garnet-olivine mineral combination only the garnet is a problematic member because it can incorporate significant amounts of Fe^{3+} in its structure. The presence of a Fe^{3+} component has a considerable influence on the calculated temperatures. The comparison of estimated temperatures for several garnet-olivine pairs with temperatures obtained from two-pyroxene thermometers has shown, that in the case of garnet-olivine thermometer the Fe^{3+} content in garnets can be ignored and all Fe treated as Fe^{2+} (Canil & O'Neill, 1996).

Garnet-orthopyroxene Fe^{2+}-Mg exchange geothermometery

The garnet-orthopyroxene Fe^{2+}-Mg exchange thermometer is based on the distribution of Fe^{2+} and Mg between garnet and orthopyroxene according to the reaction:

2 *pyrope* + 3 *ferrosilite* → 2 *almandine* + 3 *enstatite*

One of the reliable calibrations of this geothermometer which is applicable to garnet peridotites and granulites was made by Harley (1984):

$$T_{H-84}(^{\circ}C) = \frac{3740 + 1400 \cdot X_{Ca}^{grt} + 22.86 \cdot P}{R \cdot \ln K_D + 1.96} - 273$$

where P is pressure in kbars and R is the universal gas constant (8.3143 J/K mol). The distribution coefficient is given by:

$$K_D = \frac{X_{Fe}^{grt}}{X_{Mg}^{grt}} \cdot \frac{X_{Mg}^{opx}}{X_{Fe}^{opx}} = \frac{\left(Fe^{2+}/Mg\right)^{grt}}{\left(Fe^{2+}/Mg\right)^{opx}}$$

and

$$X_{Ca}^{grt} = \frac{Ca}{Ca + Mn + Fe^{2+} + Mg}$$

The distribution of Fe^{2+} and Mg between garnet and orthopyroxene produces a good geothermometer with required high dP/dT slope and a range in K_D of 4 to 1.5 over geologically attainable P-T conditions. At low temperatures the precision of the geothermometer is limited by analytical uncertainties. An error in K_D of only ±0.1 is equivalent to ±40–60 °C error in temperature estimation (Harley, 1984).

The effects of Fe^{3+} calculations are very important when using garnet-orthopyroxene Fe^{2+}-Mg exchange thermometer. Normally, in natural assemblages Fe^{3+} preferentially enters garnet rather than orthopyroxene. K_D values calculated by simply assuming $Fe^{tot} = Fe^{2+}$ will therefore be greater than those calculated by estimating Fe^{3+} with some consistent charge- and mass-balance algorithm. Even a small decrease of K_D, resulting from Fe^{3+} calculation, may raise estimated temperatures by 20–100 °C, which is a significant amount (Harley, 1984). In natural systems, T_{H-84} temperatures calculated with upper equation by ignoring Fe^{3+} should be regarded as minimum temperatures.

Al-in-orthopyroxene geobarometry

Reliable geobarometers suitable for HP/UHP rocks are mostly based on net-transfer reactions involving transfer of Al from tetrahedral to octahedral coordination sites. The Al-in-orthopyroxene barometer has been widely used. The content of Al^{3+} in octahedral sites in orthopyroxene coexisting with garnet is particularly pressure de-

pendent and hence serves as an adequate indicator of the pressure conditions at which the rock has been equilibrated. Several calibrations of this barometer have been performed, as summarized by Krogh Ravna & Paquin (2003). To date, the Brey & Köhler (1990) calibration seems to be the most reliable for pressure calculations over a wide pressure range. Pressure is calculated according to the equation:

$$P(kbar) = \frac{-C_2 - \sqrt{C_2^2 + \frac{4 \cdot C_3 C_1}{1000}}}{2 \cdot C_3}$$

with

$$\begin{aligned} C_1 = & -R \cdot T \cdot \ln K_D - 5510 + 88.91 \cdot T - 19 \cdot T^{1.2} + \\ & + 3 \cdot (X_{Ca}^{grt})^2 \cdot 82458 + X_{Mg}^{M1} \cdot X_{Fe}^{M1} \cdot (80942 - 46.7 \cdot T) - \\ & - 3 \cdot X_{Fe}^{grt} \cdot X_{Ca}^{grt} \cdot 17793 - X_{Ca}^{grt} \cdot X_{Cr}^{grt} \cdot (1.164 \cdot 10^6 - \\ & - 420.4 \cdot T) - X_{Fe}^{grt} \cdot X_{Cr}^{grt} \cdot (-1.25 \cdot 10^6 + 565 \cdot T) \\ C_2 = & -832 - 8.78 \cdot 10^{-5} \cdot (T - 298) + 3 \cdot (X_{Ca}^{grt})^2 \cdot 3305 - \\ & - X_{Ca}^{grt} \cdot X_{Cr}^{grt} \cdot 13.45 + X_{Fe}^{grt} \cdot X_{Cr}^{grt} \cdot 10.5 \\ C_3 = & 16.6 \cdot 10^{-4} \end{aligned}$$

R is the universal gas constant (8.3143 J/K mol) and the distribution coefficient is calculated as:

$$K_D = \frac{(1 - X_{Ca}^{grt})^3 \cdot X_{Al}^{grt}}{X_{MF}^{M1} \cdot (X_{MF}^{M2})^2 \cdot X_{Al,TS}^{M1}}$$

Site occupancies for pyroxenes are taken from Nickel & Green (1985) and Carswell & Gibb (1987) and are defined as:

$$X_{Al}^{M1} = \frac{Al + Na - Cr - Fe^{3+} - 2 \cdot Ti}{2}$$

$$X_{Al,TS}^{M1} = \frac{Al + Na - Cr - Fe^{3+} - 2 \cdot Ti}{2} \quad (for\ Jd < 0)$$

$$X_{Al,TS}^{M1} = \frac{Al - Na + Cr + Fe^{3+} + 2 \cdot Ti}{2} \quad (for\ Jd > 0)$$

$$X_{Mg}^{Mi} = X_{MF}^{Mi} \cdot X_{MF} \quad (i = 1, 2)$$

$$X_{Fe}^{M1} = X_{MF}^{M1} \cdot (1 - X_{MF})$$

$$X_{MF}^{M1} = (1 - X_{Al}^{M1} - Cr - Fe^{3+} - Ti)$$

$$X_{MF}^{M2} = (1 - Ca - Na - Mn)$$

$$X_{MF} = \frac{Mg}{Mg + Fe^{2+}}$$

Site occupancies for garnet are as follows:

$$X_{Ca}^{grt} = \frac{Ca}{Ca + Mg + Fe^{2+} + Mn}$$

$$X_{Fe}^{grt} = \frac{Fe^{2+}}{Ca + Mg + Fe^{2+} + Mn}$$

$$X_{Mg}^{grt} = \frac{Mg}{Ca + Mg + Fe^{2+} + Mn}$$

$$X_{Al}^{grt} = \frac{Al}{Al + Cr}$$

$$X_{Cr}^{grt} = \frac{Cr}{Al + Cr}$$

Like in the Fe^{2+}-Mg geothermometry, the oxidation state of present iron has significant influence. Fe^{3+} is replacing Al^{3+} in octahedral places in orthopyroxene structure. Consequently, equal amounts of Al^{3+} in tetrahedral sites are required to retain charge balance. This results in a limited amount of Al^{3+} available for the substitution, therefore calculated activity of the $MgAl_2SiO_6$ component in orthopyroxene is considerably underestimated.

Results

Petrography and mineral chemistry

Several samples of relatively well-preserved garnet peridotites from two known localities were investigated: one locality is outcroping within the SBUC near Visole; the other one is exposed farther west, near Prihovca (Figure 3). In Visole the garnet-bearing peridotites occur as very small lenses within the extensively serpentinized ultrabasites while in Prihovca area garnet peridotite bodies of up to several metres in size are exposed within the rocks of continental crustal origin, mainly micaschists and gneisses. Garnet peridotites exhibit rather massive and relatively homogeneous textures without any distinct compositional layering visible in the outcrop, hand-specimen and thin-section scale. In well preserved garnet peridotites big pinkish-red colored garnet grains are surrounded by a black matrix whereas more serpentinized varieties contain completely white colored garnets.

Garnet peridotites consist of garnet, olivine, orthopyroxene, clinopyroxene and brown spinel, which are to a variable extent replaced by amphibole, green spinel, serpentine, talc and chlorite. They show higher modal amounts of garnet and clinopyroxene relative to olivine, therefore they are mainly classified as pyroxenites (garnet-olivine websterites), some of the samples even as garnet orthopyroxenites. However, because of intensive retrogression of these rocks, the abundance of primary minerals is largely obscured.

Garnet mostly forms big porphyroblastic grains with irregular boundaries (Figure 4a). Only rarely it is found in idiomorphic forms with well developed crystal faces. Garnet is also found as exsolution lamellas from clinopyroxene, in form of irregular, bleb-resembling inclusions in orthopyroxene and in coronas around Cr-spinel. All garnets are pyrope-rich, belonging to almandine-pyrope-grossular series. End member compositions are ranging from 53–68 mol% of pyrope, 18–33 mol% of almandine and spessartine, and 8–20 mol% of grossular and andradite. Garnets in samples from Prihovca contain slightly higher pyrope content (56–68 mol%) than garnets from Visole (54–66 mol%).

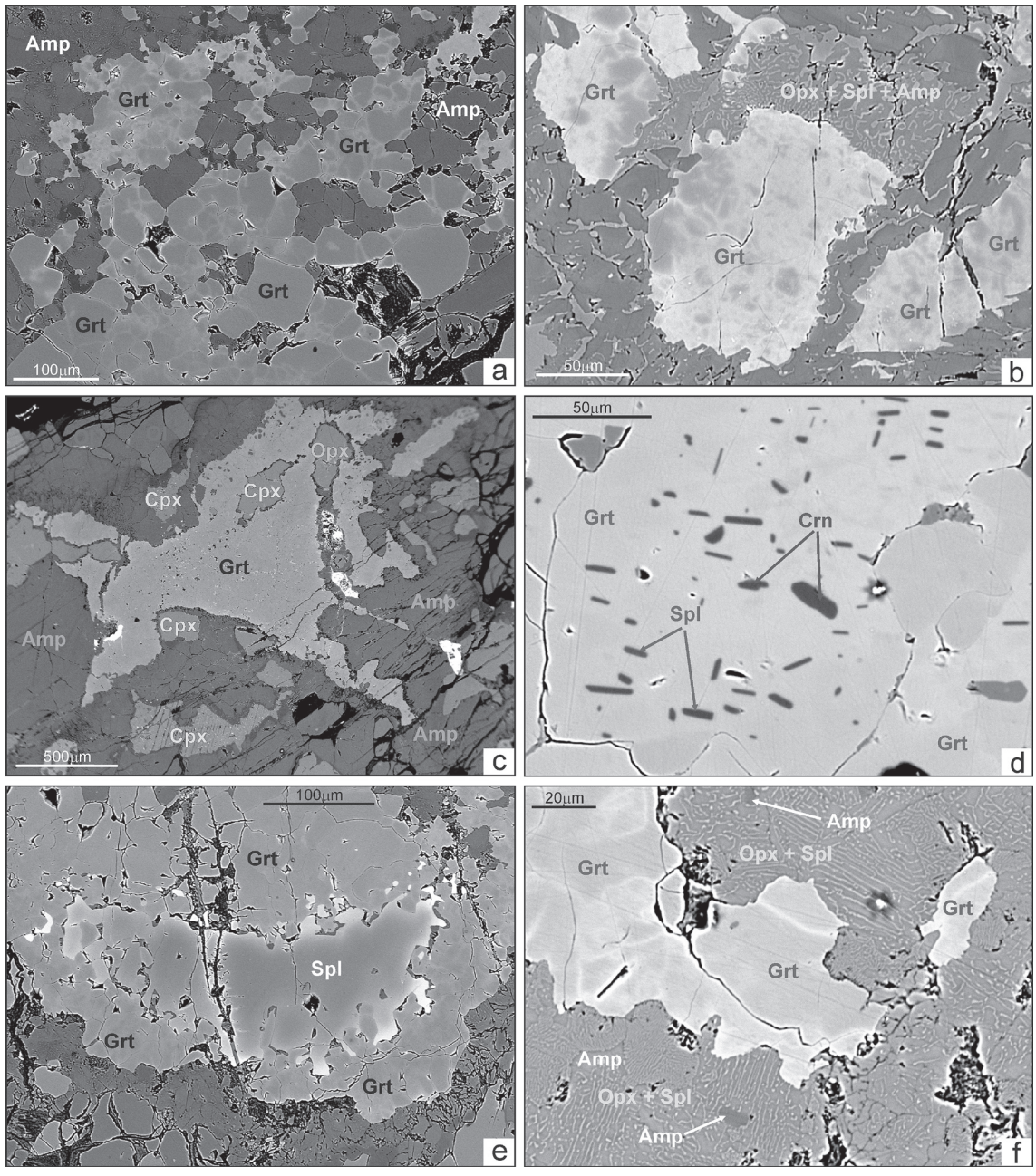

Figure 4. Garnets from garnet peridotites in photomicrographs – backscattered electron images (BSE).
(a) Inhomogeneous garnet porphyroblasts are mainly found in shape of xenomorphic grains with irregular boundaries.
(b) Patchy garnet grains surrounded by secondary symplectites of spinel, amphibole and orthopyroxene. Difference between high-Mg dark parts and low-Mg bright parts within same garnet grain is well displayed.
(c) Big garnet grain with irregular boundaries comprises clinopyroxene and orthopyroxene inclusions. Garnet is surrounded by amphibole and appears homogeneous due to relatively small magnification.
(d) Corundum and spinel inclusions in inhomogeneous garnet display semi-parallel orientation. Spinel inclusions in this case might be interpreted as remnants of primary low-pressure stage or as secondary minerals. It is also not clear whether corundum minerals are real inclusions or maybe exsolutions from garnet.
(e) Cr-Spinel inclusion in garnet represents primary spinel overgrown by garnet during subduction.
(f) Garnet rims are replaced by symplectitic intergrowth of Al-orthopyroxene, Al-spinel, diopside and Prg-amphibole. As a result of retrogression, garnet shows a decrease in Mg (darker parts) and increase in Fe (brighter parts). Amp-amphibole, Cpx-clinopyroxene, Crn-corundum, Grt-garnet, Ol-olivine, Opx-orthopyroxene, Spl-spinel.

The most pronounced feature of garnets from the studied garnet peridotites is their patchy appearance (Figure 4b) caused by chemical inhomogeneity. Patchy garnets were found in samples from both localities, although garnets from Prihovca are slightly more homogeneous than those from Visole. Dark parts of garnets are Mg-rich with 60 to 68 mol% of pyrope and are corresponding to peak pressure compositions. Bright parts are Ca- and Fe-rich, but Mg-poor with much lower pyrope content (54 to 56 mol%). During decompression, Mg is moving out of garnet which results in enrichment of Ca and Fe. Compositional change between the dark and bright parts in garnets can be well expressed with magnesium number (Mg#):

$$Mg\#=100\cdot X_{Mg}^{grt}=100\cdot\frac{Mg}{Mg+Fe^{2+}}$$

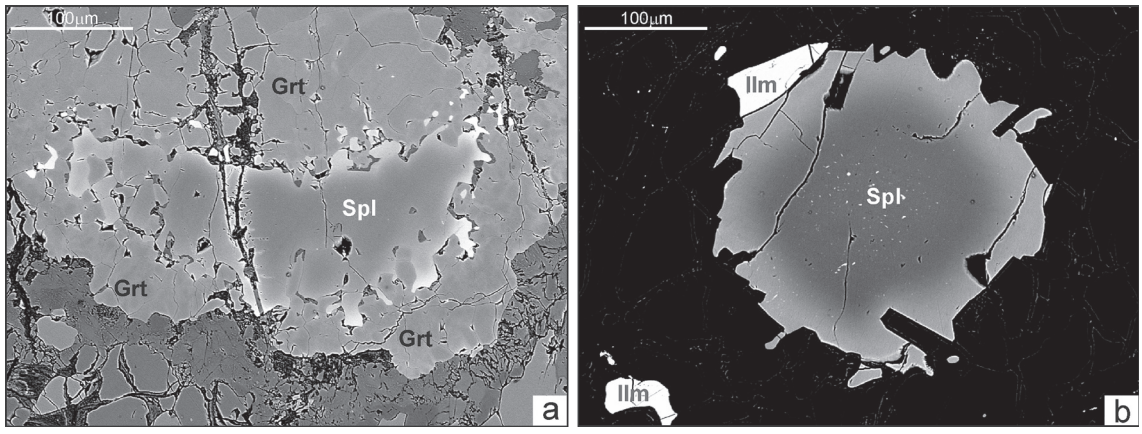

Figure 5. Chromian-rich spinel occurring in matrix (BSE). Matrix minerals in (b) are mostly olivine and amphibole. Both grains show weak zonation indicating an increase of Cr content from core to rim. Amp-amphibole, Cpx-clinopyroxene, Ilm-ilmenite, Ol-olivine, Opx-orthopyroxene, Spl-spinel.

In the dark parts Mg# is reaching 0.78, whereas it never exceeds 0.68 in the bright parts. Relatively slow diffusion processes caused an irregular distribution of composition that resulted in patchy texture of garnet.

Inclusions in garnets are typically clinopyroxene, orthopyroxene (Figure 4c), corundum (Figure 4d) and spinel (Figure 4e). Mg# of garnet close to the interface with clinopyroxene inclusion (0.74) is slightly lower than Mg# of garnet next to orthopyroxene inclusion (0.76) indicating that compositional modification of garnet is higher next to clinopyroxene than next to orthopyroxene. Cr-spinel inclusions are remnants of the primary low-pressure stage that was overgrown by garnet during subduction. Pressure increase and possibly cooling governed formation of garnet on expense of spinel, clinopyroxene and orthopyroxene.

Garnets are replaced by kelyphitic rims consisting of symplectitic intergrowth of high-Al orthopyroxene, Al-rich spinel, diopside and pargasitic amphibole (Figure 4f). Chromium number (Cr*) in Al-spinel is ranging from 0.6–0.9 and is calculated from:

$$Cr^* = 100 \cdot \frac{Cr}{Cr + Al}$$

Kelyphitic assemblage around garnets formed during the exhumation-related decompression of these rocks. Decompressional breakdown of garnet caused the diffusion of Mg and Al in spinel and Ca in clinopyroxene. As a result of retrogression, garnet shows a decrease in Mg and increase in Fe.

Spinel group minerals form two generations, the brown chromian-rich spinel and the green aluminum-rich spinel. Cr-spinel occurs in the matrix (Figure 5a) and as inclusions in garnet (Figure 4d, e). Cr-spinel inclusions are remnants of the primary low-pressure stage that was overgrown by garnet (Figure 4e) during subduction due to pressure increase and possibly cooling.

The composition of Cr-spinel ranges from Al_2O_3 = 24.3–53.5 wt%, Cr_2O_3 = 13.9–38.7 wt% and Mg# = 40.7–68.2. Cr-spinel shows a weak zoning with mainly lighter rims and darker cores (Figure 5b). The lighter spinel has a higher chromium number (Cr* = 47–52) than the darker spinel (Cr* = 22–43). During the growth, garnet takes up the Al from the spinel, which consecutively becomes more Cr-rich at the rim and thus lighter in color. Al-spinel represents a second generation that may be found in symplectites, mostly with Al-orthopyroxene replacing garnet (Figure 4f). The composition of Al-spinel ranges from Al_2O_3 = 57.7–69.6 wt%, Cr_2O_3 = 0–2.8 wt%, Mg# = 76.3–85.5 and Cr* = 0–3.1.

Olivine grains are unzoned and nearly homogeneous in composition (Figure 6a). The chemical homogeneity of olivine may be explained by the fact that olivine is a mineral with fastest diffusion of elements. Fe-Mg diffusion in olivine is about two orders of magnitude faster than in pyroxene and garnet (Brenker & Brey, 1997). Olivine mainly occurs as matrix mineral sometimes containing clinopyroxene (Figure 6a) and orthopyroxene inclusions. Forsterite content of the studied olivine is ranging in very wide range from 77.0 to 91.0. Olivine contains 0.02–0.28 wt% MnO, <0.07 wt% CaO, <0.02 wt% TiO_2 and <0.15 wt% Cr_2O_3. NiO content is rather variable and is reaching up to 0.38 wt%.

Olivine is intensively fractured and broken down into smaller grains due to retrogression (Figure 6b). Cracks are filled with secondary opaque minerals. In the contact zones between olivine and garnet extensive kelyphitic coronas have been developed (Figure 6b). They consist of diopsidic clinopyroxene, orthopyroxene, Al-spinel and pargasitic amphibole. Kelyphitisation results from a metamorphic reaction between olivine and garnet during retrogression. The relative abundance of amphibole and clinopyroxene in kelyphitic rims probably reflects local fluctuations of P_{H2O} during kelyphite growth (Godard & Martin, 2000).

Orthopyroxenes occur as four different types of grains: (1) small inclusions in garnet (Figure 4c); (2) symplectitic intergrowth with Al-spinel replacing garnet (Figure 4f); (3) oriented lamellar exsolutions from clinopyroxene; and (2) individu-

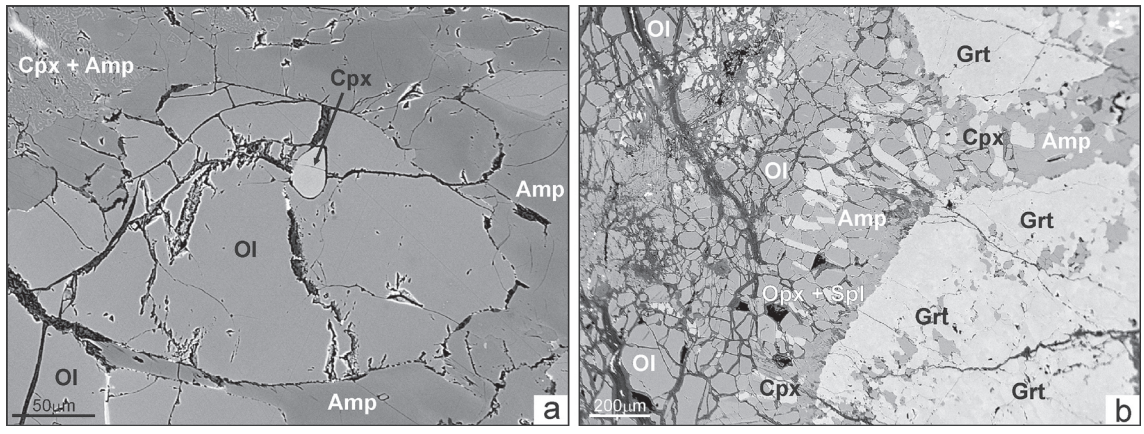

Figure 6. Olivine grains in BSE.
(a) Homogeneous olivine with small clinopyroxene inclusion.
(b) Kelyphitic corona in contact between garnet and olivine. Olivine grains are broken down into numerous individual particles due to retrogression and weathering. Cracks are often filled with opaque secondary minerals. Amp-amphibole, Cpx clinopyroxene, Grt-garnet, Ol-olivine, Opx-orthopyroxene, Spl-spinel.

al matrix grains (Figure 7). Regardless of their occurrence, grain size and textural origin, the analyzed orthopyroxene grains are very similar in composition. All orthopyroxenes are enstatites (En = 83.7–92.1) with Mg-numbers varying from 83.9 to 92.4. Al_2O_3 and Cr_2O_3 concentrations range form 0.73–2.98 wt% and 0–0.20 wt%, respectively. CaO and TiO_2 contents in all measured orthopyroxenes are low with <0.56 wt% for CaO and <0.05 wt% for TiO_2. MgO (31.67–35.70 wt%) and MnO contents are typical for worldwide orthopyroxene compositions with MnO in some cases extended to slightly higher values (up to 0.26 wt%).

Matrix orthopyroxenes are found in the form of small rounded grains (Figure 7a) or as large anhedral minerals (Figure 7b). The latter commonly reveal intracrystalline exsolution microstructures, consisting of numerous oriented ilmenite and clinopyroxene lamellas, which precipitated from a suprasaturated high-T orthopyroxene host (van Roermund et al., 2002). Exsolution lamellas exhibit parallel orientation and are concentrated in the central parts of the orthopyroxene grains. The rims of orthopyroxenes are free of exsolutions due to re-crystallization. Some of the orthopyroxenes reveal internally folded exsolution lamellas (Figure 7b), suggesting that exsolution process was either accompanied or postdated by deformation. Some matrix orthopyroxenes also contain small exsolutions of pargasitic amphibole and garnet. Interstitial garnet exsolutions show very distinct bleb-like shapes (Figure 7b) and are mostly present along the orthopyroxene exsolution-free grain boundary. They show similar microstructures to those reported from garnet websterites in Norway (van Roermund et al., 2002).

Large matrix orthopyroxene grains are often very low in Al_2O_3 content (down to 0.73 wt%), which reflects high-pressure conditions during their formation. Al content in orthopyroxene is a good diagnostic criteria for revealing pressure variations during the metamorphic evolution. In general, Al decrease can be due to increase in pressure or decrease in temperature (cooling). Inversely, increase in Al content is caused by decompression or heating. High-temperature orthopyroxenes are thus characterized by low Al and high Ca contents. In the analyzed orthopyroxenes the distribution of Al shows lowest Al and highest Ca content in the core. This indicates a decrease in

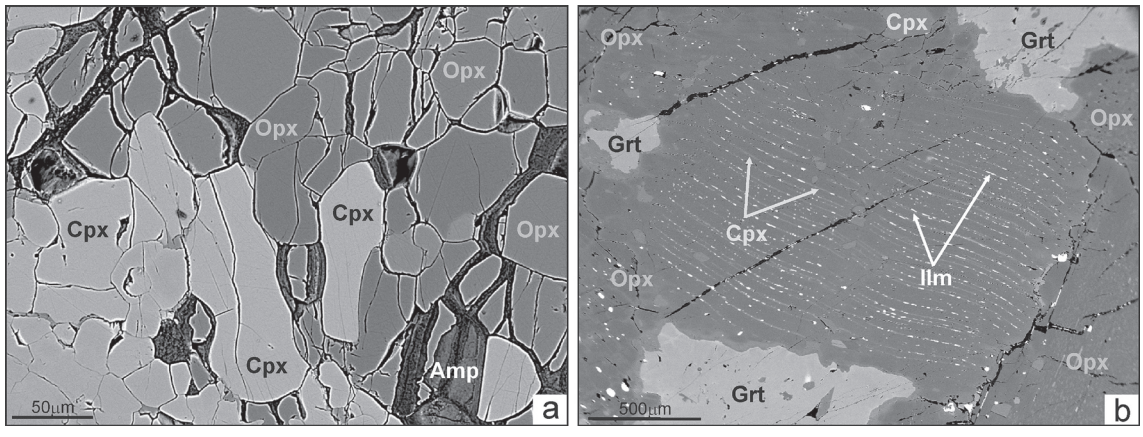

Figure 7. Matrix orthopyroxenes (BSE).
(a) Small rounded orthopyroxene grains in contact with clinopyroxenes and amphiboles.
(b) Bended exsolutions occupying the central part of orthopyroxene grain with re-crystallized, exsolution-free rim. Garnet blebs are arranged along the orthopyroxene grain boundary. Amp-amphibole, Cpx-clinopyroxene, Grt-garnet, Ilm-ilmenite, Opx-orthopyroxene.

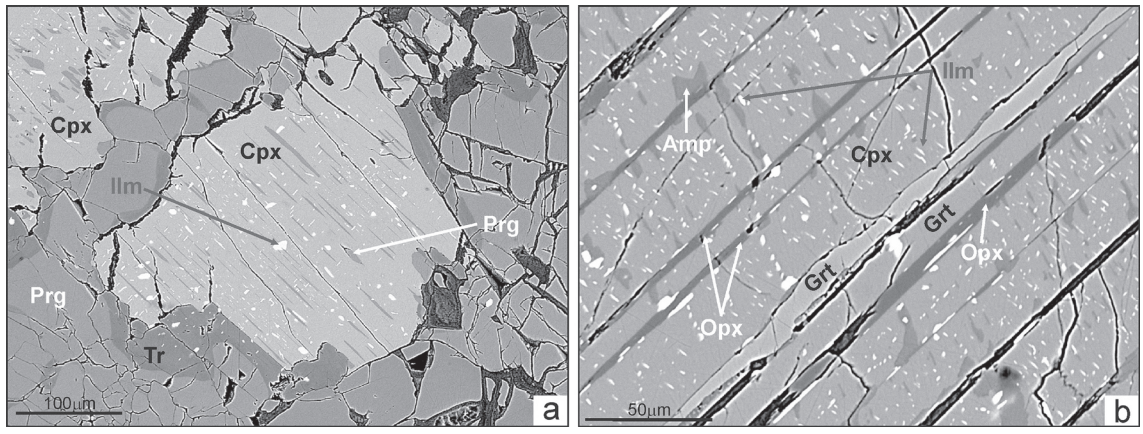

Figure 8. Matrix clinopyroxene grains (BSE).
(a) Individual matrix clinopyroxene grain is rimmed by amphibole and is representing the relict phase of primary material; clinopyroxene inclusions in olivine are also observable.
(b) Garnet, ilmenite and clinopyroxene exsolutions within orthopyroxene host exhibit a clearly visible parallel orientation; in some cases the exsolutions occur in two perpendicular sets. Amp-amphibole, Cpx-clinopyroxene, Grt-garnet, Ilm-ilmenite, Opx-orthopyroxene, Prg-pargasite, Tr-tremolite.

pressure and temperature from core to rim, consistent with exhumation and decompression of the rocks.

Clinopyroxene occurs in form of matrix grains (Figure 8a), inclusions in garnet (Figure 4c), olivine (Figure 6a) and orthopyroxene, exsolutions from orthopyroxene (Figure 7b) and in complex coronas in contact zone between olivine and garnet (Figure 6b). All analyzed clinopyroxenes are diopsides (En = 46.6–57.8, Fs = 0.1–6.1, Wo = 36.1–51.0) with Mg-numbers ranging from 90.0–99.8. They have low Na_2O and Cr_2O_3 content varying from 0.19–0.82 wt% and 0–0.67 wt%, respectively. The Al_2O_3 content is ranging from 0.73–4.87 wt% but TiO_2 content is mostly below 0.13 wt%. No significant compositional differences between clinopyroxene minerals with different occurrence and textural type can be observed. This is taken as good evidence for equilibrium conditions.

Coarse-grained matrix clinopyroxene minerals often contain numerous exsolution lamellas of garnet, low-Al orthopyroxene, ilmenite and pargasitic amphibole (Figure 8b). The size of lamellas is very varied and is ranging from very tiny rods (<10 μm) of ilmenite and orthopyroxene to larger elongated exsolutions (up to several 100 μm in length) of garnet and orthopyroxene. Amphibole and some orthopyroxene exsolutions are remarkably thicker and relatively short. The obvious intergrowth of different exsolution lamellas and the lack of a clear-cut relationship might suggest a nearly simultaneous generation (Xu et al., 2004). All garnet exsolutions lie in a direction parallel to the c axis. Some ilmenite lamellas occur in two orientations with nearly perpendicular intersections (Figure 8b), suggesting a topotactical intergrowth due to exsolution rather than being a primary intergrowth or epitaxial replacement (Zhang & Liou, 2003).

Matrix clinopyroxene grains are in most cases rimmed by amphiboles of pargasitic and tremolitic composition (Figure 8a).

Other minerals present in the analyzed garnet peridotites and pyroxenites were formed after peak pressure conditions and are related to retrogression due to the exhumation of these rocks. These are typically amphibole, chlorite, serpentine and talc. With decreasing temperature, pargasitic amphibole that is replacing clinopyroxene and which might be stable at pressure conditions up to 25 kbar, is successfully transformed to tremolite, chlorite and serpentine minerals.

Amphibole occurs in 3 different generations: (1) pargasite; (2) tremolite; and (3) gedrite. Bright Na-rich amphibole belongs to pargasite compositions with Mg-number ranging from 89.9-98.1. Pargasitic amphiboles occur around matrix clinopyroxene grains in form of retrogressive rims (Figure 8a), as exsolutions in clinopyroxene (Figure 8) and in kelyphitic intergrowth replacing the contact zone between garnet and olivine (Figure 6b). A common retrogression product of ultramafic rocks is also orthoamphibole of gedritic composition. It is known to be forming in lower amphibolite facies conditions, possibly by reactions involving chlorite. The amphibolitization process postdated the formation of symplectitic replacement rims around major mineral phases. In some cases amphibole grains resemble inclusions or have idiomorphic forms, but they are always connected to the periphery with fluid channels and are thus indisputably of secondary origin.

Chlorite, serpentine and talc formed under lowest P-T conditions as late retrogressive stages partly replacing olivine and pyroxene minerals.

Geothermobarometry

Metamorphic conditions for the formation of garnet peridotites have been calculated from a combination of the garnet-olivine (O'Neill & Wood, 1979; O'Neill, 1980) and garnet-orthopyroxene (Harley, 1984) Fe^{2+}-Mg exchange thermometers, and Al-in-orthopyroxene barometer (Brey & Köhler, 1990).

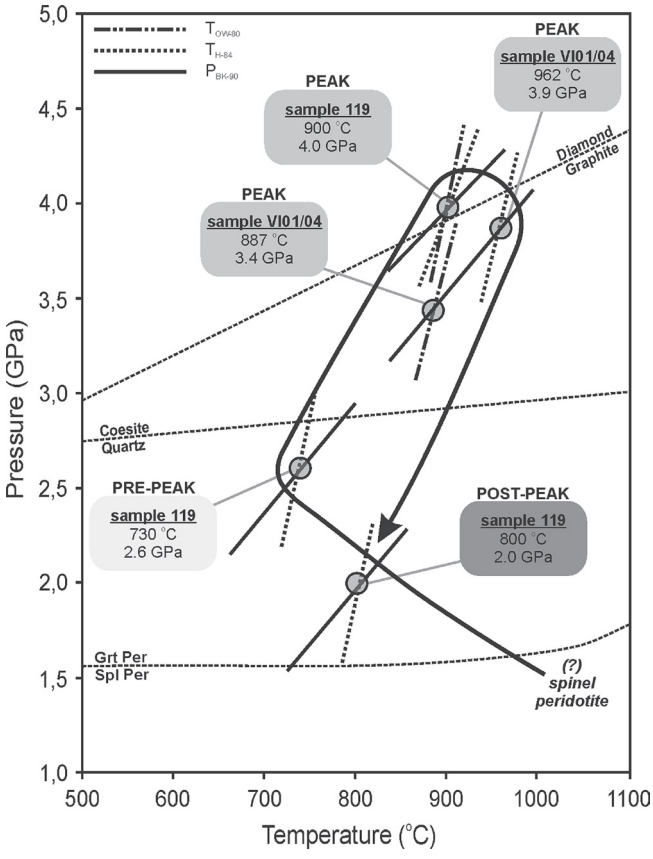

Figure 9. Estimated pressure and temperature conditions with suggested metamorphic P-T path for Pohorje garnet peridotites. A combination of garnet-olivine Fe^{2+}-Mg exchange thermobarometer (OW-80; O'Neill & Wood, 1979), garnet-orthopyroxene Fe^{2+}-Mg exchange thermobarometer (H-84; Harley, 1984), and Al-in-orthopyroxene barometer (BK-90; Brey & Köhler, 1990). Shown for reference are equilibria for diamond-graphite (Bundy, 1980), coesite-quartz (Bohlen & Boettcher, 1982), and spinel-garnet peridotite (O'Hara et al. 1971).

The initial (pre-peak) metamorphic conditions have been calculated with the application of Fe^{2+}-Mg garnet-orthopyroxene exchange thermometer together with the Al-in orthopyroxene barometer to the garnet and orthopyroxene exsolutions in primary clinopyroxene. Estimated P-T values are 730 °C at pressure of 2.6 GPa.

Porphyroblastic garnet with the highest pyrope content and orthopyroxene with the lowest Al content together with relatively homogeneous olivine have been chosen to calculate peak P-T conditions, as it is generally recommended (e.g. Brey & Köhler, 1990; Brenker & Brey, 1997; Krogh Ravna & Paquin, 2003). The results indicate that the peak of metamorphism occurred at temperatures of 887–962 °C and pressures of 3.4–4.0 GPa (Figure 9). The equilibrium P-T conditions for the sample 119 cluster in a narrow range, close to values of 900 °C and 4 GPa. There is a very good consistency between the garnet-olivine and garnet-orthopyroxene Fe^{2+}-Mg exchange thermometers for this sample. The P-T conditions for sample VI01/04, obtained from the garnet-olivine thermometer and the Al-in-orthopyroxene barometer, are 887 °C and 3.4 GPa, whereas the intersection between the garnet-orthopyroxene thermometer and the Al-in-orthopyroxene barometer yields 962 °C and 3.9 GPa. This discrepancy may result from partial disequilibrium between garnet, olivine and orthopyroxene during post-peak decompression. Additionally, since all Fe has been treated as Fe^{2+} in the calculations, the temperature obtained by garnet-orthopyroxene thermometer should only be regarded as minimum peak temperature (Harley, 1984).

The post-peak metamorphic conditions have been deduced from the composition of orthopyroxene in symplectites with Al-rich spinel that form kelyphitic rims around garnet. The garnet-orthopyroxene Fe^{2+}-Mg exchange thermometer in combination with the Al-in-orthopyroxene barometer yields P-T conditions of ~800 °C and 2 GPa.

Discussion and Conclusions

The geothermobarometrical data obtained from garnet peridotites, with peak P-T conditions of 887–962 °C and 3.4–4.0 GPa, clearly confirm the existence of UHP metamorphism in the Pohorje area. Recorded peak metamorphic conditions are in the same range as peak conditions determined for the associated kyanite eclogites (Janák et al., 2004; Vrabec, 2010). This confirms that the southeasternmost parts of the Austroalpine nappes in the Alps reached UHP metamorphic conditions during the Cretaceous orogeny at ca. 91–92 Ma. Garnet peridotites were most probably introduced to the subducting plate from the overlying mantle wedge and later on subducted further to the depths of at least 120 km.

From observed mineral assemblages and estimated P-T conditions a metamorphic P-T path can be deduced (Figure 9). The reaction textures, mineral compositions and thermobarometric evidence indicates that garnet-bearing peridotites have undergone a complex history, including at least four stages of recrystallization: protolith stage, metamorphic stage, decompression stage, and retrogression stage.

Stage I: the protolith stage, is garnet-free and is defined by assemblage of olivine + Al-orthopyroxene + Al-clinopyroxene + Cr-spinel. Al-orthopyroxene occurs as inclusions in garnet, whereas Cr-spinel is additionaly preserved in the matrix. The initial composition of the investigated peridotite most probably corresponded to spinel lherzolite. The occurrence of Cr-spinel as inclusions in garnet indicates that garnet peridotites evolved from spinel-bearing protolith, which could therefore represent pieces of intermediate to shallow-level lithospheric mantle.

Stage II: the metamorphic stage, is defined by the matrix assemblage of garnet + clinopyroxene + orthopyroxene + olivine + Cr-spinel. Garnet occurs as coronas around Cr-spinel, as exsolutions from clinopyroxene, and as large porphyroblasts in the matrix. Primary, coarse-grained clinopyroxene contains exsolution rods of garnet, low-Al

orthopyroxene, pargasitic amphibole, Cr-spinel and ilmenite.

Formation of garnet exsolutions from clinopyroxene could have started at P-T conditions of about 700–750 °C and 2.5 GPa, as deduced from geothermobarometry. The exsolution process may correspond to the incorporation of peridotite from the overlying mantle wedge into subducting crust. The interaction between the hot mantle and the relatively colder subducting crust probably caused nearly isobaric cooling from spinel to garnet stability field. Similar exsolutions have been observed in other HP and UHP ultramafic rocks, e.g. garnet peridotite and pyroxenite from Nonsberg area, Eastern Alps (Godard et al., 1996), garnet clinopyroxenite from Sulu, eastern China (Zhang & Liou, 2003) and garnet websterite from Bardane, western Norway (Carswell & van Roermund, 2005). The formation of exsolutions in clinopyroxene is undoubtedly caused by reactions driven by changes in temperature and pressure, but the accurate conditions are difficult to estimate. The parent phase of such intergrowths of clinopyroxene + garnet + ilmenite could have been the primary clinopyroxene (Zhang & Liou, 2003). Formation of garnet lamellas in clinopyroxene has generally been interpreted as a result of exsolution from primary clinopyroxene (Dawson & Reid, 1970; Harte & Gurney, 1975; Sautter & Harte, 1988). According to experimental work of Harte & Gurney (1975) a single clinopyroxene is stable in a wedge shaped P-T stability field below the solidus (~3.4–3.8 GPa at 1380–1400 °C; 2.6 GPa at 1370 °C). With decreasing temperature, garnet first appears at ~1400 °C and 3.4–3.6 GPa, joining the clinopyroxene and forming a clinopyroxene + garnet assemblage. Hence, the exsolution of garnet from clinopyroxene has been suggested to be related mainly to cooling from near-solidus conditions toward normal mantle lithosphere temperatures. Although the effect of Ti was not evaluated in Harte & Gurney (1975) experiments, a similar clinopyroxene precursor of the garnet + ilmenite + clinopyroxene intergrowth is suggested, as the solubility of clinopyroxene ($CaMgSi_2O_6$) in garnet is limited except for majorite formed at very high pressures (see Fig. 6 in Zhang & Liou, 2003).

During the peak of metamorphism large porphyroblastic garnet was formed from primary, Al-bearing phases such as spinel, clinopyroxene and orthopyroxene. The increased chromium content in the rims implies that Cr-rich spinel (Cr* = c. 50) remained stable at peak metamorphic conditions, since chromium moves the spinel-garnet transition boundary towards higher pressures (Webb & Wood, 1986; Klemme, 2004). P-T conditions of the peak metamorphic stage calculated from geothermobarometry are 887–962 °C and 3.4–4.0 GPa, that is well within the stability field of coesite.

Stage III: the decompression stage, occurred after peak pressure conditions and is manifested by formation of kelyphitic rims of high-Al orthopyroxene, Al-spinel, diopside and pargasitic amphibole replacing garnet. After having reached their metamorphic peak, the garnet peridotites were exhumed to mid-crustal levels. The composition of orthopyroxene in symplectites with Al-rich spinel was used to obtain P-T conditions during decompresion. The garnet-orthopyroxene Fe^{2+}-Mg exchange thermometer in combination with the Al-in-orthopyroxene barometer yields P-T conditions of ~800 °C and 2 GPa.

Stage IV: the retrogression stage, occurred under lowest P-T conditions and is characterized by the formation of tremolitic amphibole, gedrite, chlorite, serpentine and talc. Pargasitic amphibole was partly replaced by tremolite, pyroxene by serpentine and chlorite, and olivine by serpentine and talc. It is assumed that pressure and temperature further decreased during this stage. The increased activity of H_2O caused retrogression under low P-T conditions.

References

Becker, H. 1993: Garnet peridotite and eclogite Sm-Nd mineral ages from the lepontine dome (Swiss Alps): new evidence for Eocene high-pressure metamorphism in the central Alps. Geology (New York) 21: 599–602.

Bohlen, S.R. & Boettcher, A.L. 1982: The quartz-coesite transformation: A precise determination and effects of other components. J. Geophys. Res. (Washington) 87: 7073–7078.

Brenker, F.E. & Brey, G.P. 1997: Reconstruction of the exhumation path of the Alpe Arami garnet-peridotite body from depths exceeding 160 km. J. Metamorphic Geol. (Oxford) 15: 581–592.

Brey, G.P. & Köhler, T. 1990: Geothermobarometry in four-phase lherzolites II. New thermometers, and practical assessment of existing thermobarometers. J. Petrol. (Oxford) 31: 1353–1378.

Brueckner, H.K. & Medaris, L.G. 2000: A general model for the intrusion and evolution of 'mantle'garnet peridotites in high-pressure and ultra-high-pressure metamorphic terranes. J. Metamorphic Geol. (Oxford) 18: 123–133.

Bundy, F.R. 1980: The P, T phase and reaction diagram for elemental carbon. J. Geophys. Res. (Washington) 85: 6930–6936.

Canil, D. & O'Neill H. St. C. 1996: Distribution of ferric iron in some upper mantle assemblages. J. Petrol. (Oxford) 37: 609–635.

Carswell, D.A. & Gibb, F.G.F. 1987: Evaluation of mineral thermometers and barometers applicable to garnet lherzolite assemblages. Contrib. Mineral. Petrol. (Berlin) 95: 499–511.

Carswell, D.A. & Compagnoni, R. 2003: Introduction with review of the definition, distribution and geotectonic significance of ultrahigh-pressure metamorphism. In: Carswell, D.A. & Compagnoni, R. (eds.): Ultra-high pressure metamorphism. EMU Notes in Mineralogy, 5. Eötvös University Press (Budapest): 1–508 cd-rom.

Carswell, D.A. & van Roermund, H.L.M. 2005: On multi-phase mineral inclusions associated with microdiamond formation in mantle-derived

peridotite lens at Bardane on Fjortoft, west Norway. Eur. J. Mineral. (Stuttgart) 17: 31–42.

Chopin, C. 2003: Ultrahigh-pressure metamorphism: tracing continental crust into the mantle. Earth Planet. Sci. Lett. (Amsterdam) 212: 1–14.

Dawson, J.B. & Reid, A.M. 1970: A pyroxene-ilmenite intergrowth from the Monastery Mine, South Africa. Contrib. Mineral. Petrol. (Berlin) 26: 296–301.

Dobrzhinetskaya, L.F., Green, H.W. & Wang, S. 1996: Alpe Arami: a Peridotite Massif from depths of more than 300 km. Science (Washington) 271: 1841–1845.

Ernst, W.G. 1978: Petrochemical study of lherzolitic rocks from the Western Alps. J. Petrol. (Oxford) 19: 341–392.

Fodor, L., Jelen, B., Márton, E., Zupančič, N., Trajanova, M., Rifelj, H., Pécskay, Z., Balogh, K., Koroknai, B., Dunkl, I., Horváth, P., Vrabec, M., Kraljič, M. & Kevrič, R. 2002: Connection of Neogene basin formation, magmatism and cooling of metamorphics in NE Slovenia. Geol. Carpathica (Bratislava) 53: 3 cd-rom.

Fodor, L., Balogh, K., Dunkl, I., Pécskay, Z., Koroknai, B., Trajanova, M., Vrabec, M., Vrabec, M., Horváth, P., Janák, M., Lupták, B., Frisch, W., Jelen, B. & Rifelj, H. 2003: Structural evolution and exhumation of the Pohorje-Kozjak Mts., Slovenia. Annales Universitatis Scientarum Budapestinensis, Sectio Geologica (Budapest) 35: 118–119.

Fodor, L., Gerdes, A. ,Dunkl, I., Koroknai, B., Pécskay, Z., Trajanova, M., Balogh, K., Horváth, P., Jelen, B., Vrabec, M. & Vrabec, M. 2007: Formation age, exhumation and deformation of the Pohorje pluton: implications for Cretaceous and Miocene deformations of the Eastern Alps - Pannonian basin junction. Abstract volume, 8th Workshop on Alpine Geological Studies, Davos, 10.-12. October 2007, (Davos): 18–19.

Gebauer, D. 1996: A P-T-t path for an (ultra?) high pressure ultramafic/mafic rock-association and its felsic countrz-rocks based on SHRIMP-dating of magmatic and metamorphic zircon domains. Example: Alpe Arami (Central Swiss Alps). In Basau, A. & Hart, S. (eds.): Earth Processes. Reading the Isotopic Code. American Geophysical Union (Washington), Geophysical Monograph 95: 307–329.

Godard, G. & Martin, S. 2000: Petrogenesis of kelyphites in garnet peridotites: a case study from the Ulten zone, Italian Alps. J. Geodynamics (New York) 30: 117–145.

Godard, G., Martin, S., Prosser, G., Kienast, J.R. & Morten, L. 1996: Variscan migmatites, eclogites and garnet-peridotites of the Ulten zone, Eastern Austroalpine system. Tectonophysics (New York) 259: 313–341.

Harley, S.L. 1984: An experimental study of the partitioning of Fe and Mg between garnet and orthopyroxene. Contrib. Mineral. Petrol. (Berlin) 86: 359–373.

Harte, B. & Gurney, J.J. 1975: Evolution of clinopyroxene and garnet in an eclogite nodule from the Roberts Victor kimberlite pipe, South Africa. Physics and Chemistry of the Earth (New York) 9: 367–387.

Hinterlechner-Ravnik, A. 1987: Granatov peridotit na Pohorju. Geologija (Ljubljana) 30: 149–181.

Hinterlechner-Ravnik, A., Sassi, F.P. & Visona, D. 1991: The Austridic eclogites, metabasites and metaultrabasites from the Pohorje area (Eastern Alps, Yugoslavia): 2. 2. The metabasites and metaultrabasites, and concluding considerations. Rendiconti Fisiche Accademia Lincei (Milano) 2: 175–190.

Hoinkes, G., Koller, F., Rantitsch, G., Dachs, E., Höck, V., Neubauer, F. & Schuster, R. 1999: Alpine metamorphism of the Eastern Alps. Schweiz. Mineral. Petrogr. Mitt. (Zürich) 79: 155–181.

Janák, M., Froitzheim, N., Lupták, B., Vrabec, M. & Krogh Ravna, E.J. 2004: First evidence for ultrahigh-pressure metamorphism of eclogites in Pohorje, Slovenia: Tracing deep continental subduction in the Eastern Alps. Tectonics, (Washington) 23: TC5014, doi:10.1029/2004TC001641.

Janák, M., Froitzheim, N., Vrabec, M., Krogh Ravna, E.J. & De Hoog, J.C.M. 2006: Ultrahigh-pressure metamorphism and exhumation of garnet peridotite in Pohorje, Eastern Alps. J. Metamorphic Geol. (Oxford) 24/1: 19–31.

Janák, M., Cornell, D., Froitzheim, N., De Hoog, J.C.M., Broska, I., Vrabec, M., Hurai, V. 2009: Eclogite-hosting metapelites from the Pohorje Mountains (Eastern Alps): P-T evolution, zircon geochronology and tectonic implications. Eur. J. Mineral. (Stuttgart) 21/6: 1191–1212.

Klemme, S. 2004: The influence of Cr on the garnet-spinel transition in the Earth's mantle: experiments in the system MgO-Cr_2O_3-SiO_2 and thermodynamic modelling. Lithos (Amsterdam) 77: 639–646.

Krogh Ravna, E.J. & Paquin, J. 2003: Thermobarometric metodologies applicable to eclogites and garnet ultrabasites. In: Carswell, D.A. & Compagnoni, R. (eds.): Ultra-high pressure metamorphism. EMU Notes in Mineralogy, 5. Eötvös University Press (Budapest): 1–508 cd-rom.

Liou, J.G., Hang, W.G.E., Rumble, D. & Maruyama, S. 1998: High-pressure minerals from deeply subducted metamorphic rocks. In: Hemley, R.J. (ed.): Ultrahigh pressure mineralogy: Physics and chemistry of the Earth's deep interior. Reviews in Mineralogy, 37. Mineral. Soc. Am.: (Washington): 33–96.

Medaris, L.G. 2000: Garnet peridotites in Eurasian high-pressure and ultrahigh-pressure terranes: A diversity of origins and thermal histories. In: Ernst, W.G. & Liou, J.G. (eds.): Ultrahigh-pressure metamorphism and geodynamics in collision-type orogenic belts. International Book Series 4. Geol. Soc. Am. (New York): 57–73.

Miller, C. & Thöni, M. 1997: Eo-Alpine eclogitisation of Permian MORB-type gabbros in the Koralpe (Eastern Alps, Austria): new geochronological, geochemical and petrological data. Chem. Geol. (New York) 137: 283–310.

Miller, C., Mundil, R., Thöni, M. & Konzett, J. 2005: Refining the timing of eclogite metamorphism: a geochemical, petrological, Sm-Nd and U-Pb case study from the Pohorje Mountains, Slovenia (Eastern Alps). Contrib. Mineral. Petrol. (Berlin) 150: 70–84.

Mioč, P. & Žnidarčič, M. 1977: Osnovna geološka karta SFRJ, list Slovenj Gradec, 1 : 100.000. Zvezni geološki zavod (Beograd).

Neubauer, F. & Höck, V. 2000: Aspects of geology in Austria and adjoining areas: introduction. Mitt. Öster. Min. Ges. (Vienna) 92: 7–14.

Nickel, K.G. & Green D.H. 1985: Empirical geothermobarometry for garnet peridotites and applications for the nature of the lithosphere, kimberlites and diamonds. Earth Planet. Sci. Lett. (Amsterdam) 73: 158–170.

Nimis, P. & Morten, L. 2000: P-T evolution of 'crustal' garnet peridotites and included pyroxenites from Nonsberg area (upper Austroalpine), NE Italy: from the wedge to the slab. J. Geodynamics (New York) 30: 93–115.

Nimis, P. & Trommsdorff, V. 2001: Revised thermobarometry of Alpe Arami and other garnet peridotites from the Central Alps. J. Petrol. (Oxford) 42: 103–115.

Obata, M. & Morten, L. 1987: Transformation of spinel lherzolite to garnet lherzolite in ultrmafic lenses of the austridic crystalline complex, Northern Italy. J. Petrol. (Oxford) 28: 599–623.

O'Hara, M.J., Richardson, S.W. & Wilson, G. 1971: Garnet-peridotite stability and occurrence in crust and mantle. Contrib. Mineral. Petrol. (Berlin) 32: 48–68.

O'Neill, H.St.C. 1980: An experimental study of Fe-Mg partitioning between garnet and olivine and its calibration as a geothermometer: corrections. Contrib. Mineral. Petrol. (Berlin) 72: 337.

O'Neill, H.St.C. & Wood, B.J. 1979: An experimental study of Fe-Mg partitioning between garnet and olivine and its calibration as a geothermometer. Contrib. Mineral. Petrol. (Berlin) 70: 59–70.

Paquin, J. & Altherr, R. 2001: New constraints on the P-T evolution of the Alpe Arami garnet peridotite body (Central Alps, Switzerland). J. Petrol. (Oxford) 42: 1119–1140.

Sautter, V. & Harte, B. 1988: Diffusion gradients in an eclogite xenolith from the Roberts Victor kimberlite pipe: 1. Mechanism and evolution of garnet exsolution in Al_2O_3-rich clinopyroxene. J. Petrol. (Oxford) 29: 1325–1352.

Schmid, S.M., Fügenschuh, E., Kissling, E. & Schuster, R. 2004: Tectonic map and overall architecture of the Alpine orogen. Eclog. Geol. Helv. (BAsel) 97: 93–117.

Schuster, R., Koller, F., Hoecke, V., Hoinkes, G. & Bousquet, R. 2004: Metamorphic structure of the Alps: Eastern Alps. In: Oberhänsli, R. (ed.): Explanatory notes to the Map of Metamorphic Structures of the Alps. Mitt. Öster. Min. Ges. (Vienna) 149: 175–199.

Takahashi, E. 1986: Melting of a dry peridotite KLB-1 up to 14 GPa: Implications on the origin of peridotitic upper mantle. J. Geophys. Res. (WAshington) 91: 9367–9382.

Thöni, M. 2002: Sm-Nd isotope systematics in garnet from different lithologies (Eastern Alps): age results, and an evaluation of potential problems for garnet Sm-Nd chronometry. Chem. Geol. (New York) 185: 255–281.

Thöni, M. & Jagoutz, E. 1992: Some new aspects of dating eclogites in orogenic belts: Sm-Nd, Rb-Sr, and Pb-Pb isotopic results from the Austroalpine Saualpe and Koralpe type locality (Carinthia/Styria, southeastern Austria). Geochim. Cosmochim. Acta (New York) 56: 347–368.

Thöni, M. & Miller, C. 1996: Garnet Sm-Nd data from the Saualpe and the Koralpe (Eastern Alps, Austria): chronological and P-T constraints on the thermal and tectonic history. J. Metamorphic Geol. (Oxford) 14: 453–466.

Trajanova, M., Pécskay, Z., Itaya, T. 2008: K-Ar geochronology and petrography of the Miocene Pohorje Mountains batholith (Slovenia). Geol. Carpath. (Bratislava) 59: 247–260.

Tumiati, S., Thöni, M., Nimis, P., Martin, S. & Mair, V. 2003: Mantle-crust interactions during Variscan subduction in the Eastern Alps (Nonsberg-Ulten zone): geochronology and new petrological constraints. Earth Planet. Sci. Lett. (Amsterdam) 210: 509–526.

Van Roermund, H.L.M. & Drury, M.R. 1998: Ultrahigh pressure (P>6 GPa) garnet peridotites in Western Norway: exhumation of mantle rocks from >185 km depth. Terra Nova (Oxford) 10: 295–301.

Van Roermund, H.L.M., Carswell, D.A., Drury, M.R. & Heijboer, T.C. 2002: Micro-diamonds in a megacrystic garnet-websterite pod from Bardane on the island of Fjørtoft, western Norway. Geology (New York) 30: 959–962.

Visona, D., Hinterlechner-Ravnik, A. & Sassi, F.P. 1991: Geochemistry and crustal P-T polymetamorphic path of the mantle-derived rocks from the Pohorje area (Austrides, Eastern Alps, Slovenia). Mineralia Slovaca (Bratislava) 23: 515–525.

Vrabec, M. 2010: Pohorje eclogites revisited: Evidence for ultrahigh-pressure metamorphic conditions. Geologija (Ljubljana) 53/1: see this issue.

Webb, S.A. & Wood, B.J. 1986: Spinel-pyroxene-garnet relationships and their dependence on Cr/Al ratio. Contrib. Mineral. Petrol. (Berlin) 92: 471–480.

Xu, W., Liu, X., Wang, Q., Lin, J. & Wang, D. 2004: Garnet exolution in garnet clinopyroxenite and clinopyroxenite xenoliths in early Cretaceous intrusions from the Xuzhou region, eastern China. Mineralogical Magazine (London) 68/3: 443–453.

Zhang, R.Y., Liou, J.G. & Cong B. 1994: Petrogenesis of garnet-bearing ultramafic rocks and associated eclogites in the Su-Lu ultrahigh-P metamorphic terrane, eastern China. J. Metamorphic Geol. (Oxford) 12: 169–186.

Zhang, R.Y. & Liou, J.G. 2003: Clinopyroxenite from the Sulu ultrahigh-pressure terrane, eastern China: Origin and evolution of garnet exolution in clinopyroxene. Am. Mineral. (Washington) 88: 1592–1600.

Zupančič, N. 1994. Petrografske značilnosti in klasifikacija pohorskih magmatskih kamnin. Rudarsko metalurški zbornik (Ljubljana) 41: 101–112.

GEOLOGIJA *53/1*, 37–46, Ljubljana 2010

Geochemical characteristics of surface waters and groundwaters in the Velenje Basin, Slovenia

Geokemične značilnosti površinskih in podzemnih vod v Velenjskem bazenu

Tjaša KANDUČ[1], Sergej JAMNIKAR[2] & Jennifer McINTOSH[3]

Prejeto / Received 1. 3. 2010; Sprejeto / Accepted 15. 5. 2010

[1]Department of Environmental Sciences, Jožef Stefan Institute, Jamova 39, SI-1000 Ljubljana, Slovenia;
e-mail: tjasa.kanduc@gmail.com
[2]Velenje Coal Mine, Partizanska 78, SI-3320 Velenje, Slovenia
[3]Department of Hydrology and Water Resources, University of Arizona, 1133 E. James E. Rogers Way, Tucson, Arizona, USA

Key words: geochemistry, stable isotopes, carbon, surface waters, groundwaters, Velenje basin, Slovenia
Ključne besede: geokemija, stabilni izotopi, ogljik, površinske vode, podzemne vode, Velenjski bazen, Slovenija

Abstract

The geochemical and isotopic composition of surface water and groundwaters in the Velenje Basin, Slovenia, were investigated to gain a better understanding of the origin of surface and groundwaters. Surface waters and groundwaters from the Triassic aquifer are dominated by HCO_3^-, Ca^{2+}, and Mg^{2+} from dissolution of carbonate minerals, while groundwaters from the Pliocene and Lithotamnium aquifers have distinct geochemical signatures, enriched in Na^+ and K^+. Surface waters are controlled by calcite dissolution, while groundwaters from the Triassic aquifer are controlled by dolomite dissolution. The partial pressure of CO_2 in surface waters and groundwaters is well above atmospheric concentrations, indicating that these waters are a potential source of CO_2 to the atmosphere. The $\delta^{13}C_{DIC}$ values of surface waters are shown to be controlled by biogeochemical processes in the terrestrial environment, such as dissolution of carbonates, degradation of organic matter, and exchange with atmospheric CO_2, which is more pronounced in the lake waters. The $\delta^{13}C_{DIC}$ values of groundwater from the Triassic aquifer are consistent with degradation of CO_2 and dissolution of dolomite. Groundwaters from the Pliocene and Lithotamnium aquifers have $\delta^{13}C_{DIC}$ values suggestive of biogenic CO_2 reduction and degradation of organic matter.

Izvleček

Raziskane so bile geokemijske in izotopske značilnosti površinskih in podzemnih vod v Velenjskem bazenu. Površinske vode in podzemne vode, ki pripadajo triasnemu vodonosniku imajo kemijsko sestavo HCO_3^--Ca^{2+}-Mg^{2+}, medtem ko imajo podzemne vode, ki pripadajo pliocenskemu in litotamnijskemu vodonosniku drug vir napajanja in so obogatene z Na^+ in K^+. Kemijsko sestavo površinskih vod kontrolira raztapljanje kalcita, medtem ko je kemijska sestava triasnih podzemnih vod kontrolirana z raztapljanjem dolomita. Parcialni tlak je nad atmosferskim CO_2 v površinskih in podzemnih vodah in predstavlja vir CO_2 v ozračje. Vrednosti $\delta^{13}C_{DIC}$ v površinskih vodah so odvisne od biogeokemijskih procesov v terestričnem okolju: raztapljanje karbonatov, razgradnja organske snovi in izmenjava z atmosferskim CO_2, ki se odraža v jezerih. Na vrednosti $\delta^{13}C_{DIC}$ v triasnih vodonosnikih vplivajo razgradnja organske snovi in raztapljanje dolomita, medtem ko na vrednosti $\delta^{13}C_{DIC}$ v pliocenskih in litotamnijskih vodonosnikih vplivata razgradnja organske snovi in bakterijska CO_2 redukcija.

Introduction

The geochemical study of river water allows important information to be obtained on chemical weathering of rocks and soil and the chemical and isotopic compositions of the drainage basin (Gibbs, 1972; Reeder et al., 1972; Hu et al., 1982; Stallard & Edmond, 1983; Goldstein & Jacobsen, 1987; Elderfield et al., 1990; Zhang et al., 1995; Huh et al., 1998). Since carbonate weathering largely dominates the chemistry of river waters, characterization of the water chemistry of rivers draining carbonate-dominated terrain is crucial to precisely identify the various contributions of the different sources to water solutes (Fairchild et al., 1999, 2000; Gaillardet et al., 1999; Liu & Zhao, 2000). Surface water hydrochemistry depends on multiple natural factors such as the intensity and composition of precipitation, chemical reactions between water and soil or sediment, biochemical reactions, and surface water-groundwater interactions, as well

as on anthropogenic activities. The use of stable isotopes of carbon as an additional method is crucial to evaluate biogeochemical processes in rivers (Brunke & Gauser, 1997; Sophacleous, 2002; Wachinew, 2006).

Many hydrogeological studies use stable isotopes of the water molecule to determine groundwater quality, origin, recharge mechanisms, and rock-water interactions. Stable isotopes of carbon, nitrogen and sulphur can give valuable information about reactions involving these elements and to trace biogeochemical processes in aquatic systems (Adelana, 2005). The isotopic characterization of the groundwater is also needed to fully evaluate the processes and origin of gases in coal basins (Aravena et al., 2003).

This paper analyses several lines of evidence, including hydrogeological, chemical, and isotopic information on surface and groundwaters to evaluate different sources of fluids in the Velenje basin. This study represents the systematic study of geochemical (chemical and isotopic) variables of surface and groundwaters and is also a part of major project aimed at evaluating the hydrogeology and hydrochemistry of a coal seam gas (CSG) exploration area and searching for locations of the Velenje basin most appropriate for CO_2 sequestration.

Study area

The study area and geological sketch map are represented on Figure 1 A. The Velenje Basin is situated in the NE part of Slovenia. It is located at the junction of the WNW – ESE – trending Šoštanj Fault and the E – W trending Periadriatic Fault Zone, bounded to the south by the Smrekovec Fault segment. The Šoštanj and Smrekovec Faults were generated due to the collision of continental plates. The study area is within the Southern Karavanke. In the pre – Pliocene basement of the basin, Triassic limestones and dolomites prevail on the north-eastern side of the Velenje Fault. Oligocene to Miocene clastic strata, consisting predominantly of marls, sandstones and volcanoclastics prevail on the south-western side (Figure 1 A). More details about Velenje Basin geology, petrology and tectonics are presented in Brezigar et al., 1988; Markič & Sachsenhofer, 1997, Vrabec, 1999 and the references therein. The age of the groundwater in the Triassic section of the basin was previously investigated by Veselič & Pezdič, 1998, while statistical processing of chemical data of different groundwaters of the Velenje Basin was published in Mali, 1992.

The three artificial lakes investigated in this paper (Lake Velenje, 54 m deep on average; Lake Škale and Lake Družmirje) were formed due to excavation of coal and subsidence of the terrain (Figure 1 B). Lake Velenje was polluted by introduction of ash, transported from the Šoštanj power plant, up until 1983. The lake waters reached a pH of 12. Beginning in 1994, a closed system of deashing was constructed for the power plant, and the quality of surface waters has since improved (Šterbenk & Ramšak, 1995).

The headwaters of the River Paka are in the Volovica on Pohorje Mountain. The streams Bečovnica, Velunja and Toplica flow into the River Paka through Pliocene and Quaternary sediments (Figure 1 B). The River Paka tends to be characterized by flash floods (torrential runoff events), with the highest discharge in the spring (3.52 m^3/s) and the lowest discharge in the summer (1.86 m^3/s). Upstream of the cities of Velenje and Šoštanj, the River Paka is relatively pristine. Near Velenje and Šoštanj, the River Paka becomes highly polluted from sewage sludge discharge (Gams & Zupan,

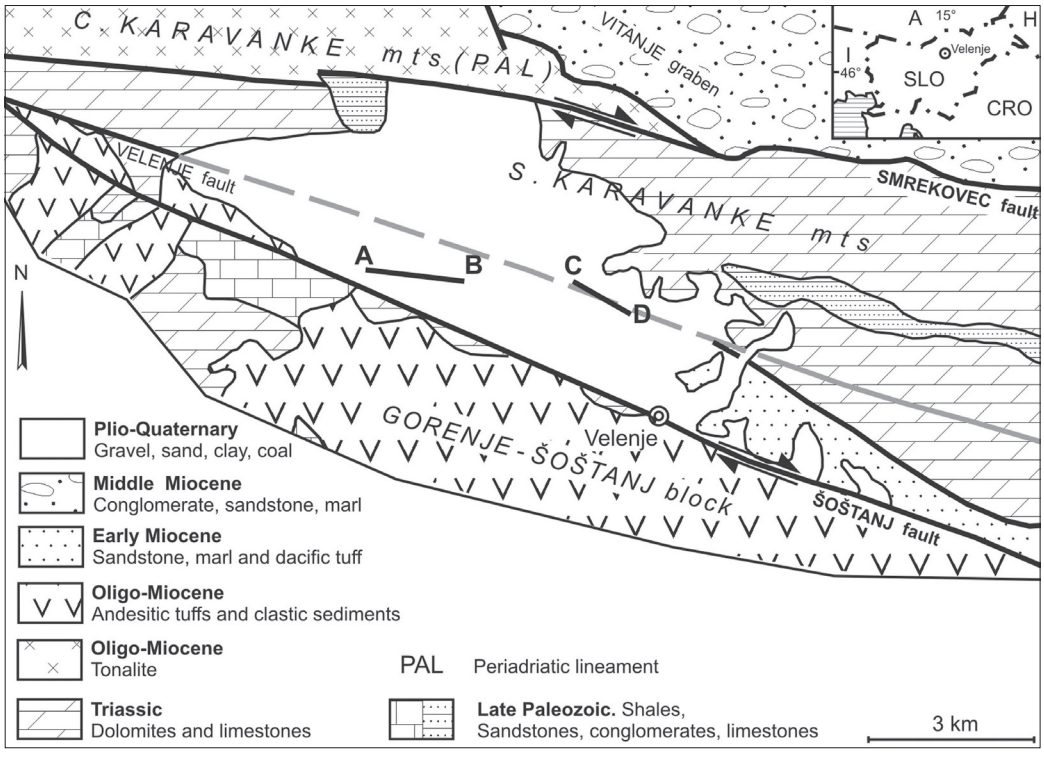

Figure 1 A. Geological sketch map of the Velenje Basin is also presented. Profiles A-B and C-D present locations of groundwater sampling.

1994). In the Velenje area the watershed of the River Paka is composed of Triassic limestone and Pliocene and Quaternary sediments.

The headwaters of the River Velunja drain rocks and sediments of the Velunja overthrust belt, composed of sericite and chlorite schist with sandstones and diabase of Ordovician and Devonian age. In the central part of the River Velunja drainage area, the watershed is composed of rocks of Miocene age, which were deposited on Devonian schist, composed of conglomerate, sandstones and clays. In its lower reach the River Velunja drains Pliocene and Quaternary sediments composed of sands, clays and gravels (Mioč & Žnidarčič, 1972). The gravels are composed of magmatic and metamorphic rocks, which were eroded from the upper part of the watershed.

The watershed of Rivers Bečovnica and Klančica are composed of limestone, breccias, and sandstones of Permian age and Pliocene and Quaternary sediments composed of gravel and sandy clays. The watersheds of streams Toplica, Lepena, Ljubela are composed of Triassic massive limestone in their upper reaches, while their lower reaches are composed of Pliocene and Quaternary gravels. Discharge from the Topolšica thermal spring contributes to Toplica stream waters. Thermal waters are 29 and 31 °C, discharge at approximately 28 l/s, and come to the surface at the section between the Smrekovec Fault and cross section faults between the contact of Triassic limestone and impermeable Tertiary sediments (Mioč & Žnidarčič, 1972).

Profiles A-B and C-D are presented on Figures 1 A and B. The Velenje coalmine in the Velenje Basin is separated into two parts: the Preloge coalmine and the Škale coalmine; the latter was closed for mining in the year 2008 (Figure 1 B). Groundwater in the Velenje coalmine is drained by hanging filters to prevent ingress of water into the mine. The average discharge of water from Pliocene sands varies from 490 l/min, the average discharge of water from Litotamnium limestone is 24 l/min and the average discharge from Triassic limestone is 236 l/min (Jamnikar & Fijavž, 2006). In the Velenje coal basin, the shallow aquifers are classified as Quaternary or Pliocene aquifers. Pliocene aquifers, found in the Preloge coalmine, are further divided into: 1) aquifers right above the coal (Pl 1), 2) aquifers 20-80 m above the coal (Pl 2), and upper Pliocene aquifers (Pl 3). The Pliocene aquifers are composed of clastic sediments, such as sand and gravel. The northern part of the Preloge coalmine, on the southern side of the Velenje Fault, is underlain by the Lithotamnium limestone (Oligocene and Miocene age) (Figures 1 A and C). The Lithotamnium limestone forms a local lens-shaped aquifer, which is confined by an impermeable barrier. The Škale coalmine contains a Triassic aquifer composed of Scythian and Anisian age limestone and dolomite (Figures 1A and C), which is of interest for water supply management (Fijavž, 2002).

Materials and methods

Sample collection

A map of the sampling locations of surface waters is presented on Figure 1 B. A map of sampling locations of groundwaters is presented on Figure 1 B. Sampling of surface waters and groundwaters was performed in October 2003. Water samples from 10 surface water locations, 3 lakes, and 7 streams were collected (Table 1, Fig. 1B). In addition, 31 groundwaters were collected from Pliocene aquifers (16 samples from P11 and P12 aquifers), 13 groundwaters were collected from Triassic aquifers and 2 groundwaters were collected from Litotamnium aquifers. All water samples were analyzed for geochemical and stable isotopic parameters (Table 2, Fig. 2A). Temperature and pH were measured in the field. Because pH is sensitive

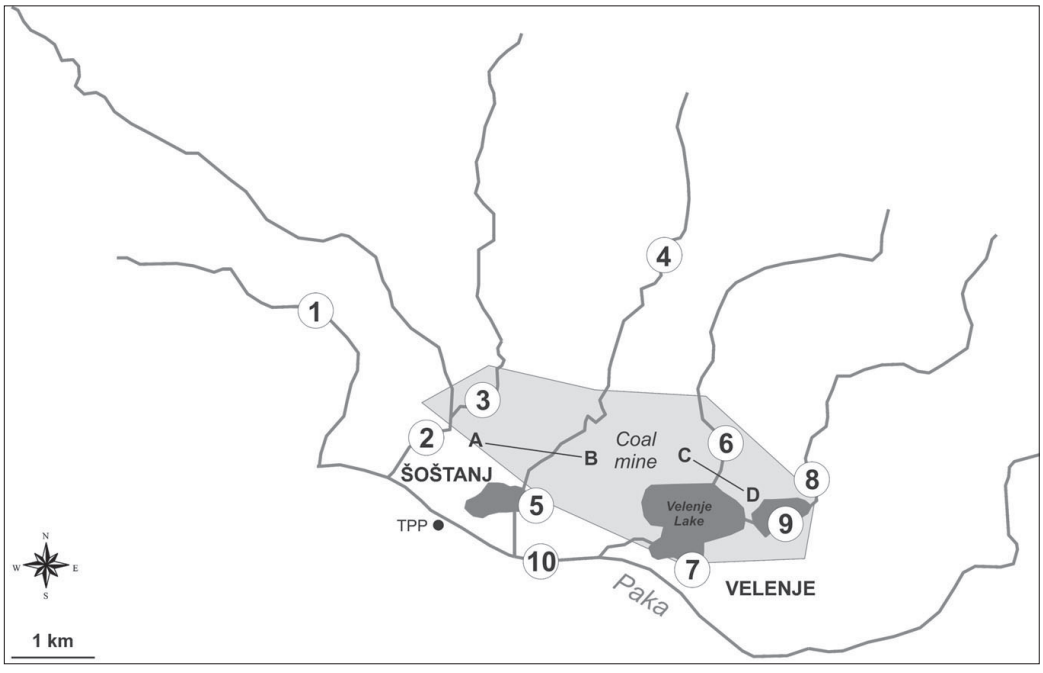

Figure 1 B. Map of surface water sampling locations. Numbers of location correspond to Table 1.

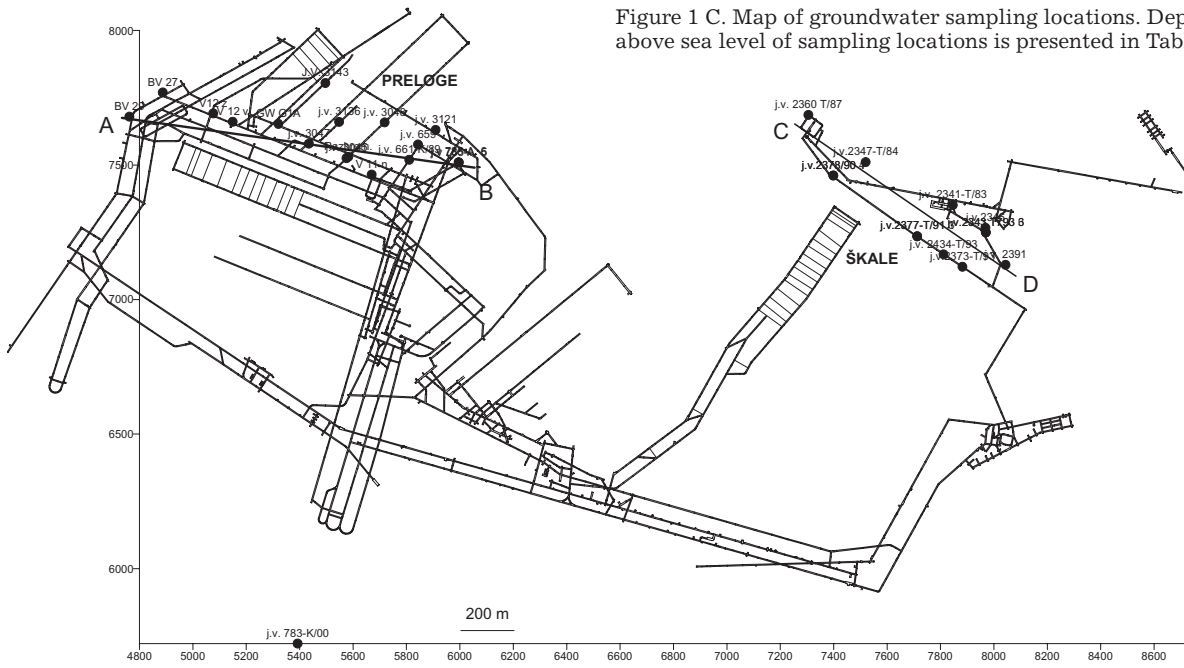

Figure 1 C. Map of groundwater sampling locations. Depth above sea level of sampling locations is presented in Table 2.

Table 1. Chemical and isotopic data for surface waters in the Velenje Basin

Sampling point	Location	T (°C)	pH	Total alkalinity (meq/l)	Ca^{2+} (mM)	Mg^{2+} (mM)	Na^{+} (mM)	K^{+} (mM)	Si (mM)	SO_4^{2-} (mM)	NO_3^{-} (mM)	Cl^{-} (mM)	DOC (mg/l)	$\delta^{13}C_{DIC}$ (‰)	$\delta^{18}O$ (‰)
1	River Toplica	9.7	7.73	3.74	1.44	0.33	0.11	0.03	0.13	0.19	0.12	0.09	1.49	-12.6	-8.3
2	River Bečovnica	9.9	7.93	2.71	1.24	0.43	0.31	0.05	0.22	0.26	0.19	0.28	5.90	-11.7	-8.3
3	River Klančica	10.4	7.81	2.83	1.17	0.48	0.42	0.06	0.26	0.20	0.11	0.24	3.17	-12.8	-8.4
4	River Velunja	9.2	8.04	2.69	0.90	0.51	0.16	0.03	0.14	0.28	0.08	0.12		-11.0	-8.6
5	Lake Družmirje	15.0	8.30	2.29	1.01	0.60	0.32	0.07	0.04	0.45	0.04	0.14	6.20	-8.5	-9.8
6	River Ljubela	11.2	8.30	4.61	1.91	0.71	0.23	0.04	0.14	0.16	0.05	0.18		-12.0	-9.2
7	Lake Velenje	18.6	8.22	1.89	3.87	0.57	2.64	1.26	0.02	5.05	0.06	0.76	4.50	-6.6	n.a.
8	River Lepena	17.0	8.48	5.52	1.90	1.05	0.39	0.08	0.09	0.31	0.00	0.41		-10.9	-9.2
9	Lake Škale	16.1	7.95	3.91	1.27	0.99	0.52	0.07	0.03	0.50	0.04	0.27	6.42	-7.5	n.a.
10	River Paka	17.0	8.30	3.15	2.45	0.69	1.45	0.57	0.07	2.27	0.03	0.56	2.91	-8.7	-8.0

Table 2. Chemical and isotopic data for groundwaters dewatering different strata above the coal seam in the Velenje Basin

Location	Depth above sea level (m)	Geology	T (°C)	pH	Total alkalinity (meq/l)	Ca^{2+} (mM)	Mg^{2+} (mM)	Na^{+} (mM)	K^{+} (mM)	Si (mM)	SO_4^{2-} (mM)	NO_3^{-} (mM)	Cl^{-} (mM)	DOC (mg/l)	$\delta^{13}C_{DIC}$ (‰)	$\delta^{18}O$ (‰)
BV 29	417.0	Pliocene1,2	19.0	7.00	19.92	2.18	4.43	3.02	0.14	1.25	0.00	0.02	0.10	7.24	-2.5	n.a.
BV 27	413.0	Pliocene1,2	16.7	7.12	11.92	1.76	2.39	1.65	0.08	0.95	0.00	0.00	0.07	4.00	-3.2	-10.7
V 12 z	387.0	Pliocene1,2	18.6	6.70	32.44	3.61	8.46	4.55	0.19	1.37	0.00	0.00	0.19	6.93	-3.3	-11.3
V 12 v	385.0	Pliocene1,2	18.6	6.50	27.38	3.05	6.89	3.66	0.16	1.26	0.00	0.00	0.15	n.a.	-2.9	n.a.
GW G1A	-61.2	Pliocene 1	n.a.	n.a.	31.64	4.44	5.45	12.42	0.35	0.86	1.11	0.00	0.51	n.a.	-9.1	n.a.
j.v. 3121	-60.0	Pliocene 1	20.1	6.62	32.91	2.86	8.51	8.56	0.14	1.91	0.00	0.00	0.22	6.99	-2.4	-11.1
J.V. 3143	-45.0	Pliocene 1	20.1	6.35	33.53	4.17	8.16	7.30	0.14	1.71	0.00	0.00	0.20	8.22	0.2	-10.8
j.v. 783-K/00	-71.5	Pliocene 1	20.5	6.45	52.15	4.12	15.47	13.09	0.18	1.79	0.20	0.00	0.41	14.69	-2.6	-10.7
j.v. 3136	-63.9	Pliocene 1	20.5	6.49	38.19	3.18	10.11	9.98	0.15	1.84	0.00	0.08	0.23	9.75	-1.7	-10.4
j.v. 3048	-62.0	Pliocene 1	19.5	6.51	25.99	2.52	7.07	5.19	0.11	1.65	0.00	0.01	0.17	5.52	-3.6	-10.5
j.v. 3047	-79.0	Pliocene 1	21.4	6.43	43.09	3.63	12.65	10.33	0.16	1.81	0.01	0.01	0.41	12.56	-3.1	-10.0
j.v. 3045	-91.2	Pliocene 1	20.6	6.36	32.56	2.79	10.01	6.86	0.14	1.76	0.01	0.00	0.21	n.a.	-5.5	-10.4
razbremenilna	-60.0	Pliocene 1,2	20.8	6.53	51.59	3.60	16.34	12.79	0.20	1.91	0.00	0.00	0.40	n.a.	-4.8	-10.5
V 11 n	373.0	Pliocene 1,2	20.1	7.38	61.95	4.25	21.74	11.30	0.26	1.72	0.00	0.00	0.54	n.a.	-3.3	-10.4
j.v. 661-K/89	-106.6	Pliocene 1,2	20.8	7.01	59.78	4.50	20.77	11.45	0.25	1.83	0.01	0.08	0.53	11.99	-3.5	-10.4
j.v. 659	-106.0	Pliocene 1	21.0	6.93	44.33	3.53	13.60	9.47	0.19	1.82	0.00	0.00	0.33	11.44	-2.6	-10.9
j.v 785-A 6	-149.9	Litotamnium limestone	30.2	7.18	39.93	1.19	1.29	54.00	0.50	0.22	0.00	0.00	2.08	152.20	-2.6	-10.7
j.v 785-A 5	-149.7	Litotamnium limestone	30.0	7.30	38.06	1.29	1.22	50.73	0.48	0.23	0.00	0.00	2.01	n.a.	-1.9	-10.7
j.v.2373-T/93	85.9	Triass-anisian	18.4	7.08	9.88	2.37	2.02	0.42	0.03	0.16	1.98	0.01	0.03	2.17	-8.4	n.a.
j.v.2346	121.0	Triass-anisian	17.7	7.06	5.94	2.03	1.54	0.07	0.01	0.16	0.78	0.01	0.05	11.80	n.a.	-9.7
j.v.2343 T793 6	121.0	Triass -anisian	17.1	7.13	5.88	1.99	1.50	0.07	0.01	0.15	0.64	0.00	0.05	1.54	-11.0	n.a.
j.v. 2341-T/83	121.6	Triass-anisian	16.0	7.11	6.68	2.70	1.46	0.10	0.01	0.16	1.06	0.01	0.10	2.53	-17.4	-9.6
j.v.2347-T/84	73.7	Triass-anisian	18.9	6.90	5.79	2.68	1.76	0.17	0.03	0.17	1.81	0.01	0.12	n.a.	-8.7	-9.6
j.v. 2391	85.6	Triass-anisian	14.2	7.08	5.57	1.68	1.34	0.11	0.01	0.11	0.35	0.05	0.11	n.a.	-12.8	-9.5
j.v.2343 T793 3	121.0	Triass-anisian	16.4	7.11	5.79	2.15	1.46	0.07	0.01	0.14	0.56	0.00	0.06	n.a.	-12.5	-9.1
j.v. 2360 T/87	27.0	Triass-scythian	20.6	6.94	5.56	3.19	2.32	1.57	0.08	0.19	3.61	0.00	0.24	2.22	-9.3	-9.6
j.v.2378/90 1	30.2	Triass-scythian	20.1	6.74	6.66	4.46	3.16	1.51	0.08	0.17	5.37	0.01	0.15	n.a.	-8.3	-10.1
j.v.2378/90 4	30.2	Triass-scythian	19.8	6.61	7.65	4.63	2.36	0.91	0.17	0.16	n.a.	n.a.	n.a.	5.76	-10.1	-9.7
j.v.2377-T/91 1	33.6	Triass-scythian	15.3	6.91	6.89	3.68	1.73	0.18	0.02	0.15	2.07	0.00	0.12	2.05	-8.6	-9.8
j.v.2377-T/91 3	33.6	Triass-scythian	18.7	6.58	10.57	3.70	2.38	1.51	0.07	0.14	n.a.	n.a.	n.a.	8.17	-3.2	-9.3
j.v. 2434-T/93	50.0	Triass-scythian	20.0	6.66	n.a.	2.97	1.64	3.98	0.11	0.15	1.44	0.00	0.19	n.a.	-8.1	-9.6

to degassing and warming, water samples were collected in a large volume, air-tight container and the pH was measured at least twice to verify electrode stability. The field pH was determined on the NBS scale using two buffer calibrations with a reproducibility of ± 0.02 pH units.

Sample aliquots collected for chemical analysis were passed through a 0.45 µm nylon filter into bottles and kept refrigerated until analysed. Samples for cation (treated with HNO_3), anion and alkalinity analyses were collected in HDPE bottles. Samples for $\delta^{13}C_{DIC}$ analyses were stored in glass bottles and filled to the top, with no headspace. Samples for $\delta^{18}O$ analyses were collected in HDPE bottles.

Analytical methods

Total alkalinity was measured within 24 h of sample collection by Gran titration (Gieskes, 1974) with a precision of ± 1 %. Concentrations of dissolved Ca^{2+}, Mg^{2+}, Na^+, K^+ and Si were determined using a Jobin Yvon Horiba ICP-OES with an analytical precision of ±2 %. Anions (SO_4^{2-}, NO_3^-, Cl^-) were analyzed on a Dionex ICS-2500 with an analytical precision of ±2 %. Concentrations of DIC were determined on a UIC Coulometrics CO_2 coulometer with a precision of ±2 %. Dissolved organic carbon (DOC) concentrations were measured using high-temperature platinum-catalyzed combustion followed by infrared detection of CO_2 (Shimadzu TOC-5000A) with a precision of ±2 %.

The stable isotope composition of dissolved inorganic carbon ($\delta^{13}C_{DIC}$) was determined with a Europa Scientific 20-20 continuous flow IRMS ANCA - TG preparation module. Phosphoric acid (100 %) was added (100-200 µl) to a septum-sealed vial which was then purged with pure He. The water sample (6 ml) was injected into the septum tube and headspace CO_2 was measured (modified after Miyajima et al. 1995; Spötl, 2005). In order to determine the optimal extraction procedure for surface water samples, a standard solution of Na_2CO_3 (Carlo Erba) with a known $\delta^{13}C_{DIC}$ of –10.8 ±0.2 ‰ was prepared with a concentration of either 4.8 meq/l (for samples with an alkalinity above 2 meq/l) or of 2.4 meq/l (for samples with alkalinity below 2 meq/l).

The isotopic composition of oxygen in water ($\delta^{18}O$) was measured after equilibration with reference CO_2 at 25 °C for 24 h (Epstein & Mayeda, 1953). The measurement was performed on a Varian MAT 250 mass spectrometer. Stable isotope results for O are reported using conventional delta (δ) notation $\delta^{18}O$, in permil (‰) relative to VSMOW. The precision of measurements was ±0.1 ‰ for $\delta^{18}O$.

Thermodynamic modelling was used to evaluate pCO_2 and the saturation state of calcite ($SI_{calcite}$) using pH, alkalinity and temperature as inputs to the PHREEQC speciation program (Parkhurst & Appelo, 1999).

Results and discussion

Major and stable isotope geochemistry of surface waters

Surface waters are primarily composed of HCO_3^-, Ca^{2+} and Mg^{2+} (Table 1). Dissolved Ca^{2+} and Mg^{2+} are largely supplied by the weathering of carbonates with smaller contributions from silicate weathering, as indicated by the relatively high HCO_3^- and low Si concentrations (Figures 2A and 3A). Dissolved Na^+ and K^+ originate from the leaching of feldspars from clastics rocks also composing the watershed. The concentrations of alkalinity varied from 1.89 to 5.52 meq/l, concentrations of Ca^{2+} ranged from 0.9 to 3.87 mM, concentrations of Mg^{2+} from 0.33 to 1.05 mM (Table 1) and are comparable to sampling locations from the River Sava watershed (Kanduč et. al., 2007). Figure 2A presents Ca^{2+} + Mg^{2+} versus alkalinity. Most of the samples have a 2:1 mole ratio of HCO_3^- to Ca^{2+} + Mg^{2+} following the reactions:

Calcite: $CaCO_3 + CO_{2(g)} + H_2O \Leftrightarrow Ca^{2+} + 2HCO_3^-$

Dolomite: $CaMg(CO_3)_2 + 2CO_2 + 2H_2O \Leftrightarrow Ca^{2+} + Mg^{2+} + 4HCO_3^-$

Differences in HCO_3^- concentrations in carbonate-bearing watersheds are related to the geological composition of the watershed, relief, mean annual temperature, the depth of the weathering zone, the soil thickness and residence time in the system (Gaillardet et al., 1999). Most surface waters indicate that weathering of calcite is dominant (Figure 2B). A Mg^{2+}/Ca^{2+} ratio around 0.75, which is typical of weathering of dolomite with calcium, is characteristic only in location 9 (Lake Škale). Concentrations of K^+ and Na^+ in surface waters were low, except in Lake Velenje and the River Paka, where higher concentrations were observed (Figure 3). Na^+ and K^+ concentrations are derived from weathering of feldspars in the watershed.

Concentrations of dissolved organic carbon (DOC) ranged from 1.49 to 6.42 mg/l (Table 1), which is typical of unpolluted rivers (Tao, 1998). All of the surface water samples, except for Lake Velenje and River Paka, had low concentrations of dissolved sulfate (<0.50 mM; see Table 1). Sulfate concentrations in Lake Velenje were 5.05 mM, likely due to leaching of sulphur from nearby coal deposits. Sulphur in coal is found in both inorganic and organic forms (Davidson, 1993). Inorganic sulphur in coal is mostly pyrite (FeS_2), with minor amounts of marcasite and sulphates. The sulphate content of coal is usually low unless pyrite has been oxidized. Forms of organic sulphur are less well established (Davidson, 1993). River Boben, which is draining mining area district in Zasavje region (Kanduč, 2006) and River Paka (from this study) had slightly elevated sulfate values (1.13 and 2.27 mM, respectively). Sulfur and oxygen isotopes of SO_4^{2-}, although not measured as part of this study, could help to further elucidate the sources of sulfate to surface waters.

Oxygen isotope values of all surface water samples ranged from -9.8 ‰ to -8.0 ‰ (Table 1). $\delta^{18}O$ values in surface waters are dependent on several factors: precipitation, evaporation, evapotranspiration, infiltration and equilibration with run-off (Yee et al., 1990). Measured $\delta^{18}O$ values in river water are comparable with $\delta^{18}O$ values obtained in the River Sava ($\delta^{18}O$ ranged from -10.0 to -8.8 ‰) sampled in fall 2004 (Kanduč, 2006). More positive $\delta^{18}O$ values could be attributed to evaporation (Gonfiantini, 1986). Carbon isotope values of dissolved inorganic carbon (DIC) ranged from -12.8 ‰ to -6.6 ‰ (Table 1) and indicate different processes in the surface water system: dissolution of carbonates, degradation of organic matter and equilibration with atmospheric CO_2. Calculated CO_2 partial pressure (pCO_2) varied from near atmospheric values (354 ppmv) to values that are over 10-fold supersaturated (3388 ppmv), which is typical of surface water (Kanduč et al., 2007). Higher pCO_2 values are probably due to higher degradation of organic matter in surface waters (Dever et al., 1983).

The $\delta^{13}C_{DIC}$ values of surface waters were used to determine the contributions of organic matter decomposition, carbonate mineral dissolution, and exchange with atmospheric CO_2 to DIC in the watershed. An average $\delta^{13}C_{POC}$ value of –26.6 ‰ was assumed to calculate the isotopic composition of DIC derived from in-stream respiration (see Figure 4). Open system equilibration of DIC with CO_2 enriches DIC in ^{13}C by about 9 ‰ (Mook et al., 1974), thus yielding the estimate of –17.6 ‰ shown in Figure 4. Nonequilibrium dissolution of carbonates with one part of DIC originating from soil CO_2 (–26.6 ‰) and the other from carbonate dissolution with an average $\delta^{13}C_{Ca}$ of 2.0 ‰ (Kanduč et al., 2007) produces an intermediate $\delta^{13}C_{DIC}$ value of –12.3 ‰ (Figure 4). Given the isotopic composition of atmospheric CO_2 (–7.8 ‰; Levin et al., 1987) and equilibrium fractionation with DIC of +9 ‰, DIC in equilibrium with the atmosphere should have a $\delta^{13}C_{DIC}$ value of about 1.6 ‰ (Figure 4). Most surface water samples fall around the line of nonequilibrium carbonate dissolution by carbonic acid produced from soil zone with a $\delta^{13}C_{CO2}$ of -26.6 ‰. Higher $\delta^{13}C_{DIC}$ values were observed in lakes, indicating open system DIC equilibration with the atmosphere since the long residence time of water in lakes allows dissolved CO_2 to equilibrate with the atmosphere.

The calcite saturation index ($SI_{calcite} = \log ([Ca^{2+}] \cdot [CO_3^{2-}])/K_{calcite}$; using the solubility products of calcite ($K_{calcite}$)) is near and well above equilibrium ($SI_{calcite} = 0$) and ranges from -0.03 to 1.55, indicating that calcite is supersaturated and precipitation is thermodynamically favoured in most of the surface waters.

Major and stable isotope geochemistry of groundwater

From the geochemical and stable isotope results of sampled groundwater (Table 2) three different aquifers can be identified: 1) A Pliocene aquifer with an alkalinity from 11.92 to 61.95 meq/l, concentrations of Ca^{2+} from 1.76 to 4.50 mM, concentrations of Mg^{2+} from 2.39-21.74 mM, concentrations of Na^+ from 1.65 to 13.09, concentrations of Si from 0.86 to 1.91 mM, $\delta^{13}C_{DIC}$ values from -9.1 to 0.2 ‰, and $\delta^{18}O$ values from -11.3 to -10.0 ‰; 2) A Triassic aquifer with an alkalinity from 5.56 to 10.57 meq/l, concentrations of Ca^{2+} from 1.68 to 4.63 mM, concentrations of Mg^{2+} from 1.34 to 3.16 mM, concentrations of Na^+ from 0.07 to 3.98 mM, concentrations of Si from 0.11 to 0.19 mM, $\delta^{13}C_{DIC}$ values from -17.4 to -3.2 ‰. and $\delta^{18}O$ values from -10.1 to -9.1 ‰; and 3) A Lithotamnium aquifer with an average alkalinity of 39.00 meq/l, an average concentration of Ca^{2+} of 1.24 mM, an average concentration of Mg^{2+} of 1.26 mM, an average concentration of Na^+ of 52.36 mM, an average concentration of Si of 0.23 mM, a $\delta^{13}C_{DIC}$ value of -2.2 ‰, and an average $\delta^{18}O$ value of -10.7 ‰ (Table 2).

Groundwaters from the Triassic aquifer have HCO_3^- to $Ca^{2+} + Mg^{2+}$ ratios close to 2, plotting along the 1:2 line shown in Figure 2A, indicating that weathering of carbonates is the major contributor of solutes, as seen for surface waters. Furthermore, it was found that the Mg^{2+}/Ca^{2+} ratio in the Triassic aquifer is higher than 0.5, indicating that weathering of dolomite is dominant (Figure 2 B). Groundwater from the Pliocene aquifer plots near the 2:1 line, but slightly below (Figure 2A) suggesting contribution of additional cations (Na^+) likely due to cation exchange. In contrast, groundwater from the Lithotamnium aquifer has no relationship to the 1:2 line, plotting with high HCO_3^- and low $Ca^{2+} + Mg^{2+}$ concentrations (Figure 2A). This suggests that carbonate weathering is not an important contributor of solutes to the Lithotamnium aquifer groundwaters.

Groundwaters from the Triassic aquifer have similar major ion chemistries, including K^+, Na^+, Si, Ca^{2+}, Mg^{2+}, and HCO_3^- concentrations as surface waters (Figures 2 and 3), whereas groundwater from the Pliocene and Lithotamnium aquifers display different chemical signatures. Groundwater from the Pliocene aquifer have relatively high K^+, Na^+ and Si concentrations (Figure 3), likely from leaching of feldspars in the aquifer sand, marl and mud units. It cannot be excluded that the water recharging Pliocene aquifers is discharged from the Periadriatic lineament. Groundwater from the Lithotamnium aquifer has low Si concentrations and high Na^+ and K^+ concentrations (Figure 3).

DOC (dissolved organic carbon) was investigated in the aquifers as it plays an important role in reduction-oxidation (redox) reactions. The most common soil–derived organic materials are humic substances, defined by their high molecular weight. In non-contaminated groundwaters, low molecular weight (LMW) compounds make up the remainder of the DOC. LMW DOC includes cellulose, proteins, and organic acids such as carboxylic, acetic and amino acids (Clark & Fritz, 1997). Concentrations of DOC in the Pliocene and Triassic aquifers in the Velenje basin are relatively low

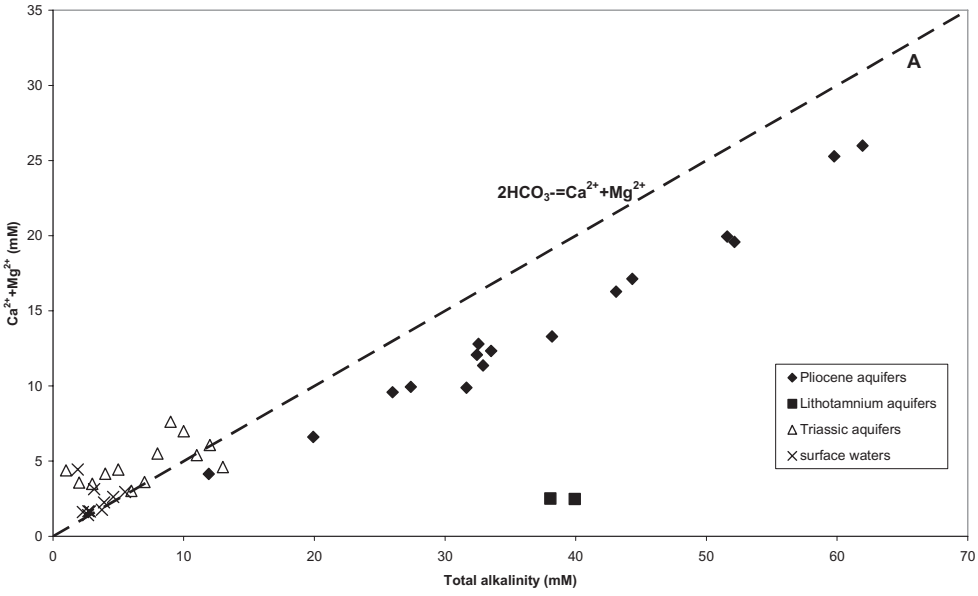

Figure 2. A. Ca^{2+} + Mg^{2+} versus alkalinity concentrations; the dotted line indicates weathering of carbonates.

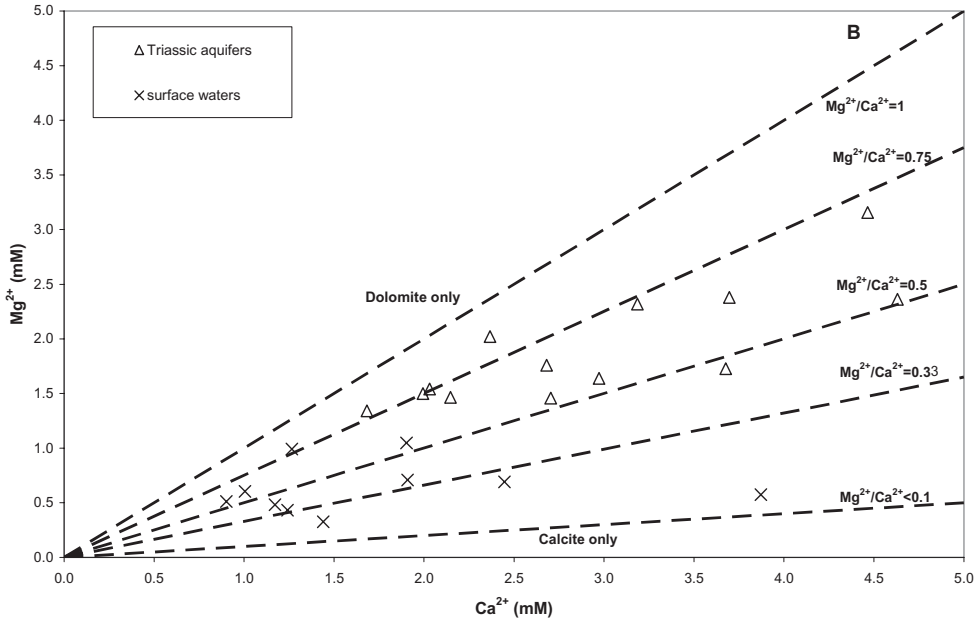

B. Mg^{2+} versus Ca^{2+} concentrations indicating the importance of dolomite versus calcite weathering.

(from 1.54 to 14.69 mg/l; Table 2). In comparison, groundwaters associated with organic-rich shales in the Michigan Basin contain DOC concentrations up to 840 mg/l (Martini et al., 1996). An elevated concentration of DOC (152.20 mg/l) was measured in the Lithotamnium aquifer, which is probably related to the higher organic matter content compared to the other aquifers.

Calculated CO_2 partial pressures (pCO_2) of groundwater varied from 22908 ppm to 870964 ppm (location j.v. 783-K/00), which is from 57 to 2180-fold supersaturated relative to atmospheric CO_2 (400 ppm; Clark & Fritz, 1997). The calcite saturation index ($SI_{calcite}$) of groundwater was generally well above equilibrium ($SI_{calcite} = 0$), indicating that calcite was supersaturated and precipitation was thermodynamically favoured in samples from the Pliocene and Lithotamnium aquifers ($SI_{calcite}$ ranged from -0.07 to 1.25), while Triassic aquifers were under saturated or close to saturation with respect to calcite ($SI_{calcite}$ ranged from -0.2 to 0.16). Groundwaters belonging to the Triassic aquifer have similar $\delta^{18}O$ values as surface waters, indicating similar water sources. In contrast, Pliocene and Lithotamnium aquifers had lower $\delta^{18}O$ values ranging from -11.3 to -10.0 ‰ (Table 2). $\delta^{18}O$ values from Pliocene and Lithotamnium groundwaters are lower in comparison with groundwaters in the Sava River Basin (Kanduč, 2006). Aravena et al., 2003 found very depleted $\delta^{18}O$ and δD values (around -20 ‰ for $\delta^{18}O$ and -150 ‰ for δD), which were attributed to CO_2 reduction processes.

Figure 4 indicates processes influencing the $\delta^{13}C_{DIC}$ value in groundwaters. It can be seen that groundwaters from the Triassic aquifer have similar $\delta^{13}C_{DIC}$ values as surface waters and fall around the line of nonequilibrium carbonate dissolution by carbonic acid produced from the soil zone with a $\delta^{13}C_{CO2}$ of -26.6 ‰. Groundwaters belonging to the Pliocene and Lithotamnium aquifers have higher $\delta^{13}C_{DIC}$ values, which could be attributed to bacterial CO_2 reduction, causing enrichment with ^{13}C. Investigation of origin of methane in the Elk Valley coalfield, southeastern British Columbia, Canada also confirmed bacterial origin of methane with $\delta^{13}C_{DIC}$ values from monitoring wells up

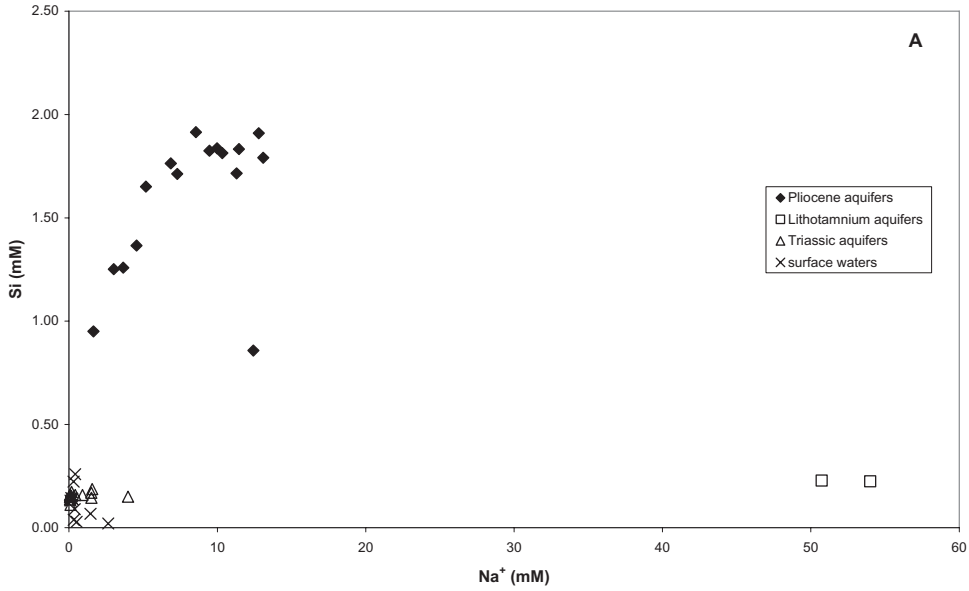

Figure 3. A. Si versus Na^+ concentration of surface waters and groundwaters from the Velenje Basin.

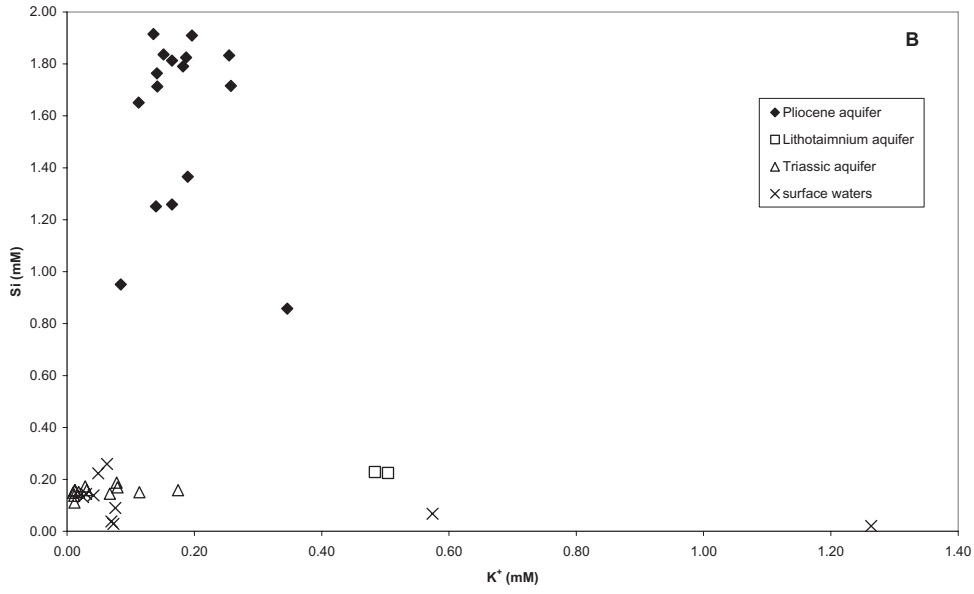

B. Si versus K^+ concentrations of surface waters and groundwaters from the Velenje Basin.

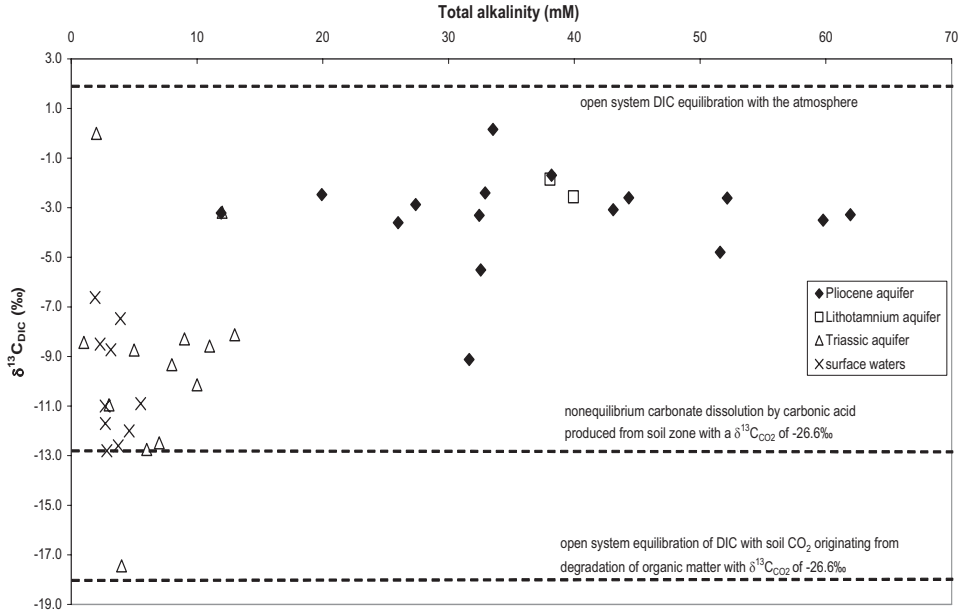

Figure 4. Variation in $\delta^{13}C_{DIC}$ values of surface waters and groundwaters compared to alkalinity concentrations, with lines indicating processes likely occurring in the Velenje Basin. These include values calculated for: 1) open system DIC in equilibration with the atmosphere, 2) nonequilibrium carbonate dissolution by carbonic acid produced from soil zone CO_2, and 3) open system equilibration of DIC with soil CO_2 originating from degradation of organic matter with $\delta^{13}C_{soil}$ = -26.6 ‰.

to +34.9 ‰ (Aravena et al., 2003). Since groundwaters represent a closed system, the process of open system equilibration with the atmosphere is negligible. The isotopic composition of CO_2 in the Velenje Basin also indicated a bacterial origin (besides endogenic CO_2) of CO_2 and is further discussed in Kanduč & Pezdič, 2005.

Conclusion

The major solute composition of surface waters in the Velenje Basin is dominated by HCO_3^-, Ca^{2+} and Mg^{2+}. Total alkalinity concentrations ranged from 2.69 to 5.52 mM in rivers, while in lakes concentrations of HCO_3^- ranged from 1.89 to 3.91 mM. The concentration of solutes decreases according to the sequence HCO_3^->Mg^{2+}>Na^+>Ca^{2+} in the Pliocene aquifer, Na^+>HCO_3^->Mg^{2+} in the Lithotamnium aquifer, and HCO_3^->Ca^{2+}>Mg^{2+} in the Triassic aquifer. Alkalinity values reached up to 61.95 mM in the Pliocene aquifer, 39.93 mM in the Lithotamnium aquifer, and 10.57 mM in the Triassic aquifer. Observed $\delta^{13}C_{DIC}$ values in lakes reached up to -7.5 ‰, which is related to longer equilibration time with atmospheric CO_2, while river water had lower $\delta^{13}C_{DIC}$ values similar to those observed in the Triassic aquifer. Higher $\delta^{13}C_{DIC}$ values up to 0.2 ‰ in the Pliocene and Lithotamnium aquifers could be attributed to the bacterial CO_2 reduction process.

Since the Velenje Basin is located in a tectonically complex system, the study confirms the different origins of groundwaters in this area. It seems that Pliocene groundwaters (Preloge mining area) recharging the Velenje Basin are related to coalbed gas generation in the coalbed seam, since waters with high alkalinities (mineralization) accelerate bacterial activity. It still remains a question how much bacterial gas in the Preloge mining area is of recent generation and how much bacterial gas remains trapped in the coalbed seam since formation of the basin. Triassic groundwaters (located in the Škale mining area) have similar chemical and isotopic composition as surface waters and are mostly controlled by dissolution of carbonates and degradation of CO_2.

This study was performed in the framework of a larger study called "Sequestration of CO_2 in geological media: criteria and approach for site selection as a response to climate change" in the Velenje Basin and represents the first results of a systematic study of the chemical and isotopic composition of surface waters and groundwaters in this area. It should be emphasized that the Velenje coalmine is located near Šoštanj power plant, which emits around 4 Mt/year of CO_2 into the atmosphere. Hence the question arises about sequestration of CO_2 in the Velenje Basin to satisfy the Kjoto protocol, which was ratified in the year 2002.

Acknowledgements

This study was conducted in the framework of the project Z1-2052 funded by the Slovenian Research Agency (ARRS) and the Velenje coalmine. The project was also financially supported by the National Science Foundation, USA (NSF-EAR#0208182). The authors are grateful to Mr. Marko Ranzinger and Mr. Igor Medved for technical support and assistance in the field sampling. Sincere thanks to Dr. Anthony Byrne for improving the English of the manuscript.

References

Adelana, S. 2005: Environmental isotopes in hydrogeology. In: Lehr J. H., Keeley J. (eds.). Water encyclopedia groundwater. Wiley-Interscience, A John Wiley & Sons, Inc., Hoboken (New Jersey): 1–836.

Aravena, R., Harrison, S. M., Barker, J. F., Abercrombie, H., & Rudolph, D. 2003: Origin of methane in the Elk Valley coalfield, southeastern British Columbia, Canada. Chem. Geol. 195: 219–227.

Brezigar, A., Ogorelec, B., Rijavec, L. & Mioč, P. 1988: Geologic setting of the Pre – Pliocene basement of the Velenje depression and its surroundings. Geologija (Ljubljana) 30 (1987): 31–65 (in Slovene).

Brunke, M. & Gonser, T. 1997: The ecological significance of exchange processes between rivers and groundwater. Fresh. Biol. 37: 1–33.

Clark, I. & Fritz, P. 1997: Environmental Isotopes in Hydrology. Lewis Publishers (New York): 1–328.

Davidson, R. M. 1993: Organic sulphur in coal. IAE Coal Research (London): 1–79.

Dever, L, Durand, R, Fontes, J. Ch. & Vaicher, P. 1983: Etude pédogénétique et isotopique des néoformations de calcite dans un sol sur craie. Caractéristiques et origines. Geochim. Cosmochim. Acta 47: 2079–2090.

Elderfield, H., Upstill-Goddard, R. & Sholkovitz, E. R. 1990: The rare earth elements in rivers, estuaries and coastal seas and their significance to the composition of ocean waters. Geochim. Cosmochim. Acta 54: 971–997.

Epstein, S. & Mayeda, T. 1953: Variations of ^{18}O contents of water from natural sources. Geochim. Cosmochim. Acta 4: 213–224.

Fairchild, I. J., Killawee, J. A., Hubbard, B. & Dreybrodt, W. 1999: Interactions of calcareous suspended sediment with glacial meltwater, a field test of dissolution behaviour. Chem. Geol. 155: 243–263.

Fairchild, I. J., Borsato, A., Tooth, A. F., Frisia, S., Hawkesworth, C. J. Huang, Y., McDermott, F. & Spiro, B. 2000: Controls on trace element (Sr-Mg) compositions of carbonate cave waters: implications for spelothem climatic records. Chem. Geol. 166: 255–269.

Fijavž, O. 2002: Monitoring odvodnjevalnih procesov v jamah Premogovnika Velenje, Diploma work (Velenje):1–42 (in Slovene).

Gaillardet, J., Dupré, B. & Allègre, C. J. 1999: Global silicate weathering and CO_2 consump-

tion rates deduced from the chemistry of large rivers. Chem Geol. 159: 3–30.

Gams, I. & Zupan, M. 1994: Paka. In: Voglar D. (ed): Encyclopedia Slovenia (Mladinska knjiga) 8/1–224 (in Slovene).

Gonfiantini, R. 1986: Environmental isotopes in lake studies. In: Fritz P. & Fontes J. Ch. (eds.). Handbook of Environmental Isotope Geochemistry (Elsevier) 2: 113–168.

Gibbs, R. J. 1972: Water chemistry of the Amazon River. Geochim. Cosmochim. Acta 36: 1061–1066.

Gieskes, J. M. 1974: The alkalinity-total carbon dioxide system in seawater. In: Goldberg E.D. (ed): Marine Chemistry of the Sea. John Wiley and Sons (New York) 5: 123–151.

Goldstein, S. J. & Jacobsen, S. B. 1987: Rare earth element in river waters. Earth Planet. Sci. Lett. 89: 35–47.

Huh, Y., Tsoi, M. Y., Zaitsev, A. & Edmond, J. M. 1998: The fluvial geochemistry of the rivers of Eastern Siberia: I. Tributaries of the Lena River draining the sedimentary platform of the Siberian Craton. Geochim. Cosmochim. Acta 62: 1657–1676.

Hu, M. H., Stallard, R. F. & Edmond, J. M. 1982: Major ion chemistry of some large Chinese rivers. Nature 298: 550–553.

Jamnikar, S. & Fijavž, O. 2006: Hidrogeološko poročilo za leto 2006, Premogovnik Velenje d.d., 1–21.

Kanduč, T. 2006: Hidrogeokemične značilnosti in kroženje ogljika v porečju reke Save v Sloveniji: doktorska disertacija. Ljubljana: 1–141 (Ph. D Thesis in Slovene).

Kanduč, T. & Pezdič, J. 2005: Origin and distribution of coalbed gases from the Velenje Basin, Slovenia. Geochem. J. 39: 397–409.

Kanduč, T, Szramek, K, Ogrinc, N. & Walter, L. M. 2007: Origin and cycling of riverine inorganic carbon in the Sava River watershed (Slovenia) inferred from major solutes and stable carbon isotopes. Biogeochem 86: 137–154.

Levin, I., Kromer, B., Wagenback, D. & Minnich, K. O. 1987: Carbon isotope measurements of atmospheric CO_2 at a coastal station in Antarctica. Tellus 39 B: 89–95.

Liu, Z. & Zhao, J. 2000: Contribution of carbonate rock weathering to the atmospheric CO_2 sink. Environ. Geol. 39: 1053–1058.

Mali, N. 1992: Uporaba multivariatnih statističnih metod pri ločevanju rudniških vod. RMZ (Ljubljana) 39: 348–361 (in Slovene).

Markič, M. & Sachenhofer, R. F. 1997: Petrographic composition and depositional environments of the Pliocene Velenje lignite seam (Slovenia). Internat. J Coal Geol. 33: 229–254.

Martini, A. M., Budai J. M., Walter L. M. & Schoell, M. 1996: Microbial generation of economic accumulations of methane within a shallow organic – rich shale. Nature 383: 155–157.

Mioč, P. & Žnidarčič, M. 1972: Osnovna geološka karta SFRJ 1 : 100000. Tolmač lista Slovenj Gradec, L33-34, Zvezni geološki zavod Beograd, 1–39. (in Slovene).

Miyajima, T., Yamada, Y. & Hanba, Y.T. 1995: Determining the stable isotope ratio of total dissolved inorganic carbon in lake water by GC/C/IRMS. Limnol. Oceanogr. 40/5: 994–1000.

Mook, W.G., Bommerson, J.C. & Staverman, W.H. 1974: Carbon isotope fractionation between dissolved bicarbonate and gaseous carbon dioxide. Earth Planet. Sci. Lett. 22:169–176.

Parkhurst, D. L. & Appelo, C. A. J. 1999: User's guide to PHREEQC for Windows (version 2) – a computer program for speciation, batch – reaction, one – dimensional transport, and inverse geochemical calculations. Water – Resources Investigations Report 99–4259.

Reeder, S. W., Hitchon, B. & Levinson, A. A. 1972: Hydrogeochemistry of the surface waters of the Mackenzie River drainage basin, Canada: 1. Factors controlling inorganic composition. Geochim. Cosmochim. Acta 36: 181–192.

Sophocleous, M. A. 2002: Interactions between groundwater and surface water. The state of the science. Hydrogeol. J. 10/1: 52–67.

Stallard, R. F. & Edmond, J. M. 1983: Geochemistry of the Amazon: 2. The influence of geology and weathering environment on the dissolved load. Geophys. Res. J. 88: 9671–9688.

Spötl, C. 2005: A robust and fast method of sampling and analysis of $\delta^{13}C$ of dissolved inorganic carbon in ground waters. Isotopes Environ. Health Stud. 41: 217–221.

Šterbenk, E. & Ramšak, R. 1995: Velenjsko jezero znova živi. Naš čas 27/95. Velenje.

Tao, S. 1998: Spatial and temporal variation in DOC in the Yichun River, China. Wat Res. 32: 2205–2210.

Veselič, M. & Pezdič, J. 1998: Hydrogeological aspects of lignite mine Velenje: environmental isotope study. RMZ (Ljubljana) 45: 192–196.

Vrabec, M. 1999: Style of postsedimentary deformation in the Plio – Quaternary Velenje basin, Slovenia. Neues Jahrbuch für Geologie und Paläontologie 8: 449–463.

Wachinew, P. 2006: Isotopic composition of dissolved inorganic carbon in a large polluted river: The Vistula, Poland. Chem Geol. 233: 293–308.

Zhang, J., Quay, P. D. & Wilbur, D. O. 1995: Carbon isotope fractionation during gas – water exchange and dissolution of CO_2. Geochim. Cosmochim. Acta 59/1: 107–1146.

Yee, P., Edgett, R. & Eberhardt, A. 1990: Great lakes – St. Lawrence River regulation; what it means and how it works. Joint publication of Environment Canada Ontario Region and the U. S. Army Corps of Engineers.

GEOLOGIJA *53/1*, 47-54, Ljubljana 2010

Loforanine iz eocenskih plasti osrednje Istre

Lophoraninas from Eocene beds in central Istria, Croatia

Vasja MIKUŽ

Univerza v Ljubljani, Naravoslovnotehniška fakulteta, Oddelek za geologijo, Privoz 11, SI-1000 Ljubljana, Slovenija; e-mail: vasja.mikuz@ntf.uni-lj.si

Prejeto / Received 6. 4. 2010; Sprejeto / Accepted 15. 4. 2010

Ključne besede: rakovice, *Lophoranina*, srednji eocen, lutetij, fliš, Ćopi, Istra, Hrvaška
Key words: crabs, *Lophoranina*, Middle Eocene, Lutetian, flysch, Ćopi, Istria, Croatia

Izvleček

V prispevku so obravnavani ostanki srednjeeocenske rakovice vrste *Lophoranina marestiana* (König, 1825) iz okolice zaselka Ćopi pri Pićnu v osrednji Istri na Hrvaškem. Ostanki njihovih karapaksov so najdeni v lutetijskih karbonatnih kamninah, ki so v sklopu debelih paleogenskih flišnih plasti. Primerki opisanega taksona so v najdišču razmeroma pogostni, vendar pomanjkljivo ohranjeni. Nastopajo skupaj s številnimi ostanki skeletov in kamenih jeder majhnih in večjih organizmov najrazličnejših paleontoloških skupin.

Abstract

In the contribution remains of Middle Eocene crabs of species *Lophoranina marestiana* (König, 1825) from environs of the small village of Ćopi near Pićan in central Istria, Croatia, are considered. Remains of their carapaces were found in Lutetian carbonates occuring within the thick Paleogene flysch beds sequence. Individuals of the mentioned taxon are relatively abundant of skeletons and casts of smaller and larger organisms of diverse paleontological groups.

Uvod

Ćopi leži jugovzhodno od Pazina, točneje južno od Pićna v osrednji zeleni Istri na Hrvaškem (sl. 1). Tam izdanjajo debele eocenske flišne plasti, ponekod v izredno lepih in zanimivih profilih, ki po Veliću in sod. (1995, 6) pripadajo paleogenskemu flišnemu bazenu osrednje Istre. Ostanki makrofavne so vedno vezani na plasti, kjer najdemo večje ali izredno veliko število numulitin. To so ponavadi apnenčevi peščenjaki in olistostromne breče, redkeje apnenci. Znotraj tega kompleksa je še plast, v kateri so ostanki rakovic. Njihovi ostanki so izredno redki in običajno močno poškodovani. Tako smo se vsake nove rakovičje najdbe zelo razveselili, še posebej lepo ohranjene.

Pri Ćopiju so določene plasti polne mikro in makrofosilov. V začetku smo bili pozorni predvsem na morske ježke in mehkužce. Ker smo nekajkrat našli slabo ohranjene ostanke loforanin, smo začeli iskati in zbirati tudi njihove ostanke. Po večkratnih obiskih najdišča smo zbrali toliko ostankov loforanin, da jih lahko predstavimo. Mislimo, da vsi ostanki pripadajo samo eni obliki rakovic vrste *Lophoranina marestiana*.

Dosedanje raziskave rakovic v osrednji Istri

Bittner (1875, 68) piše, da so ranine v Istri poznane in so enake vrsti *Ranina marestiana* ter da so iz zgornjega horizonta z rakovicami vrste *Harpactocarcinus punctulatus* Desmarest v najdišču pri nekdanjem Čepićkem jezeru. Toniolo (1909, 291-294) med eocensko favno okolice Roča v Istri opisuje tudi rakovice štirih oblik: *Calappa* sp., *Harpactocarcinus quadrilobatus* Desmarest, *H. punctulatus* Desmarest in *H. souwerbyi* (=*sowerbyi*) Milne-Edwards. Kakršnihkoli ostankov ranin ali loforanin iz območja okolice Roča, Toniolo (1909) ne omenja. Sacco (1924, 20-21) poroča, da so srednjeeocenske plasti bogate s fosilnimi ostanki in da izdanjajo na območju Roča, Pazina, Gračišća in drugod. Med rakovicami omenja najdbe rodov *Ranina* in *Calappa* ter vrste *Harpactocarcinus quadrilobatus*, *H. punctulatus* in *H. sowerbesi* (=*sowerbyi*) s številnimi primerki, ki tvorijo takoimenovane »plasti z rakovicami«. Kochansky-Devidé (1964, 219, sl. 292) predstavlja ostanke rakovice rodu *Ranina* iz eocenskih skladov v okolici Raše. Pavlovec in Pavšič (1987, 55) sta raziskovala plasti z rakovicami v Istri in

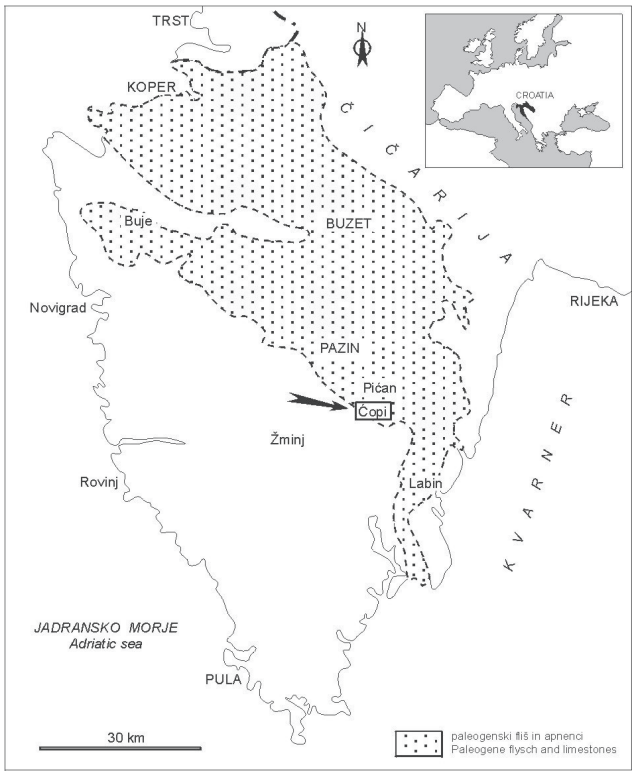

Sl. 1. Položaj najdišča eocenskih loforanin pri Ćopiju v osrednji Istri na Hrvaškem

Fig. 1.The position of site of Eocene lophoraninas at Ćopi in central Istria, Croatia

pišeta, da so tam ugotovljene rakovice *Harpactocarcinus punctulatus* Desmarest, *H. quadrilobatus* in *H. punctulatus istriensis* Bachmayer et Nosan. S pomočjo numulitin in nanoplanktona sta ugotovila, da so plasti z rakovicami na severovzhodni strani tržaško-pazinskega terciarnega bazena (Gračišče, Roč) spodnjelutetijske, na jugozahodni (Pićan) pa srednjelutetijske starosti. Nadalje še pišeta, da v primorskem pasu v bazi eocenskega fliša najdemo cono oziroma plast z rakovicami, v katerih so primerki rodov *Harpactocarcinus* in *Ranina*. Moosleitner (1996, Taf. 1) predstavlja ostanke eocenskih rakovic iz najdišča Paz v Istri. Določeni sta dve rakovici: *Ranina marestiana* Koenig in *Harpactocarcinus punctulatus* (Desmarest). Tarlao (2000, 30) omenja iz Istre štiri rakovice: *Harpactocarcinus punctulatus* Desmarest, *H. quadrilobatus* Desmarest, *H. sowerby* Edwards in *H. punctulatus istriensis* Bachmayer & Nosan. Tarlao (2000, 31) nadalje obravnava istrske rakovice iz okolice Pazina in predstavlja vrsto *Harpactoxanthopsis quadrilobata* (Desmarest 1822). Mikuž (2002) poroča, da so v letu 2001 našli lepo ohranjen primerek rakovice, ki jo opisuje kot vrsto *Harpactoxanthopsis quadrilobata*. Iz Gračišća pri Pazinu opisuje Mikuž (2004, 24) skromen primerek rakovice vrste *Lophoranina marestiana* (König, 1825). Schweitzer, Ćosović & Feldmann (2005, 664) poročajo o naslednjih eocenskih rakovicah, ki so bile najdene v Istri: *Calappa* sp., *Harpactoxanthopsis quadrilobatus*, *Harpactocarcinus punctulatus*, *Harpactoxanthopsis souverbiei* in *Lophoranina marestiana*. Schweitzer in sod. (2007, 1098) poročajo o najdbah rakovic na Hrvaškem vrste *Harpactocarcinus punctulatus*, iz Slovenije in Hrvaške pa o vrsti *Harpactocarcinus istriensis*.

Paleontološki del

Sistematika po: Glaessner, 1969

Ordo Decapoda Latreille, 1803
Subordo Pleocymeata Burkenroad, 1963
Infraordo Brachyura Latreille, 1803
Sectio Oxystomata H. Milne-Edwards, 1834
Superfamilia Raninoidea de Haan, 1841
Familia Raninidae de Haan, 1841
Genus *Lophoranina* Fabiani, 1910

Guinot (1993, 1325) opisuje družino Raninidae de Haan, 1841 in jo imenuje »frog crabs« (»žabje rakovice«). Glaessner (1969, R498) prikazuje in opisuje razlike med rodovi *Ranina*, *Lophoranina* in drugimi podobnimi oblikami iz družine Raninidae. Rod *Ranina* ima na dorzalni strani karapaksa številne vzdolžno potekajoče zrnaste izrastke, *Lophoranina* pa ima na karapaksu vzporedne in prečno potekajoče trnaste grebene. Rod *Ranina* je poznan od eocena do danes, rod *Lophoranina* je samo eocenski. Glaessner (1969) in Savazzi (1981) pišeta, da so rakovice rodu *Lophoranina* ugotovljene v srednje in zgornjeeocenskih skladih Evrope, Egipta, Irana, Indije in zahodnega Pacifika ter v oligocenskih plasteh ZDA (Alabama), Bornea in Zahodne Indije. Savazzi (1981, 233) nadalje še piše, da so ostanki pravega rodu *Lophoranina* v Evropi najdeni izključno v srednje in zgornjeeocenskih skladih. Potemtakem so loforanine za del eocena v tem prostoru do neke mere »vodilni fosili«.

Lophoranina marestiana (König, 1825)
Tab. 1, sl. 1-11

1859 *Ranina Marestiana* Kön. – Reuss, 21, Taf. 5, Fig. 1
1863 *Ranina Helli* – Schafhäutl, 223, Taf. 60, Fig. 3
1875 *Ranina Marestiana* König – Bittner, 64, Taf. 1, Figs. 1, 2a-2c
1883 *Ranina Marestiana* König. – Bittner, 300, Taf. 1, Figs. 1a-1b
1895 *Ranina Marestiana* König – Bittner, 253, Taf. 1, Fig. 5-5a
1895 *Ranina Marestiana* Koenig – Zittel, 488, Figs. 1324 a-c
1896 *Ranina Marestiana* Koenig 1828 – Oppenheim, 209
1924 *Ranina marestiana* Koen. – Parona, 515, Fig. 308
1966 *Ranina (Lophoranina) marestiana* König – Ancona, 406, Tav. 1-3
1968 *Ranina marestiana* König – Vogeltanz, 103, Abb. 10-g
1969 *Ranina (Lophoranina) marestiana* (König) – Glaessner, R498, Fig. 311,6
1970 *Lophoranina marestiana* (König) 1825 – Vía, 104, Lám. 5, Figs. 1, 1a-1b; Lám. 6, Fig. 1
1981 *Ranina (Lophoranina) marestiana* König 1859 – Savazzi, 234, Fig. 2 A

1988 *Lophoranina marestiana* (König, 1825) – Beschin in sod., 175, Fig. 6, Tav. 5, Figs. 3, 4
1992 *Ranina (Lophoranina) marestiana* König – Hagn, Darga & Schmid, 192-193, Taf. 57
1994 *Lophoranina marestiana* (König, 1825) – Beschin in sod., 173, Tav. 3, Fig. 4
1996 *Ranina marestiana* Koenig – Moosleitner, 108, Taf. 1, Fig. 1
1998 *Ranina (Lophoranina) marestiana* (König) – Schultz, 40, Taf. 12, Fig. 2
1998 *Lophoranina marestiana* (König, 1825) – Beschin in sod., 20, Figs. 6.2-3, 8.1
2004 *Lophoranina marestiana* (König, 1825) – Mikuž, 24, Tab. 1, Sl. 1-2

Material: Enajst (11) bolj ali manj okrnjenih rakovičinih karapaksov (Ćr1-Ćr11). Pri nekaterih primerkih so ohranjeni tudi posamezni deli ekstremitet. Vse primerke sta našla Vili Rakovc in avtor prispevka.

Nahajališče: Profil srednjeeocenskih flišnih plasti blizu Ćopija pri Pićnu. Primerki so najdeni v lutetijskih skladih s številnimi foraminiferami – numulitinami, diskociklinami in bolj redkimi asterociklinami, pogostimi školjkami, polži, anelidi, briozoji, morskimi lilijami in morskimi ježki.

Opis: Karapaks je podolgovat do ovalen in dorzalno polkrožno izbočen. Sprednji (anteriorni) in osrednji (centralni) širši del ohranjenega dela karapaksa je raven, ostali del je polkrožno-ovalen, zadnji (posteriorni) rob je kratek in vbočen ter na zgornji strani konkaven. Pri nekaterih primerkih je ohranjen še del frontalnega roba (tab. 1, sl. 2, 4, 7) nikjer v celoti. Na površini karapaksa so za vrsto značilni številni vzporedno potekajoči in nazobčani prečni ali transverzalni grebeni. Na primerkih iz Ćopija je 14 do 15, pri nekaterih tudi več prečnih grebenov. Grebeni v sprednjem in v zadnjem delu karapaksa potekajo zvezno od levega k desnemu robu, v osrednjem delu karapaksa se razvejijo ali izklinjajo. Grebeni so asimetrični, ukrivljeni in različnih višin. Resekventna stran grebenov je gladka in obrnjena proti zadnjemu, obsekventna in trnasti izrastki pa proti sprednjemu delu karapaksa (cefalotoraksa). Terasastostopnjasti relief na dorzalni strani karapaksa in njegovo funkcionalno vlogo je nadrobno obrazložil Savazzi (1981).

Pripombe: Ancona (1966, 406) piše, da so znotraj eocenskih rakovičjih rodov *Ranina* in *Lophoranina* določene štiri vrste: *Ranina* (*Lophoranina*) *marestiana* König, *R. (L.) bittneri* Lörenthey, *R.* (*L.) reussi* Woodward in *R.* (*L.) laevifrons* Bittner. Določitev posamezne vrste pa ni tako preprosta. Po mnenju Ancone (1966) so nekatere do sedaj določene in poimenovane vrste zelo vprašljive.

Določevalni kriteriji so zelo različni, ohranjenost loforanin je običajno zelo pomanjkljiva. Hkrati pa pri določitvah niso upoštevane variacijske širine posameznih vrst, ki jih dejansko ne poznamo. Večinoma so fosilne vrste določene po morfoloških značilnostih karapaksa, ki je pri rodovih *Lophoranina* in *Ranina* precej variabilen. Karapaks in posamezni deli ekstremitet se zaradi svoje kompaktnosti tudi največkrat ohranijo in najdejo, v celoti ohranjeni primerki opisane rakovice z vsemi detajli so najverjetneje zelo redki. Vía (1970, 128, Fig. 14) še opozarja, da so pri recentni vrsti *Ranina ranina* (Linné) opazili precejšnje razlike v oblikovanosti in velikosti predvsem frontalno-orbitalnega dela karapaksa, tako pri samcih kot tudi samicah in juvenilnih primerkih.

Če upoštevamo podatke, ki jih navaja Savazzi (1981, 233), so najdeni ostanki rodu *Lophoranina* v Evropi, značilni izključno za srednje in zgornjeeocenske sklade. To nekako sovpada s stratigrafsko razširjenostjo ostankov morskega ježka vrste *Conoclypus conoideus* in še z nekaterimi drugimi oblikami morskih ježkov in primerki iz drugih živalskih skupin.

Primerki Specimens Ćr1–Ćr11 Tab. 1 – Pl. 1	dolžina Length	Širina Width
Ćr-1, sl. 1	55	45
Ćr-2, sl. 2	39	30
Ćr-3, sl. 3	43	30
Ćr-4, sl. 4	40	30
Ćr-5, sl. 5	37	32
Ćr-6, sl. 6	28	31
Ćr-7, sl. 7	38	32
Ćr-8, sl. 8	35	33
Ćr-9, sl. 9	26	21
Ćr-10, sl. 10	14	16
Ćr-11, sl. 11	13	18

Dimenzije karapaksov loforanin iz Ćopija (v mm)

Dimensions of *Lophoranina* carapaces from Ćopi (in mm)

Stratigrafska in geografska razširjenost: Reuss (1859, 81) omenja najdbe vrste *Ranina marestiana* iz numulitnega apnenca v okolici Verone. Schafhäutl (1863, Taf. 60-61) predstavlja iz eocenskih skladov južne Bavarske vrsti *Ranina fabri* in *R. helli*. Bittner (1875) prikazuje primerek, ki je bil najden v eocenskih skladih lokalitete San Giovanni Ilarione v Italiji, Zittel (1895) pa primerek iz starostno primerljivih plasti Kressenberga na jugu Bavarske. Bittner (1883, 316, Taf. 1, Figs. 1-4) predstavlja več različnih ranin: *Ranina marestiana* König in dve novi vrsti *Ranina notopoides* in *R. simplicissima*. Vse so iz eocenskih skladov Italije. Quenstedt (1885, Taf. 31, Fig. 31) prikazuje vrsto *Ranina kressenbergensis* iz eocenskih skladov Bavarske. Bittner (1895, 247, Taf. 1, Fig. 3-4) predstavlja primerek vrste *Ranina laevifrons* Bittner iz eocenskih plasti Italije, ki ga primerja s primerki vrste *Ranina marestiana* König. Oppenheim (1896, 210) omenja ostanke vrste *Ranina marestiana* iz več najdišč (Mt. Postale, Ciuppio, Mt. Vegroni, Chiampo, Purga di Bolca) v okolici Verone. Vía (1959, 365-366) iz eocenskih skladov Španije omenja dve že obstoječi vrsti *Lophoranina marestiana* (König, 1825) in *L. reussi* (Woodward, 1866) ter opisuje novo vrsto *Lophoranina straeleni* (Vía, 1959). Vadász (1960, 594) predstavlja primerek vrste *Ranina reussi* Woodward iz zgornjeeocenskih plasti Madžarske. Ancona (1966, Tav. 1-3) predstavlja dobro ohranjene in izredno lepo prepari-

rane primerke iz srednjeeocenskih plasti nahajališča Valle del Chiampo v Italiji. Vogeltanz (1968, 103, Abb. 10) je raziskoval ostanke vrste *Ranina marestiana* König iz eocenskih plasti najdišča St. Pankraz na Salzburškem. Vía (1969, 104-125) opisuje iz eocenskih skladov Španije vrste *Lophoranina marestiana* (König) 1825, *L. reussi* Woodward, 1866 in *L. straeleni* Vía, 1959. Omenja pa še številne oblike fosilnih loforanin iz območij Indopacifika, Evrope, Afrike in Amerike. Po podatkih istega avtorja (Vía 1970, 124) je vrsta *Lophoranina marestiana* registrirana v srednje in zgornjeeocenskih skladih Italije, Švice, Nemčije, Avstrije, Španije in Egipta, iz Istre jih Vía (1970) ne omenja. Glaessner (1969) jo navaja iz severne Italije. Iz eocenskih skladov Črne Gore omenja Pavić (1970, 205) vrsto *Lophoranina bittneri* Lörenthey. Hagn, Darga & Schmid (1992, 192) omenjajo in predstavljajo dva primerka vrste *Ranina (Lophoranina) marestiana*, prvega iz spodnjecuisijskih skladov Kressenberga na Bavarskem in drugega iz lutetijskih plasti najdišča St. Pankraz pri Haunsbergu severno od Salzburga. Moosleitner (1996) jo je našel v nahajališču Paz severovzhodno od Pazina v Istri. Beschin in sod. (1988; 1994; 1998) navajajo, da je opisana vrsta ugotovljena v eocenskih skladih severne Italije in v Španiji. Morda nastopa tudi na Siciliji. Schultz (1998) piše, da je omenjena vrsta rakovice najdena v lutetijskih plasteh najdišča St. Pankraz blizu Salzburga v Avstriji. Mikuž (2004, 24) opisuje primerek vrste *Lophoranina marestiana* iz srednjeeocenskih flišnih plasti najdišča Gračišće, južnovzhodno od Pazina. Főzy & Szente (2007, 243, 2) prikazujeta primerek vrste *Lophoranina reussi* (Woodward) iz eocenskih plasti Madžarske.

Zaključki

V bližini Ćopija (sl. 1), zelo majhnega zaselka v osrednji Istri na Hrvaškem izdanjajo eocenske kamnine, ki so v sklopu paleogenskega flišnega bazena. V določenem horizontu flišnega profila so karbonatne in klastične kamnine. Znotraj le teh so posamezne plasti, ki so bogate s fosilnimi ostanki. Nekoliko višje je opaziti še »horizont z rakovicami«, v katerih je najdenih več različnih rakovic, vendar med njimi ni nobenih ostankov loforanin. Po pregledovanju izdankov, v katerih so najdene loforanine in iskanju drugega fosilnega inventarja ugotavljamo, da so prisotni še naslednji organizmi: numulitine, asterocikline, diskocikline, polži, školjke, poliheti, rakovice, mahovnjaki, morske lilije in nepravilni morski ježki. Najden je tudi skromen ostanek glavonožca. Po precej subjektivni presoji opažamo, da so med foramenifera mi najbolj pogostni ostanki numulitin, med makrofavno je veliko kamenih jeder polžev in školjk, nekoliko manj je nepravilnih morskih ježkov, še veliko manj pa vseh preostalih že navedenih fosilnih skupin. Pogrešamo ostanke koral in pravilnih morskih ježkov.

V raziskovanem najdišču pri Ćopiju so ostanki loforanin razmeroma pogostni in praviloma pripadajo vrsti *Lophoranina marestiana* (König, 1825). Večina karapaksov je manjših velikosti, sem in tja se najdejo tudi nekoliko večji primerki. Vsi predstavljeni primerki so poškodovani, popolnih karapaksov ni. Glede na tamkajšnje kamnine tudi ne moremo pričakovati bolj kompletnih, nikakor pa ne v celoti ohranjenih loforanin z vsemi njihovimi zelo občutljivimi nogami. Oblikovanost prečnih grebenov, ki so nazobčani oziroma drobno trnasti je raznolika, tudi izbočenost pri karapaksih se nekoliko razlikuje. Zaradi slabše ohranjenosti njihovih karapaksov in majhnega števila primerkov, statistična obdelava merskih podatkov takšnega fosilnega materiala ni primerna, pridobljeni statistični podatki bi lahko bili zavajajoči.

Opisana in predstavljena vrsta »istrske loforanine« (tab. 1, sl. 1-11) je značilna za lutetijske sklade Hrvaške (Istra), Italije, Španije, Avstrije in južne Nemčije ter najverjetneje kar za celoten kompleks srednjeeocenskih kamnin Evrope, predvsem njenega južnega predela ter vzhodnega dela severne Afrike. Primerki rodu *Lophoranina* so registrirani tudi vzhodneje na Madžarskem. V Sloveniji imamo velike površine prekrite tudi z eocenskim flišem, vendar še nismo našli nobenih loforanin.

Lophoraninas from Eocene beds in central Istria, Croatia

Conclusions

Close to Ćopi (Fig. 1), a very small village in central Istria, Croatia, outcrop Eocene beds that are a part of a larger Paleogene flysch basin. In a specific horizon of the flysch profile are present carbonate and clastic rocks. Certain beds within them are rich in fossil remains. Somewhat higher also a »horizon with crabs« is observed in which several distinct crab species were found, but no remains of lophoraninas. During inspection of outcrops in which lophoraninas were found and examination of the remaining fossil inventory we established also the presence of the following organisms: nummulitinas, asterocyclinas, discocyclinas, gastropods, bivalves, polychaetes, crabs, bryozoans, crinoids and irregular sea urchins.

Found was also a modest remain of a cephalopod. According to a rather subjective judgment the most frequent among foraminifers are remains of nummulitinas, among the macrofauna occur abundant casts of gastropods and bivalves, less frequent are irregular sea urchins, and even more rare the mentioned fossil groups. Missing are remains of corals and regular sea urchins.

In the studied locality at Ćopi remains of lophoraninas are relatively frequent, and they belong as a rule to species *Lophoranina marestiana* (König, 1825). Most carapaces are of moderate size, only a few individuals are larger. All presented specimens are damaged, no perfectly preserved carapaces were found. With respect to the locally occuring rocks no more completely preserved lophoraninas could be expected, considering their very delicate

legs. Morphology of transversal ridges, which are dentate resp. finely thorny is variable, and also the convexity of carapaces differs somewhat. Owing to the poor preservation state of carapaces and small number of specimens a statistical treatment of measurement data of such fossil material is not appropriate, since the results of statistics could be misleading.

The described and presented species of »Istrian lophoranina« (Pl. 1, Figs. 1-11) is characteristic for Lutetian beds of Croatia (Istria), Italy, Spain, Austria and southern Germany, and most probably also for the entire complex of Middle Eocene rocks of Europe, especially of its southern region, and the eastern part of North Africa. Specimens of genus *Lophoranina* were recorded also more to the east, in Hungary. In large areas of Slovenia Eocene flysch is also exposed, in which, however, no lophoraninas were found till now.

Zahvale

Zahvaljujemo se Viliju Rakovcu iz Kranja, ki je v najdišču pri Ćopiju našel nekaj ostankov karapaksov eocenskih rakovic ter jih podaril Oddelku za geologijo. Za situacijsko skico najdišča in drugo slikovno dokumentacijo se zahvaljujemo sodelavcu Marijanu Grmu, za prevode v angleščino pa zaslužnemu profesorju dr. Simonu Pircu.

Literatura

Ancona, L. 1966: Esemplari di *Ranina* (Decapodi Brachiuri) eccezionalmente ben conservati nell´Eocene medio della Valle del Chiampo (Vicenza). Mem. Mus. Civ. Stor. Natur. Verona (Verona) 14: 401–408, Tav. 1–3.

Beschin, C., Busulini, A., De Angeli, A. & Tessier, G. 1988: Raninidae del Terziario Berico–Lessineo (Italia settentrionale). Lavori Soc. Ven. Sc. Nat. (Venezia) 13: 155–215.

Beschin, C., Busulini, A., De Angeli, A. & Tessier, G. 1994: I Crostacei eocenici della cava »Boschetto« di Nigarole Vicentino (Vicenza – Italia settentrionale). Lavori Soc. Ven. Sc. Nat. (Venezia) 19: 159–215.

Beschin, C., Busulini, A., De Angeli, A., Tessier, G. & Ungaro, S. 1998: Crostacei eocenici di »Cava Rossi« presso Monte di Malo (Vicenza – Italia settentrionale). Studi Trentini Sci. Natur., Acta Geol. (1996) (Trento) 73: 7–34.

Bittner, A. 1875: Die Brachyuren des Vicentinischen Tertiärgebirges. Denkschr. Akad. Wiss. mathem.–naturwiss. Cl. (Wien) 34: 63–106, Taf. 1–5.

Bittner, A. 1883: Neue Beiträge zur Kenntniss der Brachyuren–Fauna des Alttertiärs von Vicenza und Verona. Denkschr. Akad. Wiss. (Wien) 46: 299–316, Taf. 1.

Bittner, A. 1895: Über zwei ungenügend bekannte brachyure Crustaceen des Vicentinischen Eocäns. Sitzungsb. Akad. Wiss. Mathem.–naturw. Cl. (Wien) 104 (1): 247–253, Taf. 1.

Főzy, I. & Szente, I. 2007: A Kárpát – medence ősmaradványai. Gondolat Kiadó (Budapest): 1–456.

Glaessner, M. F. 1969: Decapoda. – In: Moore, R. C. (Edit.), Treatise on Invertebrate Paleontology, Part R, Arthropoda 4/2. The Geological Society of America Inc. and The University of Kansas (Lawrence): R399–R533.

Guinot, D. 1993: Données nouvelles sur les Raninoidea de Haan, 1841 (Crustacea Decapoda Brachyura Podotremata). C. R. Acad. Sci Paris, Sciences de la vie (Paris) 316: 1324–1331.

Hagn, H., Darga, R. & Schmid, R. 1992: Erdgeschichte und Urwelt im Raum Siegsdorf. Fossilien als Zeugen der geologischen Vergangenheit. Im Eigenverlag der Gemeinde Siegsdorf (Siegsdorf): 1–241.

Kochansky-Devidé, V. 1964: Paleozoologija. Izdavačko poduzeće »Školska knjiga« (Zagreb): XI, 1–451.

Mikuž, V. 2002: Nova najdba rakovice *Harpactoxanthopsis quadrilobata* (Desmarest) v eocenskem flišu pri Gračišću blizu Pazina v Istri (Hrvaška). (New finding of crab *Harpactoxanthopsis quadrilobata* (Desmarest) in the Eocene flysch at Gračišće near Pazin in Istria (Croatia)). Geologija (Ljubljana) 45 (1): 97–102, (Tab. 1).

Mikuž, V. 2004: *Lophoranina marestiana* iz srednjeeocenskih flišnih plasti pri Gračišću v Istri. (*Lophoranina marestiana* from Middle Eocene flysch beds at Gračišće in Istria, Croatia). Geologija (Ljubljana) 47/1: 23–27, (Tab. 1).

Moosleitner, G. 1996: Fossilien aus dem Mittel–Eozän von Istrien. Fossilien (Korb) 2: 105–110.

Oppenheim, P. 1896: Die Eocaenfauna des Monte Postale bei Bolca im Veronesischen. Palaeontographica (Stuttgart) 43: 125–221, Taf. 12–19.

Parona, C. F. 1924: Trattato di geologia con speciale riguardo alla geologia d´Italia. Seconda edizione. Casa Editrice Dottor Francesco Vallardi (Milano): XIV, 1–648.

Pavić, A. 1970: Marinski paleogen Crne Gore. Stratigrafija, tektonika, paleogeografija. Zavod za geološka istraživanja Crne Gore (Titograd): 1–205, Tab. 1–20.

Pavlovec, R. & Pavšič, J. 1987: Biostratigrafija plasti z rakovicami v Istri. (Biostratigraphy of beds with crabs in Istria). Geologija (1985/86) (Ljubljana) 28–29: 55–68, (Tab. 1–3).

Quenstedt, A. 1885: Atlas zum Handbuch der Petrefaktenkunde. Dritte umgearbeitete und vermehrte Auflage. Verlag der H. Laupp´schen Buchhandlung (Tübingen): Tab. 1–100.

Reuss, A. 1859: Zur Kentniss fossiler Krabben. Denkschr. Akad. Wiss. mathem.–naturwiss. Cl. (Wien) 17: 1–90, Taf. 1–24.

Sacco, F. 1924: L´Istria. Cenni geologici generali. Memorie descrittive della Carta geologica d´Italia (Mondovi) 19: 1–105.

Savazzi, E. 1981: Functional morphology of the cuticular terraces in *Ranina (Lophoranina)* (brachyuran decapods; Eocene of NE Italy). N. Jb. Geol. Paläont. Abh. (Stuttgart) 162 (2): 231–243.

TABLA 1 – PLATE 1

1 *Lophoranina marestiana* (König, 1825), primerek Ćr-1, karapaks z zgornje strani, Ćopi, x 1
Lophoranina marestiana (König, 1825), specimen Ćr-1, carapace from the dorsal side, Ćopi, x 1

2 *Lophoranina marestiana* (König, 1825), primerek Ćr-2, zgornja stran oklepa, Ćopi, x 1,2
Lophoranina marestiana (König, 1825), specimen Ćr-2, dorsal view, Ćopi, x 1,2

3 *Lophoranina marestiana* (König, 1825), primerek Ćr-3, zgornja stran oklepa, Ćopi, x 1,4
Lophoranina marestiana (König, 1825), specimen Ćr-3, dorsal view, Ćopi, x 1,4

4 *Lophoranina marestiana* (König, 1825), primerek Ćr-4, zgornja stran oklepa, Ćopi, x 1,3
Lophoranina marestiana (König, 1825), specimen Ćr-4, dorsal view, Ćopi, x 1,3

5 *Lophoranina marestiana* (König, 1825), primerek Ćr-5, zgornja stran oklepa, Ćopi, x 1,5
Lophoranina marestiana (König, 1825), specimen Ćr-5, dorsal view, Ćopi, x 1,5

6 *Lophoranina marestiana* (König, 1825), primerek Ćr-6, zgornja stran oklepa, Ćopi, x 1,5
Lophoranina marestiana (König, 1825), specimen Ćr-6, dorsal view, Ćopi, x 1,5

7 *Lophoranina marestiana* (König, 1825), primerek Ćr-7, zgornja stran oklepa, Ćopi, x 1,4
Lophoranina marestiana (König, 1825), specimen Ćr-7, dorsal view, Ćopi, x 1,4

8 *Lophoranina marestiana* (König, 1825), primerek Ćr-8, zgornja stran oklepa, Ćopi, x 1,5
Lophoranina marestiana (König, 1825), specimen Ćr-8, dorsal view, Ćopi, x 1,5

9 *Lophoranina marestiana* (König, 1825), primerek Ćr-9, zgornja stran dela oklepa, Ćopi, x 1,5
Lophoranina marestiana (König, 1825), specimen Ćr-9, dorsal view, Ćopi, x 1,5

10 *Lophoranina marestiana* (König, 1825), primerek Ćr-10, del zadnjega dela oklepa, Ćopi, x 1,3
Lophoranina marestiana (König, 1825), specimen Ćr-10, dorsal view, Ćopi, x 1,3

11 *Lophoranina marestiana* (König, 1825), primerek Ćr-11, del oklepa, Ćopi, x 1,4
Lophoranina marestiana (König, 1825), specimen Ćr-11, dorsal view, Ćopi, x 1,4

Fotografije (Photos): Marijan Grm

TABLA 1 – PLATE 1

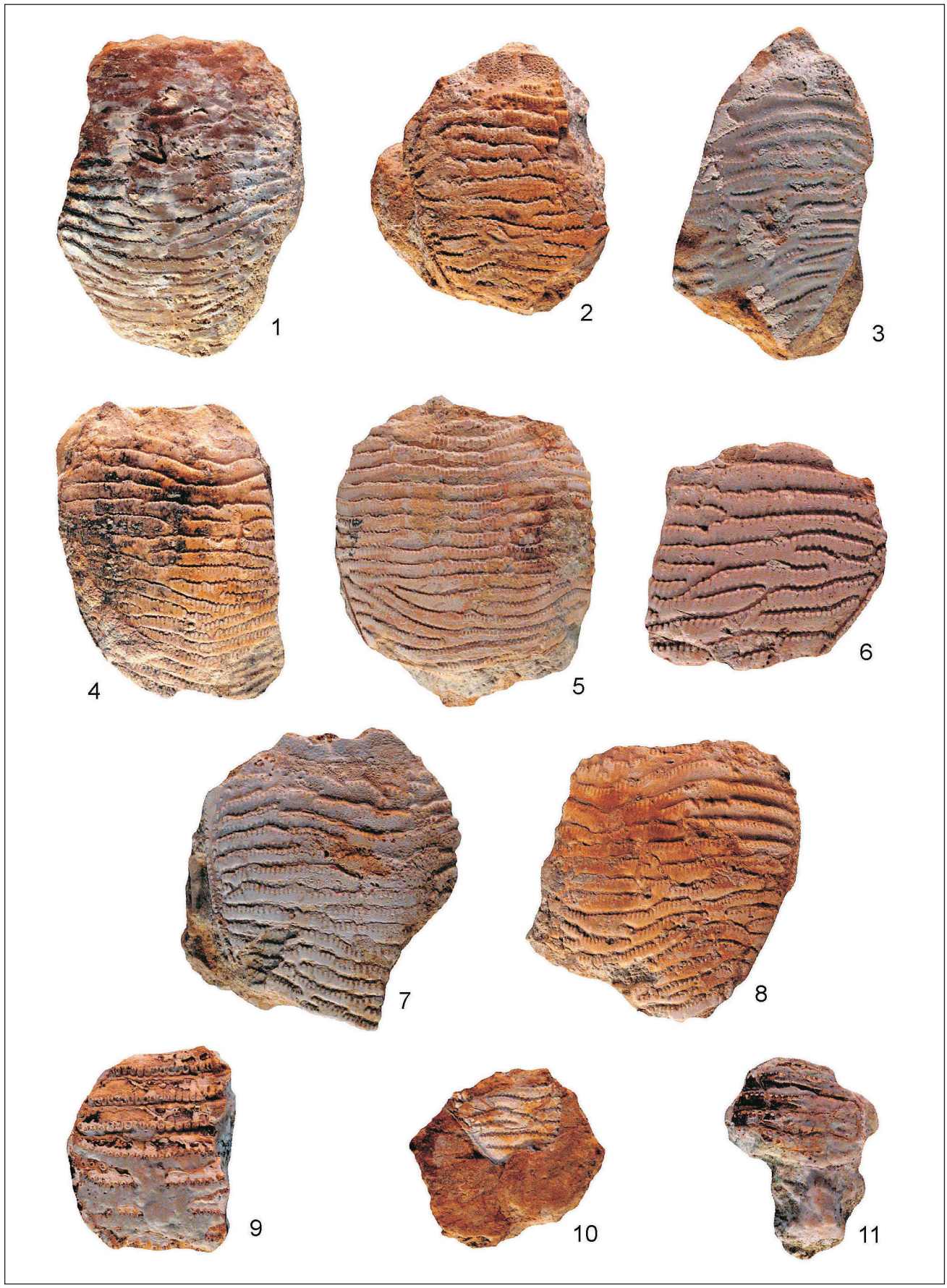

Schafhäutl, K. E. 1863: Süd–Bayerns Lethaea Geognostica. Der Kressenberg und die südlich von ihm gelegenen Hochalpen geognostisch betrachtet in ihren Petrefacten. (Leipzig): XVII, 1–487, Taf. 1–86.

Schultz, O. 1998: Tertiärfossilien Österreichs. Wirbellose, niedere Wirbeltiere und marine Säugetiere. Goldschneck–Verlag (Korb): 1–159.

Schweitzer, C. E., Ćosović, V. & Feldmann, R. M. 2005: *Harpactocarcinus* from the Eocene of Istria, Croatia, and the paleoecology of the Zanthopsidae Via, 1959 (Crustacea: Decapoda: Brachyura). J. Paleont. (Tulsa) 79 (4): 663–669.

Schweitzer, C. E., Shirk, A. M., Ćosović, V., Okan, Y., Feldmann, R. M. & Hoşgör, I. 2007: New species of *Harpactocarcinus* from the Tethyan Eocene and their paleoecological setting. J. Paleont. (Tulsa) 81 (5): 1091–1110.

Tarlao, A. 2000: Considerazioni sui Decapodi Brachiuri dellžIstria e loro attribuzione a *Harpactoxanthopsis quadrilobata* (Desmarest, 1822). Natura Nascosta (Monfalcone) 21: 29–34.

Toniolo, R. A. 1909: L´Eocene dei dintorni di Rozzo in Istria e la sua fauna. Paleontographia Italica, Mem. Palaeont. (Bologna): 15, 237–295, Tav. 1–3.

Vadász, E. 1960: Magyarország Földtana. Akadémiai Kiadó (Budapest): 1–646, (Táb. 1–51).

Velić, I., Tišljar, J., Matičec, D. & Vlahović, I. 1995: Opći prikaz geološke građe Istre. 1. Hrvatski geološki kongres, Vodič ekskurzija (Zagreb): 5–30.

Vía, L. 1959: Decápodos fósiles del Eocene español. Bol. Ist. Geol. Min. Español (Madrid) 70: 331–402.

Vía, L. 1970: Crustáceos Decápodos del Eocene Español. Pirineos, Rev. Inst. Est. Pirenaicos (1969) (Jaca) 25 (91–94): 1–479, Lám. 1–39.

Vogeltanz, R. 1968: Beitrag zur Kenntnis der fossilen Crustacea Decapoda aus dem Eozän des Südhelvetikums von Salzburg. N. Jb. Geol. Paläont. Abh. (Stuttgart) 130 (1): 78–105.

Zittel, K. A. 1895: Grundzüge der Palaeontologie (Palaeozoologie). Druck und Verlag von R. Oldenbourg (München und Leipzig): VIII, 1–971.

GEOLOGIJA *53/1*, 55–86, Ljubljana 2010

The bases for understanding of the NW Dinarides and Istria Peninsula tectonics

Osnove razumevanja tektonske zgradbe NW Dinaridov in polotoka Istre

Ladislav PLACER[1], Marko VRABEC[2] & Bogomir CELARC[1]

[1]Geološki zavod Slovenije, Dimičeva ul. 14, SI-1000 Ljubljana;
e-mail: ladislav.placer@geo-zs.si; bogomir.celarc@geo-zs.si
[2]Univerza v Ljubljani, Naravoslovnotehniška fakulteta, Aškerčeva 20, SI-1000 Ljubljana;
e-mail: mvrabec@ntfgeo.uni-lj.si

Prejeto / Received 24. 3. 2010; Sprejeto / Accepted 24. 5. 2010

Key words: Neogene and recent movements, Istria-Friuli Underthrust Zone, rigid indenter of Adria Microplate
Ključne besede: Neogenski in recentni premiki, Istrsko-Furlanska podrivna cona, trdno jedro Jadranske mikroplošče

Abstract

Thrust structure of the northeastern part of the External Dinarides is depended upon paleogeography of the **Adriatic–Dinaric Mesozoic Carbonate Platform,** which was in the southeast (in the recent position) composed of Dinaric and Adriatic segment with intermediate Budva Trough. In the northwest in the area of the present Slovenia, it represents uniform platform. In the northwestern continuation of the Budva Trough, shallow halftrough formed and more to the west, shallow Friuli Paleogene Basin came in to being, which separated so called Friuli Carbonate Platform from the central part of the carbonate platform. Area of Istria was separated from Adriatic segment with Kvarner Fault, originated already in the Mesozoic.

External Dinaric Thrust Belt formed in the final phase of the Dinarides overthrusting. It originated from Dinaric segment of the Mesozoic Carbonate Platform at the end of the Eocene and was thrusted on the Adriatic segment of the Mesozoic Carbonate Platform. Whole process also triggered formation of the **External Dinaric Imbricate Belt** with Thrust Front of the External Dinarides against Adriatic-Apulian Foreland. Later also represents rigid indenter of the Adria Lithospheric Microplate ("Adria"), and External Dinaric Imbricate Belt represents its deformed margin, therefore we place it to the rigid indenter.

Segmentation of the "Adria" occurred in the Miocene or later. It roughly disintegrated in the Padan and Adriatic part along Kvarner Fault. During rotation of the Padan part in the counter clockwise sense, the corner part, representing Istria Peninsula, rotated and underthrusted towards northeast under External Dinarides. As a result, **Istria-Friuli Underthrust Zone** formed, structurally conditioned with the position of the Friuli Paleogene Basin, and vast **Istria Pushed Area** between Southern Alps, Velebit Mts. and Želimlje Fault. This process is still active recently.

During Istria underthrusting and pushing in the northwest direction, Raša Fault and Thrust Front of the External Dinaric Thrust Belt bended, and as a consequence, strike-slip movements along those planes were hindered. From the tip of the Kvarner Bay towards Idrija and Ravne Faults in the Upper Soča Valley, conditions for formation of the en echalon strike-slip belt were set up. The strike-slip belt is defined with segment of the Raša Fault southeast from Ilirska Bistrica, seismically active area between Ilirska Bistrica – Hruševje stretch, Vipava Fault, Predjama Fault and northwestern part of the Idrija and Ravne Fault. Therefore we postulate, that a segment of the External Dinaric Thrust Belt Front and shear boundary between the tip of Kvarner Bay and Upper Soča Valley, with extended branches of the Idrija and Ravne Faults, represents new attached block of the Adria Microplate rigid indenter edge.

Izvleček

Narivna zgradba severozahodnega dela Zunanjih Dinaridov je pogojena s paleogeografsko podobo **Jadransko-dinarske mezozojske karbonatne platforme**, ki je bila na jugovzhodu v današnji legi zgrajena iz dinarskega in jadranskega segmenta platforme z vmesnim **Budvanskim jarkom**, na severozahodu na območju današnje Slovenije pa je tvorila enotno platformo. V podaljšku Budvanskega jarka proti severozahodu, se je v paleogenu izoblikoval plitek poljarek, zahodno od tod pa plitek **Furlanski paleogenski bazen**, ki je tedaj ločil t. i. Furlansko karbonatno platformo od osrednjega dela karbonatne platforme. Območje Istre je bilo od Jadranskega segmenta platforme ločeno s **Kvarnerskim prelomom**, ki je bil zasnovan že v mezozoiku.

V končni fazi krovnega narivanja Dinaridov je iz dinarskega segmenta mezozojske karbonatne platforme konec eocena nastal **Zunanjedinarski narivni pas**, ki se je narinil na jadranski segment mezozojske karbonatne platforme in izzval nastanek **Zunanjedinarskega naluskanega pasu** katerega čelo predstavlja **Narivno čelo Zunanjih Dinaridov** nasproti **Jadransko-apulijskemu predgorju**. Slednje predstavlja trdno jedro Jadranske litosferne mikroplošče ("Adrie"), Zunanjedinarski naluskani pas pa njeno deformirano obrobje in ga zato prištevamo k trdnemu jedru.

V miocenu ali pozneje je prišlo do segmentacije "Adrie". Ta je v grobem razpadla ob Kvarnerskem prelomu na padski in jadranski segment. Pri rotaciji padskega segmenta v nasprotni smeri urinega kazalca, se je njen vogalni del kjer leži polotok Istra, zasukal in se podrinil proti severovzhodu pod Zunanje Dinaride. Nastala je **Istrsko-furlanska podrivna cona**, ki je strukturno pogojena z lego Furlanskega paleogenskega bazena in obsežno **Istrsko potisno območje**, ki zajema prostor med Južnimi Alpami, Velebitom in Želimeljskim prelomom. Ta proces je recentno aktiven.

Pri podrivanju in potiskanju Istre proti severovzhodu se je usločil Raški prelom in čelni nariv Zunanjedinarskega narivnega pasu, zaradi česar je bilo zmikanje ob teh ploskvah oteženo. Ustvarili so se pogoji za nastanek ešalonskega zmičnega pasu od vrha Kvarnerskega zaliva proti Idrijskemu in Ravenskemu prelomu v dolini zgornje Soče. Pas je definiran s segmentom Raškega preloma jugovzhodno od Ilirske Bistrice, pasom pogoste seizmične aktivnosti Ilirska Bistrica – Hruševje, Vipavskim prelomom, Predjamskim prelomim ter severozahodnim delom Idrijskega in Ravenskega preloma. Postavljamo domnevo, da predstavlja segment med Čelom Zunanjedinarskega narivnega pasu in strižno mejo med vrhom Kvarnerskega zaliva ter zgornjim Posočjem s podaljšanima vejama Idrijskega in Ravenskega preloma proti zahodu nov priključeni blok mejnega pasu trdnega jedra Jadranske mikroplošče.

Introduction

The idea about tectonic structure of the northwestern part of the External Dinarides is based on the data of structural mapping and hypothetic assumption of the Adria Microplate indenter underthrusting below External Dinarides (Blašković & Aljinović, 1981; Blašković, 1991, 1998, 1999; Placer, 2002, 2005, 2007; Placer et al., 2004), on the analysis of repeated leveling line campaigns data (Rižnar et al., 2007) and GPS measurements (Weber et. al., 2010).

The question of structure of the northwestern part of Dinarides in hinterland of Trieste Bay, Istria Peninsula and Kvarner Bay (Fig. 1) is important for understanding the dynamics of tectonic processes and establishment of trace of northeastern boundary of the rigid indenter of the Adria Lithospheric Microplate. It is also closely related with discussion on existence of a single or two Mesozoic carbonate platforms. The concept of a single platform has been recently maintained by Velić et al. (2002) and Vlahović et al. (2005), and the term Adriatic Carbonate Platform was proposed, which also includes several intraplatform basins that assumed various positions in the evolution process of the platform. In structural sense, Budva Trough (T_3 – K) divides central and southern part of the platform into two segments. Two platforms, the Adriatic and the Dinaric one, with the interplatform Budva Trough, have been advocated by Herak (1986,1999), Tari (2002) and Korbar (2009).

The analysis of the thrust structure of northwestern part of Dinarides described in the present paper supports the assumption that the model by Velić et al. (2002) and Vlahović et al. (2005) more closely corresponds to the situation in the field, whereas Tari's model, although established in the central and southeastern part of the External Dinarides, provides an appropriate basis for structural and genetic presentation of problems. Since according to our research the Budva Trough was larger in size than believed by Vlahović et al.

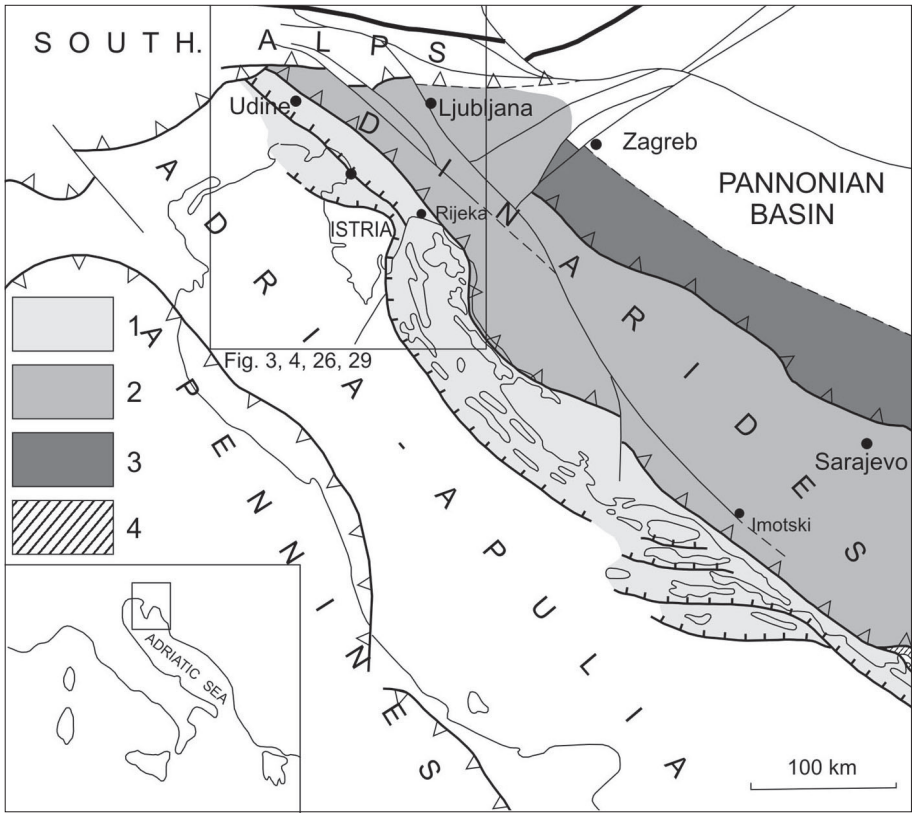

Fig. 1. **Orientation sketch. Thrust subdivision of the Dinarides.**
1. External Dinaric Imbricated Belt;
2. External Dinaric Thrust Belt;
3. Internal Dinaric Thrust Belt;
4. Budva Trough.

(2005), and had therefore a stronger influence on formation of the thrust structure, we believe it is more appropriate to use the term Adriatic-Dinaric Carbonate Platform (Pamić et al., 1998) consisting of Adriatic and a Dinaric segment. Therefore we accordingly modified Tari's (2002) structural terminology.

Tari (2002) subdivided the Dinaric thrust structure into the Eastern Thrust Belt and the Western Thrust Belt whose overthrusts verge toward SW. The Eastern Thrust Belt consists of rocks of the prerifting and rifting stages, and the most characteristic overthrust structure in it is the front nappe of ophiolitic melange. The latter is overthrust on the Western Thrust Belt whose northeastern part consists of Jurassic and Cretaceous flysch filling the pre-thrust basin of the Eastern Thrust Belt, and its central and southwestern parts comprise rocks of the Dinaric Mesozoic carbonate platform that comprises the foreland of the Eastern Thrust Belt. The southwestern boundary of the Western Thrust Belt is constituted by the Frontal Thrust of the Dinaric carbonate platform that passes along the Adriatic coast. Below the Frontal Thrust is underthrust the marginal part of the Adriatic Carbonate Platform, as a result of which the Imbricated belt of the Adriatic Carbonate Platform is formed. Rocks of the Budva Basin are covered by overthrusts of the Western Thrust Belt. The thrust structure of Dinarides progressed in time and space from northeast toward southwest. The Eastern Thrust Belt, however, started to form after the continental progressive convergence at the end of Jurassic, while the Frontal Thrust of the Western Thrust Belt ended its evolution in the Older Eocene. The imbricated belt of the Adriatic Carbonate Platform might have originated in the last thrusting stage of the Western Thrust Belt already, its evolution continued by underthrusting of the rigid indenter of the Adria Lithospheric Microplate under Dinarides in Oligocene, and has been still active in Pleistocene.

In the paper the classical structural subdivision into the Internal and External Dinarides, and their foreland is used (Fig. 1). Tari's (2002) Eastern Thrust Belt is considered as the **Internal Dinaric Thrust Belt**, and Western Thrust Belt as the **External Dinaric Thrust Belt**. For southwestern boundary of the External Dinaric Thrust Belt it seems better to use the term **Frontal Zone of the External Dinaric Thrust Belt** than the term Frontal Thrust of the Western Thrust Belt, since it better corresponds to reality. Its trace is identical with the classic Overthrust of High Karst in the sense of Herak (1999), Pamić & Hrvatović (2003), Prelogović et al. (2004), and others. The **External Dinaric Imbricated Belt** is identical in its central and southeastern coastal part to Tari's Imbricated Belt of the Adriatic Carbonate Platform that represents in structural sense marginal part of the rigid indenter of Adria Lithospheric Microplate. The southwestern boundary of the External Dinaric Imbricated Belt is the **Thrust Front of External Dinarides**.

The overthrust model by Korbar (2009) cannot be included into this concept, since his understanding of the size of the Dinaric and Adriatic segments of the Mesozoic Carbonate Platform differs from all previous ideas. Korbar included into the Dinaric segment also the central part of our External Dinaric Imbricated Belt, respectively of TARI´S Imbricated Belt of the Adriatic Platform between Istria and Brač which is a part of the Adriatic branch of the Adriatic-Dinaric Carbonate Platform, or a separate carbonate platform in previous models.

In the studied region, Paleozoic clastites and Upper Permian to Carnian bedded carbonates and clastites are exposed, followed by rocks of the Adriatic-Dinaric Carbonate Platform from Norian to Upper Cretaceous and Paleocene, and on the top by Upper Cretaceous and Tertiary marly calcareous and clastic rocks which are degradation products of the platform. The geometry of the thrust structure is controlled by the Budva intraplatform troughs, and by two horizons of more ductile rocks which underlie and overlie the carbonate platform deposits (Fig. 2). The lower horizon is divided in External Dinarides in two levels, the lower one consisting of Carboniferous-Permian clastites, that include the Gröden (Val Gardena) Group (Fig. 2, b – dark grey shading), and the upper one composed of Upper Permian, Lower Triassic and Anisian layered carbonates and clastites, Ladinian and Carnian clastites (Fig. 2, a – light grey shading). This distinction is generally not feasible in the region of the Adriatic segment of carbonate platform owing to lack

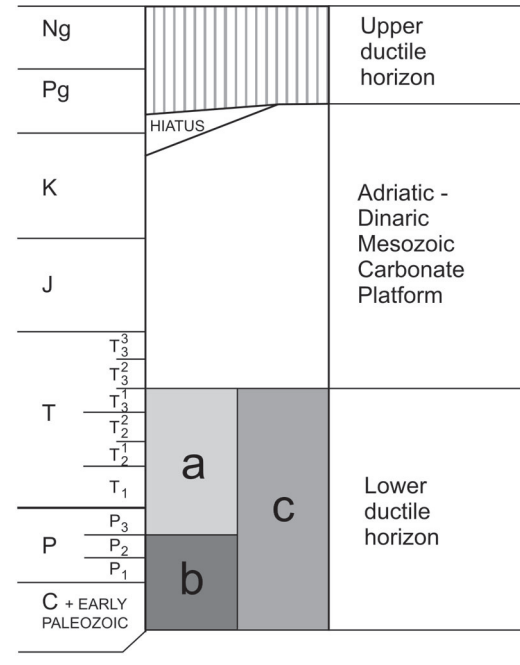

Fig. 2. **Lithostratigraphic column.**
Upper ductile horizon: flysch and molasse; *Adriatic-Dinaric Mesozoic Carbonate Platform*: Upper Triassic, Jurassic and Cretaceous carbonates; *Lower ductile horizon*:
a – Upper level: Carnian clastites, Middle Triassic clastites and volcanic rocks, Anisian carbonates, Lower Triassic carbonates, marlstones and clastites and Permian carbonates;
b – Lower level: Middle and Lower Permian clastites and carbonates and oldest clastites;
c – Upper and Lower level undifferentiated.

of data; so the entire horizon is marked by grey shading (Fig. 2, c – grey shading). For the sake of better distinctness on the tectonic map in Fig. 3 only the lower level of the lower ductile horizon is drawn next to the upper ductile horizon (Fig. 2, b – dark grey shading).

In this article, the age of thrust deformations is based on the Eocene age of flysch in the southeastern part of the External Dinarides. New findings about Miocene age of flysch (Mikes et al., 2008) are not verified yet, so they were not taken in to the consideration.

The boundary with Southern Alps is considered in the present paper formally, without regard to the internal structure of the Southern Alps. The concept of the Southern Alpine Boundary is understood in the sense as presented by Slejko et al. (1986), Carulli et al. (1990), Nussbaum (2000), Merlini et al. (2002) and Peruzza et al. (2002).

The rigid indenter of the Adria Microplate, abridged "Adria" in the quotation marks, will be used in the further text.

Tectonic structure

Interpretation of tectonic structure of Istria and its hinterland between Southern Alps and Velebit Mts. (Fig. 3) is based on data of the Basic Geologic Map of Yugoslavia of scale 1:100.000 (Buser et al., 1967; Buser, 1968, 1969, 1978, 1986, 1987; Grad & Ferjančič, 1974, 1976; Magaš, 1968; Mamužić et. al., 1969; Pleničar et al., 1969; Pleničar et al., 1973; Polšak, 1967; Polšak & Šikić, 1973; Premru, 1983; Savić & Dozet, 1985; Šikić et al., 1969; Šikić et al., 1972; Šušnjar et al., 1970), of the compilation map Structural Model of Italy and Gravity Map, sheet 2 of scale 1 : 500.000 (Bigi et al., 1990) and Geologic Map of Friuli Venezia Giulia of scale 1 : 150.000 (Carulli, 2006). In addition, all more important results from published works are considered (Biondić et al., 1997; Blašković, 1999; Colizza et al., 1989; Cucchi et al., 1989a,b; Čar & Gospodarič, 1983/84; Jurkovšek et al., 1996; Poljak & Rižnar, 1996; Marinčić & Matičec, 1991; Matičec, 1994; Mlakar, 1969; Mlakar & Placer, 2000; Peruzza et al., 2002; Placer & Čar, 1997; Placer, 1981,1982, 1996, 2005, 2007, 2008a, 2008b; Ponton, 2002). This paper is also based on published data from structural mapping of the motorway section Divača – Koper across the Istria-Friuli Underthrust Zone in years 1999 – 2005, and Razdrto – Vipava, as well as the data from additional mapping of Razdrto – Senožeče road section, and of the seashore from Lazaret to Piran, and field inspections of key structural localities in the region between the Southern Alps and Velebit Mts.

Thrust structure of External Dinarides

In the northwestern part of Dinarides, with respect to age and genesis, there exist three thrust systems that verge toward southwest, and for which the reduction of space in SW-NE direction is characteristic. The three thrust systems are from northeast to southwest: 1. External Dinaric Thrust Belt with its frontal zone of complex structure, 2. External Dinaric Imbricated Belt with its distinct thrust front formed at overthrusting of Dinarides southwestwards, and 3. underthrusting of the "Adria" northeastwards.

Within the External Dinaric Imbricated Belt occurs the Istria-Friuli Underthrust Zone that formed in the younger stage of underthrusting of the "Adria". The movements of Istria resulted in hinterland into the broad Istria Pushed Area that extends from Southern Alps to the Velebit Mountains. All mentioned thrust systems are underthrust under the Southern Alps. In this paper only the formal subdivision of the Southern Alpine Thrust Boundary is described.

In addition to the thrust deformations, there exist also the Dinaric NW-SE striking faults which are an important indicator of dynamics of the Dinarides.

In this article, the age of thrust deformations is based on the Eocene age of flysch in the southeastern part of the External Dinarides. New findings about Miocene age of flysch (MIKES et al., 2008) are not verified yet, so they were not taken in consideration

External Dinaric Thrust Belt
(Middle Eocene – Younger Eocene)

The External Dinaric Thrust Belt comprises nappes of the External Dinarides. Structurally highest is the Trnovo Nappe with two accompanying lower order structures, the Hrušica Nappe and the Sovič Thrust Block. These three units are associated in the Trnovo Thrust Series. Below it lies the Snežnik Thrust Unit that continues in the Vinodol Thrust Unit and the Velebit Thrust Unit. The latter three thrust units are conditionally associated in the "Velebit Thrust Series" in which, however, the relations between thrust units are not as clear as in the Trnovo Thrust Series.

Trnovo Thrust Series

Interpretation of the Trnovo Nappe is based on the data of the Basic Geologic Map (Buser et al., 1967; Buser, 1968, 1987) and works of Mlakar (1969) and Placer (1973, 1981, 1999, 2008b) that originated from study of the Idrija mercury deposit and Žirovski vrh uranium deposit respectively. Deep drilling at Cerkno (Placer et al., 2000) confirmed the nappe structure with clear internal regularity. In the section across the Idrija deposit, the Trnovo Nappe is thrust for 32 km southwestward with respect to the Hrušica Nappe, and the Hrušica Nappe is shifted for 19 km with respect to the Sovič Thurst (Placer, 1981). The length of shift has not been constructed for the Sovič Thrust, but is estimated to be in order of several kilometers. Thrusting directions toward southwest are proved by axes of hectometric and dekametric folds in all

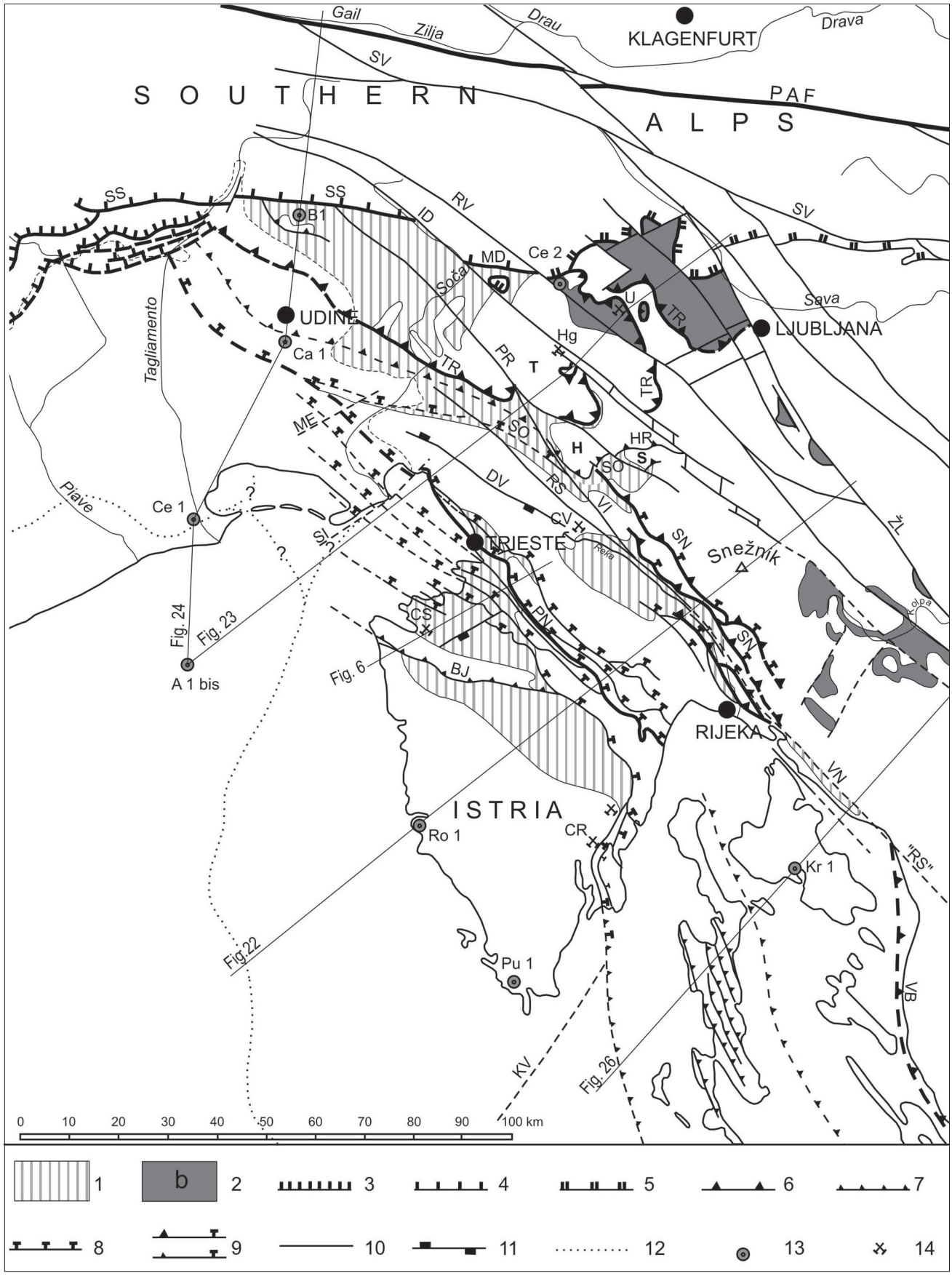

Fig. 3. **Tectonic sketch.** 1. Upper ductile horizon; 2. Lower ductile horizon southwest of the Želimlje fault: **b** – Middle and Lower Permian and Carboniferous clastites (Explanation on Fig. 2); *Boundary of underthrusting below the Southern Alps*: 3. Thrust Faults SW-NE, WSW-ENE; 4. Thrust Faults E-W weste of the RV – Ravne Fault: SS – Staro selo Fault, MD – Modrej Fault; 5. Thrust Faults W-E easth of the RV – Ravne Fault; *External Dinarides*: 6. Thrusts of the External Dinarides Thrust Belt: TR – Trnovo Nappe Fault, HR – Hrušica Nappe Fault, SČ – Sovič Thrust Fault, SN – Snežnik Thrust Fault Zone, VN – Vinodol Thrust Fault Zone, VB – Velebit Thrust Fault Zone; 7. Trusts of the External Dinaric Imbricated Belt: BJ – Buje Thrust Fault; 8. The thrusts of the Istria-Friuli Underthrust Zone and Autside: PN – Palmanova Thrust Fault; 9. Reactivated thrust faults of the Istria Pushed Area; 10. *Faults*: SV – Sava Fault, ID – Idrija Fault, RV – Ravne Fault, ŽL – Želimlje Fault, PR – Predjama Fault, VI – Vipava Fault, RS – Raša Fault, SE – Sistiana (Sesljan) Fault, ME – Medea (Medeja) Fault, KV – Kvarner Fault, PAF – Periadriatic Fault Zone; 11. DV – Divača Pivot Fault; 12. Autside border of the carbonate platform; 13. *Boreholes*: A 1 bis – Amanda, Ce 1 – Cesarolo, Ca 1 Cargniacco, B 1 – Bernadia, Ce 2 – Cerkno, Ro 1 – Rovinj, Pu 1 – Pula, Kr 1 – Krk; 14. *Abandoned metal and coal mines*: Hg – Idrija (mercury), U – Žirovski vrh (uranium), CV – Vremski Britof (bituminous coal), CS – Sečovlje (bituminous coal), CR – Raša (bituminous coal).

of the three units, and rotation of macrolithons consisting of Triassic structural blocks in the Idrija mercury deposit (Placer, 1982), and cleavage of microlithons in the Žirovski vrh uranium deposit (Mlakar & Placer, 2000) within the Trnovo Nappe, as well as direction of thrusting megalineation in the thrust plane of the Hrušica Nappe (Placer, 1994/95).

The Trnovo Nappe consists of rocks of the Paleozoic and Triassic basement of the Adriatic-Dinaric Carbonate Platform, which are over lain by rocks of the carbonate platform aged from Upper Triassic to Upper Cretaceous. In the northwestern part of the nappe Upper Cretaceous and Paleogene rocks were unconformably deposited in the mobile part of platform that dip toward NW, owing to which we suppose that the considered part of the Trnovo Nappe represents the northwestern part of the Adriatic-Dinaric Carbonate Platform (in present orientation).

The relations in the Hrušica Nappe are different; there occur rocks of Mesozoic carbonate platform, on which the Paleogene beds of carbonate marly and flysch habitus are unconformab deposited.

The Trnovo Nappe is the oldest nappe unit of External Dinarides in the studied region. During the overthrusting toward southwest, it initiated the origin of the Hrušica Nappe, and subsequently the formation of the Sovič Thrust. With regard to its position in space, the Trnovo Nappe is unique, since in the studied area it is separated from the remaining External Dinarides nappe units. On the north it is cut by the Southern Alpine Boundary, and on the east by the Želimlje Fault which is the most important fault of the Ljubljana – Imotski Fault Zone (Tari, 2002, Miocene strike slip; Placer, 2008b, Ljubljana – Imotski Fault Zone), and represents an important structural boundary of the External Dinarids. The Hrušica Nappe, after Čar & Gospodarič (1983/84), is clearly associated with nappe structure of the remaining part of the External Dinarides, its fault plane toward southeast being hidden in the fault zone of the Idrija Fault. The Sovič Thrust is a miniature pendant of the Hrušica Nappe (Placer, 1996). The problem of connection of thrust planes of the Trnovo and Hrušica Thrust Nappes and of the Sovič Thrust Fault toward northwest consists in the fact, that the thrust planes visible in southeast owing to carbonates being overthrust on flysch, become extensively ramified where the thrusts are developed in flysch, as the joints develop into integral thrust planes. Since the problem of structural connecting in the field has not yet been accomplished, it is only indicated it in the present paper (Fig. 3). Similar conditions in Istria (Placer, 2007) could have been solved only by structural mapping which, however, has not yet been undertaken in the Vipava Valley area.

The main thrust plane of the Trnovo Nappe is gently folded in Dinaric direction in a wide frontal synform, and in a corresponding antiform in northeast, where it forms a tectonic half-window called the Poljane-Vrhnika belt. Both forms are indications of post-thrusting pression in SW-NE direction. The thrust boundary of Southern Alps that covers the mentioned folds is not folded.

The formation of the Trnovo Thrust Series could be temporally attributed to the time and space between the Internal Dinaric Thrust Belt, supposed to have started forming in Younger Jurassic, and its frontal zone, whose evolution might have been accomplished in Older Eocene (Tari, 2002). According to our opinion, however, it could have lasted, considering the age of the flysch beds in the Vipava Valley, to the end of Middle, or to the Younger Eocene.

Velebit Thrust Series

The region of the "Velebit Thrust Series" southeast of the Trnovo Thrust Series is not evaluated. Subdivision into the Velebit Nappe unit and the Vinodol and Snežnik thrust units is formal. The thrust front of this belt in northwest is covered with the thrust front of the Sovič or Hrušica Nappe fault.

Frontal Zone of the External Dinaric Thrust Belt (Younger Eocene)

The Frontal Zone of the External Dinaric Thrust Belt is an important structural element of the thrust structure of Dinarides. In hinterland of Kvarner and Istria to the Postojna Basin it is identical with frontal zones of the Velebit, Vinodol and Snežnik Thrust Faults, where it is covered with the Sovič or Hrušica Nappe fault. Two possible variants of its course from there towards northwest are found in the literature. According to the first one (Herak 1999, Premru 1980, 2005), the frontal parts of the Snežnik Thrust Block and of Hrušica and Trnovo Nappe are connected with a single thrust zone, against which is supposed to lean the Hrušica and Trnovo Thrust Fault; whereas according to the second variant (Buser et al., 1967; Buser, 1968; Placer, 1999, 2008b), the unique frontal zone has supposedly split into the Hrušica and Trnovo Thrust Faults. The first variant is based on sedimentological-paleontological research that resulted in the hypothesis of existence of two separated carbonate platforms, the Adriatic and the Dinaric one. The second variant is based on analysis of structural relationships and on the hypothesis that the differences in Upper Cretaceous, and later in Paleogene, are a result of formation of intraplatform troughs of Dinaric direction with specific environments (Šribar, 1995), which permitted the coexistence of various developments at relatively short distances. This could explain the differences in development on the opposite sides of the Snežnik Thrust Fault in the area of the Postojna Flysch Basin. During mapping of the Razdrto – Vipava motorway section and at a preliminary field inspection of the southeastern part of the Vipava Synclinorium it has been found that the thrust planes of the Trnovo Nappe Series in their frontal part do not follow the regional dip of

nappe units toward northwest, because they were deformed during formation of the "Adria" unit.

The External Dinaric Imbricated Belt
(Marginal belt of "Adria")
(Oligocene)

The External Dinaric Imbricated Belt (Fig. 4) in the region of Dalmatia and Kvarner is identical with the imbricated margin of Adriatic segment of the carbonate platform. In northeast it is bordered by the Frontal Zone of the External Dinaric Thrust Belt, and in southwest by the **Thrust Front of External Dinarides**. The latter represents the boundary of the imbricated margin of the "Adria" towards its solid core. The Thrust Front of External Dinarides lies in the middle Adriatic parallel to the Frontal Zone of External Dinaric Thrust Belt, whereas in the Istrian peninsula it is considerably displaced northeastwards, which resulted in a substantial shortening of the External Dinaric Imbricated Belt. The Buje Fault in Istria represents a relic of the Thrust Front of External Dinarides. The reason for deformation and narrowing of the imbricated belt is the Miocene and Post-Miocene separate underthrusting and displacement of Istria towards northeast. Towards northwest the belt widens again.

The External Dinaric Imbricated Belt in the Kvarner region and southeast from there, consists of folds and slices with characteristic lystric thrust planes hypothetically connected in depth with ductile horizons. The part of belt situated closer to Frontal Zone of the External Dinaric Thrusts is typically less imbricated. This part consists of folds in Ravni Kotari, on the islands of Pag, Rab and Krk, and in hinterland of Istria, the Bay of Trieste and in Friuli. In hinterland of Istria and Bay of Trieste the folds are referred to as the Kras-Notranjsko Folded Structure (Placer, 2005). The latter comprises Anticlinorium of Čičarija and Trieste-Komen, Synclinorium of Brkini and Vipava, and the Ravnik Anticline. Characteristic for this group of folds is their en-echelon spatial arrangement. The southwestern half of the External Dinaric Imbricated Belt is more intensely imbricated in the Kvarner area, its structure being visible on the island of Cres. In Istria there are no visible proofs of lystric faults with the only exception of the Buzet Fault in the area of Northern Istria Structural Wedge.

Istria – Friuli Underthrust Zone
(Miocene – Recent)

The Istria-Friuli Underthrust Zone is visible from Sesljan in the Bay of Trieste to the eastern coast of Istria Peninsula along the Kvarner Bay (Fig. 4). The zone was defined during the mapping of the Kozina – Koper motorway section.

Formation of the Istria-Friuli Underthrust Zone, preliminarily called the Istria-Friuli block, was a result of separate underthrusting of a part of the "Adria" northeastwards. Underthrusting is believed to have started in post-Miocene time, according to the Synthetic structural-kinematic map of Italy already in Oligocene (Bigi et al., 2000), and is probably still active at present. The recent activity of the zone is established in Istria (Rižnar et al., 2007), while its Paleocene and Pleistocene activity in Friuli is being proved (Merlini et al., 2002). According to structural data, the southeastern boundary of separate underthrusting of the Istria-Friuli block is a transversal fault, or swarm of faults, that cuts the Adriatic segment of the carbonate platform. After Grandić et al. (1997b), this fault zone could have originated already in Middle Triassic, and has been reactivated later. It is called by Korbar (2009) the Kvarner Fault Zone. It seems possible that the Kimmeridgian emersion and bauxite occurrences in Istria (Vlahović et al. 2005) were a consequence of displacements along this zone. The role of this zone is explained in the following text.

The central structural element of the Istria-Friuli Underthrust Zone is the Palmanova Thrust Fault, locally named the Črni Kal Thrust Fault (Placer, 2007), that is accompanied in the hanging wall and footwall limbs by several thrust faults. The section of the underthrust zone has been mapped in detail in the Kozina-Koper motorway segment (Placer, 2007, Fig. 3), and is schematically shown in Fig. 6. The named thrust faults are shown on ground-plan in Fig. 5. In the hanging wall block the thrusts are arranged in the way, that the displacement along the highest, the Petrinje Thrust Fault, is the shortest (400-500 m horizontal displacement), and that it increases downward along the following thrusts. The displacement along the second thrust is around 1475 m, along the third one around 2900 m, while along the fourth, the Palmanova (Črni Kal) Thrust Fault the displacement in this profile is considerably larger, although it could not be reconstructed with sufficient accuracy. By extrapolation, allowing errors of up to 100%, it amounts to more than 10 km. The dip angle of the highest thrust fault varies between 35° and 30°, and of others from 25° to 20°. Traces of thrust faults in the hanging wall block can be followed on surface from Sistiana (Sesljan) northwest of Trieste to Mt. Učka just next to the Kvarner Bay, where even tectonic windows and outliers occur, indicating the nappe character of overthrusts in the area (Šikić et al., 1969, 1972). Hence it follows that displacements increase toward southeast. The plane of the Palmanova Thrust Fault in the Mt. Učka area is subhorizontal, while east of the ridge, passing parallel with the seashore and forming the core of a monocline, it gets together with beds tilted downwards. As a result of rotation the fault trace strikes approximately north-south, consequently different than in the case if the beds had retained the Dinaric NW-SE direction.

The position of thrust faults in the footwall side is different. Their dip angle decreases toward southwest from 25°-30° for the Palmanova Thrust Fault, to 10°- 20° for the Buzet Thrust Fault, and

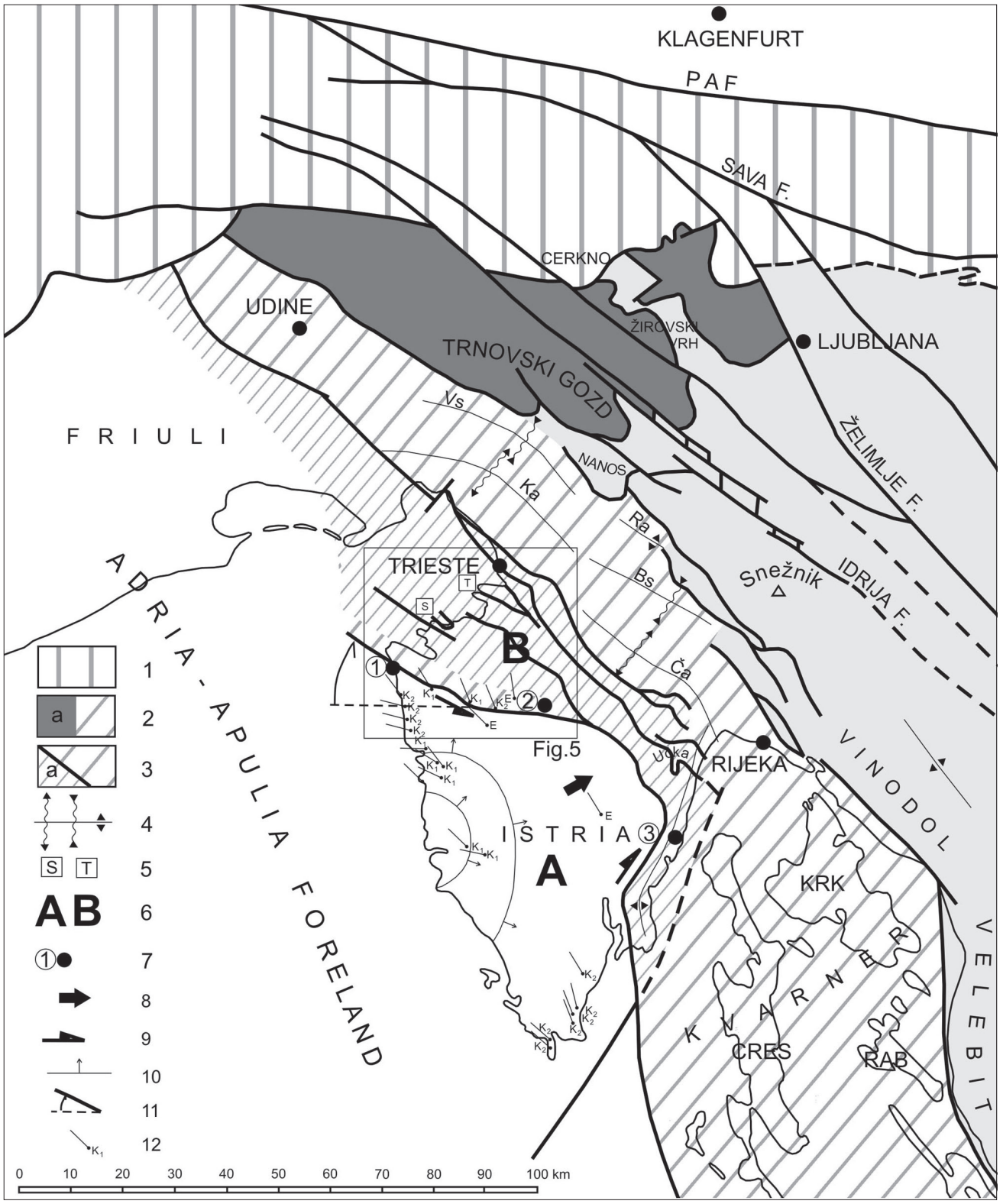

Fig. 4. **Subdivision of thrusts.**

1. Southern Alps;
2. External Dinaric Thrust Belt: a – Trnovo Nappe;
3. External Dinaric Imbricated Belt: a – Istria-Friuli Underthrust Zone;
4. Kras-Notranjsko Folded Structure (Vs – Vipava Synclinorium, Ra – Ravnik Anticline, Ka – Trieste (Trst) - Komen Anticlinorium, Bs – Barka Synclinorium, Ča – Čičarija Anticlinorium);
5. S – Strunjan Structure, T – Tinjan Structure;
6. A – Southern Istria Structural Wedge, B – Northern Istria Structural Wedge;
7. Measuring sites: (1) – Zambratija, (2) – Mlun, (3) – Vidikovac;
8. Direction of the maximal underthrusting and pushing;
9. Direction of movements in flanks of the Southern Istria Structural Wedge;
10. Dip of beds;
11. Rotation of western part of the Buje Anticline;
12. Direction of paleomagnetic pole, stratigraphic age of sample.

to 0° for the Simon Thrust Fault, which approaches to interlayer displacements in subhorizontal beds in the Izola area. The Simon Thrust Fault forms the Izola tectonic window in the frame of the Strunjan Structure, Fig. 5. On map in Fig. 4 the underthrust zone is asymmetrical. In hinterland of central Istria it is compressed and narrowed, the displacement of underthrusting being here at maximum. The thrust front of External Dinarides, initially of NW-SE direction, was here shifted farthest to northeast, and it currently consists of two asymmetric branches. The southeastern branch is bent more, and it only slightly deviates of the direction of the eastern Istrian coastline, whereas the northwestern branch, the Buje Fault, is bent considerably less, and it constitutes the SSW boundary of the Buje Anticlinal ridge. In the southeastern part, at the eastern Istria coast, the thrust faults of the External Dinaric Imbricated Belt from the Kvarner area obliquely lean on the frontal thrust plane, while in the northwestern part they are radially dispersed between the Buje Fault and the Palmanova Thrust Fault. Their continuation northwest of Istria is hypothetical, and it is based on data of the Cesarolo 1 (Cati et al., 1989) and Cargnacco 1 (Venturini, 2002) boreholes. The Buje Fault is of expressively hybrid structure which reflects its disproportionate transformation from the Frontal Thrust Fault of External Dinarides, which has a characteristic listric shape (Matičec, 1994) at Zambratija, into a gently dipping thrust fault in the narrowed part of underthrust zone at Račice. The transformation is recognized by the observation, that at Zambratija

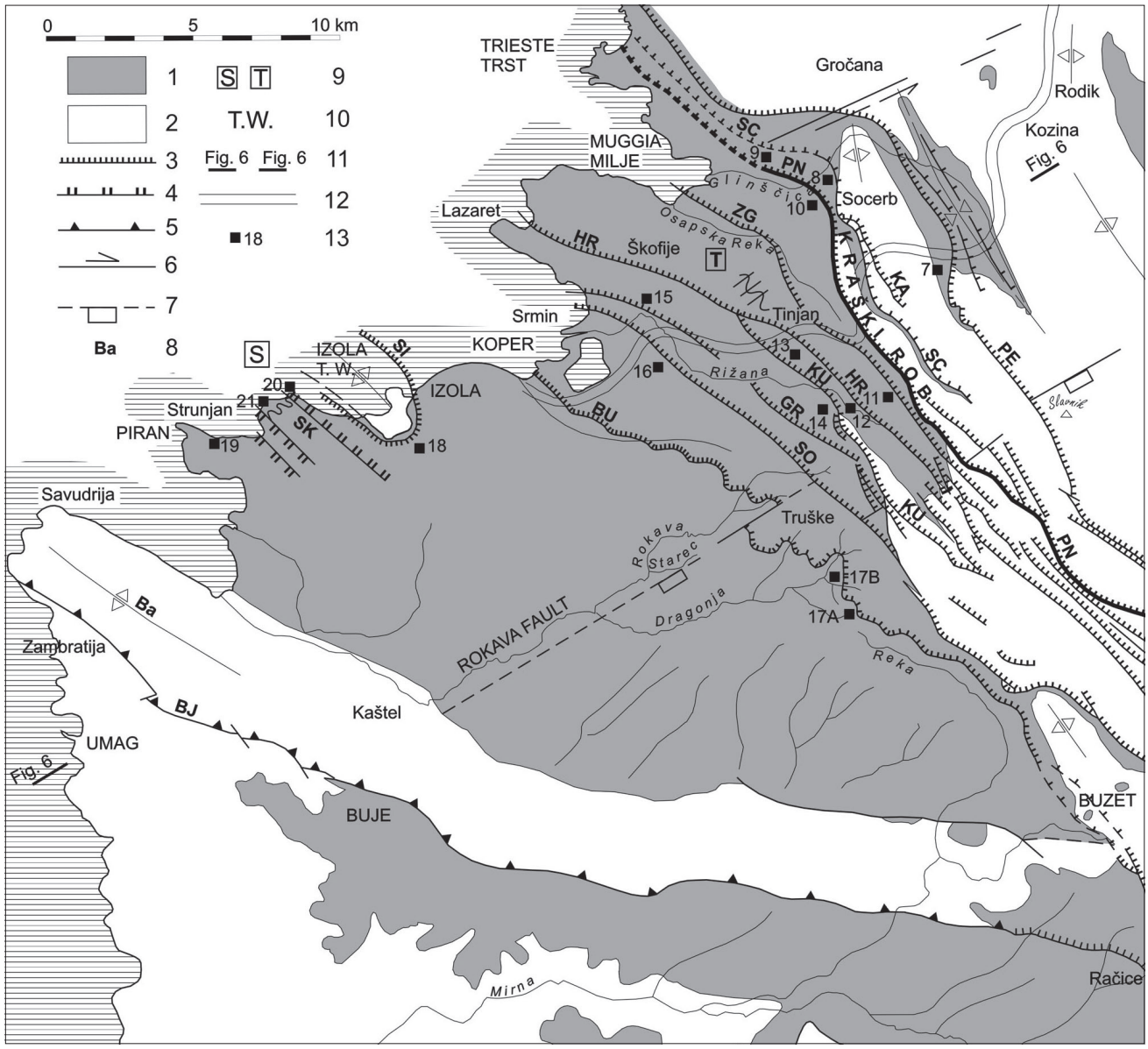

Fig. 5. **Istria-Friuli Underthrust Zone**. 1. Upper ductile horizon: flysch; 2. Platform carbonates; 3. Thrust faults: PE – Petrinje Thrust Fault, KA – Kastelec Thrust Fault, SC – Socerb Thrust Fault, PN – Palmanova Thrust Fault (local Črni Kal Thrust Fault), ZG – Zanigrad Thrust Fault, HR – Hrastovlje Thrust Fault, KU – Kubed Thrust Fault, GR – Gračišče Thrust Fault, SO – Sočerga Thrust Fault, BU – Buzet Thrust Fault, SI – Simon Thrust Fault; 4. Secondary thrust faults of the Strunjan Structure: SK – Sv. Križ Thrust Fault; 5. Thrust Front of External Dinarides: BJ – Buje Fault; 6. Strike-slipe fault; 7. Normal fault; 8. Ba – Buje Anticline; 9. S – Strunjan Structure, T – Tinjan Structure; 10. Izola Tectonic Window; 11. Fig. 6 - Fig. 6 – Synthetic profile Umag – Kozina on Fig. 6; 12. Motorway.

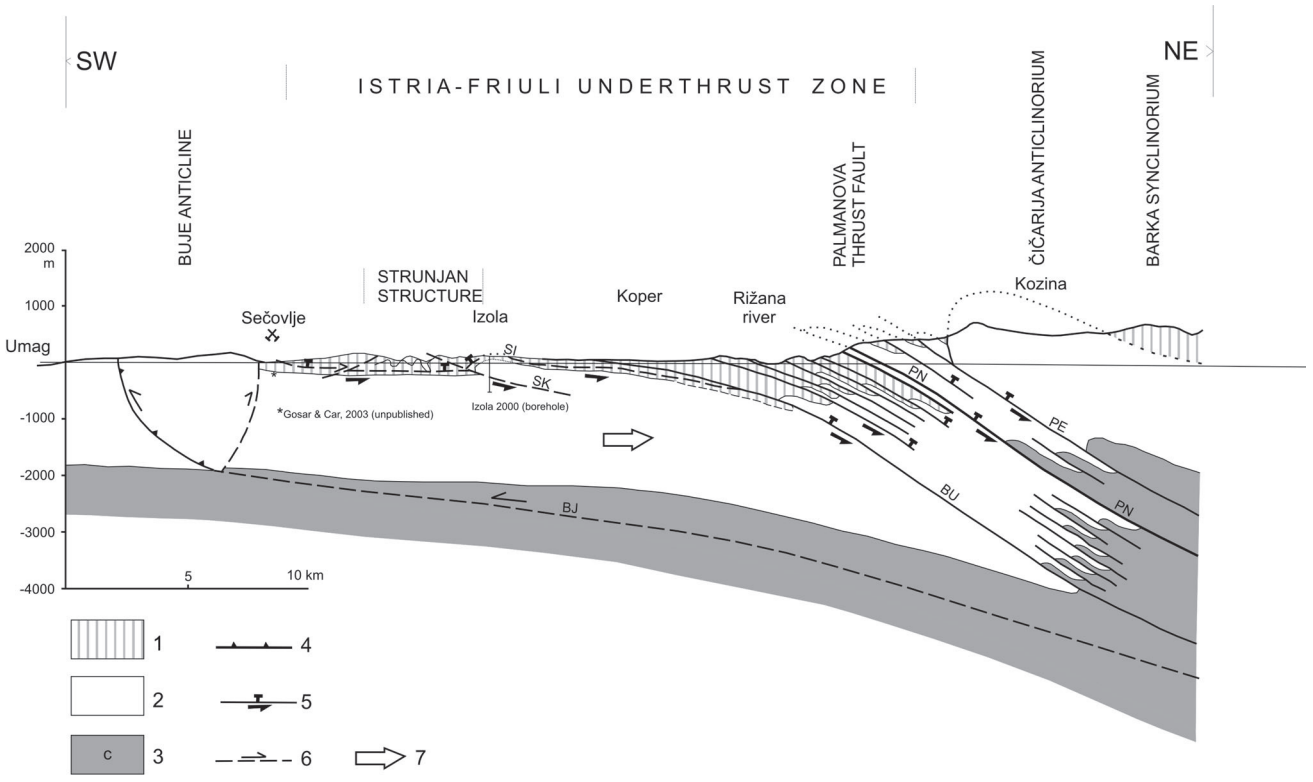

Fig. 6. **Synthetic profile** Umag – Kozina across the Istria-Friuli Underthrust Zone. See Fig. 3 and Fig. 5 for position of the profile: 1. Upper ductile horizon: flysch; 2. Carbonate platform; 3. Lower ductile horizon: **c** – Carnian and older beds, explanation in Fig. 2; 4. Thrust Front of External Dinarides: BJ – Buje Fault; 5. Thrust faults of the Istria-Friuli Underthrust Zone, underthrust direction: PE – Petrinje Thrust Fault, PN – Palmanova Thrust Fault (local Črni Kal Thrust Fault), BU – Buzet Thrust Fault, SI – Simon Thrust Fault; 6. Thrust faults of the Strunjan Structure: thrust direction: SK – Sv. Križ Thrust Fault; 7. Push direction.

it has properties of a strike-slip fault with measured subhorizontal slickensides and indications of transpression towards the east above Račice, and where it turns toward southeast it acts as a typical gentle thrust fault with a vast sequence of overturned flysch beds in the footwall. Between the two extremes occur intermediate forms, although the strike-slip component is observable at Istarske Toplice, and even farther eastward. Transformation has occurred only east of there.

The Strunjan Structure (Placer, 2005) is a secondary element within the Istria-Friuli Underthrust Zone (Figs. 4, 5 and 6). It formed due of the clockwise rotation of western branch of the Savudrija Anticline crest as a result of pushing, and not of underthrusting. By rotation of the western part of the Savudrija Anticline crest the symmetric Strunjan Structure formed with several overthrusts directed to northeast, and a single one to southwest (Sv. Križ Thrust). The Izola Anticline with a tectonic window was formed as a result of anticlinal bending of the hanging wall side of the Sv. Križ Thrust.

Thrust faults of the Istria-Friuli Underthrust Zone have been documented by reconnaissance (Fig. 5) and by photographs in figures, from the highest Petrinje Thrust Fault (Fig. 7) and Socerb Thrust Fault (Fig. 8), Palmanova (Figs. 9 and 10), Zanigrad (Fig 11), Hrastovlje (Figs. 12 and 13), Kubed (Fig. 14), Gračišče (Fig. 15), Sočerga (Fig. 16), Buzet (Fig. 17) and Simon Thrust Fault (Fig. 18), and the probable tectonical intralayer slips in the Piran Cliff (Fig. 19). The deformations of the Strunjan Structure indicated the Sv. Križ Thrust Fault (Fig. 20) and the folds in its core (Fig. 21).

Istria is divided by the Buje Fault into two wedge-shaped structural blocks. The block between this fault and the southeastern branch of the Thrust Front of External Dinarides at the Istria east coast is the **Southern Istria Structural Wedge** (A in Fig. 4), and the block between the Buje Fault and the Palmanova Thrust Fault the **Northern Istria Structural Wedge** (B in Fig. 4). The underthrusting mechanism is reflected in dynamics of these two structural wedges. The tip of the Southern Istria Structural Wedge is directed to northeast, and its symmetral coincides with direction of maximum of the underthrusting. We presume that due to the shift in direction of the tip the wedge became laterally compressed and gently folded (the South Istria Anticline). Because of gentle dip of beds, the true direction of its axis is difficult to determine. The direction of displacement of the South Istria Structural Wedge is consequently controlled by its lateral boundaries.

Kinematics of the South Istria Structural Wedge has been established after the microstructural analysis in the Buje Fault and in the east coast of Istria. Point 1 is located within the core of the Zambratija Fault that belongs to the wider zone of the Buje fault. Here sinistral strike-slip displacements occur along NW-SE to WNW-ESE striking planes with steep NE to NNE dip, indicating compression in the W-E direction. The Zambratija

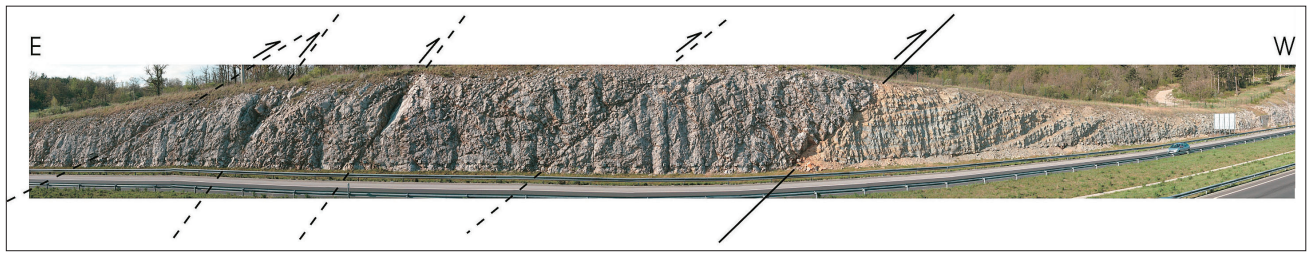

Fig. 7. **Petrinje Thrust Fault,** diagonal transverse section of footwall block of the fault zone. Southern face of highway cut east of the Kastelec tunnel near Petrinje. Small thrust of Eocene Transitional marly limestone on the Transitional marlstone, and other small thrusts. View from north to south.

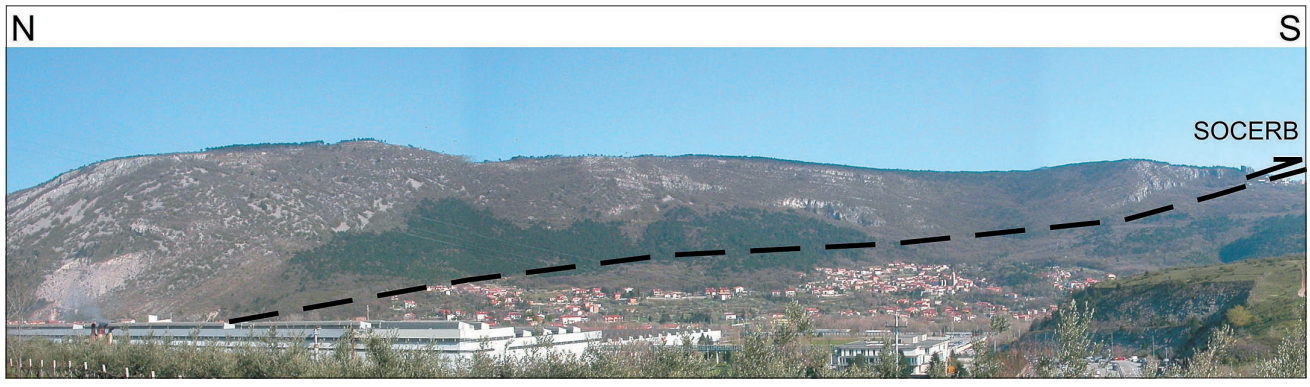

Fig. 8. **Socerb Thrust Fault,** diagonal transverse section. View from Čelo hill opposite to Dolina (S. Dorligo della Valle) near Boljunec village towards Socerb castle and thrust of the Eocene Alveoline – nummulitid limestone on flysch. Inclination of the thrust plane about 20°. View from northwest to southeast.

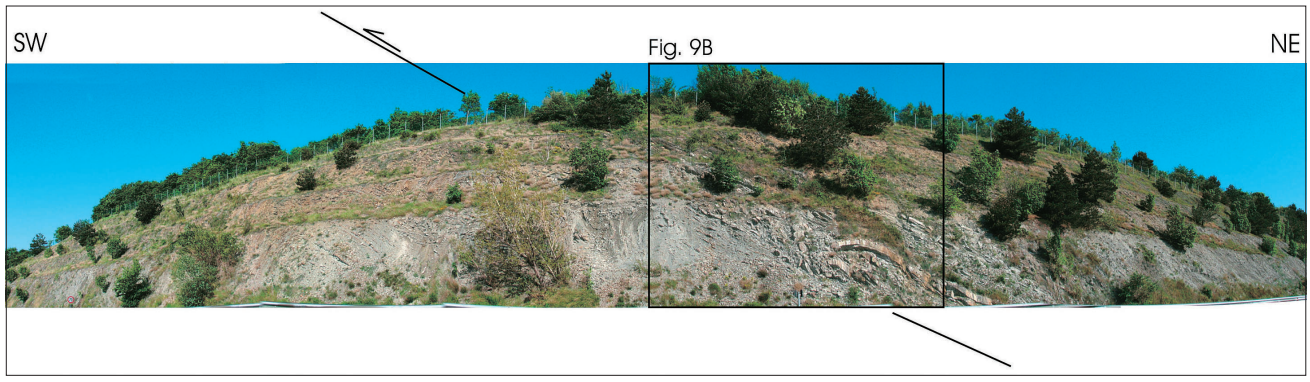

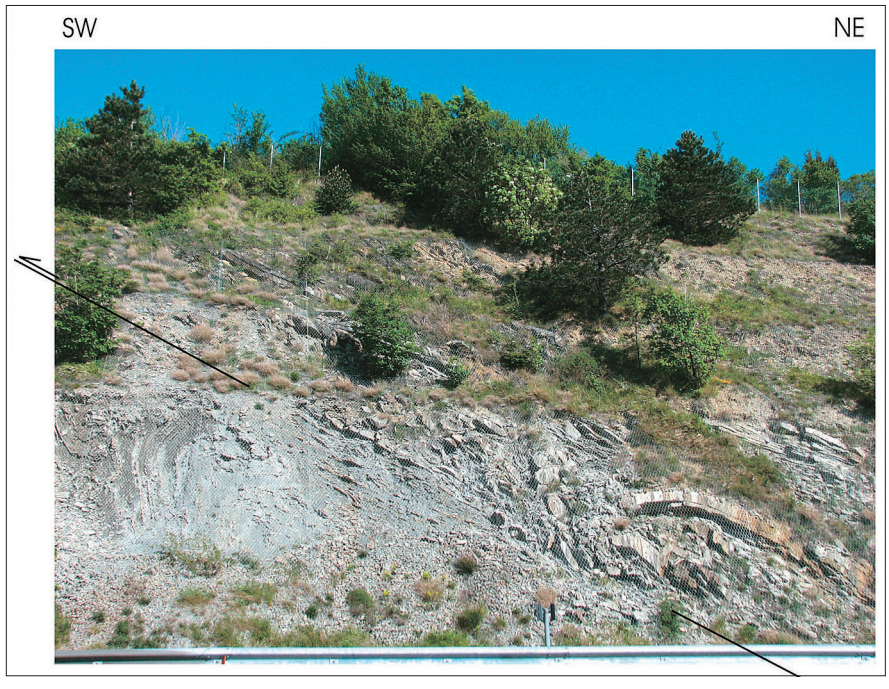

Fig. 9. **Palmanova Thrust Fault,** transverse section.

A – NW face of the highway cut under Čelo hill opposite to Dolina (S. Dorligo delle Valle) village. Thrust fault together with large part of thrust zone in hanging- and footwall is visible.

B – Detail of main thrust plane in the thrust zone. View from southeast to northwest.

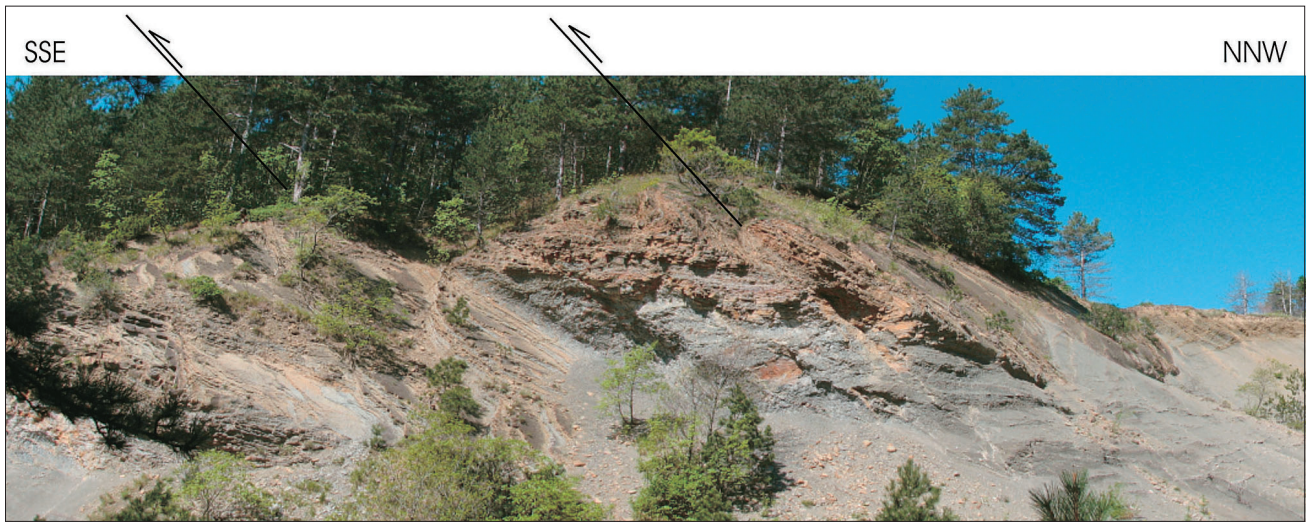

Fig. 10. **Palmanova Thrust Fault** (locally Črni Kal Thrust Fault), diagonal transverse section of part of the fault zone. Overturned folds in the ravine under Prebeng (Prebenico) village. View from east to west.

Fig. 11A. **Zanigrad Thrust Fault.** View on the fault zone over the Predloka village under Črni Kal village, longitudinal section. View from southwest to northeast.

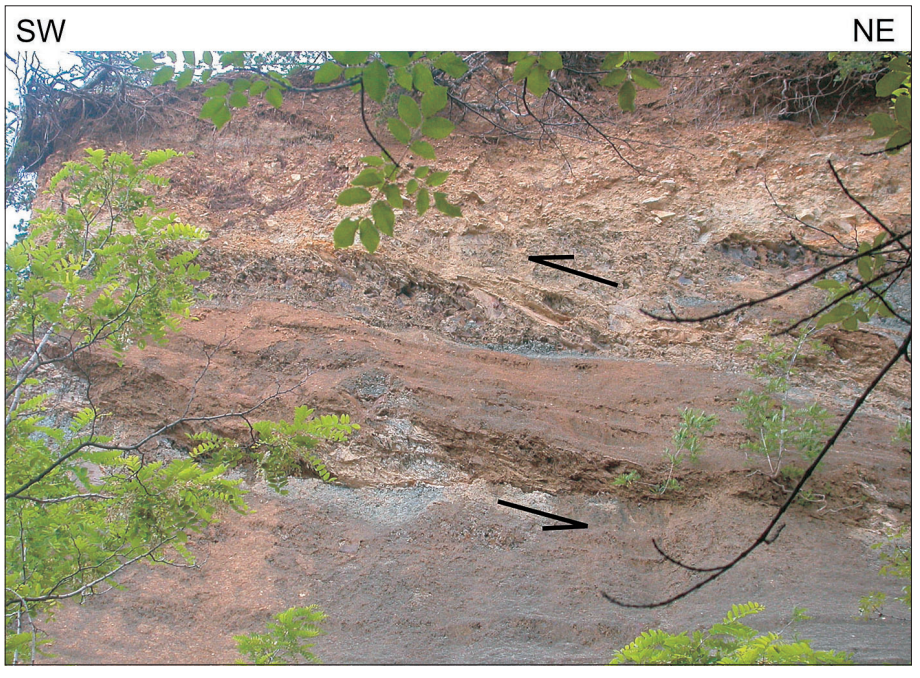

Fig. 11B – Fault zone detail, transverse section. View from southeast to northwest.

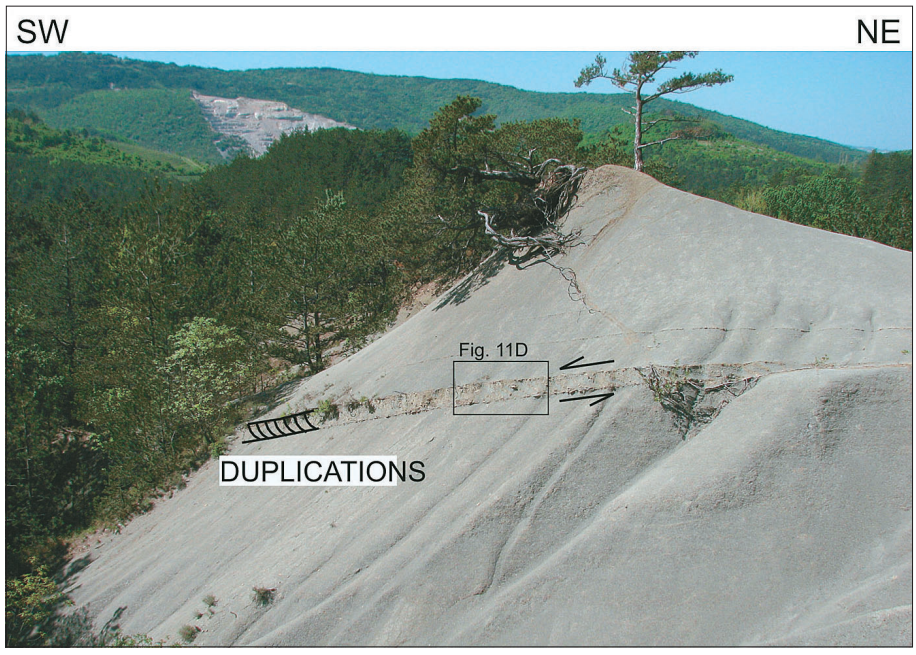

Fig. 11C – Duplications in the footwall block, transverse section. View from southeast to northwest.

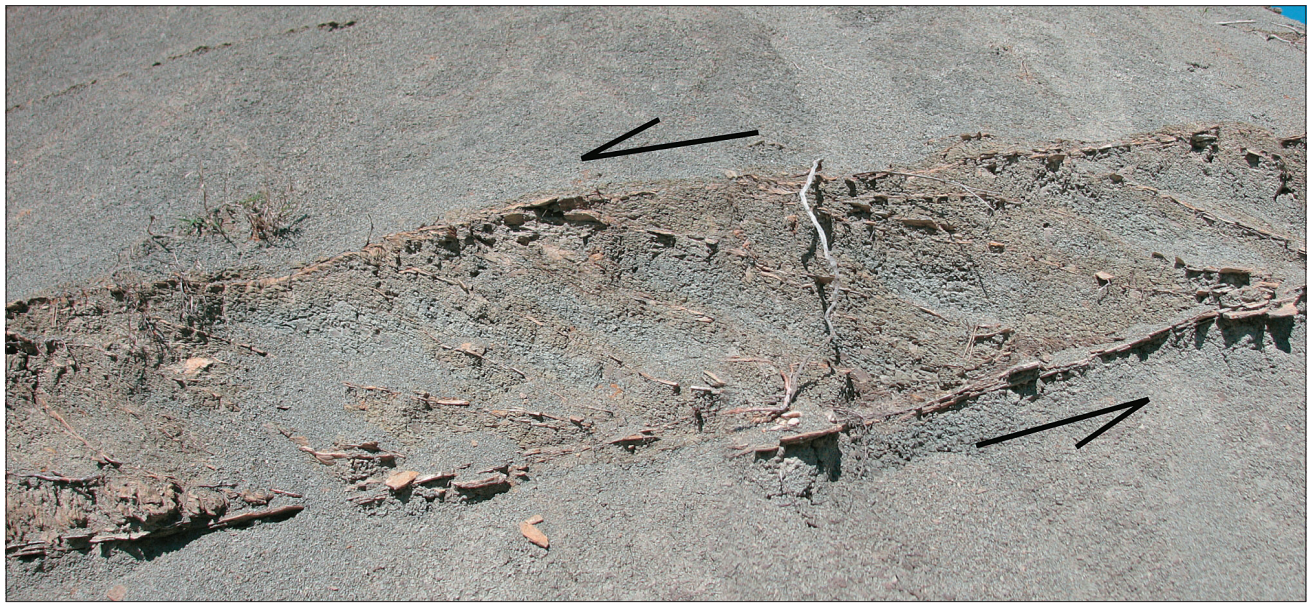

Fig.11D – Detail.

fault is parallel to the Buje fault, hence a similar displacement along the latter is presumed. At the southern road to Veliki Mlun (point 2) similar oblique sinistral displacements occur along subvertical joint planes of W-E strike, which indicate compression in the WSW-ENE direction. These displacements can also be applied to the Buje Fault. Theses on sinistral displacements along the Buje Fault are also supported by data of Marton (1987), who mentions extreme counterclockwise rotation in the southern side of the fault.

Important for confirmation of kinematics of the Southern Istrian Structural Wedge is the Vidikovac outcrop (point 3) which is situated outside of the fault zones. Dextral strike-slip activity parallel with the eastern edge of the Southern Istria Structural Wedge appears in joints, striking parallel with the coastline and genty dipping to the ESE.

Conditions in the area of Northern Istria Structural Wedge are different. Here we present indications of the compression in SW-NE direction (Strunjan Structure – S), and lateral extension toward NW (Tinjan Structure – T) (Placer, 2005). Which structures are pre-recent and which recent could be determined only by future structural measurements. Data by Weber et al. (2010) about recent displacements give just a general trend.

Secondary folding of thrust planes and repeated weak thrusting are common characteristics of the Istria-Friuli Underthrust Zone. The intensity of this process is modest, but its presence in Istria is a general phenomenon which is in some places the reason for an essentially steeper dip (more than 25°) to northeast of thrust planes; in other places the dip is subhorizontal, and somewhere even pointing to the southwest (Figs. 11C and 11D). The underthrusting of the Istria-Friuli block was evidently a polyphase process.

Important from the standpoint of underthrusting mechanism of the Istria-Friuli block is the

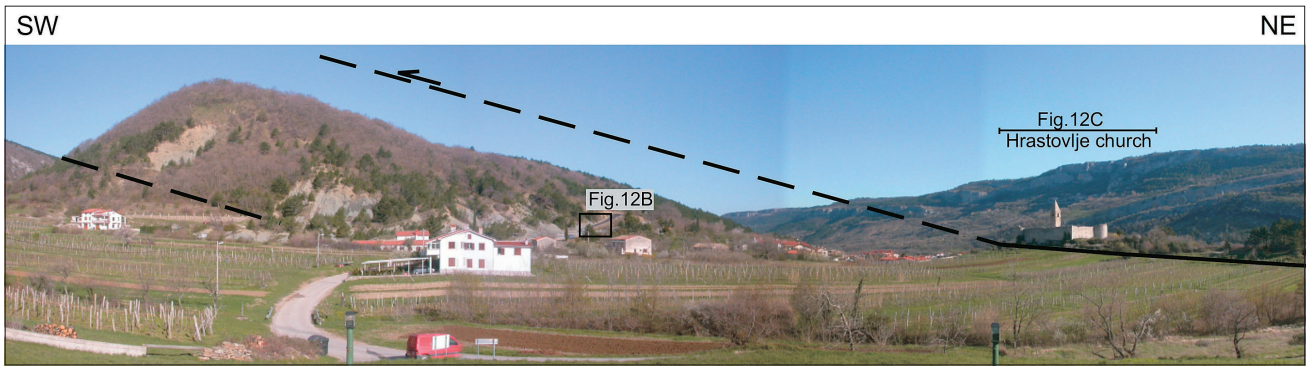

Fig. 12A. **Hrastovlje Thrust Fault,** transverse section.
View on southeast slopes of the Vrh hill above Hrastovlje village, which is completely positioned in the thrust zone. View from southeast to northwest.

Fig. 12B. Detail of the fault zone in the marlstones.

Fig. 12C. View to the principal fault plane, Alveoline – nummulitid limestone thrust on flysch.

Fig. 13. **Hrastovlje Thrust Fault,** transversal section of part of the fault zone. Cut face behind hunter cabin in Kortine settlement. Fault zone in sandstones and siltstones. View from southeast to northwest.

question of trace, structure and age of the Palmanova Thrust Fault in its continuation towards northwest, under sediments of the Friuli Plain. Competent data on this are furnished by Venturini (2002), Merlini et al. (2002), Peruzza et al. (2002) and Fantoni et al. (2002). It follows from records of the Cargnacco 1 borehole and from seismic profiles that the Palmanova Thrust Fault continues under the alluvium deposits of the Friuli Plains to the Southern Alpine Thrust Boundary. Its morphologic expression under alluvial deposits of the Friuli Lowland and the width of the thrust zone diminish in the northwestern direction, as manifested in profiles across Istria (Fig. 22), over the Kras edge (Fig. 6), Sistiana (Sesljan) (Fig. 23) and across the Southern Alpine Thrust Boundary (Fig. 24). Considered in the latter profile are the data of cross-section across the Cargnacco 1 borehole – Ca 1 on Fig. 3 (Merlini et al. 2002, Fig. 3B) and profile between Gemona (Gumin) and Udine (Videm) (Fantoni et al. 2002, Fig. 5; Merlini et al., 2002, Fig. 3A). According to these data, the Palmanova Thrust Fault should have been still active in Pliocene and Pleistocene. The seismic profiles of Merlini et al. indicate that in the Cargnacco 1 profile and to the northwest of there no other thrust faults are present southwest of the Palmanova Thrust Fault.

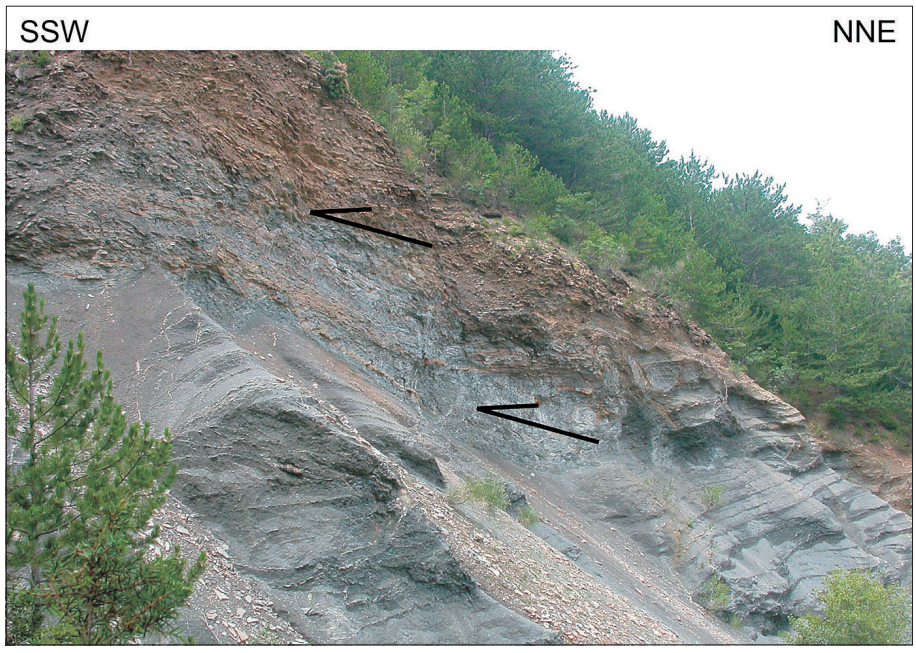

Fig. 14. **Kubed Thrust Fault,** diagonal transversal section of part of the fault zone. South slopes of Ivačevec hill (226m). Fault zone; in the lower part in marlstones, in the upper part in sandstones and siltstones. View from south to north.

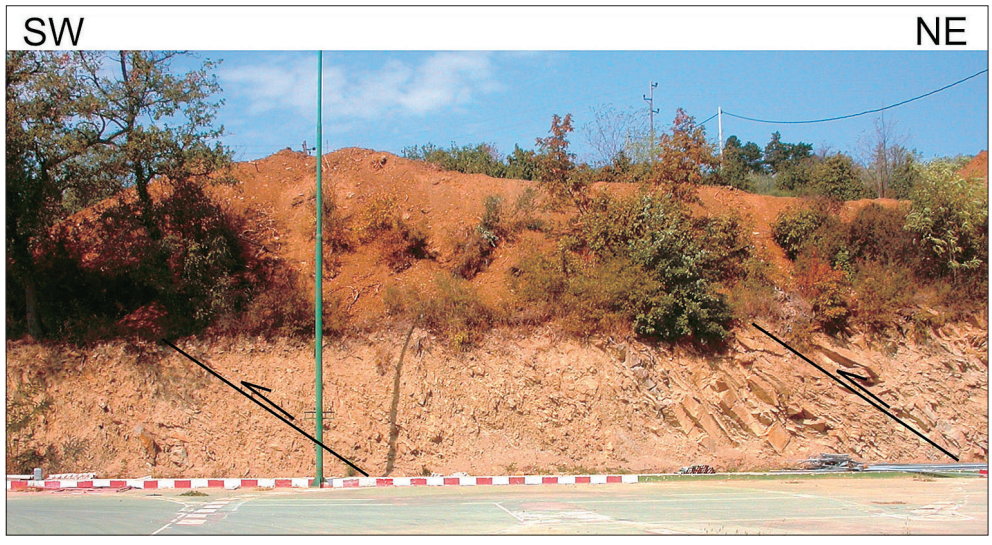

Fig. 15. **Gračišče Thrust Fault,** diagonal transversal section of part of the fault zone. Excavation of playground behind tavern in the Valmarin settlement. Fault zone in sandstone and siltstone beds. View from southeast to northwest.

Fig. 16. **Sočerga Thrust Fault,** transversal section of part of the fault zone (in building pit). Excavation in Pobegi village. Fault zone in sandstone and siltstone beds.

Fig. 17A. **Buzet Thrust Fault.** Waterfall on the Stranica creek south from Trebeše village. View on inverse calcarenite megabeds in the footwall block of thrust. View from northwest to southeast.

Fig. 17B. Part of the fault zone along Dragonja River north of Trebeše village. View from west to east.

The Kras edge originated by underthrusting of the southeastern part of the Istria-Friuli block. As underthrusting experienced its maximum intensity in the southeast, the maximum uplift affected the southeastern part of the Čičarija Anticlinorium, to an elevation of 1394 m a.s.l. (Mt. Učka), whereas northwestwards the territory gradually lowers to a few tens of meters a.s.l. at the Soča River, where the Trieste-Komen Anticlinorium "sinks" under alluvial deposits of the Friuli Lowland. The morphologically elevated thrust front, however, continues also below these deposits.

With increasing underthrusting intensity towards southeast, all to Mt. Učka, arises the question of transition of the Istria-Friuli Underthrust Zone into structures of the External Dinaric Imbricated Belt in the Kvarner area. Genesis of the transition structure is schematically shown in Fig. 25. We assume that before the separate displacement of the Istria-Friuli block northeastward the External Dinaric Imbricated Belt was not deformed, and that its strike was NW-SE oriented. The displacement of Istria to northeast was indubitably associated with dextral slip along the Kvarner Fault Zone, and with the slight counterclockwise rotation of the Istria-Friuli block. Judging from interpretation by Grandić et al. (1997a, 1997b, 2004), the Kvarner Fault Zone after reactivation never cut and displaced the frontal thrust of the External Dinaric Imbricated Belt, but it extended northeastwars below the separating plane of the imbricated structure. There formed the broader dextral strike-slip fault zone due to which an extensive S structure was generated, which is manifested in the Kvarner area, with clockwise rotation of islands of Susak, Cres, Lošinj and partly Krk, and, on the other side of the Kvarner Fault Zone, as pushing and underthrusting which were most intense in the tip of the Southern Istrian Structural Wedge. This is the reason for occurrence of elements of nappe structure in Mt. Učka (Fig. 3). The distinct difference in internal structure between the underthrust belt in Istria that consists of gentle dipping thrust faults with elements of nappe structure in Mt. Učka area (Figs. 6, 22) and the imbricated structure of Kvarner with characteristic listric thrust faults (Fig. 26) illustrates the im-

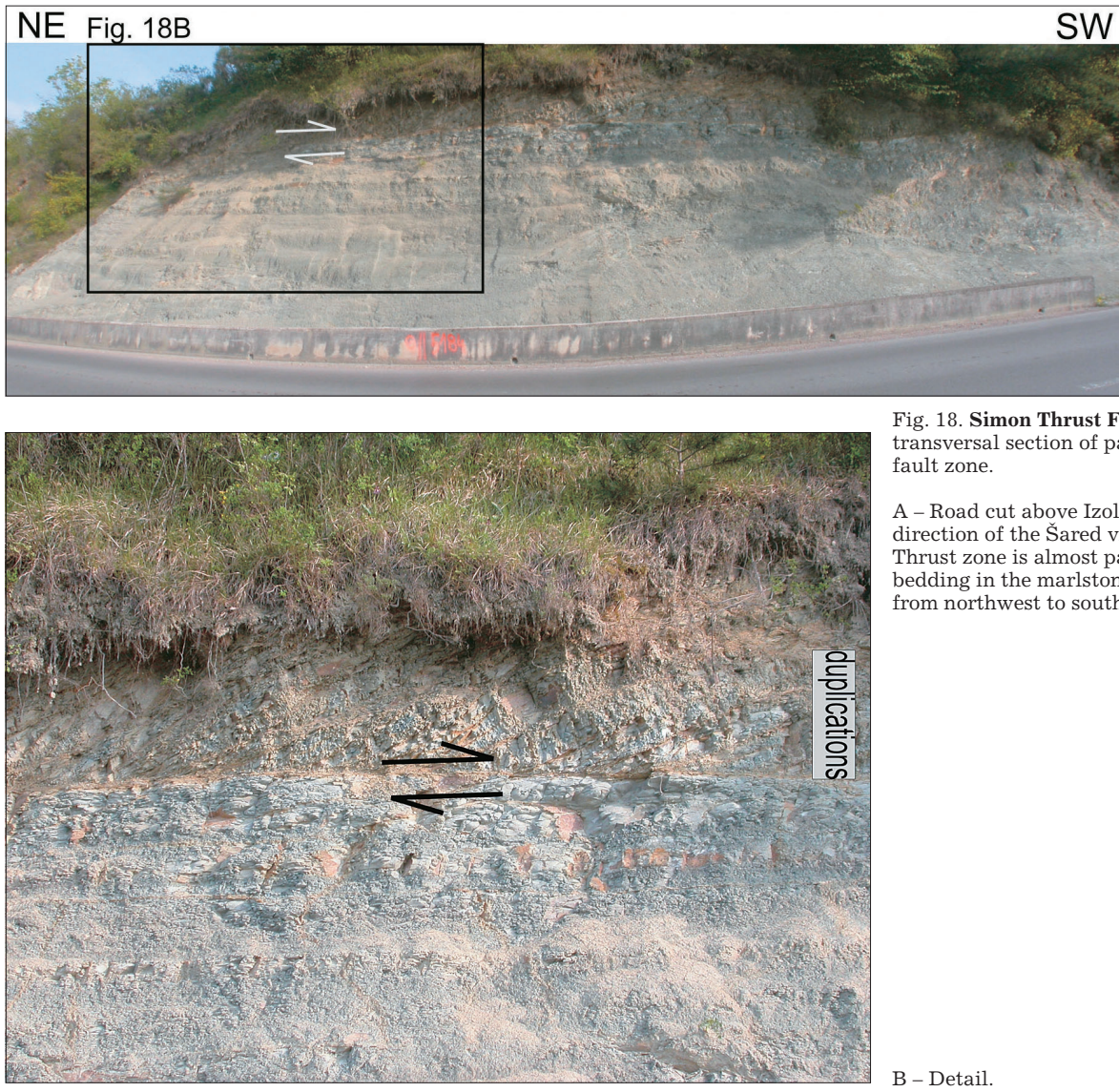

Fig. 18. **Simon Thrust Fault,** transversal section of part of the fault zone.

A – Road cut above Izola in direction of the Šared village. Thrust zone is almost parallel to bedding in the marlstones. View from northwest to southeast.

B – Detail.

portance of the Kvarner Fault Zone. The structure in this profile has been summarized from data of surface mapping and from deep drillings published for Kvarner by Đurasek et al. (1981), and for the Dalmatia region by Tari (2002) and Grandić et al. (2004). Del Ben et al. (1991) presumed at the eastern Istrian coast and in part inland northwest of Rijeka a transtensional fault which they named the Istrian Fault. Korbar (2009) presumes the existence of a similar fault which he named the Kvarner Fault Zone. On land, however, Šikić et al. (1972) and Matičec (1994) were not able to find proofs for its existence.

The Palmanova Thrust Fault cannot be connected in eastern Istria with the deformed Thrust Front of External Dinarides. The fault passes across Učka to the Kvarner area, where according to our hypothesis its continuation could not be expected.

Reactivation of the transversal Kvarner Fault Zone and displacement of the Istria-Friuli block, combined with underthrusting is the expression of a more radical differentiation of the "Adria" into the Padan and Adriatic parts, the same as in Weber et al. (2010).

The Istria Pushed Area
(Miocene - Recent)

The displacement of the Istria-Friuli block northeastwards created next to the Istria-Friuli Underthrust Zone also a wide, northeastwards pushed area whose boundray could not be precisely determined. It comprises in general the External Dinarides from the Southern Alps to Velebit Mts. and Mali Kvarner, and can be tracked in the direction of the push all to the Želimlje Fault. We named it the **Istria Pushed Area** (Fig. 27). The most conspicuous is the lateral bending of older structures toward NE, and consequences of the push are manifested also by secondary underthrusting below the Istria-Friuli Underthrust Zone. Pushing and underthrusting was polyphase, the two processes having taken place, and are still taking place, in parallel and alternatively. This mechanism is a object of future investigations. The present state of displacements is described in a treatise about the recent movements of the "Adria" (Weber et al. 2010).

Effects of push are subdivided here into: 1. Bending of the oldest structures toward NE, 2. Secondary underthrusting outside of the Istria-

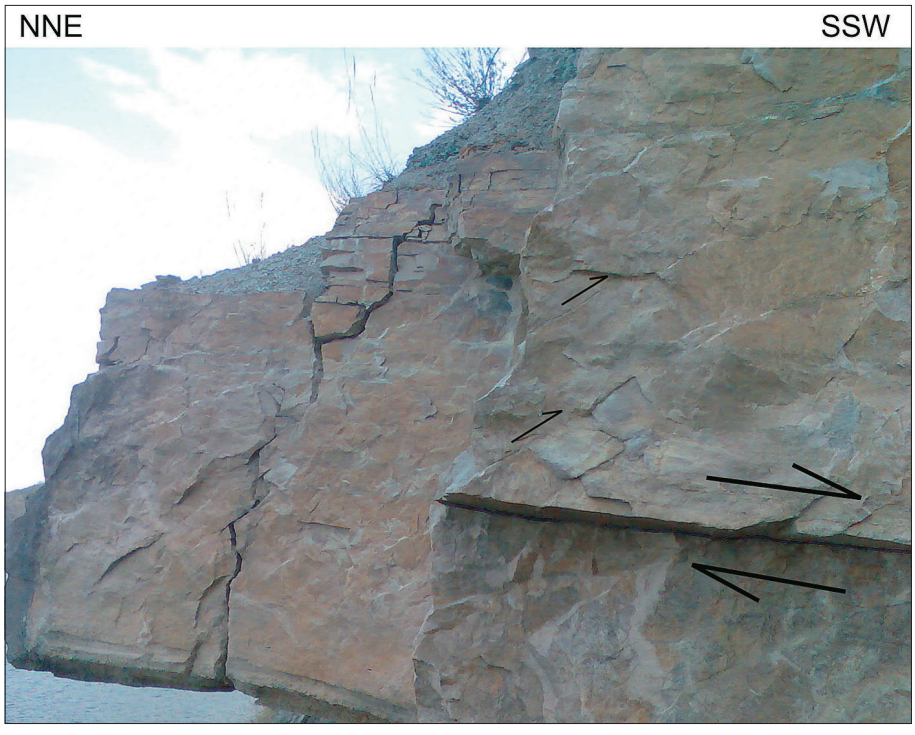

Fig. 19. **Interbedding movements in subhorizontal beds near Piran.**

A – Limestone block with system joints, which are bent due to internal rotation. It was triggered by bedding-plane slides. Tectonical movement or synsedimentary slides.

B – Oriented shear joints in sandy marlstone bed of the cliff east of Piran.

Friuli Underthrust Zone, 3. Special effects, and 4. Disintegration of the Istria-Friuli block.

1. The bended structures are developed in three areas: **A.** In the core of the push area, the southeastern part of the Čičarija Anticlinorium and of Brkini Synclinorium was moved farthest northeastward. Both units are bent owing to their position in the prolongation of bisector of the Southern Istrian Structural Wedge (Fig. 27). Less perceptibly bent is the thrust plane of the Snežnik Thrust Fault and the dinaric-striking Raša Fault. The bending is cleary expressed on the digital elevation model of Istria (Fig. 28A, B).

B. The most prominent in the northwestern side of the pushed area is the bending of the northwestern part of the Trieste-Komen Anticlinorium and Vipava Synclinorium.

C. In the southeastern side of the pushed area occurs a perceptible clockwise rotation of the Kvarner islands Susak, Cres and Lošinj what is being interpreted as a consequence of rotation at the dextral strike-slip Kvarner Fault Zone.

2. Secondary underthrusting at existing thrust planes is the most explicit in continuation of the Southern Istria Structural Wedge axis. After data of the Basic Geologic Map (Šikić et al., 1972) the

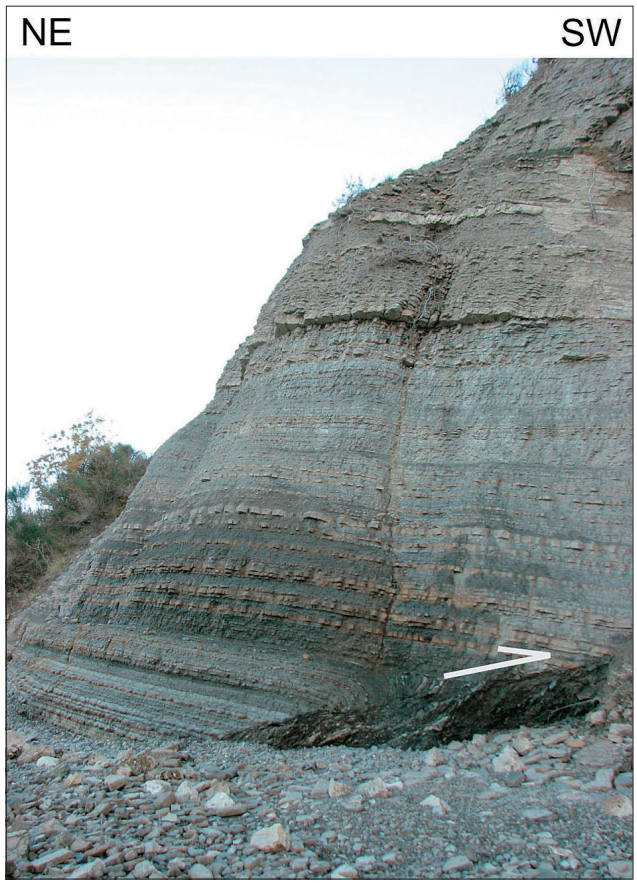

Fig. 20. **Sv. Križ Thrust Fault, part of the Strunjan Structure.** Cliff above Sv. Križ Bay near the Strunjan village.

density of reverse faults is here significantly increased. Especially illustrative is the Snežnik Thrust Fault southeast of the Pivka structure which shows in this segment the characteristics of the nappe structure (Fig. 3). Here recumbent folds can be found and erosion windows in overturned beds (PLENIČAR, 1959). Underthrusting is manifested in the area of the Snežnik Thrust Fault in addition to the mentioned nappe geometry also in the way how the axes of folds of the Ravnik Anticline and Brkini Synclinorium obliquely lean to the front of the Snežnik Thrust. The same was recognized also by PREMRU (2005). This means that in the apical part of the Southern Istria Pushed Area the Southern Istria Structural Wedge is pushed under the Snežnik Thrust Unit.

Important for comparison are conditions along the northeastern coast of Kvarner, where BLAŠKOVIĆ (1999) mentions underthrusting along the Vinodol Thrust Fault. The described structures do not have characteristics of nappe structure as observed along the Snežnik Thrust Fault, but suggest a different mechanism of shortening. This is shown in Fig. 26. Shortening due to clockwise rotation of the Kvarner islands is here compensated by extensive anticlinal arching of the External Dinaric Thrust Belt in the Gorski Kotar area, where as consequence also Paleozoic beds are exposed. On the island of Krk in the zone of maximum compression occur also folds of NE vergence.

3. In addition to pushing and underthrusting also other effects associated with one process or the other are observable, and having specific kinematics owing to various reasons. Three effects should be mentioned, the Divača Fault, blind valleys of Matarsko podolje, and the Ljubljana Moor.

A. The Divača Fault is a pivot fault with its southwestern side rotated in the way to uplift its southeastern part (JURKOVŠEK et al. 1996). The southwestern block situated closer to Istria is thus uplifted, or in the kinematic sennse, moved to the underthrust block that experienced a larger displacement. The Divača Fault was consequently reactivated in the stage of asymmetric underthrusting of the Istria-Friuli block, its southwestern side having a similar symmetry as the Kras edge which is the highest uplifted in southeast (Mt. Učka, 1264 m).

B. The blind valleys in Matarsko podolje are developed in axis of the Southern Istria Structural Wedge in two or three levels (MIHEVC, 1994, 2007).

Fig. 21. **Folded core of the Strunjan Structure** (see Fig. 6), diagonal transversal section. The cliff face in Strunjan village north of the Stjuža Bay. The fold verges in direction opposite to vergence of the Sv. Križ Thrust. View from west to east.

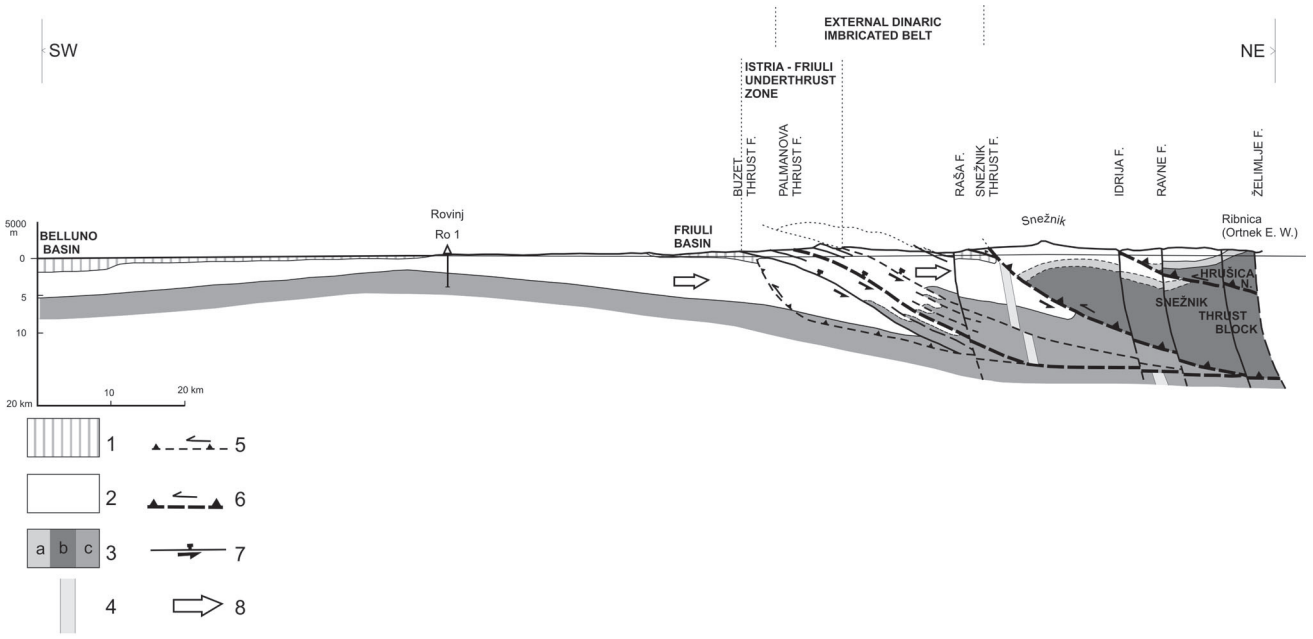

Fig. 22. **Profile** Rovinj – Mount Snežnik – Ribnica (Ortnek). Position of the profile in Fig. 3: 1. Upper ductile horizon: flysch; 2. Carbonate platform; 3. Lower ductile horizon: **a** – Upper level: Carnian clastites, Middle Triassic clastites and vulcanites, Anisian carbonates, Lower Triassic carbonates, marlstones and clastites and Upper Permian carbonates; **b** – Lower level: Middle and Lower Permian clastites and Carboniferous, and older clastites; **c** – Upper and Lower level ; 4. Hypothetic fault structure in Adriatic – Dinaric Mesozoic Carbonate Platform in the continuation of the Budva Trough, see Fig. 29; 5. Thrust faults of External Dinaric Imbricated Belt, Thrust Front of External Dinarides; 6. Thrust fault of External Dinaric Thrust Belt, thrust direction; 7. Thrust fault of Istria – Friuli Underthrust Zone, underthrust direction; 8. Push direction.

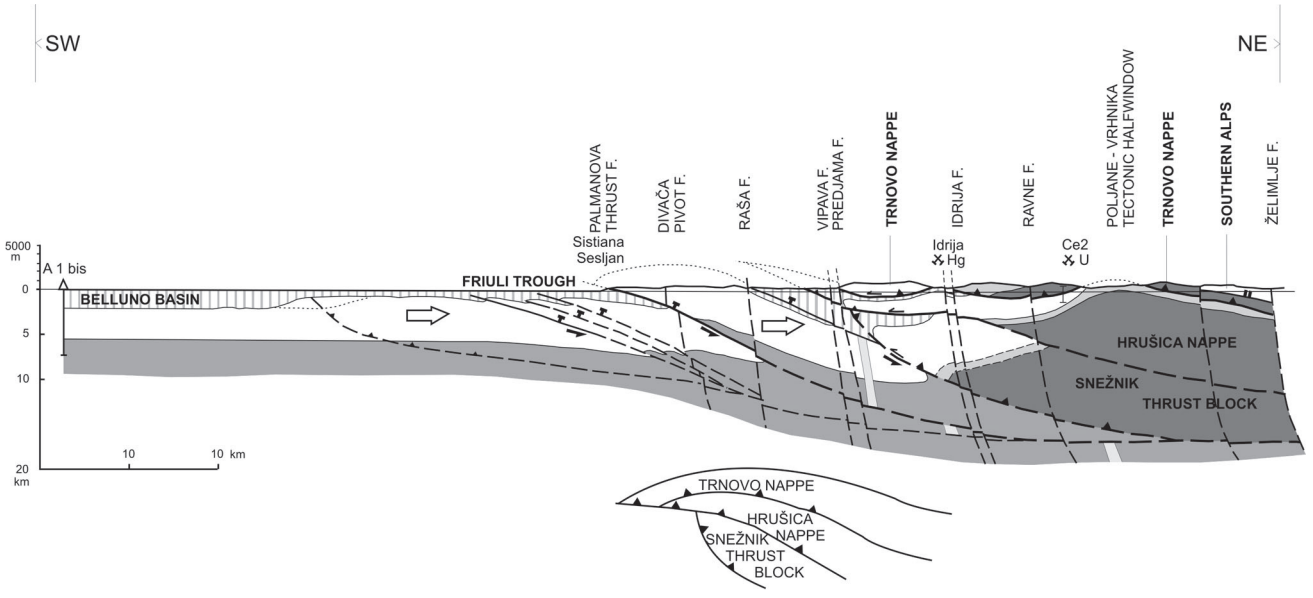

Fig. 23. **Profile** boreholes Amanda-1 bis – Sistiana (Sesljan) village – Idrija Hg ore deposit – Žirovski vrh U ore deposit. Position of profile in Fig. 3 (Explanation in Fig. 22).

C. The Ljubljana Moor formed, and is still forming, as a result of expressing of the Ljubljana Wedge (Placer, 2008b, 2009) between the Želimlje Fault, and the faults of the series which comprises the Ravne, Sovodenj, Borovnica and Ravnik Faults. The regional frame for the expressing mechanism is the tension state within the Istria Pushed Area.

4. During underthrusting the Istria–Friuli block disintegrated into three segments separated by three transversal faults. The most important is the bordering Kvarner Fault Zone. The second, Sistiana (Sesljan) Fault, passes across the Sistiana inlet (Carulli, 2006), and the third one is the hypothetic fault along the Middle Soča (Isonzo) Valley between Solkan and Turriaco (Turjak), the Medea Fault. The result of the Kvarner Fault Zone has been discussed already. The fault across the Sistiana inlet was recognized on Slovenian territory as a fracture zone connecting the areas of arching of the Trieste–Komen Anticlinorium and Vipava Synclinorium, and can be followed to the Bela Valley between Trnovski gozd and Nanos. The fault evidently continues also under the sea, and is connected with the paleogeographic boundary between Istria and Friuli Platform. With regard to intense arching of the Trieste–Komen Anticlino-

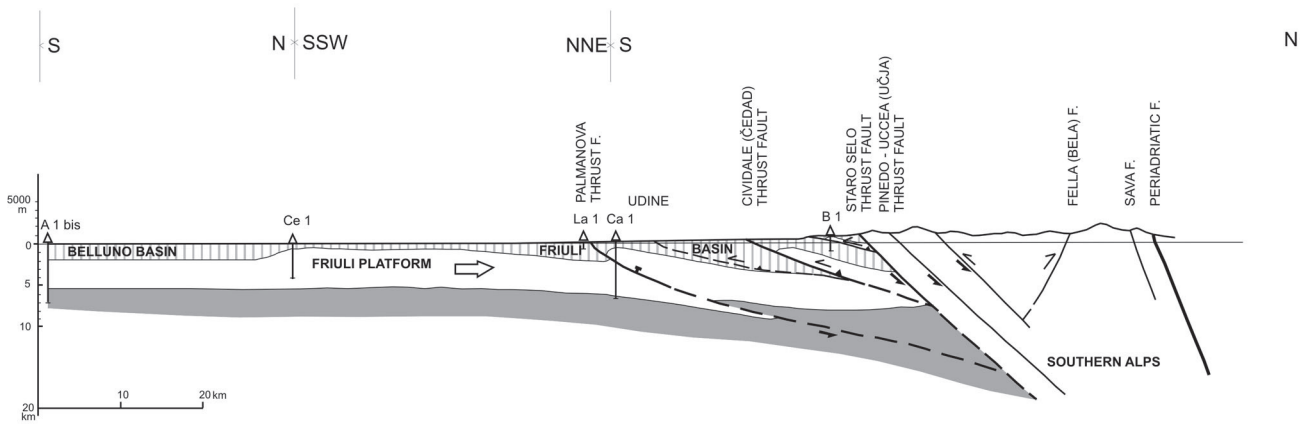

Fig. 24. **Profile** borehole Amanda (A1 bis) – Cesarolo (Ce1) – Cargniacco (Ca1) – Bernadia (B1) – Staro selo Fault – Periadriatic Fault Zone. Position of profile in Fig. 3 (Explanation on Fig. 22).

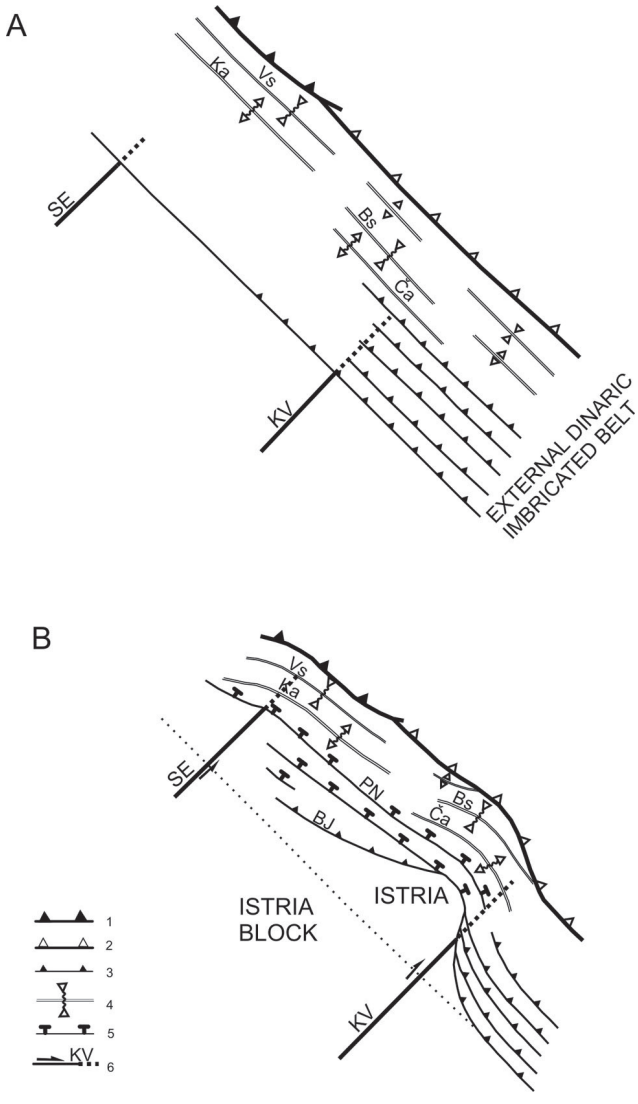

Fig 25. **Kynematic model** of Istria – Friuli Underthrust Zone. **A** Position before underthrusting; **B** Position after underthrusting. 1. Frontal Zone of External Dinaric Thrust Belt, Trnovo Thrust Series; 2. Frontal Zone of the External Dinaric Thrust Belt, Velebit Thrust Series; 3. Thrust faults of the External Dinaric Imbricated Belt: BJ – Buje Fault; 4. Folds of External Dinaric Imbricated Belt: Vs – Vipava Synclinorium, Ka – Trieste (Trst) - Kras Anticlinorium, Bs – Brkini Synclinorium, Ča – Čičarija Anticlinorium; 5. Thrust faults of Istria-Friuli Underthrust Zone: PN – Palmanova Thrust Fault; 6. Faults of stable part of the carbonate platform: KV – Kvarner Fault, SE – Sistiana (Sesljan) Fault, covered fault.

rium and Vipava Synclinorium we presume the origin of deformation being located in the disintegrated platform, underthrust below the overthrust block of the Palmanova Thrust Fault. Indications for existence of the fault along the Middle Soča (Isonzo) Valley are the orientation of the valley and anomalies of the thrust structure on the Medea Hill (Carulli, 2006).

Boundary of underthrusting below the Southern Alps (Miocene – Recent)

Underthrusting of Dinarides under Southern Alps is a complex process that started in Miocene, and is still active at present in the frame of "Adria". The complexity of its evolution is witnessed by present structure of the Southern Alpine Thrust Front (Fig. 3) which is divided in the W-E direction in three segments each with distinct characteristics.

The first segment of this boundary between the Želimlje and Ravne Faults consists of a gentle thrust fault which dips 20°-30° to southwest and is interrupted in several places by a younger steep fault of transversal dinaric strike. Position and dip of the thrust fault plane was determined during investigations of the Knape polymetallic deposit. Along the thrust plane outcrop Paleozoic clastic rocks of the Trnovo Nappe, and Triassic rocks in footwall of the Trnovo Nappe underthrust below Mesozoic rocks of the Southern Alps, belonging to the Slovenian Basin (Buser, 1989).

The second segment of boundary west of the Ravne Fault is a fault of W-E strike and 40°-50° dip north. Between the Ravne Fault and Idrija Fault it is named the Modrej Fault (Buser, 1986). It is displaced to northwest at the Idrija Fault and continues as the Staro selo Fault of the same strike and dip. West of the Tagliamento River Valley, in front of Gemona, in the W-E direction two thrust faults pass (Nicolich et al., 2004). South of the Modrej Fault in the Trnovo Nappe the Ponikve Tectonic Klippe is situated, consisting of rocks of the Slovenian Basin and therefore belonging to the Southern Alps. Its thrust plane is subhorizontal, and therefore we compare it with the bordering thrust plane east of the Ravne Fault.

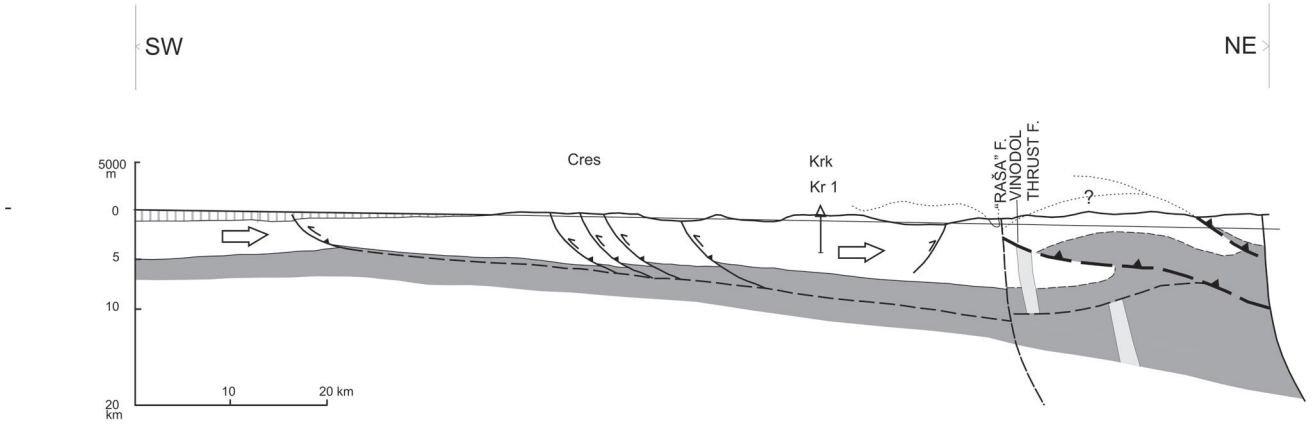

Fig. 26. **Profile** Kvarner – Gorski Kotar. Position of profile in Fig. 3 (Explanation in Fig. 22).

On relationships in third segment of the boundary south and southwest of Tagliamento River Valley, the authors of recent publications disagree (Nussbaum, 2000; Peruzza et al., 2002, Nicolich et al., 2004), and no reliable interpretation is available. Important is, however, that according to Nicolich et al. (2004), the WSW-ENE striking Barcis Thrust Fault leans on the W-E striking thrust fault west of Tagliamento River. The same is presumed also for the SW-NE striking Bassano Thrust Fault. It is indicative that both thrust faults lean on the W-E thrust fault in the continuation of the Raša Fault. Relation of other SW-NE striking thrust faults southeast of the Bassano Thrust Fault is not clear. We presume that differences in interpretation are associated with recent displacements. Important for explanation of dynamics, however, is the fact that the dip angle of the Barcis and Bassano Thrust Faults is around 30° as estimated on profile in Nicolich et al. (2004), which is significantly less than dip of the Staro selo Fault. The roles of N-S striking sinistral strike-slip faults in the Tagliamento River Valley are not considered here.

The different characteristics of the Southern Alpine Thrust Front in the area between the Želimlje

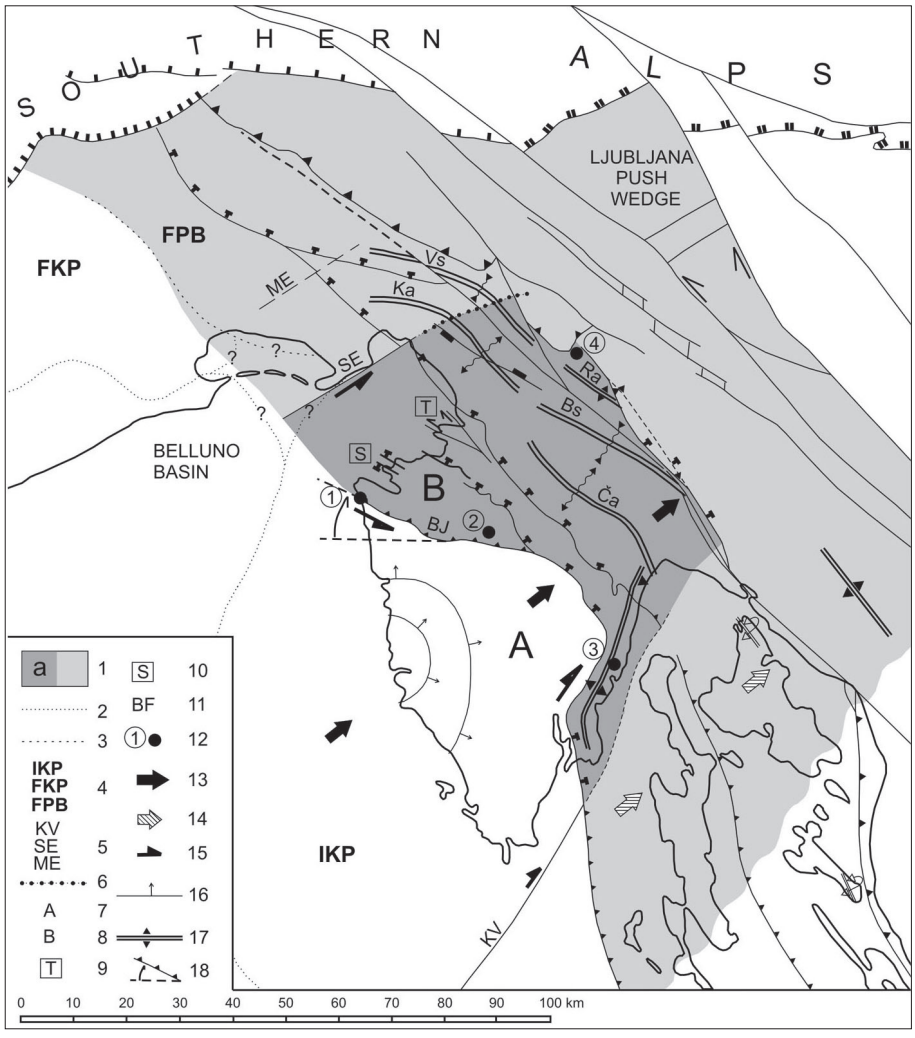

Fig. 27. **Istrian Pushed Area.**
1. Istrian Pushed Area: **a** – Initial area; 2. External edge of carbonate platform; 3. Platform edge towards internal Paleogene basin;
4. Units of Adriatic - Dinaric Carbonate Platform: **IKP** – Istria part of carbonate platform, **FKP** – Friuli Carbonate Platform, **FPB** – Friuli Paleogene Basin;
5. Faults: KV – Kvarner Fault, SE – Sistiana (Sesljan) Fault, ME – Medea (Medeja) Fault;
6. Zone Sistiana (Sesljan) village – Bela brook, the boundary belt between Istria and Friuli structural block; 7. **A** – Southern Istria Structural Wedge; 8. **B** – Northern Istria Structural Wedge;
9. T – Tinjan lateral push wedge;
10. S – Strunjan compressive structure; 11. BJ – Buje Fault;
12. Location of microstructural analyses: (1) – Zambratija, (2) – Mlun, (3) – Vidikovac, (4) – Ubeljsko; 13. Direction of maximal underthrusting and pushing; 14. Direction of pushing on Kvarner area; 15. Direction of strike-sliping; 16. Dip of beds;
17. Kras – Notranjsko Folded Structure (Ra – Ravnik Anticline, Ča – Čičarija Anticlinorium, Ka – Trieste (Trst) - Komen Anticlinorium, Vs – Vipava Synclinorium, Bs – Brkini Synclinorium); 18. Rotation of western flank of the Buje Anticline.

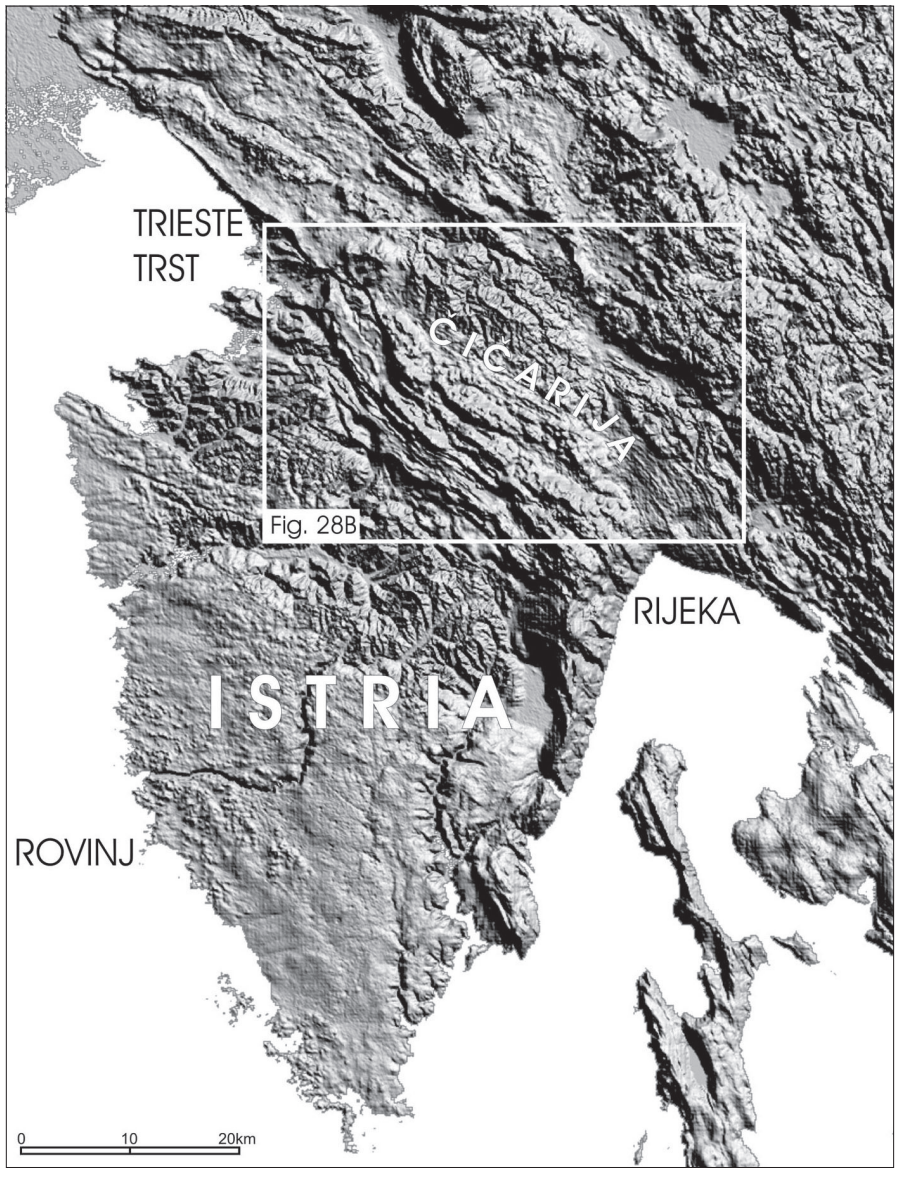

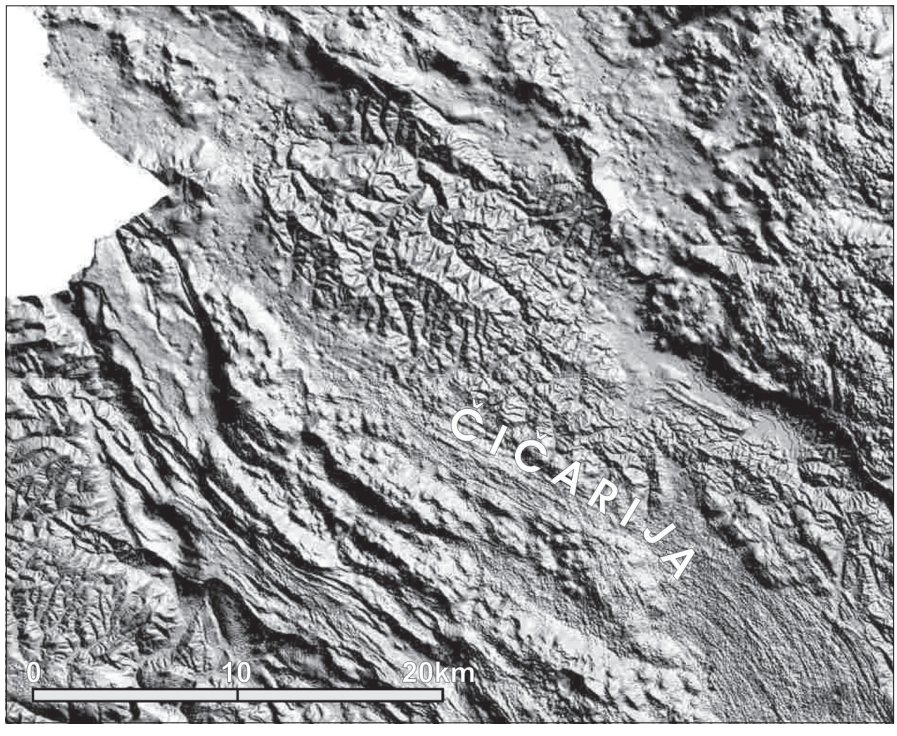

Fig. 28. **Digital elevation model** of Istria.

A Deformation of southern Čičarija hills in continuation of Southern Istria Structural Wedge (see Fig. 27);

B Detail with bent structure of Čičarija.

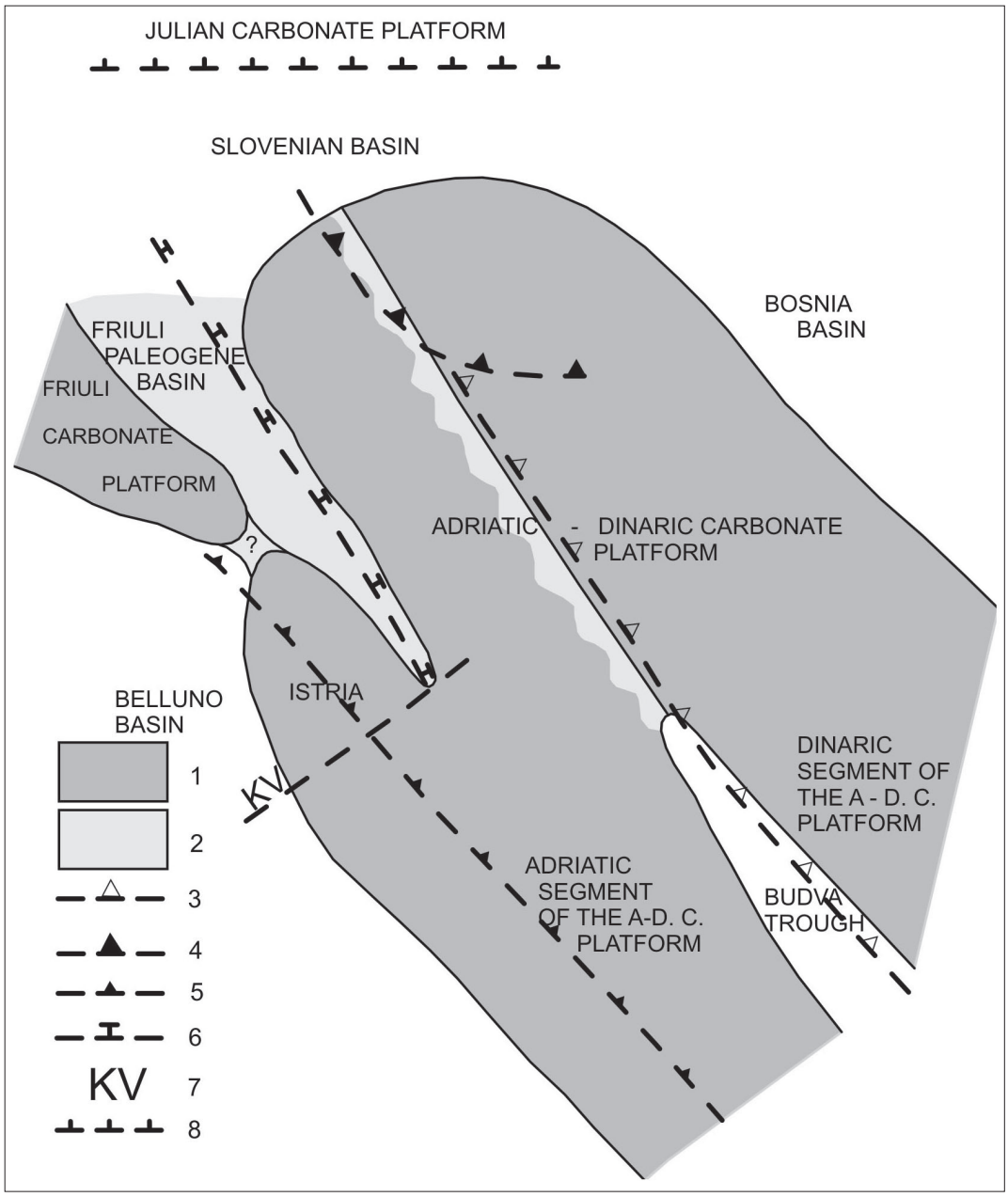

Fig. 29. **Paleogeographic model** of Adriatic - Dinaric Carbonate Platform; paleogeographic predisposition of External Dinarides tectonic model. 1. Carbonate platform; 2. Paleogene basin or trough; 3. Predisposition of Frontal Zone of External Dinaric Thrust Belt, "Velebit Thrust Series"; 4. Predisposition of Frontal Zone of External Dinaric Thrust Belt, Trnovo Thrust Series; 5. Predisposition of Trust Front of External Dinarides; 6. Predisposition of Istria – Friuli Underthrust Zone; 7. KV – Kvarner Fault; 8. Predisposition of boundary of underthrusting below the Southern Alps.

Fault and west of Tagliamento River are an indication of different stages of its evolution.

The relation between the Southern Alps, External Dinarides and Adriatic-Apulian foreland is schematically presented in Fig. 24.

NW-SE faults

The network of NW-SE striking dinaric faults in the study area of northwestern Dinarides is presented schematically. The basic data sources for this system are Basic Geologic Maps and papers by Buser (1976), Vrabec (1994), Jurkovšek et al. (1996) and Placer (2008a, b).

In general, three groups of faults that evolved in the course of geologic history from various stress fields and specific conditions are important. The first group comprises the Ljubljana - Imotski Fault Zone (Tari, 2002, Miocene strike slip; Placer, 2008b, Ljubljana – Imotski Fault Zone) of which is most important the Želimlje Fault, the second is fault zone of the Idrija Fault, and the third is a group of faults southwest of the Idrija Fault, with the more important Predjama, Vipava, Raša and Divača Faults.

The Želimlje Fault represents an important structural boundary. Its importance is based on the differences in thrust structure of the Dinarides southwest and northwest of this fault zone (Placer, 2008b).

The Idrija Fault has been relatively well studied. Two kilometers of dextral displacement of the mercury deposit at Idrija along this fault has been determined by Mlakar (1964) and Placer

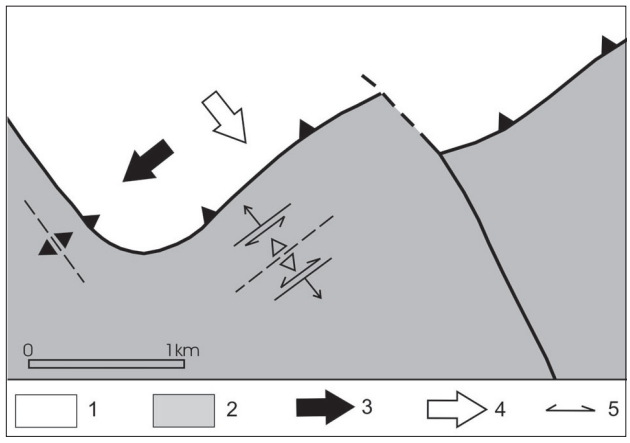

Fig. 30. **Secondary thrusting of Hrušica nappe toward SE. Location 4 on Fig. 27.** 1. Hrušica nappe; 2. Upper ductile horizon, flysch; 3. Thrusting direction of Hrušica nappe, Upper Eocene – Lower Oligocene; 4. Direction of secondary thrusting, Pliocene – Quaternary; 5. Horizontal interbed slipping.

(1982). Genesis of karst poljes southeast of Idrija was investigated by Poljak (1986) and Vrabec (1994). The displacement of the Southern Alpine Thrust Front, however, was not reconstructed to a more precise detail because of impossibility of determining the intersections of the Modrej and Staro selo Faults wih the Idrija Fault. The estimate of the horizontal displacement is about 10 km. The wider fault zone of the Idrija Fault comprises a number of parallel faults, of which the Ravne Fault is the most important. The Sovodnje, Borovnica and Ravnik Faults are arranged in en echelon series between the Ravne and the Želimlje Faults. Farther southeast they lean on the Želimlje Fault, respectively the Ljubljana – Imotski Fault zone also the Idrija Fault (Placer, 2008b). In 1998 (Zupančič et al., 2001) and 2004 (Vidrih & Ribičič, 2004) occurred earthquakes with horizontal focal displacement at the Ravne Fault.

For understanding the dynamics of the considered region also the Predjama, Vipava, Raša and Divača Faults are important. These faults were variously deformed after the disintegration of the "Adria" into the Padan and Adriatic parts, and formation of the Istria Pushed Area. From the temporal succession and type of these deformations, the deformation model for the northeastern corner of the "Adria" will have to be constructed.

Discussion

On the basis of the above presented structure of the northwestern part of External Dinarides the following should be underlined:

Adriatic-Dinaric Mesozoic Carbonate Platform (Fig. 29). The initial structure of the thrust and nappe structure of External Dinarides is the paleogeography of the Mesozoic Carbonate Platform and its internal structure. With regard to the present structural relations in northwestern part of External Dinarides, the most suitable is the conservative concept of an Adriatic-Dinaric Mesozoic Carbonate Platform consisting of a Dinaric and an Adriatic segment of the platform, between which the Budva Trough is situated. In northwest these segments have to merge into a single carbonate platform. In prolongation of the Budva Trough, the existence of a shallow Paleogene trough, or semi-trough, is not excluded. Istria and Friuli are parts of the Adriatic-Dinaric Carbonate Platform. They are separated from its central part by shallow Friulan Paleogene Basin. Friuli is separated from Istria by a shallow Paleogene passage. Istria is separated from the Adriatic segment of the Adriatic –Dinaric Carbonate Platform by a fault zone originating according to Grandić (1997b) most probably already in the Middle Triassic, and having been later reactivated as the Kvarner Fault Zone.

Differences in development of the Upper Triassic, Upper Cretaceous and Paleogene beds on the carbonate platform are a consequence of its incipient disintegration to Dinaric striking troughs and horsts (Šribar, 1995), and smaller shallow basins with a more or less continuous sedimentation in subsided parts, and various levels of erosion in the uplifted parts. Therefore differences in the upper part of platform cannot be used for establishing large tectonic displacements without objective material proofs for them. Also the differences in development between the Adriatic and Dinaric segment of platform cannot serve as a realistic base for extreme mobilistic explanations, but rather as stimulation for careful structural mapping of the contact areas. In this light the ideas of Herak (1999), Tari (2002) and Korbar (2009) should be considered.

2. Nappe structure of External Dinarides (Figs. 27 and 29). External Dinarides were formed in thrust processes in Paleocene and Eocene, and in the underthrusting stage of the "Adria" from Miocene on. The External Dinaric Thrust Belt developed predominantly from the Dinaric segment of platform and its prolongation toward northwest, where the Dinaric and Adriatic segments of platform were merged, which is the reason for existence of two areas of different internal geometry. In northwest, where the platform is uniform, the southwestern part of the External Dinaric Thrust Belt consists of the Trnovo Thrust Series, known from the analysis of nappe structure of the Idrija area and its wider surroundings. All mentioned units in it, the Trnovo and Hrušica Nappes and the Sovič Thrust Unit, have an identical geometry. Towards southeast, where the External Dinaric Thrust Belt consists of the Dinaric platform segments, extend from northwest to southeast the Snežnik, and Vinodol and Velebit Thrust Units. According to the structural data, inferred from situation on the surface, the exent of displacement increases from the Snežnik Thrust Unit southeastwards, and therefore we facultatively speak of the "Velebit Thrust Series". The Trnovo Thrust Series covers the "Velebit Thrust Series", so that the Frontal Zone of the External Dinaric Thrust Belt comprises the Frontal Zone of the "Velebit Thrust Series", which is

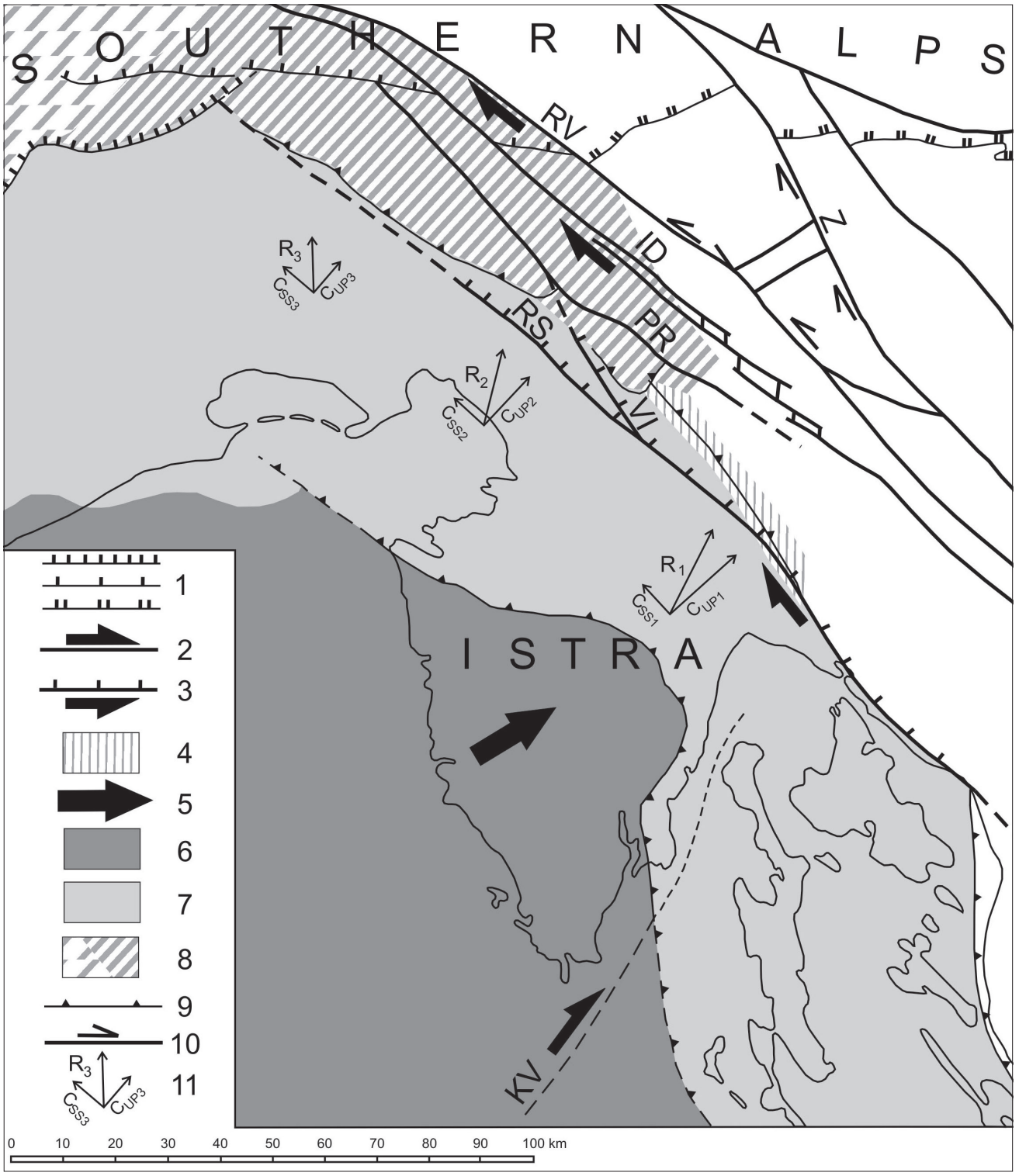

Fig. 31. **Recent dynamic model.** 1. Thrust faults of Southalpine Thrust Boundary; 2. Important strike-slip faults; 3. Transpressive faults; 4. Seismic active zone Ilirska Bistrica – Hruševje; 5. Direction of relative movement of Southern Istria Structural Wedge; 6. "Adria"; 7. Imbricated margin of "Adria"; 8. Neotectonic-recent segment incorporated in external edge of margin of "Adria"; 9. Thrust Front of External Dinarides; 10. Border faults of Ljubljana Wedge; 11. R_1, R_2, R_3 –relative vectors of resultant movements, C_{SS} – strike slip component of displacement ($C_{SS1} \approx C_{SS2} \approx C_{SS3}$), C_{UP} – sum of underthrusting and pushing displacement component ($C_{UP1} > C_{UP2} > C_{UP3}$).

linear, and the Frontal Zone of the Trnovo Thrust Series, which is, owing to the northwest regional dip of the units, segmented according to fronts of individual thrust and nappe units.

The External Dinaric Thrust Belt is overthrust in southeast, in the area of the "Velebit Thrust Series", across the Budva Trough on the northeastern margin of the Adriatic platform segment which became therefore folded and partly imbricated. In northwest, where the platform segments are joined, predominate en echelon arranged folds of the Kras-Notranjsko Folded Structure.

Decreasing of displacements in front of the "Velebit Thrust Series" towards northwest is connected with pinching out of the Budva Trough. The difference in development of Cretaceous and

Paleogene between the Snežnik Thrust Unit and its basement is connected with structural differentiation of the platform and the resulting consequences.

3. Underthrusting below Southern Alps caused beside formation of the Southern Alpine Thrust Boundary also existence of the accompanied structures in Dinarides. They are well defined in the ductile formations of the lower and upper detachment horizon. Folds in the W-E direction in the Permocarboniferous clastites of the Trnovo Nappe are observable in the lower and folds in the SW-NE direction in the flysch of the upper detachment horizon under southeastern or left flank of the Hrušica Nappe near Ubeljsko (point 4 in Figs. 27 and 31). W-E directed folds are positioned east from Idria Fault and were formed in the first phase of the post-Sarmatian underthrusting. Younger, SW-NE directed folds are positioned west from Idria Fault. They formed as consequence of the contemporaneous lateral movement along Idria Fault and underthrusting below Southern Alps. Gentle secondary thrusting of the Trnovo and Hrušica Nappe in the southeast direction is also the effect of the above mentioned folding. PREMRU (1980) believed that Trnovo and Hrušica Nappes, as they are treated in our article, were secondary thrusted to the south, and arguments this with W-E directed folds. He didn't discuss the extent of thrusting.

4. The Istria-Friuli Underthrust Zone (Figs. 4 and 25) and the **Istria Pushed Area** (Fig. 27) are two phenomena that in sense of dynamics cannot be separated. Both phenomena are connected with formation of the "Adria" and its separation by the Kvarner Fault Zone into the Padan and Adriatic part. The movements started in Miocene. Already during the first displacement stage the dextral strike-slip movements along the Kvarner Fault Zone had to occur, and underthrusting under the frontal part of the Snežnik Thrust Fault, as evidenced by dipping of the Ravnik Anticline and Brkini Synclinorium axis under the Snežnik Thrust Unit. Underthrusting resulted also in deformation of the front of the Hrušica and Trnovo Nappes. We see the reasons for such interpretations in the lateral displacement between beds of the secondary fold (point 4 in Fig. 27, detail in Fig. 31). We presume that the Istria-Friuli Underthrust Zone started forming at a time when further underthrusting below the Snežnik Thrust Unit was not possible any more. It developed after the weakened part of platform in the place of the Friulan Paleogene Basin. In principle the Istria-Friuli Underthrust Zone accepted the displacements that were not possible any more in hinterland of Istria in the Frontal Zone of the External Dinaric Thrust Belt. Extensive underthrusting below the Snežnik Thrust Unit was probably limited to a narrow space between the apical part of the Southern Istrian Structural Wedge and the Kvarner Fault Zone in the depth. The limited capability for underthrusting below the Snežnik thrust block is associated with the unique platform.

The effect of push, expressed in deformation of the frontal part of Hrušica and Trnovo Nappes, can be recognized by disability of reconstructing the thrust planes of the both nappe units in flysch according to principles of expected geometry of the overthrust units.

Formation of the Istria-Friuli Underthrust Zone and of Istrian Pushed Area was a polyphase process. The polyphase character can be observed e.g. in internal structure of the Istria – Friuli Underthrust Zone, in which alternate phases of underthrusting and folding, and also in relation between the Dinaric striking faults and laterally deformed arcuate structures, as in continuation of the Southern Istrian Structural Wedge in which the Raša Fault and Čičarija Synclinorium are arched, whereas the fault itself together with the Trieste-Komen Anticlinorium and Vipava Synclinorium are not arched, etc.

5. "Adria" (Fig. 30). If accepting the hypothesis that the original structure of the rigid indenter of "Adria" has been the Adriatic segment of the Adriatic – Dinaric Mesozoic Carbonate Platform, it could be deduced from interpretation of the present structure of the External Dinarides that the boundary of the "Adria" is identical with the Frontal Zone of the External Dinaric Thrust Belt. However, this impression is only apparent, more acceptable seems the hypothesis that the original structure of the rigid indenter of microplate is identical with the lithologic boundary of the northeastern margin of the Adriatic segment of carbonate platform in the depth, which in places coincides spatially with the Frontal Zone, and with fault deformations that have arisen along this boundary. In northwestern part of External Dinarides, where the Adriatic and the Dinaric segment of carbonate platform should have been joined, the original structure should have been subjected to other criteria. We presume on the basis of deformation geometry at least two principal phases of evolution of northwestern boundary of the "Adria", accompanied with interphase events as sketched under point 3. Two phases are presumed with respect to segmentation of underthrusting boundary of the External Dinarides under Southern Alps west of the Ravne Fault, which is attributed to the broader zone of the Idrija Fault (Fig. 3). It is subdivided into the Modrej Fault, respectively Staro selo steep Thrust Fault of W-E strike, and a zone of gently inclined thrust faults striking ENE-WSW to NE-SW west of Tagliamento that lean on the W-E striking faults. The area of the intersecting line of SW (WSW)-NE (ENE) and W-E striking thrust faults lies, at least theoretically, in the structural prolongation of the Budva Trough below the Trnovo Thrust Series. The area of actual displacements along the Ravne Fault, respectively the broader fault zone of the Idrija Fault, lies on the trace of a wider zone of en echelon arranged dinaric, NW-SE striking faults, that passes from tip of the Kvarner Bay to central Soča River area. The zone is defined by the Raša Fault at the segment from eastern Kvarner coast

to the Ilirska Bistrica, active seismic zone Rupa – Postojna, Predjama Fault and the northwestern section of the Idrija and Ravne Faults. The connection between Kvarner and central Soča River area seems to be of a younger date. It formed after deformation of the Raša Fault in prolongation of the tip of Southern Istria Structural Wedge. Formation of this zone is conspicuously indicated by the linear arrangement of earthquake hypocenters in the Ilirska Bistrica – Hruševje zone. The mentioned boundaries of the "Adria", older and younger, reflect the subrecent and recent fragmentation process of northeastern part of the "Adria". The mechanism of this process is suggested by results of GPS measurements in the considered area (Weber et al., 2010) that was generated by separate rotation of the Padan part of the "Adria" in whose edge Istria is situated opposite to the southern or Adriatic part. The rotation generates pushing of Southern Istria Structural Wedge northeastwards and strike-slip along faults of en echelon zone between Kvarner and the central Soča River area. Recent displacements along the Črni Kal Thrust Fault (Rižnar et al., 2007) indicate integral displacement of smaller structural blocks that will have to be determined by measurements. Such blocks are in addition to the Southern Istria Structural Wedge also the Northern Istria Structural Wedge, the Istrian block with respect to the Friulan block, etc..

An idea about incorporation of the new segment of the crust in the "Adria" opens the question about its northern boundary. It is positioned in the western continuation of the Idria or Ravne Fault respectively. From this point of view, the South Alpine Thrust Front Boundary west from Idrija Fault and original NW boundary of the "Adria" in the structural continuation of the Budva trough under the Hrušica and Trnovo nappe plain has to be newly defined.

The kinematics of the eastern part of the Padan segment of the "Adria" is represented with resultant vectors of single parts of its boundary belt movements. According to the most intensive underthrusting and pushing in the Istria and gradual declining to the northwest, which is represented on the profiles across Istria (Fig. 22, C_{UP1} component), across Trieste – Karst Plateau (Fig. 23, C_{UP2} component) and Friuli (Fig. 24, C_{UP3} component), the relation between relative components of the underthrusting and pushing is as follows: $C_{UP1} > C_{UP2} > C_{UP3}$. If we presume that the component of displacement owing to the strike slip in the northeastern direction (C_{SS}) is roughly the same in the whole area, then $C_{SS1} = C_{SS2} = C_{SS3}$ Relative resultant movements R_1, R_2 and R_3 are therefore distorted in the counter-clockwise direction as deduced from reduced movements based on the GPS measurements (Weber et al. 2010).

References

Bigi, G., Consentino, D., Parotto, M., Sartori, R. & Scandone, P. 1990: Structural Model of Italy and Gravity Map, 1: 500.000. Sheet 2, Edit.: Bigi et al., Consiglio Nazionale delle Ricerche, 1990 (1983).

Bigi, G., Castellarin, A., Catalano, R., Coli, M., Cosentino, D., Dal Piaz, G. V., Lentini, F., Parotto, M., Patacca, E., Praturlon, A., Salvini, F., Sartori, R., Scandone, P. & Vai, B. 2000: Syntetic Structural – Kinematic Map of Italy, 1 : 2.000.000. Edit.: Bigi et al., Consiglio Nazionale delle Ricerche, 2000 (1989).

Biondić, B., Dukarić, F., Kuhta, M. & Biondić, R. 1997: Hydrogeological Exploration of the Rječina River Spring in the Dinaric Karst. Geol. Croat. (Zagreb) 50/2: 279–288.

Blašković, I. & Aljanović, B. 1981: Mikrotektonski elementi kao osnova za model tektonske građe šireg područja Kvarnera (Microtectonic elements as a basis for tectonic model of the broader Kvarner area). Simp. Kompleksna naftno-geološka problematika podmorja i priobalnih djelova Jadranskog mora, Split, Zbornik radova (Proceedings), 87–100, Zagreb.

Blašković, I. 1991: Raspored uzdužnih, reversnih i normalnih rasjeda i konstrukcija oblika i dubina ploha podvlačenja (Disposition of the longitudinal, reverse and normal faults and the construction of the forms and depths of the underthrusting surfaces). Geol. vjesnik (Zagreb) 44: 247–256.

Blašković, I. 1998: The Two Stages of Structural Formation of the Coastal Belt of the External Dinarides. Geol. Croat. (Zagreb) 51/1: 75–89.

Blašković, I. 1999: Tectonics of Part of the Vinodol Valley with in the Model of the Continental Crust Subduction. Geol. Croat. (Zagreb) 52/2: 153–189.

Buser, S. Grad, K. & Pleničar, M. 1967: Osnovna geološka karta Jugoslavije 1:100.000, list Postojna (Basic geological map of Yugoslavia, sheet Postojna). Savezni geološki zavod, Beograd.

Buser, S. 1968: Osnovna geološka karta Jugoslavije 1 : 100.000, list Gorica (Basic geological map of Yugoslavia, sheet Gorica). Savezni geološki zavod, Beograd.

Buser, S. 1969: Osnovna geološka karta Jugoslavije 1 : 100.000, list Ribnica (Basic geological map of Yugoslavia, sheet Ribnica). Savezni geološki zavod, Beograd.

Buser, S. 1976: Tektonska zgradba južnozahodne Slovenije (Tektonischer Aufbau Südwest-Sloweniens). 8. jugosl. Geol. kongres, Bled 1974, 3: 45–57, Ljubljana.

Buser, S. 1978: Osnovna geološka karta Jugoslavije 1 : 100.000, list Celje (Basic geological map of Yugoslavia, sheet Celja). Savezni geološki zavod, Beograd.

Buser, S. 1986: Osnovna geološka karta Jugoslavije 1 : 100.000, tolmač lista Tolmin in Videm (Udine) (Basic geological map of Yugoslavia, guidebook for sheet Tolmin in Videm (Udine). Savezni geološki zavod, Beograd.

Buser, S. 1987: Osnovna geološka karta Jugoslavije 1 : 100.000, list Tolmin in Videm (Udine) (Basic geological map of Yugoslavia, sheet Tolmin in Videm (Udine)). Savezni geološki zavod, Beograd.

Buser, S. 1989: Development of the Dinaric and the Julian carbonate platforms and of the intermediate Slovenian basin (NW Yugoslavia). Mem. Soc. Geol. It. (Roma) 40 (1987): 313–320.

Carulli, G. B., Nicolich, R., Rebez, A. & Slejko, D. 1990: Seismotectonics of the Northwest External Dinarides. Tectonophysics, 179: 11–25.

Carulli, G. B. 2006: Carta geologica del Friuli Venezia Giulia 1:150.000 (Geological map of the Friuli Venezia Giulia 1 : 150.000). Edit.: Carulli, Universita degli studi di Trieste, Universita degli studi di Udine, Firenze.

Cati, A., Sartorio, D. & Venturini, S. 1989: Carbonate platforms in the subsurface of the northern Adriatic area. Mem. Soc. Geol. It. (Roma) 40 (1987): 295–308.

Colizza, E., Costa, R., Cucchi, F., Knezaurek, G., Pirini Radrizzani, G., Pugliese, N., Ulcigrai, P. & Zucchi Stolfa, M. L. 1989: The geology of the San Pelagio area (Karst of Trieste, Italy). Mem. Soc. Geol. It. (Roma) 40 (1987): 45–51.

Cucchi, F., Pirini Radrizzani, C. & Pugliese, N. 1989a: The carbonate stratigraphic sequence of the Karst of Trieste (Italy). Mem. Soc. Geol. It. (Roma) 40 (1987): 35–44.

Cucchi, F., Vaia, F. & Finocchiaro, F. 1989b: The geology of T. Rosandra valley (Karst of Trieste, Italy). Mem. Soc. Geol. It. (Roma) 40 (1987): 67–72.

Čar, J. & Gospodarič, R. 1983/84: O geologiji krasa med Postojno, Planino in Cerknico (About geology of karst among Postojna, Planina and Cerknica). Acta carsologica (Ljubljana) 12: 91–105.

Del Ben, A., Finetti, I., Rebez, A. & Slejko, D. 1991: Seismicity and seismotectonics at the Alps-Dinarides contact. Bollettino di Geofisica Teorica ed Applicata 33/130–131: 155–176.

Đurasek, N., Frank, G., Jenko, K., Kužina, K. & Tončić-Gregl, R. 1981: Prilog poznavanju naftno-geoloških odnosa u sjeverozapadnom dijelu jadranskog podmorja (Contribution to the understanding of oil-geological relations in NW Adriatic area). Simp. Kompleksna naftno-geološka problematika podmorja i priobalnih djelova Jadranskog mora, Split, Zbornik radova (Proceedings), Zagreb: 201–213.

Fantoni, R., Catellani, D., Merlini, S., Rogledi, S. & Venturini, S. 2002: La registrazione degli eventi deformativi cenozoici nell´avampaese Veneto-Friulano. Mem. Soc. Geol. It. (Roma) 57: 301–313.

Grad, K. & Ferjančič, L. 1974: Osnovna geološka karta Jugoslavije 1 : 100.000, list Kranj (Basic geological map of Yugoslavia, sheet Kranj). Savezni geološki zavod, Beograd.

Grad, K. & Ferjančič, L. 1976: Kranj; Osnovna geološka karta Jugoslavije 1 : 100.000, tolmač lista Kranj (Basic geological map of Yugoslavia, guidebook for sheet Kranj). Savezni geološki zavod, Beograd.

Grandić, S., Boromisa-Balaš, E. & Šušteršić, M. 1997a: Exploration concept and characteristic of the Dinarides stratigraphic and structural model in the Croatian offshore area (Part I). Nafta (Zagreb) 48/4: 117–128.

Grandić, S., Boromisa-Balaš, E. & Šušterčić, M. 1997b: Exploration concept and characteristics of the stratigraphic and structural models of the Dinarides in Croatian offshore area (Part II.:Hydrocarbon Consideration). Nafta (Zagreb) 48/8–9: 249–266.

Grandić, S., Kratković, I., Kolbah, S. & Samaržija, J. 2004: Hydrocarbon potential of stratigraphic and structural traps of the Ravni Kotari area - Croatia. Nafta (Zagreb) 55/7–8: 311–327.

Herak, M. 1986: A new concept of geotectonics of the Dinarides. Acta geologica 16/1, Prirodoslovna istraživanja (Zagreb) 51: 1–42.

Herak, M. 1999: Tectonic Interrelation of the Dinarides and the Southern Alps. Geol. Croat. (Zagreb) 52/1: 83–98.

Jurkovšek, B., Toman, M., Ogorelec, B., Šribar, L., Drobne, K., Poljak, M & Šribar, Lj. 1996: Formacijska geološka karta južnega dela Tržaško-Komenske planote: Kredne in paleogenske karbonatne kamnine (Geological map of the southern part of the Trieste-Komen plateau: Cretaceous and Paleogene carbonate rocks). Geološki zavod Ljubljana (Ljubljana): 1–143.

Korbar, T. 2009: Orogenic evolution of the External Dinarides in the NE Adriatic region: a model constrained by tectonostratigraphy of Upper Cretaceous to Paleogene carbonates. Earth-Science Rewiews, 96/4: 296–312.

Magaš, N. 1968: Osnovna geološka karta Jugoslavije 1 : 100.000, list Cres (Basic geological map of Yugoslavia, sheet Cres). Savezni geološki zavod, Beograd.

Mamužić, P., Milan, A., Korolija, B., Borović, I. & Majcen, Ž. 1969: Osnovna geološka karta Jugoslavije 1 : 100.000, list Rab (Basic geological map of Yugoslavia, sheet Rab). Savezni geološki zavod, Beograd.

Marinčić, S. & Matičec, D. 1991: Tektonika i kinematika deformacija na primjeru Istre (Tectonics and kinematics of deformations – an Istrian Model). Geol. vjesnik (Zagreb) 44: 257–268.

Matičec, D. 1994: Neotectonic Deformations in Western Istria, Croatia. Geol. Croat. (Zagreb) 47/2: 199–204.

Marton, E. 1987: Palaeomagnetism and tectonics in the Mediterranean region. Journal of Geodynamics 7: 33–57.

Merlini, S., Doglioni, C., Fantoni, R. & Ponton, M. 2002: Analisi strutturale lungo un profilo geologico tra la linea Fella-Sava e l'avampaese adriatico (Friuli Venezia Giulia-Italia). Mem. Soc. Geol. It. (Roma) 57: 293–300.

Mihevc, A. 1994: Morfološke značilnosti Matarskega podolja. Ann. Ser. hist. nat. 4/4:163–168.

Mihevc, A. 2007: The age of karst relief in West Slovenia. Acta carsologica (Ljubljana)36/1: 35–44.

Mikes, T., Báldi-Beke, M., Kázmér, M., Dunkl, I. & Eynatten, H. 2008: Calcareous nannofossil

age constraints on Miocene flysch sedimentation in the Outer Dinarides (Slovenia, Croatia, Bosnia-Herzegovina and Montenegro. In eds. Siegesmund, S., Fügenschuh, B. & Froitzheim, N. Tectonic Aspects of the Alpine-Dinaride-Carpathian System. Geological Society, Special Publications (London) 298: 335–363.

Mlakar, I. 1964: Vloga postrudne tektonike pri iskanju novih orudenih con na območju Idrije. Rudarsko-metalurški zbornik (Ljubljana) 1: 18–25.

Mlakar, I. 1969: Krovna zgradba idrijsko žirovskega ozemlja (Nappe structure of the Idrija-Žiri Region). Geologija (Ljubljana) 12: 5–72.

Mlakar, I. & Placer, L. 2000: Geološka zgradba Žirovskega ozemlja. V Rudnik urana Žirovski vrh, Florjančič, A. P. (eds), 34–45, Didakta, Radovljica.

Nicolich, R., Della Vedova, B., Giustiniani, M. & Fantoni, R. 2004: Carta del sottosuolo della Pianura Friulana (Map of subsurface structures of the Friuli Plain), Universita di Trieste: 1–32.

Nussbaum, Ch. 2000: Neogene Tectonics and Thermal Maturity of Sediments of the Easternmost Southern Alps (Friuli Area, Italy). Thesis, Inst. de Geologie, Universite de Neuchatel.

Pamić, J., Glušić, I. & Jelaska, V. 1998: Geodynamic evolution of the Central Dinarides. Tectonophisics, 297: 251–268.

Pamić, J. & Hrvatović, H. 2003: Main large thrust structures in the Dinarides – a proposal for their classification. Nafta (Zagreb) 54/12: 443–456.

Peruzza, L., Poli, M. E., Rebez, A., Renner, G., Rogledi, S., Slejko, D. & Zanferrari, A. 2002: The 1976-1977 seismic sequence in Friuli: new seismotectonic aspects. Mem. Soc. Geol. It. (Roma) 57: 391–400.

Placer, L. 1973: Rekonstrukcija krovne zgradbe idrijsko-žirovskega ozemlja (Reconstruction of the Nappe Structure of the Idrija-Žiri Region). Geologija (Ljubljana) 16: 317–334.

Placer, L. 1981: Geološka zgradba jugozahodne Slovenije (Geologic structure of southwestern Slovenia). Geologija (Ljubljana) 24/1: 27–60.

Placer, L. 1982: Tektonski razvoj idrijskega rudišča (Structural history of the Idrija mercury deposit). Geologija (Ljubljana) 25/1: 7–94.

Placer, L. 1996: O zgradbi Soviča nad Postojno (On the structure of Sovič above Postojna). Geologija (Ljubljana) 37/38 (1994/95): 551–560.

Placer, L. & Čar, J. 1997: Structure of Mt. Blegoš between the Inner and Outher Dinarides. Geologija (Ljubljana) 40: 305–323.

Placer, L. 1999: Contribution to the macrotectonic subdivision of the border region between Southern Alps and External Dinarides. Geologija (Ljubljana) 41(1998): 223–255.

Placer, L. 2002: Predhodna objava rezultatov strukturnega profiliranja Kraškega roba in Istre, AC Kozina – Srmin, Sečovlje (Preliminary results of structural profiling of the Kras edge and Istria, Kozina – Srmin Motorway, Sečovlje). Geologija (Lubljana)45/1: 277–280.

Placer, L., Košir, A., Popit, T., Šmuc, A. & Juvan, G. 2004: The Buzet Thrust Fault in Istria and overturned carbonate megabeds in the Eocene flysch of the Dragonja Valley (Slovenia). Geologija (Ljubljana) 47/2: 193–198.

Placer, L. 2005: Strukturne posebnosti severne Istre (Structural curiosity of the northern Istria). Geologija (Ljubljana) 48/2: 245–251.

Placer, L. 2007: Kraški rob. Geološki prerez vzdolž AC Kozina – Koper (Kraški rob (landscape term). Geologic section along the motorway Kozina – Koper (Capodistria). Geologija (Ljubljana) 50/1: 29–44.

Placer, L. 2008a: Vipavski prelom. Geologija (Ljubljana) 51/1: 101–105.

Placer, L. 2008b: Principles of the tectonic subdivision of Slovenia. Geologija (Ljubljana) 51/2: 205–217.

Placer, L. 2009: Tektonska razčlenitev Slovenije (Tectonic subdivision of Slovenia). V Geologija Slovenije (In Geology of Slovenia), Uredniki/Eds. Pleničar, M. et al., Ljubljana. In print.

Pleničar, M. 1959: Tektonski okni pri Knežaku (Two tectonic windows at Knežak). Geologija (Ljubljana) 5: 5–10.

Pleničar, M., Polšak, A. & Šikić, D. 1969: Osnovna geološka karta Jugoslavije 1 : 100.000, list Trst (Trieste) (Basic geological map of Yugoslavia, sheet Trst (Trieste)). Savezni geološki zavod, Beograd.

Pleničar, M., Polšak, A. & Šikić, D. 1973: Osnovna geološka karta Jugoslavije 1 : 100.000, tolmač lista Trst (Trieste) (Basic geological map of Yugoslavia, guidebook for sheet Trst (Trieste)). Savezni geološki zavod, Beograd.

Poljak, M. 1986: Strukturna evolucija slovenskih Vanjskih Dinarida u terciaru i kvartaru (The structural evolution of the Slovene Outer Dinarides in Tertiary and Quaternaty). XI. Kongr. Geol. Jugoslavije, Knj.3, 299–322, Tara.

Poljak, M. & Rižnar, I. 1996: Structure of the Adriatic - Dinaric Platform Along the Sečovlje - Postojna Profile. Geol. Croat. (Zagreb) 49/2: 345–346.

Polšak, A. 1967: Osnovna geološka karta Jugoslavije 1 : 100.000, list Pula (Basic geological map of Yugoslavia, sheet Pula). Savezni geološki zavod, Beograd.

Polšak, A. & Šikić, D. 1973: Osnovna geološka karta Jugoslavije 1 : 100.000, list Rovinj (Basic geological map of Yugoslavia, sheet Rovinj). Savezni geološki zavod, Beograd.

Ponton, M. 2002: La tettonica del gruppo del M. Canin e la linea Val Resia-Val Coritenza (Alpi Giulie occidentali. Mem. Soc. Geol. It. (Roma) 57: 283–292.

Prelogović, E., Pribičević, B., Ivković, Ž., Dragičević, I., Buljan, R. & Tomljenović, B. 2004: Recent structural fabric of the Dinarides and tectonically active zones important for petroleum-geological exploration in Croatia. Nafta (Zagreb) 55/4 (2003): 155–161.

Premru, U. 1980: Geološka zgradba osrednje Slovenije. Geologija (Ljubljana) 23/2: 227–278.

Premru, U. 1983: Osnovna geološka karta Jugoslavije 1 : 100.000, list Ljubljana (Basic geologi-

cal map of Yugoslavia, sheet Ljubljana). Savezni geološki zavod, Beograd.

Premru, U. 2005: Tektonika in tektogeneza Slovenije (Tectonics and Tectogenesis of Slovenia). Geološki zavod Slovenije (Ljubljana): 1–515.

Rižnar, I., Koler, B. & Bavec, M. 2007: Recentna aktivnost regionalnih geoloških struktur v zahodni Sloveniji. Geologija (Ljubljana) 50/1:111–120.

Savić, D. & Dozet, S. 1985: Osnovna geološka karta Jugoslavije 1 : 100.000, list Delnice (Basic geological map of Yugoslavia, sheet Delnice). Savezni geološki zavod, Beograd.

Slejko, D., Carraro, F., Carulli, G. B., Castaldini, A., Cavallin, A., Doglioni, C., Nicolich, R., Rebez, A., Semenza, E. & Zanferrari, A. 1986: Seismotectonic Model of Northeastern Italy: an Approach. Geologia Applicata e Idrogeologia XXI/1, 153–165.

Šikić, D., Polšak, A. & Magaš, N. 1969: Osnovna geološka karta Jugoslavije 1 : 100.000, list Labin (Basic geological map of Yugoslavia, sheet Labin). Savezni geološki zavod, Beograd.

Šikić, D., Pleničar, M. & Šparica, M. 1972: Osnovna geološka karta Jugoslavije 1 : 100.000, list Ilirska Bistrica (Basic geological map of Yugoslavia, sheet Ilirska Bistrica). Savezni geološki zavod, Beograd.

Šribar, L. 1995: Evolucija gornjekredne Jadransko-Dinarske karbonatne platforme u jugozapadnoj Sloveniji. MSC Thesis, pp. 89, University of Zagreb.

Šušnjar, M, Bukovac, J., Nikler, L., Crnolatac, I., Milan, A., Šikić, D., Grimani, I., Vulić, Ž. & Blašković, I. 1970: Osnovna geološka karta Jugoslavije 1 : 100.000, list Crikvenica (Basic geological map of Yugoslavia, sheet Crikvenica). Savezni geološki zavod, Beograd.

Tari, V. 2002: Evolution of the northern and western Dinarides: a tectonostratigraphic approach. EGU Stephan Mueller Special Publication Series 1: 223–236.

Velić, I., Vlahović, I. & Matičec, D. 2002: Depositional sequences and Paleogeography of the Adriatic Carbonate Platform. Mem. Soc. Geol. It. (Roma) 57: 141–151.

Venturini, S. 2002: Il pozzo di Cargnacco 1: un punto di taratura stratigrafica nella pianura friulana. Mem. Soc. Geol. It. (Roma) 57: 11–18.

Vidrih, R. & Ribičič, M. 2004: Potres 12. julija 2004 v zgornjem Posočju – preliminarne geološke in seizmološke značilnosti (The earthquake on July 12, 2004 in Upper Soča territory - NW Slovenia – preliminary geological and seismological characteristics). Geologija (Ljubljana) 47/2: 199–220.

Vlahović, I., Tišljar, J., Velić, I. & Matičec, D. 2005: Evolution of the Adriatic Carbonate Platform: Palaeogeography, main events and depositional dynamics. Palaeogeography, Palaeoclimatology, Palaeoecology (Amsterdam) 220/3-4: 333–360.

Vrabec, M. 1994: Some thoughts on the pull-apart origin of karst poljes along the Idrija strike-slip fault zone in Slovenia. Acta carsologica (Ljubljana) 23: 158–168.

Weber, J., Vrabec, M., Pavlovčič-Prešeren, P., Dixon, T., Jiang, Y. & Stopar, B. 2010: GPS-derived motion of the Adriatic microplate from Istria Peninsula and Po Plain site, and geodynamic implications. Tectonophysics, (Amst.) 483/3–4: 214–222. doi: 10.1016/j.tecto.2009.09.001

Zupančič, P., Cecić, I., Gosar, A., Placer, L., Poljak, M. & Živčić, M. 2001: The earthquake of 12 April 1998 in the Krn Mountains (Upper Soča valley, Slovenia) and its seismotectonic characteristics. Geologija (Ljubljana) 44/1: 169–192.

GEOLOGIJA *53/1*, 87-92, Ljubljana 2010

Trepça Ore Belt and Stan Terg mine – Geological overview and interpretation, Kosovo (SE Europe)

Sylejman HYSENI[1], Bedri DURMISHAJ[1], Bislim FETAHAJ[2], Ferat SHALA[2], Avdullah BERISHA[2] & Duncan LARGE[3]

[1]University of Prishtina Geology Department Mitrovicë, 40000 Republic of Kosovo
[2]Trepça Mines Prishtine, 10000 Republic of Kosovo
[3]Exploration Manager, SE Europe 38116 Braunschweig, Germany

Prejeto / Received 25. 5. 2009; Sprejeto / Accepted 27. 5. 2010

Key words: Kosovo, Trepça Belt, Stan Terg, Mine, deposit, lead, zinc, Vardar zone, Reserves and Resources

Abstract

The Trepça Belt of Pb-Zn-Ag mineralization is located within the NNW-SSE trending Vardar zone. The Belt extends for over 80 km, and supported five mines during the period 1930-2008. It contains a number of the other Pb-Zn occurrences too. The replacement and vein type mineralization is hosted primarily by Mesozoic carbonates, but also occasionally by amphibolites, and displays a clear structural control. Mineralization is spatially and genetically related to Neogene andesite-dacite extrusives and sub-volcanic intrusives. Only Stan Terg mine is presented in this paper.

Introduction

The history of silver, lead and zinc mining in Kosovo is woven into with the history of Kosovo itself. In the modern era, the production of silver, lead and zinc has been synonymous with Trepça. This briefing note describes the current situation at Trepça and examines its future outlook.

Mining activities and smelting of the silver-bearing lead-zinc ore in Kosovo has a long history and can be dated back to even pre-Roman times as the relics of tools and diggings show. From the Roman period to the Middle Ages, the area between Serbia and Greece especially the southern part of Kosovo was intensively exploited for its lead-zinc and silver ores and at that time was one of most important sources of its kind. The Roman and Ottoman Empires fought to take control of the silver mines in Kosovo and at a later stage the Serbian Middle Kingdom produced much of its coinage from silver mined at Artana/Novo Berdo.

The British company Seltrust, founded at one stage, operated nine mines in Trepça as shown on the map (Fig. 1). Currently, only five of these have significant remaining resources, although all have the potential for extensions to the known mineralization. The mining and processing infrastructure following the conflict was in a very poor condition. However, after major effort and significant investment, four of the mines have recommenced limited production.

The successful industry of the 1960s and the historic mines were founded on the quality of the lead-zinc deposits that occur in the Trepça Mineral Belt running in a NW-SE direction from Kapaonik (Beloberdo) in the north to Kizhnica in the south. Whilst the 80s and 90s were characterized, at least partly, by a lack of exploration, the known deposits are not exhausted and mineable reserves and measured resources (Adam Wheeler

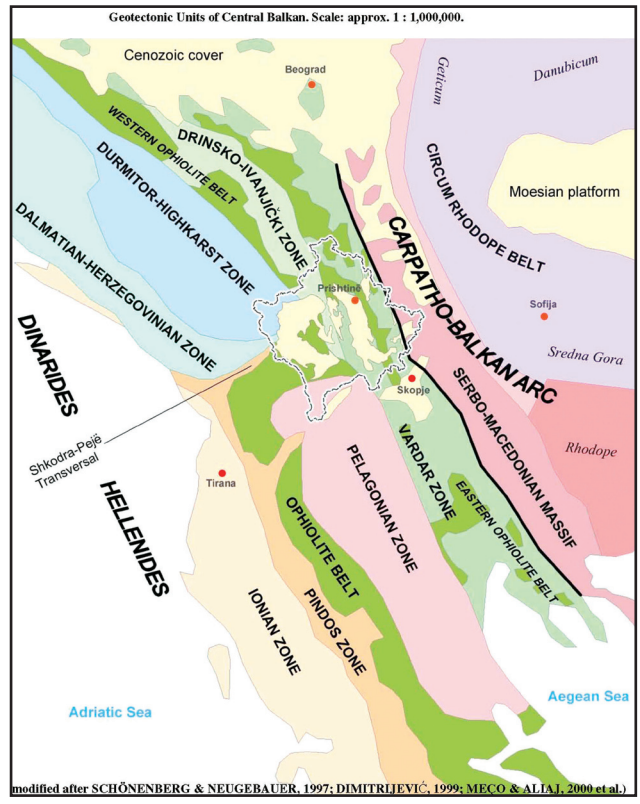

Fig. 1. Map of Kosovo in geotectonic units

study) at the five key mines total 7,068,000 tonnes of 5.46 wt% lead, 5.64 wt% zinc and 116 g/tonne silver. All deposits are open at depth or extend on strike. Recent geological work strongly indicates that the deposits within the Trepça Mineral Belt are considered highly prospective with regard to additional reserves and resources as the mineralization is structurally and/or fault controlled. Consequently, the Trepça Mineral Belts (Hyseni & Large, 2003) hold great potential, not only for lead, zinc and silver, but also for copper and gold.

Trepça Mineral Belt regional geology

The linear Trepça "Belt" of lead-zinc mineralization extends for over 80 km in northern Kosovo, and includes numerous mines and occurrences (Figs. 1, 2). Although evidence of mining dates back to the Romans, who were primarily interested in small gold occurrences, modern mining began in 1930 at the Stan Terg lead-zinc mine, which is located on the Trepca stream.

The Trepca Belt, which comprises part of what has been previously described as the Kapaonik District (Forgan, 1948; Jankovic et al., 1997), includes numerous lead-zinc deposits. On a regional scale, the Trepça Belt belongs to the Kosovo sector of the Serbo-Kosovo-Macedonian-Rhodope metallogenic belt of Oligocene-Miocene age. This includes the base and precious-metal districts in Kosovo, southern and western Serbia, Macedonia, northern Greece and southern Bulgaria (Heinrich & Neubauer, 2002).The Trepça Belt lies within the NNW-SSE trending Vardar tectonic zone (Fig. 2).

The regional structure marks the fundamental suture between the Serbo-Kosovaro-Macedonian Massif, which is underlain by late Proterozoic metamorphic successions, and the Dina rides, which are comprised of Mesozoic ones with typical Alpine deformation. The Vardar Zone contains fragments of Paleozoic crystalline schist and phyllite, with unconformable overlying Triassic clastics, phyllites, volcanoclastic rocks and Upper Triassic carbonates. Serpentinized ultrabazik rocks, gabbros, diabases and sediments of the ophiolite association characterize the Jurassic. The Cretaceous sequence consists of a complex series (sometimes described as mélange) of clastics, serpentinite, mafic volcanics and volcanoclastic rocks, and carbonates. The Tertiary (Oligocene-Miocene) andesite, trachyte and latite sub-volcanic intrusives, volcanics and pyroclastic rocks occur at several centres within the Trepça Belt, covering large areas (Miletic, 1997). They are particularly well developed in the eastern sector (the so-called Inner Vardar sub-zone) of the Vardar zone. Miocene and Pliocene shallow water sediments fill the Kosovo Basin, which borders the central and southern sectors of the Trepça Belt to the west.

Fig. 2. Vardar zone and position of Pb-Zn-Ag mineralization in Kosovo

The structure of the Trepça Belt is dominated by NNW-SSE trending structures. Overthrusts with SE vergence are dominant, some of which are demonstrably post-Oligo-Miocene in age while others are clearly older. Congruent WSW-ENE structures link the dominant NNW-SSE trending structures. It is considered that many of the Vardar structures may be reactivated Variscan structures marginal to the Serbo-Kosovaro-Macedonian Massif. The possible influence of the NW-SE structures in the Drina-Ivanjica (Drenica) structural block, which is an external unit of the Dinarides and forms the western margin of the Vardar zone, are overprinted on the dominant NNW-SSE trend.

Trepça geologists recognized three regional (NNW-SSE) trending zones of mineralization within the Belt (Fig. 3).

Zone I includes Artana-(Novoberdo-)Batllavë. Zone I follows the boundary between the Kosovo sector of the Serbo-Kosovaro-Macedonian Massif, which is marked here by extensive Neogene calc-alkaline volcanics and intrusives, with the Vardar Zone.

Zone II extends from the Hajvalia-Kizhnica district in the south to Belo Berdo in the north, and includes the Stan Terg mine and numerous other occurrences. Zone II follows the major fault that marks the eastern margin of the Miocene Prishtina basin, and its extension to the NNW and the intrusive and volcanic complexes (Fig. 3) in northern Kosovo.

Zone III includes the Crnac mine, and extends along a number of lead-zinc occurrences on the western border of the Vardar Zone, where it is in contact with the Dinaride-Drina-Ivanjica (Drenica) structural block.

Stan Terg mine

Exploration and mining history

The Stan Terg mine, which has been considered one of the best lead, zinc and silver mines in

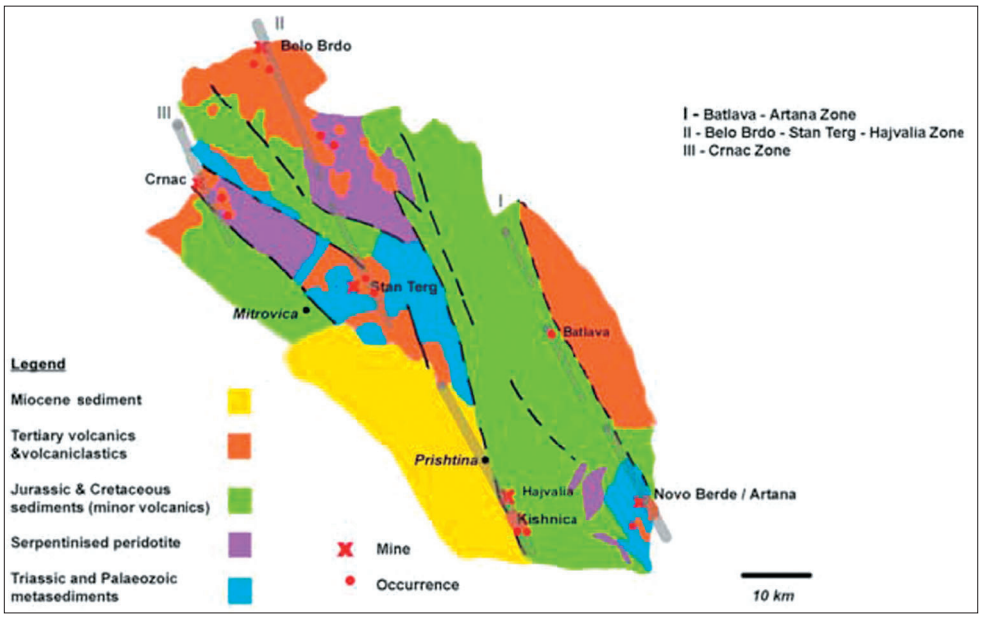

Fig. 3. Trebça mineral belt

Europe, was initially explored by Selection Trust Ltd in 1925. The deposit was discovered after exploration in the vicinity of mediaeval workings. Development commenced in 1927, and production in 1930. Production was maintained during the German-Italian occupation (1941-1945), and then continued until 1999 under state ownership. Mining has been performed from the surface down to Level 9 at a depth of 600 m below the surface. Average annual production from 1945 to 1990 was 580,000 tonnes, and it is estimated that total production has been approx. 32 million tonnes. The highest annual production was 704,000 tonnes in 1984.

In the vicinity of the Stan Terg deposit there are several occurrences of Pb-Zn ore bodies, such as Didoma, Meljenca, Rasane, Terstnea and Zijaça with all of the Stan Terg style of mineralization, holding economic potential and further resources.

Stan Terg regional geology

The Stan Terg Pb-Zn-Ag deposit is located within the Vardar zone of the Dinaride Alpine Belt, consisting of Paleozoic basement rocks, Jurassic-Cretaceous sediments and rocks of ophiolitic affinities. These rock units have been foliated during the early Tertiary (Fig. 4). During the late Tertiary, the Balkan Area was heavily affected by plutonic, sub-volcanic and volcanic processes with the deposition of mainly granodioritic magmas at depth, andesites, dacites and quartz latite flows and dykes as well as pyroclastic rocks, mostly tuffs, lapilli tuffs and ignimbrites. Structurally, the Stan Terg deposit is situated in the centre of the so-called Trepça Mineral Belt (Kapaonik Zone). This tectonic zone, within which the Balkan Pb-Zn-Ag deposits are located, is marked by very strong lineaments and a fracture zone striking NW-SE. It can be followed from Bosnia, through Kosovo and Macedonia to the Gulf of Selanik in Greece and varies in width from 40 to 60 kilometres.

Mine Geology

The overall geological structure at Stan Terg is complex, consisting of an anticline plunging at about 40° NW, with a prominent volcanic breccia pipe along the hinge of the asymmetric anticline. The core of the anticline consists of Triassic carbonates surrounded by sericite schist (Fig. 5).

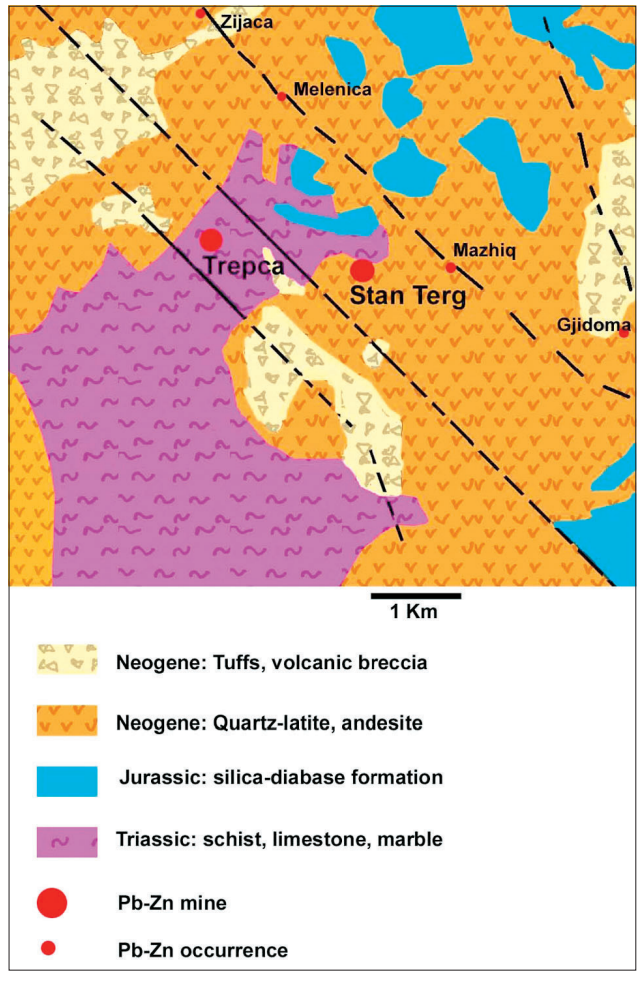

Fig. 4. Stan Terg regional Geology

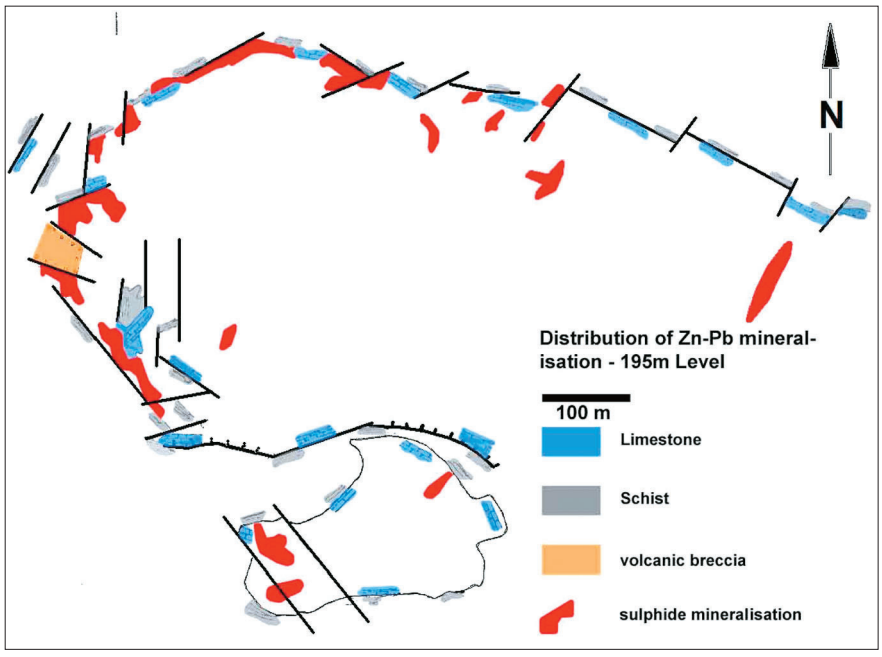

Fig. 5.
Plan of 195 m level outline of anticline

Low-grade mineralization occurs along elongated paleo-karst features and cavities, commonly associated with skarn-type alterations.

Massive sulphide ore of economic importance forms continuous, columnar shaped ore bodies of the carbonate replacement type. These are located along the carbonate-schist contact and dip parallel to the plunge of the anticline and structural fabric and the dip of the flanks. The ore bodies along this contact extend along a strike length of 1,200 m, and have been explored to a depth of 925 m below the surface (11 levels – Fig. 6).

The ore mineralogy of the deposit is dominated by pyrite, pyrrhotite, sphalerite and galena, with typical carbonate gangue minerals and minor quartz.

In detail, the ore mineralogy is very varied and includes a number of primary Pb-Zn- as well as secondary sulphides in cavities and vugs, including rare minerals such as boulangerite.

The large ore bodies along the footwall are in contact with the volcanic breccia pipe and consist of massive Pb-Zn sulphides of lower grade, including ilvaite and hedenbergite garnet as well as -magnetite, - pyrite and- chalcopyrite skarn together with Fe-rhodochrosite, siderite, ankerite and dolomite. This skarn-type mineralization also occurs together with smaller ore bodies and sub-economic pockets associated paleo-karst cavities.

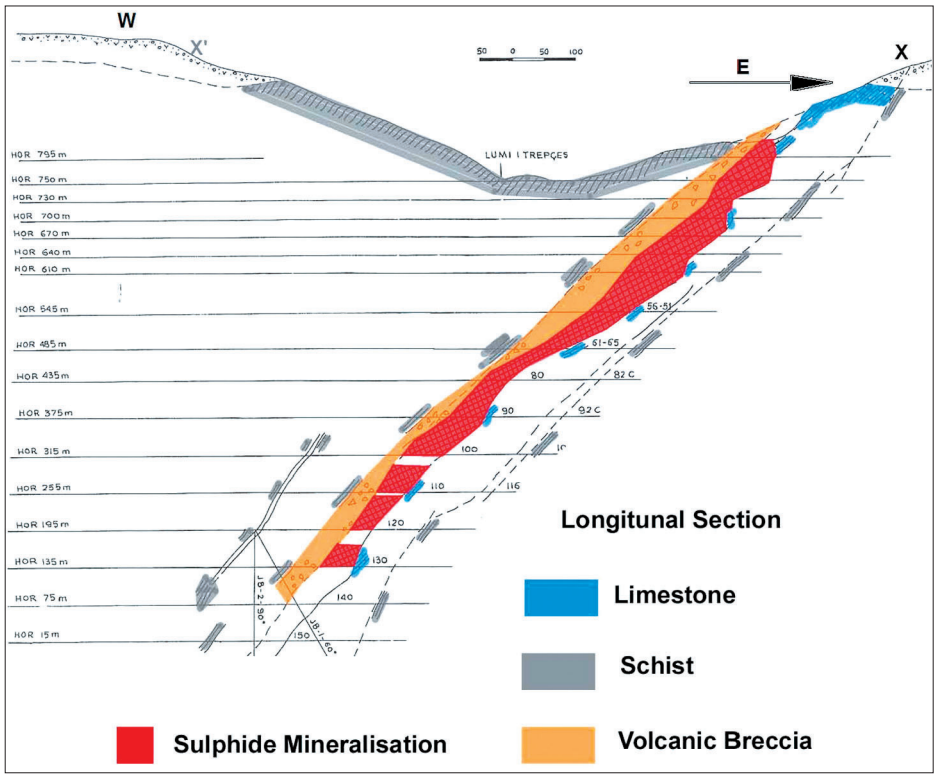

Fig. 6. Section through main mineralised zone in Stan Terg

Reserve estimation

These figures are derived from detailed reviews of previous estimates, 3D modelling using Data Mine software (Wheeler 2003), re-evaluation and re-assaying of production stops (Table 1). The resource figures pertain to 22 stopes within the bottom three levels (8-9) and have had economic cut-off calculations and mining factors applied. The figures given as probable and proven refer mainly to production stopes on Level 10 and minor to Level 9 and 11 stopes. Fig.7 does not strictly comply with CIM reporting standards due to a lack of reconciliation data.

Table 1. Stan Terg mine reserves and resources:

	Tonnes	% Pb	% Zn	g/t Ag
Proven reserves:	120,340	5.14	5.13	88.0
Probable reserves:	311,660	5.10	3.17	80.5
Total mine able reserves:	432,000	5.10	3.17	80.5
Total resources:	12,488,000	3.21	2.21	56.4

Acknowledgments

We are grateful to Professor Vahdet Pruthi University of Prishtina, who provided valuable suggestions, and improvements to the English text.

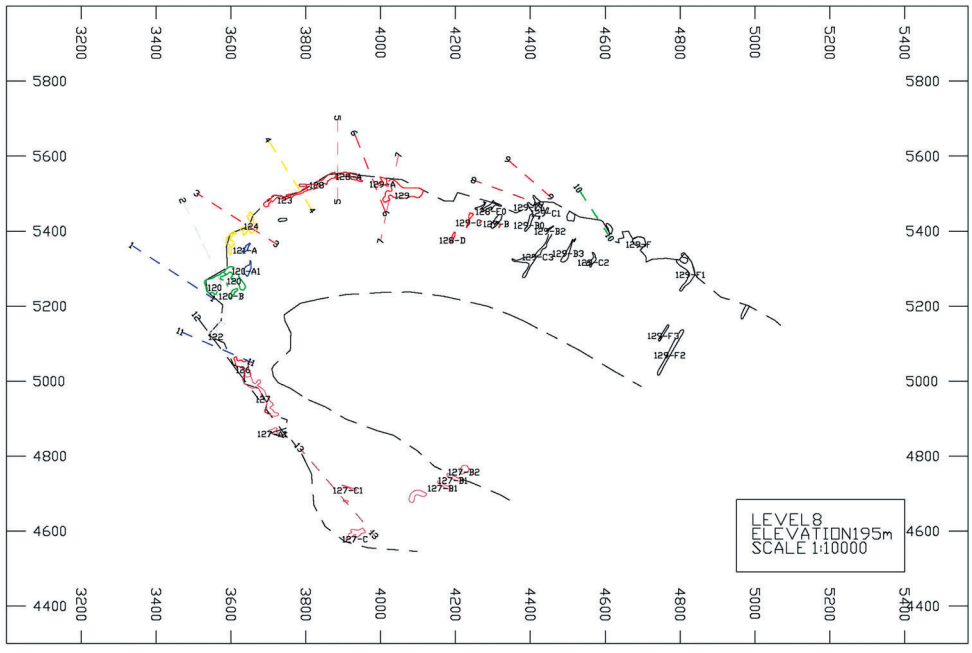

Fig. 7. The geological plane, level 8 (195m) Stan Terg mine.

References

Forgan, C.B. 1948: Ore deposits at the Stan Terg lead-zinc mine. In: The Geology, para genesis and reserves of ores of lead and zinc, 18th International Geological Congress, (London) VII: 290–307.

Heinrich, C.A. & Neubauer, F. 2002: Cu-Au-Pb-Zn-Ag Metallogenic of the Alpine – Balkan – Carpathian – Dinaride geodynamic province. Mineralium Deposita 37: 533–540.

Hyseni, S. & Large, D. 2003: The Trepca lead-zinc Mineral Belt, Kosovo – Geological Overview and Interpretation. (7th Biennial SGA Meeting on Mineral Exploration and Sustainable Development Poster 2003 Athens-Greece, 120: 1–2.

Jankovic, S. 1982: Yugoslavia. In: Dunning, F.W. Mykura, W. & Slater, D. (Eds.): Mineral deposits of Europe, SE Europe, The instruction of Mining and mineralogical society (London) 2: 143–202.

Jankovic, S. 1995: Generally metallogenic characteristics of the district of Kopaonik, Symposium (PL-IA). Geology and Metallogenic Kopaonik (Belgrade): 79–101.

Jankovic, S., Serafimovski, T., Jelenkovic, R. & Cifliganec, V. 1997: Metallogenic of the Vardar zone and the Serbo-Macedonian Mass. In: Boev, B. & Serafimovski, T. (Eds.): "Magmatism, Metamorphism and Metallurgy of the Vardar Zone and the Serbo-Macedonian Massif" Faculty of Mining and Geology Stip, 29–67.

Miletič, G. 1997: Structural control volcanic apparatus of continuous lead and zinc mineralization of the Kopaonik metallogenic district (Symposium in Serbian IRL, (Belgrade): 91–99.

Wheeler, A. 2003: Trepca Resource and Reserve Review, unpublished report, February Toronto (Canada, Strathcona Mineral Services Limited): 18–21.

GEOLOGIJA *53/1*, 93–96, Ljubljana 2010

Geološka delavnica za osnovne šole

Geological workshop for primary schools

Nina RMAN

Geološki zavod Slovenije, Dimičeva ul. 14, SI-1000 Ljubljana, Slovenija; e-mail: nina.rman@geo-zs.si

Prejeto / Received 28. 4. 2010; Sprejeto / Accepted 18. 5. 2010

Ključne besede: geologija, osnovna šola, učna delavnica, petrologija, mineralogija, paleontologija, hidrogeologija, poskus

Key words: geology, primary school, learning workshop, petrology, mineralogy, paleontology, hydrogeology, test

Izvleček

Sistematičnega poučevanja geologije v osnovni in srednji šoli v Sloveniji (še) ni. V osnovni šoli so geološke teme razdrobljene med več predmetov in razredov, zato jim je več pozornosti namenjene le v primeru izvajanja izbirnega predmeta ali geološkega krožka. S pomočjo Geološkega zavoda Slovenije že nekaj let uspešno izvajamo delavnico za osnovnošolce, ki je namenjena popularizaciji geologije. Z njo se učenci seznanijo s prepoznavanjem kamnin, mineralov in fosilov ter z lastnostmi vode.

Abstract

Systematical teaching of geology is (yet) not established in primary and secondary school in Slovenia. In primary school, geological topics are divided among numerous subjects and levels therefore they receive more attention only if alternative courses or geological circles are realized. With help of the Geological Survey of Slovenia we have been successfully performing a geological workshop for primary school pupils aiming to popularize geology. With it pupils are acquainted with methodologies for identification of rocks, minerals, fossils and properties of water.

Uvod

Spoznavanje geologije v osnovni šoli v Sloveniji je razdrobljeno med več predmetov (Majcen, 2003), geološke vsebine pa se izvajajo tudi v nekaterih Centrih šolskih in obšolskih dejavnosti. Prve informacije o kamninah in mineralih učenci pridobijo v 6. razredu pri naravoslovju, nadaljujejo v 7. razredu pri geografiji (vulkani, potresi, kras), v 8. razredu pri geografiji (tektonika, rude, podzemne vode) in biologiji (fosili) ter v 9. razredu pri geografiji Slovenije (kamnine, kras, geološka karta, tektonika). Zaradi uvrstitve v tretjo triado se zanimanje in sposobnost opazovanja narave učencev predolgo zanemarja, medtem ko nesistematično podajanje snovi otežuje nadgrajevanje že doseženega geološkega znanja. Kjer v učni literaturi obstaja neusklajena in neprimerna raba geoloških terminov (Popit, 2005), bi jo morali na podlagi obstoječega Geološkega slovarja (Pavšič, 2006) odpraviti. Za primerjavo naj omenim, da se v Mednarodni OŠ Danile Kumar v Ljubljani že učenci 2. razreda pri temi *How the world works* seznanijo s kamninami in minerali, njihovim nastankom in uporabo, v 5. razredu pri spoznavanju evolucije pa s fosili (Internetni vir 1).

Predstavitev geologije je v veliki meri prepuščena iznajdljivosti in razgledanosti učiteljev, ki se pogosto ne čutijo dovolj strokovno podkovani za uporabo praktičnih pripomočkov (npr. zbirk kamnin in mineralov, pH metra) ali nimajo znanja za prikaz določenih geoloških pojavov.

Namen predstavljene delavnice je pokazati, da lahko s preprostimi metodami in relativno poceni pripomočki opazujemo, poskušamo in določamo najrazličnejše naravne snovi. Primerna je za osnovne šole brez geoloških krožkov, a tudi takim morda poda kakšno idejo. Služi kot dopolnilo rednega pouka in izkustveno sredstvo za spoznavanje pestrosti narave.

Izvedba delavnice

Delavnica je primerna za učence od 3. do 9. razreda osnovne šole, pri čemer se zahtevnost nalog in razlaga opazovanih pojavov prilagodi njihovi sposobnosti. Zasnovana je tako, da jim približa delo terenskega geologa, torej osnove petrologije, mineralogije, paleontologije in hidrogeologije. Za izvedbo potrebujemo dovolj vzorcev kamnin, mineralov in fosilov ter nekatere tehnične pripomočke (10% raztopino HCl, povečevalna stekla, pH lističe, pH meter, merilec prevodnosti vode ipd.). Delavnico lahko izvedejo učitelji sami, zaradi razpolaganja s primernimi vzorci in drugo opremo pa

je priporočena prisotnost študentov geologije ali geologov. Trenutno delavnico izvajamo pod okriljem Geološkega zavoda Slovenije in s pomočjo študentov geologije, ki tako opravijo del študijske prakse. Izvedenih je bilo že 15 delavnic na osmih šolah, od tega 3 v angleškem jeziku na mednarodni šoli v Ljubljani.

Namen geološke delavnice je, da učenci osvojijo osnovne pojme o poimenovanju in določanju kamnin, mineralov in fosilov ter postanejo pozorni na kvaliteto pitne vode. Metode dela so opazovanje, primerjanje, opisovanje, merjenje, itd., opažanja pa učenci vpisujejo na delovne liste. Poudarek je na neformalnem podajanju snovi in subjektivnem izkustvu, saj tako učenje poteka lažje in boljše.

Na začetku delavnice učence seznanimo z osnovnimi terenskimi pripomočki geologov, izmed katerih nekatere kasneje uporabijo za reševanje nalog. Vsekakor pokažemo posebno oblikovano geološko kladivo, lupe z različno povečavo, geološko karto (Buser & Draksler, 1999), geološki kompas in varnostno opremo (očala, rokavice, čelada) ter kako se ravna z nabranimi vzorci. Po predstavitvi učenci, razdeljeni v štiri skupine, spoznavajo posamezni tematski sklop, npr. 20-30 minut za vsakega. Zadnjih 20 minut delavnice namenimo utrjevanju opazovanega. Učenci naj skupaj ali po skupinah kritično razmišljajo o novih spoznanjih, pri čemer jih usmerjamo z vprašanji, kot so:

- Kako vemo, da je vzorec stalagmit in ne stalaktit?
- Razvrsti kamnine po številu in velikosti mineralov,
- Kateri mineral reagira s kislino, ali razi steklo, ali je magneten?
- Kateri deli organizmov se pri fosilih največkrat ohranijo?
- Kako se obarva indikatorski papir v kisli in kako v alkalni raztopini?

Petrologija

Osnovno delo geologa je prepoznavanje kamnin, zato za delovni sklop o petrologiji potrebujemo vsaj 10 različnih vzorcev kamnin. Predstavljajo naj vse glavne skupine, torej magmatske, metamorfne in sedimentne kamnine. Naslednji predlogi so kamnine, ki jih lahko naberemo v Sloveniji. Magmatske globočnine predstavljata granodiorit ali tonalit s Pohorja, predornine andezit s Smrekovca ali keratofir z Jezerskega, žilnine pa pegmatitne ali aplitne žile v tonalitu. Metamorfni gnajs in skrilavec najdemo v okolici Črne na Koroškem, medtem ko blestnik na Pohorju. Sedimentne kamnine so v Sloveniji zelo dostopne. Apnenec s fosili je zanimiv na Krasu, dolomit je tipičen v Baški grapi, klastične kamnine kot npr. muljevec in peščenjak na Obali ali v Halozah, breča v Dovžanovi soteski in konglomerat v terasah ob reki Savi. Določenih kamnin, npr. bazaltne lave, obsidiana in plovca, v Sloveniji ni. Zato jih kupimo na sejmu ali naprosimo kamnoseka za ostanke pri izdelavi okenskih polic, nagrobnih kamnov ali tlakovcev.

Vsak vzorec kamnine naj bo opremljen z imenom in vrsto nastanka (npr. apnenec, sedimentna kamnina). Kamnine se makroskopsko razlikujejo predvsem po barvi in strukturi, učenci pa naj spoznajo tudi njihove druge fizikalno-kemične lastnosti. Opišejo naj barvo, specifično težo, hrapavost, odpornost proti lomljenju, število mineralov, njihovo obliko in velikost. Preverijo naj ali kamnina plava na vodi, vsebuje fosile in reagira z 10 % raztopino HCl.

Barvo kamnin in mineralov učenci določijo subjektivno (npr. temno zelena), v kolikor pa je na voljo Munsellova barvna karta (Boulder, 1995) naj učenci višjih razredov poskusijo določiti vsaj en vzorec po karti. Pomen barvne karte je v njeni objektivnosti, saj so barve standardizirane glede na ton, nasičenost in svetlost. Specifično težo vzorca je najpreprosteje določiti s subjektivnim 'tehtanjem' na roki in primerjanjem z drugimi vzorci, kajti izrazito lahki vzorci (plovec) in težki vzorci (cinabarit, galenit) jasno odstopajo. V kolikor je na razpolago dovolj časa, se lahko izvede preprost poskus z newtono metrom (Farndon, 2007, str. 47). Število mineralov v kamnini učenci določijo okvirno, glede na količino različno obarvanih zrn (npr. bela, zelena, črna), pri čemer kot obliko opišejo: okrogla, oglata, 6-kotna, ipd. Pri velikosti zrn ponudimo možnosti: zrna niso vidna (steklena osnova kot pri obsidianu in plovcu, ali pa so mikroskopska), enako ali različno velika (izmerijo, podajo razpon). Razredčena kislina HCl reagira le s kalcitom, zato so šumenje in mehurčki dokaz, da kamnina vsebuje mineral kalcit. Burna reakcija je značilna za apnenec, manj burna za laporovec. Ker kislina poškoduje sluznico in draži kožo, naj z njo ravnajo le odrasli. Shranjena mora biti v kapalki, na vzorec nanešena previdno in po oceni reakcije obrisana s papirnato brisačko.

Poleg opisovanja kamnin poudarimo pomen njihovega pravilnega in sistematičnega zbiranja. Učence spodbudimo, da za izbran vzorec napišejo kartotečni listič za zbirko, ki mora vsebovati podatke o: zaporedni številki vzorca, imenu in tipu kamnine, lokaciji najdišča, geološki starosti kamnine, kdaj in kdo je našel vzorec ter opis morebitnih posebnosti.

Mineralogija

Zbirko lahko učenci ustvarijo tudi z minerali, a najprej morajo le-te med seboj ločevati. Tudi pri tej skupini potrebujemo vsaj 10 različnih, dovolj velikih (vsaj 1–2 cm) in ne dragocenih vzorcev. Zaradi barve in sijaja priporočam pirit in galenit, zaradi barve črte na porcelanu realgar, kuprit, malahit in baker, zaradi specifične teže cinabarit, zaradi trdote lojevec, halit (kameno sol), fluorit, ortoklaz, kremen in korund, zaradi prosojnosti sadro in muskovit, zaradi reakcije s kislino pa kalcit. Kot primer organskega minerala služi jantar, ki plava v slani vodi, se ob drgnjenju naelektri in ob gorenju sprošča dišeč vonj po iglavcih.

Preprosto določljive so naslednje fizikalne lastnosti mineralov: magnetnost, specifična teža in tr-

dota. Tudi optične lastnosti, kot so barva, barva črte na porcelanu, prosojnost in sijaj, so primerne za opisovanje. Seveda vedno poskusijo reakcijo minerala s kislino.

Magnetnost učenci dokažejo, če se vzorec in magnet privlačita. Trdota mineralov je opisana s primerjalno Mohsovo lestvico. Za okvirno določanje trdote zadostujejo bakren kovanec, steklena ploščica, (svoj) noht in kristal kremena. Najprej poskusijo ali noht, kovanec in kremen razijo vzorec ter ali vzorec razi stekleno ploščico. V prvem primeru je trdota največ 2, v drugem 3, v tretjem 7, če pa vzorec razi steklo ima trdoto 7 in več. Vzorce razijo tudi med seboj, vedno domnevno mehkejšega s tršim. Na podlagi ugotovitev jih razvrstijo od najmehkejšega do najtršega. Barva črte na porcelanu je pomembna, ker je enoznačna tudi za različno obarvan mineral. Določijo jo tako, da po njem podrgnejo z vzorcem. Za porcelan lahko uporabimo keramične električne izolatorje, nebrušen del porcelanastih stenskih ploščic ali kuhinjskega porcelana. Mineral opišejo kot prozoren, če skozenj vidijo (berejo) ne glede na njegovo debelino. Prosojen preseva svetlobo, skozenj pa vidijo le, kadar je dovolj tanek. Skozi neprosojne minerale ne vidijo. Pri sijaju je dovolj, da razlikujejo med očitnimi: steklast, kovinski, peščen, masten,…

Minerali so zaradi značilnih pojavnih oblik in barv zelo primerni za urejanje v zbirke, zato učence seznanimo, da mora dobra zbirka za vsak vzorec posebej vsebovati podatke o: zaporedni številki vzorca, imenu in mineralni skupini, njegovi kemijski sestavi, nahajališču in imenu formacije v kateri je najden, kdaj in kdo ga je našel ter opis morebitnih posebnosti.

Paleontologija

Še bolj kot bleščeči minerali učenčevo domišljijo burijo fosilizirani organizmi. Zelo težko jim bomo pokazali prave dinozavrove stopinje, a kakšna kost paleolitskega medveda ali zob morskega psa sta prav tako zanimiva. Za ta sklop torej potrebujemo vsaj 10 primerkov fosilov v različnih sedimentnih kamninah. Morda jih naberemo in določimo sami (pri čemer ne ropamo zaščitenih najdišč in redkih fosilov!!!), najlaže pa se je z njimi oskrbeti na sejmih. Izmed fosilov izberemo različne preseke školjk, polžev, amonitov, koral, morskih lilij,… Zanimivi so tudi planktonski organizmi, foraminifere, alge, mahovi in drevesni listi v lehnjaku ter najrazličnejši deli rastlin v premogu. Pokažemo lahko tudi ihnofosile oz. sledove življenja (ostanki lazenja, hoje, prehranjevanja), jantar z ujetimi žuželkami in dendrite/psevdofosile/lažne fosile (mineralne tvorbe podobne fosilom). Za primerjavo naj kakšen vzorec vsebuje mikrofosile (vidni le z lupo), preostali pa naj bodo dovolj veliki za opazovanje.

Pri vzorcih je pomembno, da poleg imena fosila napišemo tudi vrsto kamnine. S tem učenci spoznajo, da se fosili nahajajo v raznovrstnih sedimentnih kamninah ter da so apnenci v Sloveniji najpogostejši nosilci fosilov in izredno različnega videza. Učenci določijo vrsto fosila, življenjsko okolje organizma, starost kamnine ter ostale lastnosti fosila (velikost, barvo, prerez, hrapavost, reakcijo s kislino) ter kamnine (barvo, hrapavost, reakcijo s kislino).

Vrsto fosila določijo na podlagi oblike, velikosti in ohranjenosti lupine. Ločujejo med odtisom oz. kamenim jedrom (ohranjen odtis notranje ali zunanje lupine), lupino, sledovi fosilov (oblika kaže na lazenje, plazenje ipd.), inkrustacijo (organizmi so prevlečeni s skorjo – lehnjak), … Za velikost izmerijo njegov najdaljši presek. Za lažjo predstavo naj uporabijo priročnike, ki prikazujejo fosile (Pavšič, 1995).

Namen te skupine je, da učenci spoznajo enkratnost in neponovljivost fosilov ter njihovo vlogo za določanje starosti kamnin in življenjskega okolja (Bavec, 1999). Poudarimo tudi pomen njihove ohranitve za naravno dediščino. Zbirka mora vsebovati podatke o: zaporedni številki vzorca, vrsti in rodu fosila, njegovi starosti, natančnem opisu nahajališča, kamninski formaciji, času najdbe in najditelju ter morebitne posebnosti.

Hidrogeologija

Ko učenci izvedo, da se geologi ukvarjamo tudi z raziskovanjem (podzemne) vode, so nemalokrat presenečeni. Vendarle pa je zaradi zanimive metodologije dela hidrogeološka skupina običajno najbolj priljubljena. Na voljo naj bodo vzorci vode, ki se uporablja v gospodinjstvu in je nenevarna za zdravje. To so npr. slana in sladka voda, voda s sodo bikarbono, voda s citronko, alkoholni ali jabolčni kis, voda iz pipe, deževnica, snežnica ali destilirana voda ter nekaj pijač, tudi gaziranih (npr. voda z limono, ledeni čaj, kokakola, fanta, jabolčni sok). Dodamo tudi neoznačen vzorec (enak enemu izmed označenih), ki ga učenci s pomočjo rezultatov preostalih testov določijo sami.

Učenci sprva opišejo vonj, barvo in motnost vzorca, in če je le mogoče še okus. Sledi določanje temperature, elektroprevodnosti in kislosti vzorca. Zadnja dva parametra glede na razumevanje določijo z različno natančnostjo (indikatorski lističi, pH meter).

Vonj določijo kot: brez vonja, oster, dišeč, ‘po kisu’,… Barva in motnost sta subjektivni oceni, opozorimo pa na vpliv debeline kozarca. Določanje okusa je izredno dobro sprejeto, a se zaradi velikega števila učencev le redko izvaja. Ker so nekatere raztopine in alkoholni kis izrazitega okusa, učence izrecno opozorimo, da vzorcev ne pijejo ter usta poplaknejo s pitno vodo. Temperaturo vode merijo sočasno s prevodnostjo raztopine, saj sta obe vrednosti podani na merilcu elektroprevodnosti vode. Visoka prevodnost vzorca kaže na veliko raztopljenih snovi (elektrolitov). Manj natančen, a nič manj zanimiv je poskus penjenja milnice (Internetni vir 2). V posamezno epruveto nalijemo nekaj centimetrov vzorca (volumen oz. višina naj bo v vseh epruvetah enaka) in vanjo dodamo po eno kapljico detergenta za pomivanje posode. Epruveto zamašimo, učenci pa jo stresejo in iz-

merijo višino pene. Višja kot je pena vzorca, manj raztopljenih snovi vsebuje oz. mehkejša je voda. Najpomembnejši pojem, ki ga učenci osvojijo pri tem sklopu je kislost vzorca. Tisti, ki še niso seznanjeni s pojmom pH, naj za določanje kislosti uporabijo indikatorske lističe s pripadajočo skalo. Najprej določijo barvo lističa, zatem iz barvne skale odčitajo vrednost pH. Tisti, ki pojem kislosti in alkalnosti vode že poznajo, lahko uporabijo pH meter, s čimer vrednost pH določijo zelo natančno, in jo primerjajo z natančnostjo določitve z barvnimi indikatorji. Pri meritvah poudarimo, da je za pitje priporočljiva nevtralna pijača, medtem ko imajo gazirane pijače običajno zelo nizek pH.

Diskusija

Opisana delavnica je nastala na željo učiteljice razrednega pouka, ki je hotela svojim učencem pokazati kamnine iz učnega načrta. Z njo učence seznanimo s štirimi pomembnimi vejami geologije: petrologijo, mineralogijo, paleontologijo in hidrogeologijo. S prikazom 'osnovnega znanja in delovanja' geologov se poznavanje geologije kot véde širi in popularizacija lahko le pozitivno pripomore k spoznavanju njenega pomena za raziskovanje in ohranjanje naravnega okolja.

Preproste raziskovalne metode ter dostopni pripomočki so primerni, da jih učenci uporabijo pri svojem raziskovanju tudi kasneje. Zahtevnost opazovanja pri posameznem sklopu je potrebno prilagoditi starosti in znanju učencev. Na podlagi izkušenj menim, da je pri mlajših najbolje spodbujati subjektivno opisovanje lastnosti. Če opišejo plovec kot *lahek luknjičast bel kamen, ki plava na vodi in ne reagira s kislino* ter ga narišejo, si ga takorekoč za vedno zapomnijo. Nasprotno so učenci zadnje triade sposobni bolj kritičnega in natančnega razmišljanja, zato jih motivira znanstveno opisovanje kot *lahka kamnina bele (5 B 9/1) barve s stekleno osnovo, plava na vodi zaradi nepovezanih por in ne reagira s kislino, ker ne vsebuje kalcita*. Spodbujati je potrebno tudi uporabo priročnikov, s katerimi lahko določijo npr. starost fosila (Pavšič, 1995), vrsto minerala (Vidrih & Mikuž, 1995), ipd. Pri hidrogeološki skupini spodbudimo razmišljanje o kemijski sestavi vzorcev, tako da na kozarce napišemo kemijske formule raztopljenih snovi in z danimi vzorci prikažemo mehčanje vode ter preproste reakcije nevtralizacije. Poleg predstavljenih poskusov je na voljo še veliko drugih, ki ponazarjajo različne mineraloške pojave, kot so npr. raztapljanje apnenca v kokakoli/vodi iz pipe, sedimentacija tal v kozarcu za vlaganje, izdelava 'sobnega vulkana' (Internetni vir 3), rast minerala iz raztopine (Bavec, 1998). Če je na voljo dovolj časa, jih lahko tudi vključimo v delavnico.

Največjo težavo pri izvedbi delavnice običajno predstavljajo primerni in raznoliki geološki vzorci. Kot omenjeno, jih z malo angažiranosti naberemo sami v naravi ali kupimo na sejemskih dogodkih (marčevska Collecta v Ljubljani, majski MINFOS v Tržiču, novembrski Mineralien Tage v Münchnu) ali pa se obrnemo na kamnoseke. Velikost delavnih skupin je posledično omejena predvsem s številom vzorcev za opazovanje. Za optimalen potek delavnic je priporočljivo 5 učencev na skupino. Seveda jih je lahko tudi več, a v tem primeru naj ima vsaka skupina svojega demonstratorja.

Zaključek

Na mladih svet stoji, zato je pomembno, da učenci spoznajo pomen geologije za vsakdanje življenje. Naj izvedo, kdo rešuje probleme s plazenjem zemljin, iskanjem mineralnih surovin, razlago okamenelih školjk ali upravljanjem s pitno vodo. Če bodo prepričani o enkratnosti geoloških pojavov, geološkem bogastvu Slovenije in pomenu njihovega varovanja, bo cilj delavnice izpolnjen. In kdo ve, morda kateri izmed učencev postane geolog(-inja).

Literatura

Bavec, M. 1999: Kamnine skrivajo okamnelo življenje. Otrok in družina (Ljubljana) 3: 46–47.

Bavec, M. 1998: Jajce je podobno jajcu. Ali je tudi kamen podoben kamnu? Otrok in družina (Ljubljana) 10: 46–47.

Boulder, 1995: Rock-color chart with genuine Munsell color Chips. Geological Society of America.

Buser, S. & Draksler, V. 1999: Geološka karta Slovenije – Šolska karta 1 : 500 000. Geodetski zavod Slovenije in Založba Mladinska knjiga (Ljubljana).

Farndon, J. 2007: The Complete Guide to Rocks & Minerals. Anness Publishing 1–256.

Majcen, T. 2003: Geologija v osnovnošolskih programih. V: Horvat, A. (ed.): Geološki zbornik 17, OG NTF (Ljubljana): 110–115.

Pavšič, J. 1995: Fosili, Zanimive okamnine iz Slovenije. Tehniška založba Slovenije (Ljubljana): 1–139.

Pavšič, J. (ed.) 2006: Geološki terminološki slovar. Založba ZRC, ZRC SAZU (Ljubljana): 1–331.

Popit, S. 2005: Geologija v šoli. V: Horvat, A. (ed.): Geološki zbornik 18, OG NTF (Ljubljana): 100–103.

Vidrih, R. & Mikuž, V. 1995: Minerali na Slovenskem. Tehniška založba Slovenije (Ljubljana): 1–379.

Internetni vir 1: dostopno 1. 4. 2010 na: http://en.os-danilekumar.si/

Internetni vir 2: dostopno 1. 4. 2010 na: http://www.osbos.si/e-kemija/e-gradivo/6-sklop/trdota_vode.html

Internetni vir 3: dostopno 1. 4. 2010 na: http://spikesworld.spike-jamie.com/science/liquids/index.html; http://pages.interlog.com/~wrenfolk/edu_exp.html; http://ga.water.usgs.gov/edu/mearth.html; http://www.earth.ox.ac.uk/~oesis/micro/index.html; http://spikesworld.spike-jamie.com/science/geology/index.html

GEOLOGIJA *53/1*, 97–102, Ljubljana 2010

Woher stammt das Wort Leibach?

Od kod izvira beseda Leibach?

What is the origin of the word Leibach?

Alfred KATSCH

Prejeto / Received 31. 3. 2010; Sprejeto / Accepted 23. 5. 2010

Müselter Weg 76, D-52080 Aachen

Schüsselwörter: Herkunft und Bedeutung des Wortes Leibach, Sprachentwicklung des Wortes Ljubljana, Bronzezeit und Mittelalter in Europa, Abbau und Verwendung von Sedimentgesteinen (Schiefer, Sandstein und Kalkstein), Lei (= Schiefer, Stein und/oder Fels).

Ključne besede: Izvor in pomen besede Leibach, jezikovni razvoj besede Ljubljana, Bronasta doba in srednji vek v Evropi, pridobavanje in uporaba sedimentnih kamnin (skrilavec, peščenjak in apnenec), Lei (=skrilavec, kamen in/ali skala).

Key words: Origin and meaning of the word Leibach, Linguistic development of the word Ljubljana, Bronze Age and Middel Ages in Europe, Quarry and use of sediment rock (schist, sandstone and limestone), Lei (=schist, stone and/or rock).

Zusammenfassung

Die Hauptstadt **Ljubljana** (Römische Kolonie Aemona Julia, Laybacum, Laibacensis, Labacensis, Lungan, Leibach, Luwigana/Lubigana und Lublana) trug in ihrer langen Geschichte einige Namen. In der deutschen Ausgabe des Stadtführers von Ljubljana wird auf das deutsche Wort **Leibach** hingewiesen. Der Name taucht von 1122 bis 1125 in den historischen Schriften der Stadt auf.

Die ersten Ansiedler aus den deutschen Ländern kamen in den südlichen Raum der Karawanken zur Merowinger- und Karolingerzeit (ca. 450 bis 900 nach unserer Zeitrechnung). Sie wanderten möglicherweise von dem Sprachgebiet Westfalen/Rheinland oder eventuell von dem Sächsischen Erzgebirge zu.

Das deutsche Wort Leibach setzt sich aus zwei Wörtern zusammen, nämlich aus „Lei“ und „Bach“ (=slowenisch: potok). Das erste Wort stammt von dem im Rheinland benutzten Wort Lei, das sich nach dem neuesten Kenntnisstand vom keltischen Wort „Ley“ ableitet. Die Bedeutung des niederdeutschen Wortes Lei haben die Gebrüder Grimm im 19. Jahrhundert ins Hochdeutsch übertragen. Danach bedeutet diese alte rheinische mundartliche Bezeichnung in Hochdeutsch „Schiefer“ (skrilavec), Stein (kamen) und Fels (skala). Die wortwörtliche Übersetzung des deutschen Wortes **Leibach** in die slowenische Sprache bedeutet schlicht und einfach „**skrilavec ob potoku**“.

Das rheinische Wort Lei lokalisiert und beschreibt hier nur eine Landfläche mit anstehenden Gesteinen (Schiefer, Stein und Fels = Lei) im Verlauf eines kleineren oder größeren Baches **(Leibach)**. Demgemäß entspricht die Bezeichnung Leibach exakt der allgemeinen Vorstellung des alten rheinischen Wortes Lei. Es wäre durchaus möglich, dass die ersten Einwanderer deshalb aus dem Bereich der Gemeinde Halle in Westfalen stammten, die der damaligen Siedlung Lubigana den deutschen Namen Leibach aufgrund der ähnlichen Gesteinsvorkommen aus ihrer alten Heimat gaben.

Izvleček

Prestolnica **Ljubljana** (rimska kolonija Aemona Julia, Laybacum, Laibacensis, Labacensis, Lungan, Leibach, Luwigana/Lubigana in Lublana) je bila poimenovana v njeni dolgi zgodovini z večimi imeni. Nemška izdaja mestnega vodiča za Ljubljano omenja nemško besedo **Leibach**. Ime se pojavi v letih od 1122 do 1125 v pisanih listinah.

Prvi naseljenci iz nemških dežel so prišli na južni prostor Karavank v merovinško-karolinški dobi (med leti 450 in 900 našega štetja). Raziskave kažejo, da so prispeli iz Vestfalije, Porenja ali morda iz saškega Rudogorja.

Nemško ime Leibach je sestavljeno iz dveh besed, in sicer „Lei“ in „Bach“ (= potok). Prva beseda prihaja iz Porenja in izvira po novejših dognanjih iz keltske besede „Ley“. Pomen besede Lei iz dolnjenemškega jezika sta prevedla brata Grimm v 19. stoletju. Po njima pomeni ta stara označba v visokonemškemu jeziku Schiefer (skrilavec), Stein (kamen) in Fels (skala). Dobesedni prevod nemške besede Leibach torej pomeni v slovenščini preprosto **skrilavec ob potoku**.

Beseda (Leibach) v Porenju označuje in opisuje pokrajino, kjer je razkrita sedimentna kamnina (=Lei) ob strugi manjšega ali večjega potoka (=Bach). Potemtaken ime **Leibach** dobro ustreza pomenu stare besede iz Porenja. Zato je, morda tudi mogoče, da prvi tukajšni nemški naseljenci izvirajo iz sedajne občine Halle v Vestfaliji, in da so poimenovali takratno naselje Lubigana z nemškim imenom glede na podobne sedimentne kamnine kakor v njihovi stari domovini.

Summary

The capital of Slovenia **Ljubljana** (Roman colony Aemona Julia, Laybacum, Laibacensis, Labacensis Lungan, Leibach, Luwigana/Lubigana, and Lublana) was known under several names during its long history. In German version of the guide-book of Ljubljana the German name **Leibach** is mentioned. The name occus from 1122 to 1125 in historic documents of the town.

The first settlers from German lands come to the southern region of the Karawanken Mountains during the Merowingian/Karolingian times (450 to 900 of our counting). They arrived possibly from the West-falian respectively Rheinlandian language area, or eventually from the Saxonian Ore Mountains.

The German expression Leibach consists of two elements, namely of the words „Lei" and „Bach"= brook (=in Slovenian: potok). The first word could originate from the term „Lei", used in Rheinland and derived according to newer understanding from the Celtic word „Ley". The meaning of the Lower German word „Lei" was transferred by the Grimm brothers in 19th century into the High German. Accordingly, this old Rhenan dialectal term means in High German Schiefer, (schist), Stein, (stone) and Fels (rock). The word-to-word translation of the German word **Leibach** in the Slovenian language means simply „**skrilavec ob potoku**", "shale at the brook".

By the Rhenan word „Lei" here only a locality with exposed rocks, Gesteinen (schist, stone and rock = Lei), along the course of a smaller or larger Bach – creek or brook – (**Leibach**) has been localized und described. In this sense the term Leibach corresponds exactly to the general idea of the old Rhenan word „Lei". It could have been possible that the first immigrants to this area originated in the Halle community in Westfalia, and that they gave the ancient settlement of Lubigana the German name Leibach owing to outcrops of the rocks similar to those in their old country.

Einleitung

Die Menschen des Mittelalters breiteten sich im Allgemeinen immer weiter von dem Mittelpunkt ihres Ursprungsgebietes aus und drangen nach und nach immer tiefer in die unbekannten europäischen Urwälder hinein, um sie sich für ihr Siedlungswerk dienstbar zu machen (Knochenhauer, 1928). An der neu gegründeten Niederlassung und in der näheren Umgebung rodeten sie die Wälder, um brauchbares Ackerland zu gewinnen. Weiter untersuchten sie dann besonders im Winter entlang der Fluss- und Bachsysteme der weiteren Gegend nach verborgenen Erzen in anstehenden Gesteinen [daher Bezeichnung wie Bleibach (= svinčeni potok), Silber- (srebrni-), Goldbach (zlati-) und Schwarzbach (črni potok) und in verschiedenen Gesteinsarten Kalkbergweg (pot na apnenčev hrib), Leiberg (skrilavi hrib) und Leienfels (skrilava skala)]. Die Siedler bezeichneten die erschlossene Landschaft auch nach den in freier Wildbahn angetroffenen Tieren [Hirsch- (jelenov-) und Fischbach (ribji potok)] und nach Früchten [Brombeerbach (robidniški potok) und Kastanienhain (kostanjev gaj)]. Die ersten Ansiedler benannten somit alle wichtigen morphologischen Standorte ihrer neuen Umgebung mit eigenen, mitgebrachten Begriffen aus der alten Heimat. So erhielten viele Orte, kleine Siedlungen und bedeutende Mineral-Fundpunkte nach oben genannten Kriterien ihren neuen Lokal-Namen. Als Beispiel soll das Wort „Buche" (bukev) dienen: Buchenbach (-potok), Buchenwald (- gozd), Buchenberg (- hrib). Die ältesten Orts- und Flurnamen beschreiben somit die Eigenart der Landschaft (z. B. Schlesien, Steiermark und Tirol), die geographische Lage der Ansiedlung (Rheinland-Pfalz) sowie die gefährlichen Orte z. B. Teufelsgraben (hudičev jarek) und die besten sonnigen Wachstumslagen für den Weinanbau z. B. Goldener Hügel (zlati grič). Diese ältesten Beschreibungen von Orts- und Flurnamen werden urkundlich aus dem Mittelalter datiert. Die Schreibweise der einzelnen alten Lokal-Namen ist nicht immer einheitlich. Die Übersetzung der einzelnen Worte in die slowenische Sprache erfolgt nach Tomšič (1964) und Anonym (2009).

In den Sagen und Märchen aller europäischen Völker des früheren Mittelalters gibt es reichliche Hinweise auf die Völkerwanderungen, Erzählungen mit tragischem Ende, Geschichten über Gold- und Silberschätze (Erzbergbau) sowie Beschreibungen der Schmiedearbeiten (Metallkunst). Es wird angenommen, dass die ersten in Deutschland tätigen Bergleute Fremdleute waren. Sie werden als kleine, schmale Personen beschrieben, weil nur sie sich in den im Querschnitt sehr eng angelegten Schächten und Stollen bewegen konnten. Diese Bergleute kamen wahrscheinlich in der Bronzezeit aus Spanien, England oder aus dem Alpenraum. Sie finden sich in den Märchen-Figuren wieder wie z. B. die sieben Zwerge in Schneewittchen (Quiring, 1929, 1935).

Überall da, wo die Natur der Erzvorkommen (besonders im späteren 13. und 14. Jahrhundert) eine lohnende und längere Betriebsdauer beim Abbau verschiedener Bodenschätze versprach, beriefen die Landesfürsten die Bergleute aus dem Ausland ein. Solche Ansiedlungen standen sehr schnell im Mittelpunkt der Einwanderung und beschleunigten den Reichtum der mächtigen Landesfürsten sowie das Wachstum der Bevölkerung (Kirnbauer, 1941; Quiring, 1941).

Vorläufige Auswertung der erzielten Ergebnisse

Die günstige geographische und geopolitische Lage der heutigen Hauptstadt Ljubljana als Siedlungsgebiet (Aemona Julia, Luwigana/Lubigana, Lungan, Leibach, Laibach, Laybach, Laybacum, Laibacensis, Labacensis und Lublana) bot in ihrer langen Geschichte den Bewohnern einen sicheren Standort, allgemeine Bürgerrechte mit zusätzlichen Freiheiten und schwunghaften Handel mit den Nachbarländern. Das Stadtgebiet ist aber auch als Naturkatastrophengebiet in die Geschichte eingegangen: mehrere stärkere Erdbeben (Vidrih, 2009), zwei verheerenden Pestepidemien mit mehreren tausend Toten (1006 und 1586), Großbrände in den Jahren 1511 und 1548 sowie am 28. April 1680 eine furchtbare Explosion des Pulverturmes (500 Zentner Schwarzpulver) mit

furchtbaren Folgen für die Bevölkerung (Vrhovec, 1886).

In der Siedlung **AEMONA JULIA** – so hieß die Hauptstadt des heutigen Sloweniens im Römischen Reich vom 1. bis 5. Jahrhundert nach unserer Zeitrechnung – benutzten die Römer bereits die Sandsteine des Karbons als Bausteine. Nach Schmid (1913) soll sich der Steinbruch am Schlossberg hinter dem Rathaus der Stadt Ljubljana befunden haben und Vrhovec (1886) berichtet nach einem Gerichtsprotokoll (1548, Fol. 98), dass dieser Steinbruch bis 1548 in Betrieb war. Die benötigten Kalksteine wurden in der Umgebung von Golovec (Kahlenberg) sowie in Podpeč gebrochen und auf dem Laibach-Fluss (Ljubljanica) in die Stadt gebracht. Der Ort Podpeč liegt ca. 11 km südwestlich von Laibach am südlichen Rand des Laibacher Moores.

Die erste deutsche Bezeichnung **Laibach** soll im Jahr 1144 erfolgen und der slowenische Name Lu**w**igana wird zwei Jahre später registriert (Anonym, 1990). Dagegen gibt Vrhovec (1886: 6) aber den slowenischen Namen als Lu**b**igana an. Die weitere sprachliche Entwicklung dieses slowenischen Namens wird in der topographischen Karte von Valvassore (1539) als **Lublana** festgehalten und entspricht beinahe heutiger Schreibweise. Die Originalarbeit von Vavassore ist nicht zugängig, deshalb näheres bei Korošec (1978: 30). Wie bereits oben erwähnt, ist die Schreibweise der Ortsnamen und Jahreszahlen in der Literatur oft nicht immer identisch. So heißt das südöstliche Hochland von Ljubljana (ca. 420 m ü. NN) zuerst „Volone“, später im 16/17 Jahrhundert „Volovec-Berge“ (Freudenberg) und im 18. Jahrhundert erfolgt eine Veränderung mit heutiger Bezeichnung „Golovec“ (Kahlenberg). Den Grund für diesen „schnellen“ Wandel des Namens in der „kurzen“ Zeit teilt Vrhovec (1886) nicht mit.

Im Stadtführer von Ljubljana wird auf den deutschen Namen **Leibach** hingewiesen, der von 1112 bis 1125 in den historischen Schriften der Stadt auftaucht, aber ohne zusätzliche Erklärung zu den folgenden Fragen: Woher stammt denn die deutsche Benennung der heutigen Hauptstadt Sloweniens und welche Bedeutung verbirgt sich eigentlich dahinter? Woher sind die Menschen in die Gegend von Ljubljana gekommen? Da diese Fragen bis heute anscheinend in Slowenien nicht geklärt sind, ist es angebracht, diesen interessanten Fragen nachzugehen. Diese Fragen sind erst teilweise in der Brockhaus Enzyklopädie (Anonym, 1990) erläutert worden. Sie können aber mit Hilfe der allgemeinen geologischen Begriffe weiter erforscht und teilweise begründet werden. Über die geschichtliche Entwicklung der Siedlungen, Märkte und Städte auf dem heutigen slowenischen Staatsgebiet wird auf die Arbeit von Kosi (2009) verwiesen.

Das deutsche Wort Leibach (auch L**ey**bach, L**ai**bach und L**ay**bach) setzt sich aus zwei Wörtern zusammen, nämlich aus „Lei“ und „Bach“ (slowenisch: potok). Das erste Wort stammt von dem im Rheinland benutzten Wort **Lei**, das sich nach dem neuesten Kenntnisstand vom keltischen Wort „**Ley**“ ableitet. Die Bedeutung des niederdeutschen Wortes Lei haben die Gebrüder Grimm (1984b) ins Hochdeutsche übertragen. Danach bedeutet diese alte rheinische mundartliche Bezeichnung in Hochdeutsch Schiefer (skrilavec), Stein (kamen) und Fels (skala). Quiring (1932) mahnt zur vorsichtigen Deutung der bergmännischen Ausdrucke Ley und/oder Lei, weil die Bezeichnung „Leyer“ (=Gesteinshauer, Gesteinsbergmann) sowohl im Dachschieferbergbau als auch bei der ältesten Basaltlavagewinnung vor 5000 Jahren in Mayen und Niedermendig (Eifel) gebräuchlich war.

Die Aussprache und die Schreibweise des Wortes Leibach sind nicht identisch, weil das „**ei**“ im Deutschen als „**ai**“ ausgesprochen wird. Die Fremdwörter werden in slowenischer Sprache entweder in ihrer Fremdform oder nach der heimatlichen Aussprache geschrieben. Die Doppellaute „ei“ (deutsche Aussprache: ai) und „eu“ (deutsche Aussprache: „oi“) sind der slowenischen Sprache fremd. Das deutsche Wort Leibach wird in slowenischer Sprache als „Laibah“ aufgeschrieben und als „Lajbah“ ausgesprochen. Die wortwörtliche Übersetzung des deutschen Wortes **Leibach** in die slowenische Sprache für die geographische Lage der bereits bestehenden Siedlung Lubigana am Laibacher-Fluss bedeutet „**skrilavec ob potoku**“ (oder vielleicht richtiger: skrilavi potok?).

Über die Bedeutung und Verwendung der karbonischen, feinkörnigen Sandsteine und dunkelgrauen Tonschiefer berichtet ausführlich Rakovec (1955). Die hellgrauen Sandsteine sind für die verschiedenen Baumaßnahmen (Brücken-, Haus- und Straßenbau) in der Stadt und Umgebung verwendet worden. Die großen Tonschiefer-Platten wurden anfänglich für die Schultafeln bzw. später für die Bedachung (Bedeckung) der Häuser benutzt. So sind viele Dächer der Häuser in der Nachbarschaft von Ljubljana mit Tonschiefer-Platten bedeckt. Weiterhin macht er wahrscheinlich, dass der heute stark eingeschnittene steile Laibacher Burghang ursprünglich flacher zum Fluss Ljubljanica verlief. Diese steil stehenden Abbauflächen des großen Steinbruches dienten bzw. bildeten beim späteren Bau der Stadthäuser als hintere Hauswand bis zum Erdgeschoss.

Die geologischen Ausführungen von Professor I. Rakovec unterstützen die Interpretation des deutschen Wortes **Leibach** in diesem Aufsatz. Das rheinische Wort **Leyendecker** trägt auch zum Verständnis und zur Richtigkeit der oben ausgeführten Begründung bei. Denn ein Leyendecker [Schieferdecker und/oder Dachdecker (krovec)] ist ein Fachmann, der die gebrochenen Rohschiefer bearbeiten und das Dach eines Hauses mit den selbst angefertigten Schiefer-Platten bedecken kann.

Die deutschen Dichter Clemens Brentano (1778–1842) und Heinrich Heine (1797–1856) benutzten als Grundlage für ihre Gedichte den Stoff aus dem Mittelalter über die tragisch endende Handlung von Lore **Ley**. Es ist interessant, dass die Schreibweise des Wortes **Lei** bei den Dichtern nicht identisch geschrieben ist. Clemens Brenta-

no benutzt das Wort L**a**y und Heinrich Heine verwendet das L**e**y.

Nach der Sage handelt es sich um eine hübsche Jungfrau mit blonden, langen Haaren. Sie zeigte sich singend und Haare kämmend den vorbeifahrenden Schiffern im Mittelrheintal. Sie bezauberte die Rheinschiffer durch ihre wunderbare Stimme, so dass sie nicht mehr auf das wilde Rheinwasser bzw. auf das gefährliche Felsenriff Acht gaben, sondern vor Staunen auf den Felsen hoch starrten, auf dem die Jungfrau saß (siehe Abb. 1). Nach der Erzählung wurden vorbeifahrende Schiffer und kleine Schiffe von den wilden Wasserwellen verschlungen und die Schuld dieser Tragödie trug die hübsche Lore Ley. Die Bevölkerung hielt sie für eine gemeine Zauberin, weil sie den Männern viel Schaden, Unglück und Unheil brachte. Da der Bischof in ihr eine unglücklich verliebte und von ihrem Ritter verschmähte Jungfrau erkannte, wurde sie in der geistlichen Gerichtsverhandlung gegen ihren Willen von der Anklage freigesprochen. Sie wurde aber ins Kloster geschickt, um dort als Nonne Gott zu dienen. Unterwegs zum Kloster bat sie ihre Bewacher, dass sie ihr erlauben mögen, ein letztes Mal das Schloss ihres Geliebten am Rhein zu sehen. Sie kletterte die hohe, steile Felswand hinauf, bis sie oben an der Felskante stand und auf den tiefen Rhein sehen konnte. Sie erblickte auf einem der kleinen Boote ihren fortgegangenen und verschollenen Liebsten. Da sie sich zu weit über den Schieferfelsen hinauslehnte, rutschte sie ab und stürzte in den tobenden Rhein. Dieser Schieferfelsen im Mittelrheinabschnitt heißt noch heute „im Tal der Lore Ley“ und ist UNESCO-Welterbe.

Dieser Aufsatz kann möglicherweise auch über die Herkunft der Einwanderer aus damaligen deutschen Ländern Auskunft gegeben. Die ersten Ansiedler aus den deutschen Ländern (wie z. B. Bayern, Franken, Hessen, Schlesien, Sachsen, Preußen, Salzburger Land und Steiermark.) kamen in den südlichen Raum der Karawanken in der Merowinger - und Karolingerzeit (450 bis 900 nach unserer Zeitrechnung). Sie stammen möglicherweise aus dem Sprachgebiet von Westfalen bzw. Rheinland oder eventuell aus dem Sächsischen Erzgebirge (siehe weiter unten).

In Deutschland leben zurzeit nach Schätzung der freien Enzyklopädie Wikipedia ca. 483 Personen, die den Familien-(Nachnamen) **Laibach** tragen. Das Wort Laibach drückt aber auch folgendes aus:

- Der Name eines **Ortsteils** von Dörzbach im Hohenlohekreis in Baden-Württemberg. Im Jahr 1307 wird dieser Ort als „Lutbach“ zum ersten Mal urkundlich genannt. Tyrolf Von Torcebach als Besitzer des alten Dorfes stammt von dem Hof Büchelich bei Laibach. Die Ortsbezeichnung Lutbach hat mit dem hier erforschten Namen nichts zu tun.
- Der Name eines **Ortsteils** von Bad Berleburg in Nordrhein-Westfalen.
- Ein **Bach** auf dem Gebiet der heutigen Gemeinde Halle (Nordrhein-Westfalen) nordwestlich Bielefeld am Südhang des Teutoburger Waldes (120 m über NN), zurzeit ca. 18 000 Einwohner. Die erste urkundliche Erwähnung wird mit dem Jahr 1241 datiert.
- Der **Familienname** des deutschen Botanikers Friedrich Laibach (1885–1967) aus Koblenz (Rheinland-Pfalz).
- In neuester Zeit nennt sich eine slowenische **Musikgruppe** „Laibach Band“.

Aus den oben genannten Fakten über die heutige Gemeinde Halle/Nordrhein-Westfalen (NRW) geht hervor, dass das Wort Leibach hier exakt der allgemeinen Vorstellung des alten rheinischen Wortes Lei entspricht. Hier stehen laut Geologischer Übersichtskarte von NRW (1 : 500 000) Schichten aus der Unterkreide (Osning-Sandstein) an. Dieser Sandstein ist morphologisch aufgrund der Gesteinshärte deutlich als Fels zu erkennen, der jedoch niemals zum bedeutenden Abbau bzw. zur größeren technischen Verwendbarkeit gelangt ist, so dass hier keine große mittelalterliche Siedlung entstehen konnte. Das rheinische Wort Lei lokalisiert und beschreibt nur eine Landfläche mit anstehenden Gesteinen (Schiefern, Steinen und Felsen = Lei) im Verlauf eines kleineren oder größeren Baches. Es wäre durchaus möglich, dass die ersten Einwanderer aus dem heutigen Bereich der Gemeinde Halle/NRW stammten, die der damaligen slowenischen Siedlung Lubigana den deutschen Namen Leibach aufgrund der ähnlichen Gesteinsvorkommen und morphologischen Gegebenheiten gaben.

Das gezielte Literaturstudium brachte aber auch neue Einblicke zum Problem des uralten indogermanischen Mischwortes Lu**w**igana/Lu**b**igana. Es kann auf die lange, allmähliche Sprachentwicklung des indogermanischen Mischwortes **Lubigana** vom Jahr 1146 über den bereits mit slowenisch klingenden Namen **Lublana** aus den 16. und 17. Jahrhunderten bis zur heutigen Bezeichnung **Ljubljana** hingewiesen werden. Vrhovec (1886) schreibt das Wort Lubigana mit dem Buchstaben „b“ und nicht wie die Brockhaus Enzyklopädie (Anonym, 1990) mit dem „w“. Durch die phonetische Transkription der Bezeichnung „Lu**w**igana“ stellte man eine Ähnlichkeit mit dem slowenischen Wort „ljubljena“(f) =„Geliebte“(f) fest. Eine andere Sprachforscher-Gruppe leitet den Namen Ljubljana von dem lateinischen Wort „Alluvion“ (f) ab und meinten damit das angeschwemmte Land um den heutigen Bach (Fluss) Ljubljanica (alluviana).

Die Lu**b**igana ist ein Mischwort und besteht aus einem urslawischen Teilwort „lubi“ und einem indogermanischen Restwort „**gan**a“. Der Buchstabe „a“ kann vom Restwort gana weggelassen werden, weil das Wort Lubigana den femininen Artikel (f) trägt. Nun ist es interessant, die beiden Worte aufzuhellen. Das urslawische Wort „lubi“ bedeutet in modernem Slowenisch „ljub“, „ljubezen“ und „ljubezniv“ (in Reihenfolge übersetzt „lieb“, „Liebe“, „liebenswürdig“). Das zweite Wort „**gan**“ ist wegen seiner Schlichtheit vermutlich uralt (Grimm (1984a). Die Gebrüder Grimm verstehen unter dem Wort „gan“ (f) *die funke* =[Funke (m) = iskra (f)] und verweisen zusätzlich auf die Mundarten in Bayern und Tirol. Aus diesem Sprachgebiet wird ein erläuterndes Beispiel

über das Wort „gan“ (f) angegeben: „*es seinen sowol die unter der asche* ***glimmenden funken*** *als die von einem brenneden körper* ***aussprühenden***“ (= to je, kot tlenje **isker** pod pepelom kakor tudi razpršene iz gorečega telesa). Im Gegensatz dazu wurde in Kärnten das Wort „gan“ (m) hauptsächlich in der Mehrzahl „ganen“ benutzt und bedeutete „funken sprühen“ (= metati iskre). Das Wort „gan“(f) kann im übertragenen Sinn durch zwei unterschiedliche Möglichkeiten gedeutet werden. Demnach steht die Bedeutung von „**glimmen**“ als Ausdruck von Passivität (verborgen, heimlich, nichtdurchschaubar und nichteinschätzbar) der Bedeutung von „**aussprühen**“ aber als Ausdruck von Aktivität (freudestrahlend, charmant, fröhlich und entgegenkommen) gegenüber.

Aus dem Gesagten kann eine vorläufige und sehr vorsichtige Interpretation der alten Bezeichnung Lu**b**igana für diesen Zeitraum gegeben werden. Dabei handelt sich um eine wortwörtliche Übersetzung mit sinngemäßer Formulierung: **Ort** „**liebeswürdiger Funken“** (= **ljubeznivi kraj isker**). Alle Bewohner der damaligen Ortschaft (Markt und/oder Stadt) nannten sich **Lubiganer** (**Liebeswürdige Funken = ljubeznive iskre**).

Es ist hoch interessant, dass sich das indogermanische Wort „**gan**“ (m/f) in den noch heute gebrauchten slowenischen Worten ci**gan** (m) - Ziegeuner (m), po**gan**stvo (f) - Heidentum (s), po**gan**jati - austreiben, sprießen; pod**gan**a (f) - Ratte (f) und prema**gan**ec (m) - Besiegter (m) erhalten hat.

In der bischöflichen Seminarbibliothek existierte eine Abschrift „Curia Labacensis Urbis Metropolis Ducatus“ von Joh. Bapt. Mayr aus dem Jahr 1680, in der nach Vrhovec (1886: 84) über das damalige Wahrzeichen der Stadt Laibach berichtet wurde. Im Rathaus standen nämlich die steinernen Skulpturen von Adam und Eva in Lebensgröße. Nach der Sage musste jeder Besucher, der erstmalig Leibach besuchte, diese beiden Statuen unbedingt küssen. So wird berichtet, dass viele Besucher, insbesondere aber die wandernden Handwerksburschen, aus Dankbarkeit für die Erhörung ihrer Fürbitte mehrfach die Hände von Adam und Eva küssten (küssen = po**ljublja**ti). An dieser Stelle spielten sich möglicherweise leidenschaftliche Szenen ab, die sich sinnbildlich über den gesamten Ort ausdehnten und sich nach einer Weile im Wort Ljubljana widerspiegeln. Demzufolge nannte man zuerst diesen Platz des Küssens und später wird die ganze Ansiedlung als der **Ort des Küssens** (kraj po**ljubljan**ja) bezeichnet.

Die verschiedene Diözesen (Aquiléia, Freisingen und Salzburg) bewahren alte Urkunden über die Pfarren Sankt Peter und Sankt Nikolai zu Laibach. Über die Auseinandersetzung wegen des Patronats der Kirche St. Petri in Laibach berichtet Pater Hitzinger (1855). Die erste Kirche erbauten die Freisinger Bischöfe zwar auf eigenen Grund und Boden, sie stand aber im Einflussbereich der Salzburger Erzbischöfe. Der Papst Urban IV. hatte sich im Jahr 1262 in diesen Streit in Lungan mit einer päptlichen Verordnung eingeschaltet und Magister Lubuvicus als Schiedsrichter ernnant. In diesen Urkunden erscheint zum ersten Mal das Wort **Lungan**. Wie die bisherigen Untersuchungen zeigen, bedeutet das Wort „gan“ (f) nach Gebrüdern Grimm (1984a) *die funke* (f). Welche Bedeutung dem Wort „lun“ (?) zugeschrieben wird, muß noch recherchiert werden. Inwieweit das Wort **Lungan** einen Ortsteil der Stadt Laibach bezeichnet, ist nach vorläufigen Literaturrecherchen nicht feststellbar. Möglicherweise kann der Name der schweizerischen Stadt Lu**gan**o, lat. Luganum, am gleichnamigen See einen wichtigen Hinweis für die Klärung des Begriffes „lun“ geben.

Die Gebrüder Grimm geben noch weitere Hinweise auf die ältere Literatur, die aber noch bestellt bzw. studiert werden muß.

Ausblick

Diese Untersuchung zeigt ferner aber auch, dass die felsartigen Sattelstrukturen wegen der Gesteinshärte in einem mäandrierenden Bach einen stärkeren Vorsprung bilden, der die Breite des Flusses bzw. Baches stark verengen kann. Dabei kann es zur Bildung der gefährlichen Stromschnellen kommen, die Wassermenge wird vergrößert und gleichzeitig die Schifffahrt gefährlich behindert. Der Vergleich derartiger morphologischer Großstrukturen kann „im Tal der Lore Ley” bzw. in Ljubljanica (Fluss Leibach) erfolgen. Im Fall der Gemeinde Halle/Westfalen soll demnächst durch eine Begehung geprüft werden, ob im dortigen Laibach diese Feststellung zutrifft. Wegen der dort anstehenden harten Sandsteine der Kreide ist es aber zu erwarten, dass diese Annahme bestätigt wird. Das führt dann zum Schlussergebnis, dass das Wort Ley in ursprünglicher keltischer Sprache möglicherweise auch den Vorsprung eines anstehenden Felsens oder die Reste der Felsabstürze in einen Fluss (Bach) bedeuteten könnte. Das hier erkannte Sprachproblem soll mit Sprachwissenschaftlern weiter diskutiert werden, um dieses hier erstmals behandelte geologisch/sprachwissenschaftliche Thema zu ergänzen und zu erweitern.

Abschießend wird noch auf folgende Tatsache hingewiesen: Beim Studium historischer Literatur erkennt man, wie früher Probleme gelöst wurden. Daraus ergibt sich zwangsweise, dass die Zukunft der Menschheit eindeutig in der vielbeschriebenen Vergangenheit liegt. Solange die Menschheit nicht in der Lage ist, das zu begreifen und daraus die richtigen Konsequenzen zu ziehen, wird auch die Lösung von Problemen der Gegenwart nicht gelingen.

Danksagung

Der Autor bedankt sich bei den Herren Universitätsprofessoren Dr. Werner Kasig und Dr. Heinrich Siemes (RWTH Aachen) für ihre vielfältige Hilfe und für die sachlichen Hinweise zur Korrektur des Aufsatzes. Weiter gilt der besondere Dank Herrn Universitätsprofessor Dr. Simon Pirc (Universität Ljubljana) für die Übersetzung der deutschen Zusammenfassung in die slowenische und in die englische Sprache. Der Dank gilt auch Frau Dipl. Bibliothekarin Andrea

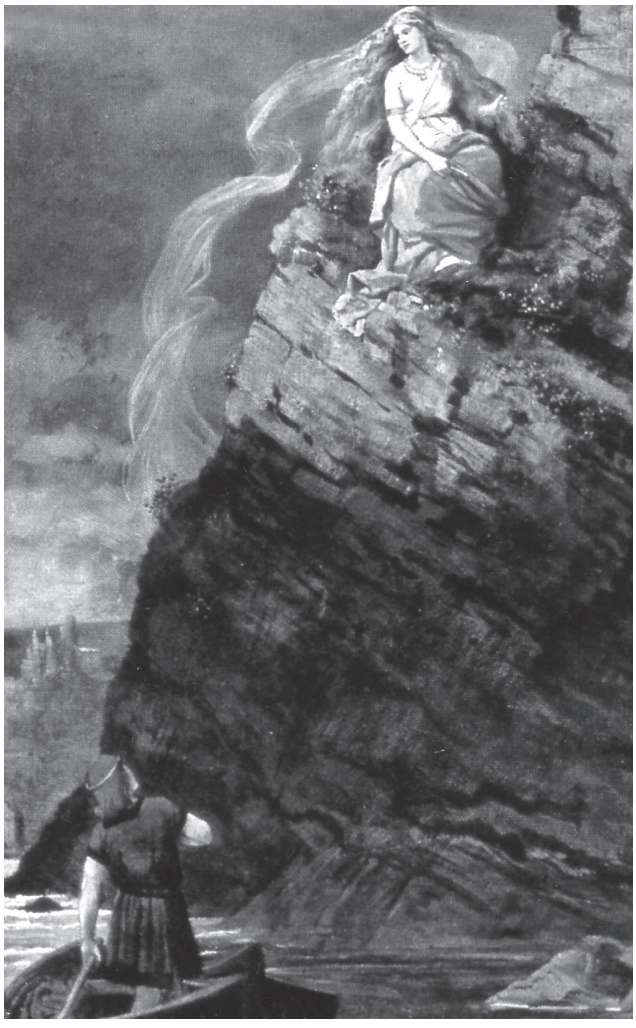

Abb. 1. Im Tal der Lore Ley (nach Vorlage einer Postkarte)
Sl. 1. V dolini Lore Ley (po razglednici)
Fig. 1. In valley Lore Ley (after a template of a postcard)

Jaek (Hochschulbibliothek der RWTH Aachen) für die Recherche bzw. schnelle Besorgung der schwer zugänglichen Literatur.

Literaturverzeichnis

Anonym, 1990: Brockhaus Enzyklopädie, 19. völlig neu bearbeitete Auflage (Mannheim) 13: 704 S.

Anonym, 2009: Kompaktwörterbuch Slowenisch (Ljubljana, Stuttgart) I–XXXII + 947 S.

Grimm, J. und W. 1984a: Deutsches Wörterbuch. Nachdruck der ersten Ausgabe 1878 (München) 4: 2151 S.

Grimm, J. und W. 1984b: Deutsches Wörterbuch. Nachdruck der ersten Ausgabe 1885 (München) 12: 2848 S.

Hitzinger, P. 1855: Zur Geschichte der Pfarren Krains. Mittheilungen des historischen Vereins für Krain und Diplomatarium Carniolicum (Laibach) 10: 28–30.

Kirnbauer, F. 1941: Deutsche Berg- und Hüttenleute als Pioniere der Technik und Kultur im europäischen Südosten. Zeitschrift für das Berg-, Hütten- und Salinenwesen (Berlin) 89: 121–131.

Knochenhauer, O. 1928: Die Wanderung der deutschen Bergleute. Zeitschrift für das Berg-, Hütten- und Salinenwesen (Berlin) 76 B259–B289.

Korošec, B. 1978: Naš prostor v času in projekciji. Oris razvoja zemljemerstva, kartografije in prostorskega urevanja na osrednjem Slovenskem (Ljubljana): 1–297.

Kosi, M. 2009: Stadtgründung und Stadtwerdung, Probleme und Beispiele aus dem slowenischen Raum. Pro Civitate Austriae: Informationen zur Stadtgeschichtsforschung in Österreich/Österreichischer Arbeitskreis für Stadtgeschichtsforschung und Ludwig Boltzmann Institut für Stadtgeschichtsforschung (Linz, Wien) 14: 5 - 21.

Quiring, H. 1929: Die Anfänge des Bergbaus in Deutschland und Herkunft der „fränkischen" Bergleute. Zeitschrift für das Berg-, Hütten- und Salinenwesen (Berlin) 77: B222–B251.

Quiring, H. 1932: Die älteste Gewinnung und Verwendung von Dachschiefer im Rheinland. Forschungen und Fortschritte, (Hrsg.) Nachrichtenblatt der deutschen Wissenschaft und Technik (Berlin) 8: 492–499.

Quiring, H. 1935: Vorgeschichtliche Studien in Bergwerken Südspaniens. Zeitschrift für das Berg-, Hütten- und Salinenwesen (Berlin) 83: 492–499.

Quiring, H. 1941: Die Anfänge der Metallverarbeitung und des Erzbergbaus in Mitteleuropa. Das Schürfwerkzeug und die Waffe der ersten metall- und erzsuchenden Erzleute. Zeitschrift für das Berg-, Hütten- und Salinenwesen (Berlin) 89: 167–187.

Rakovec, I. 1955: Zgodovina Ljubljane. I: 11–207 mit einer Geologischen Karte (1 : 75 000) der Umgebung von Ljubljana.

Schmid, W. 1913: Emona. Jahrbuch für Altertumskunde (Wien) 7: 61–186.

Tomšič, F. 1964: Deutsch-slowenisches Wörterbuch (Ljubljana): 1–987.

Vidrih, R. 2009: Nemirna zemlja. Ob 50-letnici moderne seizmologije na Slovenskem (Ljubljana): 1–120.

Vrhovec, J. 1886: Die wohllöbliche landesfürstliche Hauptstadt Laibach.

GEOLOGIJA *53/1*, 103–104, Ljubljana 2010

Nove knjige

Davorin Preisinger, 2010: **RUDNIKI Opuščeni rudniki v Sloveniji**
(**MINES Abandoned Mines in Slovenia**),
Založba Turistika, 152 strani.

V četrtek, 10. junija 2010, je v avli Mestne občine Kranj potekala predstavitev prvenca Davorina Preisingerja RUDNIKI - Opuščeni rudniki v Sloveniji. Knjigo, ki je maja 2010 izšla pri Založbi Turistika, so predstavili avtor Davorin Preisinger, urednik Matjaž Chvatal in prevajalka Nejka Kališnik. Gre za fotografsko monografijo odličnega fotografa, jamarja, drznega raziskovalca opuščenih rudniških rovov ter zbiralca kamnin, mineralov in fosilov. Avtor je v knjigi pozorno zbral fotografski material, ki ga je posnel med neštetimi akcijami v opuščene rudniške rove v zadnjih dvajsetih letih. Zanimalo ga je bogastvo mineralov v njih, rudarska dediščina, pa tudi prava mera adrenalina, ki se sprošča ob raziskovanju le-teh. Obravnavane opuščene rove je avtor opisal iz stališča vedoželjnega naravoslovnega ljubitelja in zbiralca mineralov. Podaja osnovne podatke o dostopnosti opisanih rovov, mineralni paragenezi orudenja in o odvalih, ki so v bližini. Tako so v knjigi podane osnovne informacije o 31-tih opuščenih rudnikih oz. o 50-tih opuščenih rudniških rovih barvnih kovin, kremena in premoga. Rudniški rovi so predstavljeni v samostojnih poglavjih s kratkimi, jedrnatimi teksti, ki jih dopolnjuje odlična fotografija notranjosti rudnikov in mineralov, ki se v njih nahajajo. Avtor pri vsakem rudniku posebno pozornost namenja predstavitvi mineralov, rud in kamnin. Zelo pohvalno je, da se je založnik odločil in izdal knjigo v slovenskem in angleškem jeziku.

Največji opuščeni rudnik predstavljen v knjigi je rudnik Sitarjevec pri Litiji. Na tem območju so začeli rudariti že zelo zgodaj. Domnevajo, da so v Litiji rudarili že Kelti, vendar za to ni trdnih dokazov. Najdišča žlindre v neposredni bližini Litije pričajo o rudarjenju v rimskih časih. Od srednjega veka pa vse do leta 1965 so z manjšimi prekinitvami na tem območju pridobivali svinec, cink,

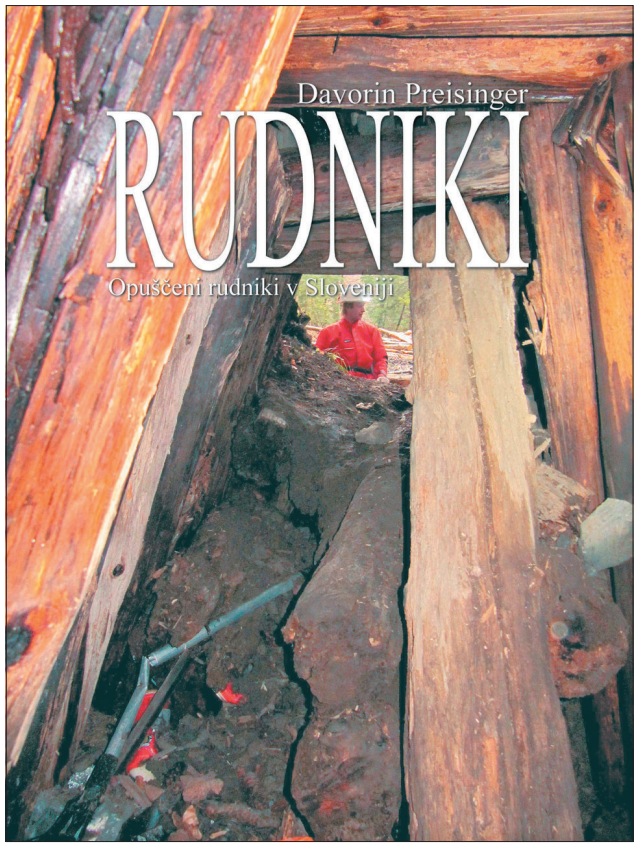

RUDNIKI
Opuščeni rudniki v Sloveniji
Jezik: slovenščina
ISBN: 978-961-6414-42-5

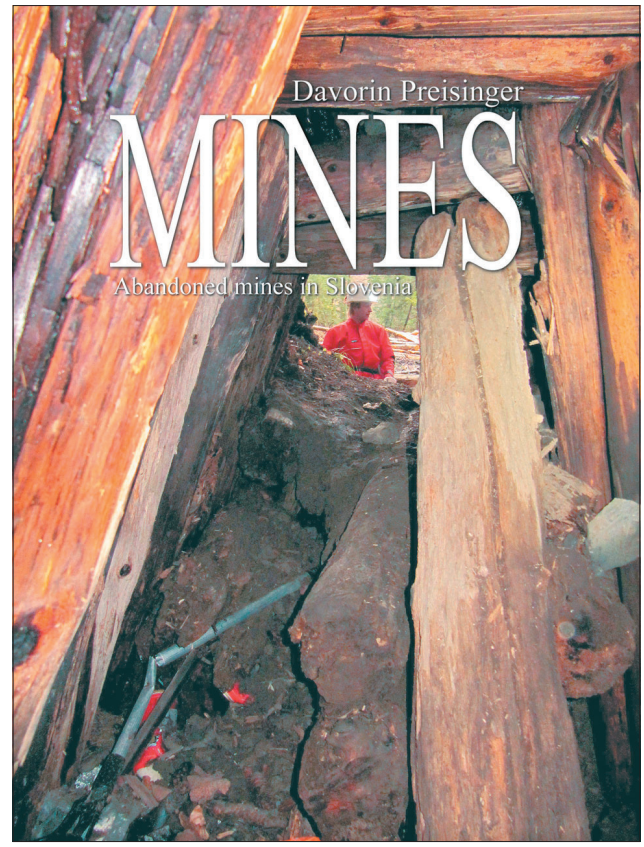

MINES
Abandoned Mines in Slovenia
Jezik: angleščina
ISBN: 978-961-6414-43-2

živo srebro, železo, barit, malo srebra in celo zlata. Kljub temu da je rudarstvo v okolici Litije pred več desetletji zamrlo, so številni sledovi rudarjenja v okolju še opazni. Najdemo številne vhode v opuščene rudniške rove, deponije siromašne rude, prikamnine in žlindre, zavedamo se ogroženosti zaradi možnosti izbruhov ujete rudniške vode v zapuščenem rudniku Sitarjevec in kislih izcednih vod, ki odtekajo iz rudnika. Ker so nekateri opuščeni rovi tik pod površjem, je prišlo do zruškov in nastale so nove povezave s površjem, ki so marsikje tudi nevarne, saj so neoznačene in skrite v podrasti gozda. Le-te so za obiskovanje zanimivega, a nevarnega podzemlja uporabljali raziskovalci starih rudniških rovov in zbiralci mineralov, med njimi tudi avtor. Sitarjevec je bil za mineraloške navdušence vedno zelo zanimiv saj slovi kot rudnik z najbolj pestro mineralno sestavo v Sloveniji. Pojavlja se preko petdeset različnih mineralov, ki so nastali v več fazah mineralizacije (cerusit, barit, cinabarit, galenit, limonitni kapniki,…). V zapuščenih in delno zarušenih rudniških rovih se tvorijo limonitni kapniki in limonitne pregrade, za katerimi zastajajo velike količine limonitnega blata in rudniške vode. Limonitnim kapnikom je v knjigi namenjeno kar veliko prostora, saj so svetovna redkost. Največji merijo že več kot 1 m. V knjigi je na kratko predstavljena geografska lega, zgodovina rudnika, mineralna parageneza in značilnosti šestih najpomembnejših rudniških rovov na Sitarjevcu. Zbrani so tudi podatki o prehodnosti in naravnih, predvsem mineraloških značilnostih in lepotah opisanih rovov. Besedilo je ilustrirano z odličnimi fotografijami, ki so nedvomno najpomembnejša odlika te knjige. Poleg sitarjevških rovov je Litijsko rudno polje v knjigi predstavljeno še z rovi Maljek, Reka Gozd in Pustov mlin, v katerih so včasih pridobivali svinčevo rudo, v glavnem galenit.

Opuščeni rudnik živega srebra v Podljubelju, ki je v knjigi opisan z imenom Šentanski rudnik, je predstavljen s sedmimi rovi. Živosrebrovo orudenje prikazujejo atraktivne slike krvavordečega cinabarita v družbi s snežno belim kalcitom in temno sivim apnencem. Prikazan je tudi svinčeni kovanec, kakršne so v Šentanskem rudniku uporabljali v drugi polovici 19. stoletja za štetje rudarskih vozičkov – huntov.

Tudi rudnik Knapovže sodi med starejše v Sloveniji, saj naj bi tam rudarili že Rimljani in v srednjem veku protestantski rudarji. Izkoriščali so žile masivnega galenita, ki so bile debele od 4 do 60 cm, tako da je ruda vsebovala povprečno kar 74 % svinca.

Rudnik bakra, svinca, cinka in srebra Remšenik slovi po pestri mineralni paragenezi. Bolj kot primarni minerali so zanimivi sekundarni minerali, ki se pojavljajo ob njih in skupaj tvorijo odlične motive za barvite fotografije.

Ostali opisani rovi so manj znani. Zato je še bolj pohvale vredno, da jih je avtor poiskal in tudi opisal. V knjigi so predstavljeni tudi nekateri raziskovalni rovi. V rudarski zgodovini Slovenije je namreč kar nekaj rudniških rovov, kjer so neuspešno poskušali srečo z iskanjem rude. Tehnologija v tistih časih ni poznala raziskovalnih vrtin, zato so vložili veliko sredstev v kopanje poskusnih, raziskovalnih rovov. Uspeha velikokrat ni bilo, zato so v nadaljevanju dela opustili.

Knjiga je pomembno delo in prispevek k spoznavanju naše ne tako oddaljene rudarske zgodovine. Namenjena je predvsem poljudnim bralcem, ki bodo ob tej knjigi spoznali, da je zgodovina rudarjenja v Sloveniji dolga in pestra. V zlati dobi rudarjenja, v drugi polovici 19. stoletja in v začetku 20. stoletja, je v Sloveniji obratovalo veliko rudnikov. Žal pa izkoriščanje rude v večini le-teh ni bilo donosno in so zato rudarjenje v njih kmalu opustili. Po drugi svetovni vojni so kovine v Sloveniji pridobivali le še Idriji in Mežici ter nekaj let še v Sitarjavcu. Ker so tudi ti rudniki danes zaprti, se naše rudarstvo danes ponaša le še s pridobivanjem premoga v Velenju in Zasavju. Ob prebiranju knjige se bodo bralci seznanili z našo dolgo in bogato rudarsko tradicijo ter spoznali pestrost mineralov, ki jih lahko pri nas najdemo.

Mateja Gosar

GEOLOGIJA *53/1*, 105–106, Ljubljana 2009

Navodila avtorjem

GEOLOGIJA objavlja znanstvene in strokovne članke s področja geologije in sorodnih ved. Revija od leta 2000 izhaja dvakrat letno v obsegu 30 avtorskih pol. Vse prispevke recenzirajo domači ali tuji strokovnjaki s področja, ki ga prispevek obravnava. Avtorji so dolžni pisno mnenje recenzentov upoštevati, ter svoje prispevke po potrebi tudi dopolniti.

Avtorstvo: Za izvirnost podatkov, predvsem pa mnenj, idej, sklepov in citirano literaturo so odgovorni avtorji. Z objavo v Geologiji se tudi obvežejo, da ne bodo drugje objavili istega prispevka.

Jezik: Članki so lahko napisani v slovenskem ali angleškem jeziku, vsi pa morajo imeti slovenski in angleški izvleček. Za prevod poskrbijo avtorji prispevkov sami.

Vrste prispevkov:

Izvirni znanstveni članek

Izvirni znanstveni članek je samo prva objava originalnih raziskovalnih rezultatov v takšni obliki, da se raziskava lahko ponovi, ugotovitve pa preverijo. Praviloma je organiziran po shemi IMRAD (Introduction, Methods, Results, And Discussion).

Pregledni znanstveni članek

Pregledni znanstveni članek je pregled najnovejših del o določenem predmetnem področju, del posameznega raziskovalca ali skupine raziskovalcev z namenom povzemati, analizirati, evalvirati ali sintetizirati informacije, ki so že bile publicirane. Prinaša nove sinteze, ki vključujejo tudi rezultate lastnega raziskovanja avtorja.

Strokovni članek

Strokovni članek je predstavitev že znanega, s poudarkom na uporabnosti rezultatov izvirnih raziskav in širjenju znanja.

Diskusija in polemika

Prispevek, v katerem avtor ocenjuje ali dokazuje pravilnost nekega dela, objavljenega v Geologiji ali z avtorjem strokovno polemizira.

Recenzija, prikaz knjige

Prispevek, v katerem avtor predstavlja vsebino nove knjige s področja geologije.

Oblika prispevka: Besedilo naj bo napisano na listih formata A4 z dvojnim presledkom, da je dovolj prostora za popravke in pripombe recenzentov. Najbolje je, da pripravite besedilo v urejevalniku Microsoft Word. Prispevki naj praviloma ne bodo daljši od 25 strani formata A4, v kar so vštete tudi slike, tabele in table. Le v izjemnih primerih je možno, ob predhodnem dogovoru z uredništvom, tiskati tudi daljše prispevke.

Prispevke oddajte uredništvu v enem tiskanem izvodu, vključno z vsemi slikami in preglednicami ter identično kopijo v elektronski obliki po naslednjem sistemu:

- *Naslov prispevka* (tudi v tujem jeziku)
- *Avtor / avtorji*
- *Ključne besede in Key words*
- *Izvleček in Abstract*
- *Tekst*
- *Literatura*
- *slike, tabele in table*

Naslovi prispevkov naj bodo kratki in naj praviloma ne presegajo 12 besed. Poleg polnega imena in priimka naj podajo avtorji tudi svoj naslov in e-pošto. Vsebine oziroma kazala pri normalno dolgih prispevkih ne objavljamo, zaželene pa niso niti opombe na dnu strani.

Citiranje: V literaturi naj avtorji prispevkov praviloma upoštevajo le tiskane vire. Rokopise naj navajajo le v izjemnih primerih z navedbo, kjer so shranjeni. V seznamu literature navajajte samo v prispevku omenjana dela. Med besedilom prispevka citirajte samo avtorjev priimek z inicialko njegovega imena, v oklepaju pa navajajte letnico izida navedenega dela in po potrebi tudi stran. Če navajate delo dveh avtorjev, izpišite med tekstom prispevka oba priimka (npr. Pleničar & Buser, 1967), pri treh ali več avtorjih pa napišite samo prvo ime in dodajte et al. z letnico (npr. Mlakar et al., 1992). Literaturo navajajte po abecednem redu avtorjev.

Imena fosilov (rod in vrsto) pa naj pišejo poševno. Pri citiranju rodov in vrst oziroma višjih taksonomskih enotah se imena avtorjev le teh pišejo normalno, npr. Apricardia pachiniana Sirna.

Primeri citiranja članka:

Mali, N., Urbanc, J. & Leis, A. 2007: Tracing of water movement through the unsaturated zone of a coarse gravel aquifer by means of dye and deuterated water. Environ. Geol., (Berlin) 51/8: 1401–1412.

Pleničar, M. 1993: Apricardia pachiniana Sirna from lower part of Liburnian beds at Divača (Triest–Komen Plateau). Geologija (Ljubljana) 35: 65–68.

Turnšek, D. & Drobne, K. 1998: Paleocene corals from the northern Adriatic platform. In: Hottinger, L. & Drobne, K. (eds.): Paleogene Shallow Benthos of the Tethys. Dela SAZU, IV. Razreda (Ljubljana) 34 (2): 129–154, incl. 10 pls.

Primer citirane knjige:

Flügel, E. 2004: Mikrofacies of Carbonate Rocks. Springer Verlag (Berlin): 1–976, cd-rom.

Jurkovšek, B., Toman, M., Ogorelec, B., Šribar, L., Drobne, K., Poljak, M. & Šribar, Lj. 1996: Formacijska geološka karta južnega dela Tržaško-komenske planote – Kredne in paleogenske kamnine 1 : 50.000. [Geological map of the southern part of the Trieste–Komen plateau – Cretaceous and Pa-leogene carbonate rocks]. Geološki zavod Slovenije (Ljubljana): 1–143, incl. 23 pls, 1 geol. map.

Slike, tabele in table: Slike (ilustracije in fotografije), tabele in table morajo biti zaporedno oštevilčene in označene kot sl. 1, sl. 2 itd., narejene v računalniškem programu (MS Excel, Word ali CorelDRAW), oddane v formatu TIFF, JPG ali EPS z ločljivostjo 300 dpi. Le izjemno je možno objaviti tudi barvne slike, vendar samo po predhodnem dogovoru z uredništvom. Obvezno je treba upoštevati zrcalo revije **172 x 259 mm**. Revija bo od leta 2008 po sklepu uredniškega odbora pričela izhajati v A4 formatu z dvokolonskim tiskom. Večjih formatov od omenjenega zrcala GEOLOGIJE ne tiskamo na zgib, je pa možno, da večje oziroma daljše slike natisnemo na dveh straneh (skupaj na levi in desni strani) z vmesnim »rezom«. Slike obeležite s številkami. V besedilu prispevka morate omeniti vsako sliko po številčnem vrstnem redu. Dovoljenja za objavo slikovnega gradiva iz drugih revij publikacij in knjig si pridobijo avtorji sami. Table pripravite v formatu zrcala naše revije.

Podnaslove k slikam, tabelam in tablam, ki morajo biti napisani v obeh jezikih, avtorji priložijo na posebnih listih enega pod drugim. Zato teh podnaslovov ne pišete med besedilom prispevka. Podnaslovi naj bodo po možnosti čim krajši.

Korekture: Te opravijo avtorji prispevkov, ki pa lahko popravijo samo tiskarske napake. Krajši dodatki ali spremembe pri korekturah so možne samo na avtorjeve stroške.

Pošiljanje prispevkov: Uredništvo sprejema prispevke do vključno 1. marca za prvo številko in najkasneje do 1. septembra za drugo številko v tekočem letu in se obveže, da bodo le-ti tiskani v tekočem letu, v kolikor bodo avtorji upoštevali pripombe recenzentov.

Avtorji prejmejo 25 separatov brezplačno, sicer pa so prispevki dostopni tudi na internetnih straneh
http://www.geologija-revija.si

Avtorje prosimo, da prispevke pošiljajo na naslov uredništva:

GEOLOGIJA
Geološki zavod Slovenije
Dimičeva ulica 14, 1000 Ljubljana ali urednik@geologija-revija.si

Uredništvo Geologije

Instructions for contributors

GEOLOGIJA publishes research and professional papers covering all aspects of geology and related sciences. The journal is issued from 2000 on twice a year in an extent of 30 authorial sheets (240 printed pages) All contributions are reviewed by Slovenian or foreign experts from the field treated by the paper. Authors are obliged to take into account their written reviews, and complete accordingly the contribution, if necessary.

Authorship: Authors are responsible for the originality of data, and especially for opinions, ideas, conclusions and the cited references. By publishing in Geologija, they are in addition obliged not to publish the same contribution elsewhere.

Language: Papers may be written in Slovenian or English, and all must contain an abstract in Slovenian and in English. The translation is at care of the authors.

Kinds of contributions:

Original scientific article

An original scientific article is only the first publication of original research results in such a form that the research could be repeated and the findings verified. As a rule it should be organized according to the IMRAD scheme (Introduction, Methods, Results, And Discussion).

Review scientific article

A review scientific article is a review of the latest works on a given field, of works of an individual researcher, or of a research group with the aim of summarizing, analyzing, evaluating or synthesizing the already published informations. It contains new syntheses that include also results of the author's own research.

Professional article

A professional article is a presentation of already known material with emphasis on the use of results of original research and on the propagation of knowledge.

Discussion and polemics

A contribution in which the author evaluates or demonstrates the correctness of a contribution that was published in Geologija, or in which he/she competently polemizes with te author.

Book review

A contribution in which the contents of a book from the field of geology are presented.

Format of contribution: The manuscript should be written on A4 size pages with double spacing to allow enough space for corrections and comments of reviewers. The contribution should be preferrably edited on a Microsoft Word word processor. As a rule contributions should not be longer than 25 A4 size pages comprising also figures, tables and plates. Longer contributions can be submitted only exceptionally after a previous agreement with the Editor.

Contributions should be submitted to the Editorial Board in a hard copy inlcuding all figures and tables, and in an identical copy in electronic form according to the following system:

- *Title of contribution* (also in foreign language)
- *Author/s*
- *Key words*
- *Abstract*
- *Text*
- *References*
- *Figures, tables and plates*

Titles of contributions should be short, as a rule not longer than 12 words. In addition to their full given name and surname the authors should indicate also their address and electronic mail address. Tables of contents with normal sized contributions are not published, and also footnotes are discouraged.

Referencing: References should contain as a rule only printed sources. Manuscript sources could be cited only exceptionally with the information on where they are available. The references cited in the text should be given in the reference list and vice versa. In the text only the surname of the author(s) with initial of the name should be cited, followed in parentheses by the year of publication and, if necessary, also the page. When citing a publication by two authors, in the text both authors' surnames should be given (e.g. Pleničar & Buser, 1967), and in case of three and more authors only the first author's surname followed by et al. and the year (e.g. Mlakar et al., 1992). The reference list should be arranged in alphabetical order of first authors. Names of fossils (genus and species) should be italicised. Authors' names in citing fossils should be written in normal type, e.g. *Apricardia pachiniana* Sirna.

References cited should follow the examples shown below:

Mali, N., Urbanc, J. & Leis, A. 2007: Tracing of water movement through the unsaturated zone of a coarse gravel aquifer by means of dye and deuterated water. Environ. Geol., (Berlin) 51/8: 1401–1412.

Pleničar, M. 1993: *Apricardia pachiniana* Sirna from lower part of Liburnian beds at Divača (Triest–Komen Plateau). Geologija (Ljubljana) 35: 65–68.

Turnšek, D. & Drobne, K. 1998: Paleocene corals from the northern Adriatic platform. In: Hottinger, L. & Drobne, K. (eds.): Paleogene Shallow Benthos of the Tethys. Dela SAZU, IV. Razreda (Ljubljana) 34 (2): 129–154, incl. 10 pls.

Examples of book references:

Flügel, E. 2004: Mikrofacies of Carbonate Rocks. Springer Verlag (Berlin): 1–976, cd-rom.

Jurkovšek, B., Toman, M., Ogorelec, B., Šribar, L., Drobne, K., Poljak, M. & Šribar, Lj. 1996: Formacijska geološka karta južnega dela Tržaško-komenske planote – Kredne in paleogenske kamnine 1 : 50.000. [Geological map of the southern part of the Trieste–Komen plateau – Cretaceous and Paleogene carbonate rocks]. Geološki zavod Slovenije (Ljubljana): 1–143, incl. 23 pls, 1 geol. map.

Figures, Tables and Plates: Figures (illustrations and photographs), tables and plates should be numbered consecutively and marked as fig. 1, fig. 2. etc. They should be produced with a suitable computer program (MS Excel, Word, CorelDraw the like), and submitted digitally in the TIFF, JPG or EPS format with 300 dpi resolution. Color figures could be published only exceptionally, and in prior arrangement with the Editor. The **172 x 259 mm** journal page format must be obligatorily considered. According to the decision of Editorial Board from 2008 on the journal is being printed in two columns on an A4 page size. Figures on folding leafs of sizes larger than the mentioned GEOLOGIJA page size will not be printed, but figures larger or longer than that may be printed on two pages (on left and on right page) with a cut inbetween. Figures shall be marked by numbers. In the text each figure should be mentioned in the proper numerical order. Permissions for publishing pictorial material from other journals, publications and books should be arranged by the authors. Plates should be prepared in the journal's page size format.

Captions to figures, tables and plates, written in both languages, are supplied by author on separate pages and listed one below the other. Please, do not write captions in the text of the contribution. If possible, captions should be concise.

Proofreading: Page proofs should be read by the authors, but they ought to correct only printing errors. Shorter additions or modifications are possible only at the author's expense.

Offprints. Authors will receive 25 offprints free. The contributions are accessible also on the web-site http://www.geologija-revija.si.

Submitting of contributions: Editorial board is accepting the contributions to 1st March for the first issue, and to 1st September for the second issue of the year, and guarantees to publish them in the given year, provided they consider the reviewers' observations.

Authors are asked to send their contributions to the mail address:

GEOLOGIJA
Geološki zavod Slovenije
Dimičeva ulica 14, SI-1000 Ljubljana
or to the electronic address:
urednik@geologija-revija.si

Editorial Board of Geologija

Geološki zavod Slovenije
Geological Survey of Slovenia
Dimičeva 14, SI-1000 Ljubljana
faks: +386(1)2809-753
tel.: +386(1)2809-700
http://www.geo-zs.si

SCANNING ELECTRON MICROSCOPE WITH ENERGY DISPERSIVE X-RAY SPECTROMETER (SEM/EDS) AT THE GEOLOGICAL SURVEY OF SLOVENIA

At the beginning of 2008, the Geological Survey of Slovenia obtained a new analytical instrument for morphological surface analysis and qualitative to semi-quantitative chemical microanalysis of materials. This instrument is a scanning electron microscope (SEM) coupled with energy dispersive spectrometer (EDS).

Basic SEM/EDS components and principles of operation:

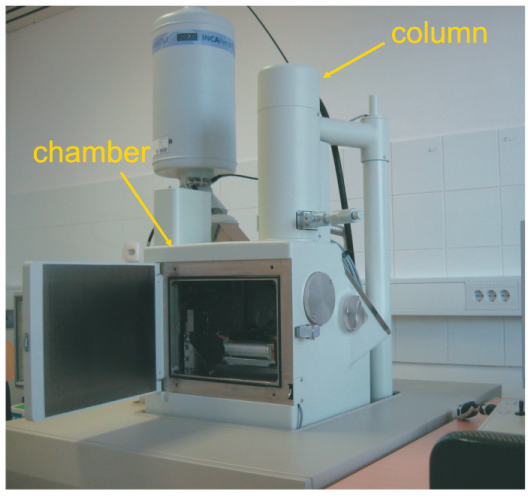

The major parts of a SEM/EDS are: vacuum specimen chamber, electron column with electron source, electromagnetic lenses, scanning coils and signal detectors (SE, BSE, EDS).

A number of signals, such as **secondary electrons** (SE), **backscattered electrons** (BSE) and **X-rays**, result from interactions of a focused scanning electron beam with the atoms of a specimen, thus providing different information about the sample.

- **SE** provide topographical image of sample surface.
- **BSE** depend on atomic number and provide relative compositional image of the sample.
- **X-rays** provide information about elemental composition of the sample.

SEM/EDS applications:

SEM/EDS at the Geological Survey of Slovenia is applied to different fields of geology.

Palaeontological studies:

Low-vacuum mode enables a non-destructive analysis of valuable samples without prior preparation.

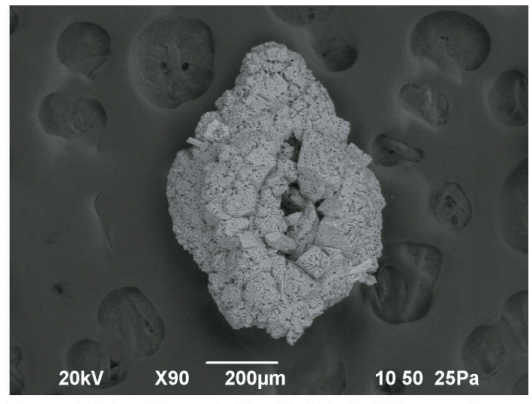

Recrystallised foraminifer *Ophthalmidium* sp. from the Bača dolomite

Sedimentary petrological studies:

High resolution and magnification can be achieved in high-vacuum mode.

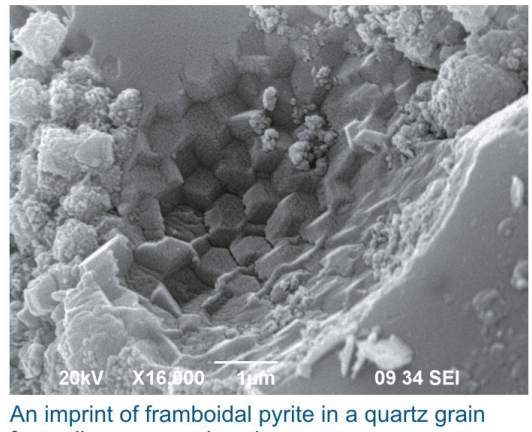

An imprint of framboidal pyrite in a quartz grain from oligocene marine clay

Coal studies:

Samples containing gases and liquids can be observed in low vacuum. High magnification image of homogeneous coal reveals flaky structure, which is important for understanding of coal porosity.

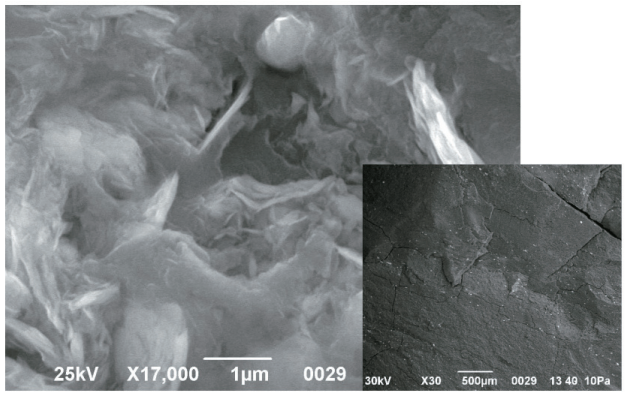

Flaky structure in homogeneous finedetritic lignite

Mineralogical studies of materials:

Mineral composition of materials can be accurately determined by semi-quantitative elemental EDS analysis of polished sections.

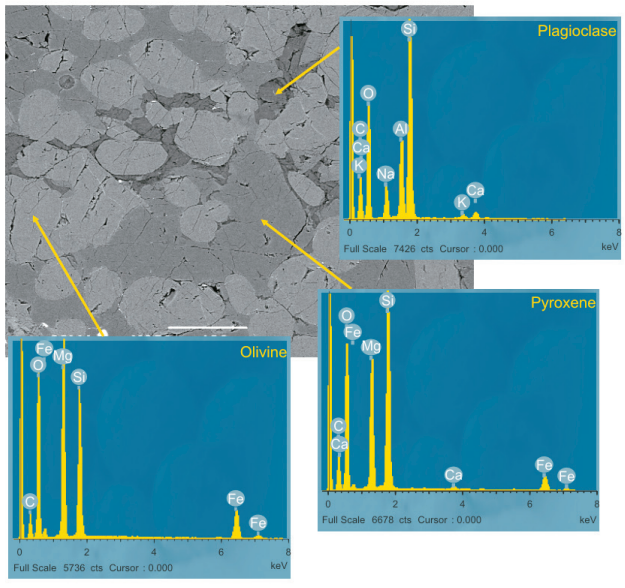

Olivine, rhombic pyroxene and plagioclase matrix with EDS spectra in chondrite meteorite

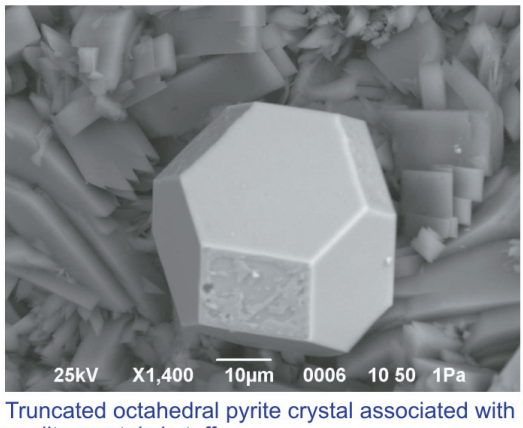

Truncated octahedral pyrite crystal associated with zeolite crystals in tuff

Geochemical studies of environmental media:

SEM/EDS supplements geochemical analyses with data on morphology, mineralogy and sources of heavy metal-bearing phases in environmental media

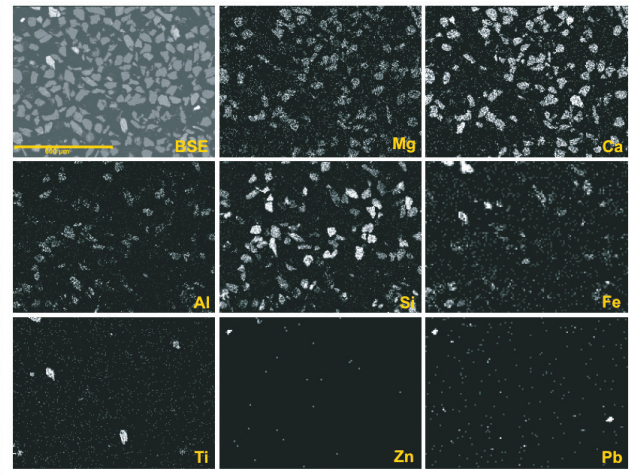

BSE image and EDS mapping of elements in river sediment

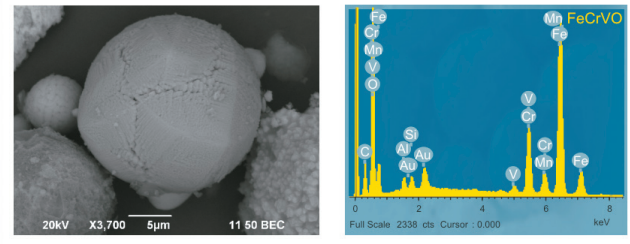

Solid spherical particle of (Cr, V, Fe)-oxide from urban snow deposit, resulting from iron and steel melting processes

Other applications:

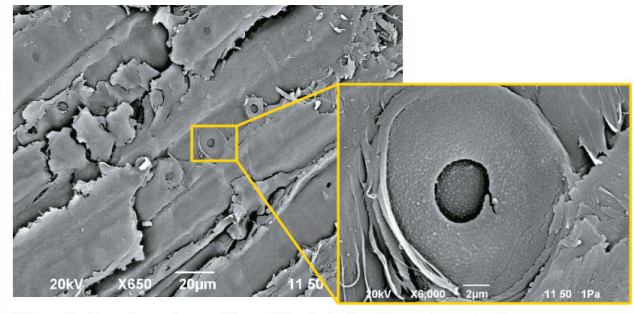

Wood structure in xylite with detail of bordered pit

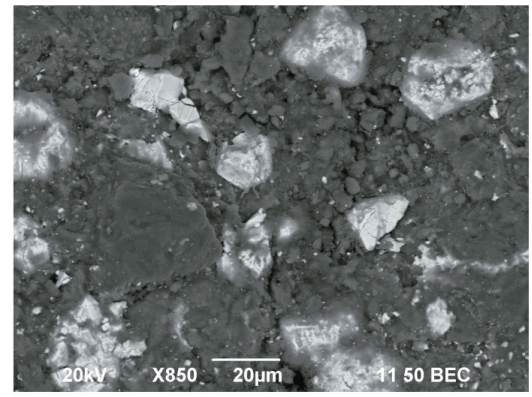

HgS on inner wall of ancient earthen vessel used for roasting of cinnabar ore

More information: Miloš Miler, tel.: +386(0)1 2809 767, e-mail: milos.miler@geo-zs.si
dr. Polona Kralj, tel.: +386(0)1 2809 746, e-mail: polona.kralj@geo-zs.si

Prepared by: Miloš Miler

GEOLOGIJA

št.: 53/1, 2010

www.geologija-revija.si

ISSN 0016-7789

Geološki zavod Slovenije
Geological Survey of Slovenia
www.geo-zs.si